

TWO-CHAMBER REACTORS AND FLOW CHEMISTRY AS VALUABLE TOOLS IN ORGANIC SYNTHESIS

Segeer VAN MILEGHEM

Supervisor:

Prof. Wim De Borggraeve

Members of the Examination Committee:

Prof. Mario Smet

Prof. Erik Van der Eycken

Prof. Wim Dehaen

Prof. Steven Verhelst

Prof. Ian Baxendale

Dissertation presented in
partial fulfilment of the
requirements for the
degree of Doctor of
Science: Chemistry

December 2017

© 2017 KU Leuven, Science, Engineering & Technology

Uitgegeven in eigen beheer, Seger Van Mileghem, Leuven, Belgium

Alle rechten voorbehouden. Niets uit deze uitgave mag worden vermenigvuldigd en/of openbaar gemaakt worden door middel van druk, fotokopie, microfilm, elektronisch of op welke andere wijze ook zonder voorafgaandelijke schriftelijke toestemming van de uitgever.

All rights reserved. No part of the publication may be reproduced in any form by print, photoprint, microfilm, electronic or any other means without written permission from the publisher.

Summary

In this thesis, organic synthesis methodologies were developed involving dangerous gases. The idea was to provide tools to the academic and industrial research society to work in a safe manner with these products. In general, in an academic lab setting, organic reactions involving gaseous reagents are avoided because of both practical and safety concerns. Therefore, alternatives for these reactions are needed.

A convenient and safe method was developed to generate carbon monoxide, a synthetically useful but highly dangerous gas. The gas is formed in a closed system where it is consumed as well. This new method uses formic acid, mesyl chloride and triethylamine to generate carbon monoxide, 3 commodity chemicals available in every organic synthesis lab and is one of the cheapest ways known to generate carbon monoxide on laboratory scale. This methodology was applied by means of a two-chamber reactor to the development of minimalist α -helix peptidomimetics, scaffolds that can display amino acid side chains in a geometrically similar way as a protein α -helix. Palladium-catalyzed aminocarbonylation reactions were used to assemble the helix mimetics. Previously unreported pyrazine based oligoamide α -helix mimetics were generated in this fashion.

Next, the use of sulfur dioxide as reactant in organic synthesis was examined. Facing similar problems as with carbon monoxide, we developed a method for the large scale laboratory synthesis of DABSO, a common gas surrogate for sulfur dioxide, again making use of two-chamber reactors.

Finally, flow chemistry was used to expand classic batch synthetic tools. In a first part, the use of carbon monoxide precursors was explored using continuous flow technology. Another chapter involves the application of flow chemistry to the synthesis of glycerol carbonate from glycerol. Glycerol is an industrial waste product of the production of biodiesel while glycerol carbonate is considered a green chemical.

Samenvatting

In deze thesis hebben we gepoogd bij te dragen aan het uitvoeren van organische reacties waarbij gassen gebruikt worden als reagens, waardoor deze toegankelijker worden voor de academische onderzoeker. In het algemeen vragen deze reacties namelijk speciale voorzieningen. Alle problemen met gassen (veiligheid, lage oplosbaarheid, hoge drukken, toxiciteit, ...) zorgen ervoor dat men niet echt staat te springen om deze te gebruiken.

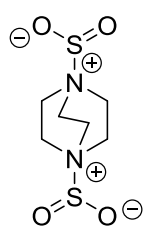
We hebben een veilige manier ontwikkeld voor het gebruik van koolstofmonoxide op laboratoriumschaal. Dit is namelijk een synthetisch interessant maar zeer toxisch gas. Het gas wordt gegenereerd én geconsumeerd in een twee-kamer reactor. De manier waarop het gas gegenereerd wordt is één van de goedkoopste methoden die gekend is, waarbij geen toxische nevenproducten worden gegenereerd. Deze methodologie werd toegepast voor de ontwikkeling van α -helix mimetica. Dit zijn verbindingen die aminozuurzijketens op dezelfde ruimtelijke manier plaatsen als een proteïne α -helix dat doet. Deze verbindingen kunnen hierdoor medisch relevant zijn. Door gebruik te maken van koolstofmonoxide via palladium-gekatalyseerde aminocarbonylering zijn we er in geslaagd om de ongerapporteerde pyrazinegebaseerde oligoamide α -helixmimetica te synthetiseren.

Ook werd het gebruik van zwaveldioxide als reagens in organische reacties onderzocht. Dit gas is gelijkaardig aan koolstofmonoxide in de zin dat het vergelijkbare interessante synthetische mogelijkheden biedt maar ook zeer gevaarlijk is om mee te werken. Vanuit die optiek hebben we een protocol ontwikkeld voor de grote schaal synthese van DABSO, een gekende gasprecursor voor zwaveldioxide, weerom gebruik makend van een twee-kamer reactor.

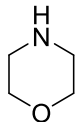
Een ander aspect van deze thesis is het gebruik van flowtechnologie als een expansie op de huidige batch synthese methodologieën. Hierbij wordt op een continue manier een synthese uitgevoerd. Dit werd toegepast voor koolstofmonoxideprecursoren alsook voor de synthese van glycerolcarbonaat, een groen reagens, uit glycerol, een industrieel afvalproduct van de biodieselsynthese.

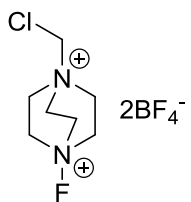
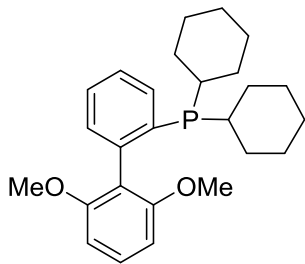
List of abbreviations

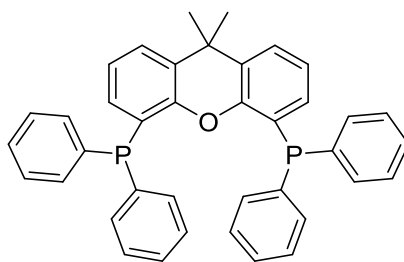
ACN	Acetonitrile
Boc	<i>tert</i> -butyloxycarbonyl, protecting group
BPR	Back pressure regulator
bs	Broad singlet
COware	Two-chamber reactor from the Skrydstrup group
CSA	Camphersulfonic acid
Da	Dalton, molecular weight unit
DABCO	1,4-diazabicyclo[2.2.2]octane



DABSO	
DCM	Dichloromethane
DIAD	Diisopropylcarbodiimide
DIPEA	<i>N,N</i> -diisopropylethylamine (Hünig's base)
DIY	Do it yourself
DMAP	4-Dimethylaminopyridine
DMC	Dimethyl carbonate
DMF	Dimethyl formamide
DMSO	Dimethyl sulfoxide
<i>e.g.</i>	exempli gratia
eq	Equivalents
FT-IR	Fourier-transform infrared spectroscopy
GC	Gas chromatography

GLC	Glycerol carbonate
GPR	Gas pressure regulator
HOMO	Highest occupied molecular orbital
HPLC	High pressure liquid chromatography
HR-MS	High resolution mass spectrometry
HTS	High-throughput screening
IC ₅₀	The half maximal inhibitory concentration
IleRS	Isoleucine tRNA synthetase
IPA	Isopropyl alcohol
LUMO	Lowest unoccupied molecular orbital
MIT	Massachusetts Institute of Technology
Morpholine	
MPLC	Medium pressure liquid chromatography
Ms	Mesyl
N/A	Not applicable
NaHMDS	Sodium hexamethyldisilazide
NBS	<i>N</i> -bromosuccinimide
NHC	<i>N</i> -heterocyclic carbene
nM	Nanomolar (concentration)
NMR	Nuclear magnetic resonance
PBR	Packed bed reactor
PPI	Protein-protein interaction
ppm	Parts per million

PS	Polymer supported
psi	Pound-force per square inch, a unit for pressure
RT	Room temperature
SAR	Structure activity relationship
<i>sec</i> -BuOH	2-butanol
SelectFluor	
S _N Ar	Nucleophilic aromatic substitution
SOMO	Single occupied molecular orbital
S-Phos	
TFA	Trifluoroacetic acid
THF	Tetrahydrofuran
ThrRS	Threonyl tRNA synthetase
TLC	Thin layer chromatography
Trt	Trityl, protecting group
Ts	Tosyl



Xantphos

Acknowledgements - Dankwoord

Het dankwoord is, een beetje tegendraads, het meest gelezen stukje van een doctoraatsthesis. Hoe zou dat komen? Maak u vooral geen illusies, we zijn allemaal een stelletje prutters! Een dankwoord is veel interessanter dan data! Ik heb het eigenlijk nooit kunnen begrijpen hoe sommige mensen op het einde van hun doctoraat heel hun dankwoord rondkrijgen op **één** pagina. Als er na een dergelijke rollercoaster van 4 jaar niet meer emoties vrijkomen dan louter de formele zaken, dan stel ik mij daar toch vragen bij. Neen, dit acht ik een moment om eens deftig uit te drukken dat ik dankbaar ben. Meer zelfs, gezien ik niet altijd een kampioen ben in emoties te uiten of zeggen waarop het staat, maak ik van deze gelegenheid graag gebruik om iedereen uitgebreid te bedanken.

Ik had eerst en vooral deze woorden nooit kunnen neerpennen als professor **Wim De Borggraeve** mij niet de kans had gegeven om te doctoreren. Hij moet het vuur in mijn ogen hebben gezien! Heel hard bedankt voor deze opportuniteit. Ik vind dat je een zeer goede begeleider bent: temperen waar nodig maar ook moed inspreken waar nodig, zonder veel wetenschappelijke vrijheid te ontnemen van je mensen. Ik heb mezelf nooit de “doorsnee” doctoraatsstudent gevoeld en heb gelukkig altijd de mogelijkheid blijven hebben om naast het doctoreren ook tijd te kunnen steken in hobby's zoals sport en vissen, een garantie die je in het academisch milieu zeker niet overal hebt, en die ik ten zeerste geapprecieerd heb.

Ook mijn assessoren en juryleden kunnen hier niet ontbreken. Professor **Mario Smet** en professor **Erik Van der Eycken**, bedankt om mijn doctoraat met veel enthousiasme op te volgen als assessoren. Mario, ook bedankt voor het organiseren van de wijnavonden. Professor **Wim Dehaen**, professor **Steven Verhelst** and professor **Ian Baxendale**, thanks a lot for being my jury members and revising this work. Your time and comments are greatly appreciated.

Iemand die ook een zeer belangrijke rol heeft gespeeld in mijn verhaal op de KU Leuven is niemand minder dan **Brecht**. Meer zelfs, moest ik aan één iemand in dit dankwoord de eigenschap uniek toekennen, ja... dan heb jij die prijs gewonnen. (Ok nee, toch niet, gedeelde eerste plaats met **Cevain**!) Of kennen de lezers van dit dankwoord misschien nog iemand die op de *security check* van de luchthaven plots beseft dat hij nog een dolk van quasi een halve meter aan zijn broek heeft hangen en dit dan ook nog eens uitgelegd krijgt

zonder confiscering van dit moordwapen? Of iemand die samen met “een man die in het bos woont” voor een dagje naar de zee gaat, vervolgens een gek Japans pak aantrekt om dan met zijn tweeën met messen te gaan vechten in de zee, gewoon “voor de leut”? Gaande van een kerel die sporadisch eens een gasfles besprong, tot de dag van vandaag waar hij recent vader geworden is, wat een metamorfose! Ik kijk ook echt op naar uw handigheid, want anders had de Pleasuretron 2000 mijn pad nooit gekruist... In ieder geval, vanaf de dagen waarin je de begeleider was van mijn masterthesis tot quasi de dag dat dit boekje gedrukt werd, zijn jouw hersenkronkels van cruciaal belang geweest in dit werk, iets wat ik nooit zal vergeten...

Iemand waarvan ik van de eerste contacten al meteen wist dat we wel eens goede maten zouden kunnen worden is **Klaas**, de schrik van Hoogstraten en *self declared* bowlingexpert, ondanks de ‘petanqueworp’. Ondertussen zijn onze paden (een beetje) gescheiden, maar dat weerhoudt ons zeker niet om vantageit eens goed bij te praten. De manier waarop wij op dagdagelijkse basis zeverden tegen elkaar in het labo, dat zijn momenten om eeuwig te koesteren. Of het nu ging over vrouwen, chemie, random zever of vrouwen (hebben we het wel 1 of 2 keer over gehad, geloof ik), de humor die er aan te pas kwam hield ons messcherp. De elegante wijze waarop jij (al dan niet geïntoxiceerd, al waren de bloemenverkopende Paki’s daar minder enthousiast over) tevens een feestje in gang kan steken, daar kan menig persoon nog iets van leren. Wereldklasse is het. De labofeestjes in de oude F zijn gewoonweg niet los te maken van een feestende Klaas. Wie weet is het dan ook geen toeval dat we dit nooit hebben kunnen evenaren in het nieuwe gebouw, we waren onze katalysator voor eeuwig en altijd kwijt... Dat we nog lang maten mogen blijven, man! En als apotheose: **AZOE EEN TIETE, PEKE!** Bij deze ben je mij een bak bier verschuldigd, graag binnen de maand aan mij bezorgd.

Over **Cevain**, Bitcoin miljonair, zou ik 10 pagina’s kunnen schrijven hier, en dan nog is het onmogelijk om een beschrijving neer te pennen zodat mensen die hem niet kennen, weten wat hun te wachten zou staan wanneer ze hem leren kennen... Ik haalde namelijk hierboven al aan dat hij met Brecht de eerste plaats deelt qua uniek zijn. Cevain, hoe jij de lijn serieus-zever kunt laten vervagen, dat is ongezien. Na ettelijke jaren goede vrienden te zijn, hangt er toch nog zoveel mystiek rond u en dat typeert u echt! De dynamiek met uw vriendin bijvoorbeeld, begrijpe wie kan?! Naast de *string theory* het

meest complexe raadsel van deze tijd. Als er maar één waarheid in het universum is, dan is het deze wel: houd Evelien goed bij u, want zo één komde echt NOOIT nimeer tegen. Ook uw kot vroeger met bijhorende bureau die begraven was onder de lege melkflessen en pizzadozen, en uw *lifting gear* in de andere hoek.. En toch niet het leven gelaten door salmonella of door de vloer gezakt te zijn, niets minder dan een wonder! Ik ben zelf iemand die regelmatig ongepaste opmerkingen kan maken, maar dat is niets vergeleken met uw kunsten op dit vlak, waarbij vooral uw timing en verrassingseffect zijn gelijke niet kent. Man, wat heb ik geschaterlacht, ongelofelijk! Ons gebulder tijdens de middag in de oude F was vaak te horen tot helemaal bij Spectro, wat waren dat de tijden!

Stijn, de keukenprinses. Waar moet ik in hemelsnaam beginnen? Sinds jaar en dag mijn maatje, mijn persoonlijk adviseur in de keuken en mijn encyclopedie van wetenschappelijke feiten rond voeding. Ik kwam nooit eerder iemand tegen wiens ogen beginnen te fonkelen als hij spreekt over koffie, of bier, of brood, of kikkererwten, of kaas, of kruiden, of... Ondanks de regelrechte *cock block* van een 6 tal jaar geleden, zijn we zeer goede maten gebleven, haha! Ook 6 weken Australië hebben we overleefd zonder elkaar (nét) niet de kop in te slaan. Jouw 'tegendraads doen om tegendraads te zijn' karakteristiek siert u, daar zal Amy zeker van kunnen meespreken. Dat is ook sowieso de hoofdrede waarom uw pa u nen 'onnozeleir' vindt! Ik kan er nog wel wat meer bedenken eigenlijk! Misschien omdat wat jij 'parate kennis' acht (en dat is VEEL), dat daar niemand u iets moet over vragen, want dan krijgen ze het deksel hard op de neus! Of uw geheimzinnigheid rond afwezigheid/vakantie misschien? Man, wat heb ik daarmee gelachen! Er zijn zoveel herinneringen, gaande van Stijn die een potje satékruiden *ad fundum* kapt en er totaal slecht van gaat, tot de verdeel en heers *kitchen overlord* op het kerstfeestje, die allemaal een speciaal plaatsje hebben gekregen. Bedankt voor alles, echt waar!

Koen, de man die gebroken heeft met peptiden om zich op gelators te storten. De peptiden zijn nog vol liefdesverdriet, arme stakkers... Een groot lawaai, dat zal ik mij vooral blijven herinneren over de heer Koen Nuyts. Enkele jaren terug toonde je een moment van tederheid tussen al dat geroep, en nam ik je onder mijn hoede om je te introduceren tot crossfit, tot op vandaag de dag nog steeds de basis voor uw breedgeschouderd postuur. *You're welcome*. Dingen zoals de Colruytripjes, uw uitbarstingen (zoals die

keer dat Cedrick als groen blaadje uw glasfilter had laten vallen), uw humor en uw Justin Bieber bureau zullen me lang bijblijven.

Johannes, de NederBelgPool! Jouw eigenschappen als chemist zijn niet van de minste. Zomaar op je eentje verschillende papers halen, dat is niet voor iedereen weggelegd. Ik ben er dan ook zeker van dat de universiteit Antwerpen er een sterke macht bijheeft. Succes!

Dan, **Joachim** van Quartier Schaerbeek, de *groupie* van Steel Panther! Er wordt regelmatig geschreven dat te laat komen in iemands bloed zit, dat hij er niet kan aan doen. Jij bent voor mij het levende voorbeeld van deze stelling! Ik denk dat ik tevens niemand ken die zo ongelofelijk goed kan luisteren als jij. Jij discussieert nooit om gewoon je eigen visie op te dringen, maar eerder om te luisteren naar de andere standpunten, en die eigenschap is op zijn zachtst uniek te noemen. Eerst en vooral: bedankt voor de ettelijke uren debat/discussie/filosofische uitwisselingen, waarbij ik soms zo hard *in the zone* geraakte dat ik bijna begon te tieren. Hier heb ik toch wel enorm veel aan gehad. Jij gaat het trouwens nog ver schoppen met je chemische kennis, jij levende literatuurlegende. Met je tondeuse daarentegen heb je dringend wat bij te leren... Het blijft mij trouwens keer op keer verbazen wat een aimabele man jij wel niet bent: bijna geen vooroordelen naar mensen toe en je tolereert zowat alles. Helaas wordt heel deze karakteristiek volledig teniet gedaan wanneer het over muziek gaat, want dan verander je plots in de meest intolerante persoon die ik ken! Liever snel naar de hel dan traag naar de hemel? "Een gevaarlijk lied met een TOTAAL verkeerde boodschap." Zingen over seks? "Puberaal gedrag van de ergste graad." Het spreekt voor zich: *Jesus would not be proud*. In ieder geval, moest je toch ooit beginnen neigen naar atheïsme moet je me zeker bellen, al zijn we beide hoogbejaard ;-). Als laatste dien ik nog te zeggen dat ik hoop dat mijn huwelijkscadeau voor wat, euh, afwisseling kan zorgen. Al is het maar uit wetenschappelijke nieuwsgierigheid!

Thomas, moderator van www.dumpert.nl, iemand die zeer creatief tot 20 kan tellen, de koning van de *logical fallacies* en nog zoveel meer. Je was ook voor een hele poos een naaste collega, met veel gelach en gegier over de jaren heen. Merci voor alle filmpjes, alle reisverhalen en je uitstekende uitvoering van 'laboverantwoordelijke' zijn. Ik zal ook nooit vergeten hoe jij voor eeuwig de geschiedenis bent ingegaan als een absolute wereldster in anti-climaxverhalen! (Voor de geïnteresseerden: vraag hem maar eens naar een Russische vrouw die kwam couch surfen, maar zorg wel dat je eerst

neerzit.) Ook tegen absoluut onbeleefde apen op congressen stonden we samen sterk! In alle eerlijkheid dien ik de lezers nog in te lichten dat Thomas een soort van geavanceerde codetaal heeft ontwikkeld die tot op heden niet te kraken valt. Het betreft hier de term “en cetera”, heel sporadisch aangevuld met “of cetera”. Na talloze vergaderingen onder collega’s zijn we tot de conclusie gekomen dat we een prijs uitreiken voor de persoon die deze *next level* code kan kraken, want ons is het tot op heden gewoonweg niet gelukt.

Wat later vervoegde **Cedrick** ons ook, de “katholieke”, ambitieuze West-Vlaming. Geloof het of niet, maar als Cedrick een doel voor ogen heeft, valt dat zelfs te merken aan zijn... manier van wandelen! Gene zever. Niemand wandelt sneller door de gangen van den F, zoveel is zeker. Het gros van de lezers beseft misschien niet meteen dat Cedrick een bekende Vlaming is, met verschijningen op nationale televisie. Hij geeft tegenwoordig nog gratis handtekeningen, maar ik zou er snel bij zijn als ik van u was... En trots dat zijn mama is! Merci voor de vele eerlijke antwoorden op mijn vaak nogal rare vragen, en alle hulp in het labo. Ik denk trouwens, zonder te zeveren, dat er voor jou een carrière in de politiek is weggelegd. Zo een extreem gladde paling als jij (al kan **Gert** er ook wat van!), ik zou het zeker een kans geven!

Laurens was ook van de partij, een man die liever met gelletjes speelt dan met vrouwtjes, tenzij het Japanse deernen betreft! Op een dag wordt hij een gekend auteur in Nature Materials, maar daar zullen we toch nog even moeten op wachten, vrees ik... Zie maar dat je deze Japanoloog nooit meevraagt, want de kans is groot dat hij niet kan omdat hij nog moet afwassen. Man, man, man! Nochtans ziet de toekomst er rooskleurig uit, gezien Laurens gekroond is tot nieuwe Chieftain van de spellekesavond. Mijn opvolging is verzekerd, een goeie zaak!

Of course, **Soultan** cannot be forgotten in this acknowledgement, although his last sighting was in the Canadian wilderness, dancing with bears... Thanks for all the laughs, the fights (the battle of the forks with Eggmantas for example!), your party spirit, your smoothness (‘Of course!’) and so much more. I’m definitely sure you will do a great job in the land of maple syrup, as you are a versatile and capable scientist. A la prochaine, mec!

Philippe ‘de Grote’, zoals Klaas het mooi doopte, gij waart, zijt en zult een serieuze meerwaarde voor de groep zijn. Buiten een harde werker en een zeer capabel chemist, durf jij *out of the box* te denken en met coole ideeën

op de proppen te komen. Daar zijn zowel de nieuwe snufjes in *the office* als op het *world wide web* levende voorbeelden van! Het is dan ook meer dan verdiend dat jij naast voltijds doctoraatsstudent ook de titel *head of innovation* hebt verdiend! Blijf vooral zo verder doen.

Dries, de lepe pé. Gij zijt ne rare snuiter ze, ma dat weet ge zelf ook wel! Ik ben er zeker van dat ge uw doctoraat in schoonheid ga afronden. Tijdens je oefenzittingen valt er door je leidinggevende positie wel eens een vrouwtje in zwijm. Helaas pindakaas zijn deze vaak “jouw type” niet. Komaan man! Standaard verlagen, mijn gedacht! Wat minder aan die badmintonraket denken? Wanneer doen we ons matchke eigenlijk? Ik ga u sowieso kloppen...

Alsof één Verschueren echt nog niet genoeg was, dan komt er prompt een andere de veteraan aflossen... *Parents, lock up your daughters*, **Rik “Ricky Gervais” Verschueren** (Henri voor de vrienden) is gearriveerd uit metropool Wortel! Ik heb oprecht spijt dat wij niet wat langer collega’s zullen zijn, want, om het zacht uit te drukken, wij hebben wel wat gemeen! Interesse in mensen, zowel qua psychologie als overtuigingen, is een zeldzame karakteristiek die we toch beiden bezitten. Ook op filosofisch vlak kwam ik zwaar aan mijn trekken door u. Het woord “*specimen*” zal mijn hele leven gelinkt blijven aan onze definitie, en terecht ook, want zeldzaam zullen ze blijven... Ge hield mij scherp, en de occasionele steek werd direct met veel geweld teruggevuurd! Ook op het vlak van humor zit het snor. *A new ‘lord of the memes’ is born*. Bedankt om deze toch wel uiterst belangrijke *legacy* voort te zetten. Merci voor de babbels, zowel diepgaand als ultraplat. Blijf vooral uw eigen gedacht volgen, want gij gaat nog ergens geraken! Hopelijk verliezen we het contact niet, dat zou een spijtige zaak zijn. Ik wens u alleszins ne *specimen* toe!

Michael, thanks for being the Australian cunt that you are. You getting married was the perfect excuse to explore *down under*! Thank you for being a nice guy in general, which can be rare among PhD students. Also for all the talks, for all the drinks (coffee, but mainly beer), for all the PhD smack talk and for letting us stay in your parents’ garage in Sydney! It appears you will be staying in Belgium for some time to come, and I can say that I like that!

Wim Dehaen Junior, ik heb helaas de titel voor ‘uniek zijn’ al weggegeven. Nochtans had jij ook wel kans op de titel nu ik erover nadenk... Helaas ben je niet blijven doctoreren op de KU Leuven, wat ik een uiterst spijtige zaak vond! Elke keer als ge terug in België passeerde en onze paden kruisten, lachte ik

me steeds opnieuw een kriebel met u. Het moet gezegd, uw outfit draagt elke keer wat meer bij aan dat gebulderlach. Haha! Als gij uw pijlen blijft richten op een academische carrière, dan kan ik u alvast verzekeren dat ge het volgens mij extreem goed gaat doen. De manier waarop jij chemie ademt en een levende encyclopedie bent, dat kent zijn gelijke niet. Een kleine twee jaar terug kregen we te horen dat je *vegan* was geworden. Was dit de Wim die keer op keer lachte met vegetariërs, op zijn kenmerkende extreem sarcastische wijze? Of was het zuiver om op te vallen? Dit was in ieder geval voor mij een cruciaal moment van zelfreflectie en verandering op het vlak van voeding, iets wat ik je misschien nog nooit verteld heb.

Lau, de klimmer en nog steeds rasechte Hasselaar. Bedankt voor het gezever door de jaren heen. Als je chemie ooit beu bent, dan zou je nog steeds cursussen beginnen geven om te leren '*party crashen*', iets waar je toch wel in uitblinkt!

Jochen, die mijn plaats innam om bij **Jeroen & Tim** te gaan wonen (zie verder), heeft ook een rol gespeeld in dit verhaal. Jochen, nu en voor altijd, gij hebt de meest aanstekelijke schaterlach ter wereld, *period*! En zoals 'Het Eiland' ons jaren geleden al leerde, 'ge kunt uwe lach niet veranderen!' Goed nieuws dus. Tot verbazing van menig onderzoeker werd je helaas niet *lord of the F*. Gij zijt een warm persoon, Jochen, misschien soms zelfs te goed voor deze wereld! Merci voor alles (bv. de rasechte Straetmanskippen®)!

Jeroen Sniekers, helaas NIET de kip met de gouden publicatie-eieren. Ik ken niemand die trotser is op Limburg dan gij! Al moet in alle eerlijkheid gezegd worden dat je een Vilvoords accent begint te krijgen. *Blame the girlfriend*! Merci voor de DSC-hulp en voor mijn ijsbeermaatje te zijn *back in the days*.

Ook **Mathias**, beter gekend als den Danny (sorry not sorry), verdient hier toch wel een aparte alinea. Het is na al die jaren nog steeds zo dat vrouwen gemiddeld meer babbelen dan mannen, met Mathias de uitzondering op die regel. Van in de dagen op Toxikon tot op het einde van mijn doctoraat kregen we op wekelijkse basis met elkaar te maken. De manier waarop jij een lab runnende houdt? Dat verdient een dikke vette opslag, ik zou zeker het IWT eens mailen. Ik zal u mij altijd blijven herinneren als 'de gekke weetjesman'. Je hoefde maar één keer iets uit te leggen aan Mathias, hij was er mee weg tot in het oneindige.

I would like to express my gratitude as well to the other LOSH members I shared the lab with: **Tamara, Hung, Nico, Benoit, Shabnam, Chiara, Ronny,**

Sarah, Seba (de meest enthousiaste stem van den F), **Gert** (de schrik van de Blackwood), **Vidmantas, Carmen, Monissa, Sam** (eindelijk iemand met dezelfde muzieksmaak!), **Ruben**, and anyone whom I might have forgotten!

Also members of other labs who I interacted with deserve a word of gratitude: **Maarten** (de droogheid zelve), **Vince** (de prins), **Jubi** (see you in Kerala my friend), **Joice, Robby, Sampad, Pavel** (I like snow, I like mountains, *ergo* I like Russia!), **Hans, Felix** (thanks for being my guide in Berlin), **Geert, Upendra, Justyna, Deepali, Wout, Koen, Pieterjan, Tom, Tomas, Thomas, Giacomo** and probably many more!

Er zijn uiteraard ook personen zonder wie de F nooit zou kunnen functioneren. Eerst en vooral **kapitein Raf**, bedankt voor alle gesprekken en uw uitstekend leiderschap. Ook **Dominique** (de Jean-Michel Saive van de KU Leuven), **Karel** (aan F-verhalen geen gebrek!), **Dirk** en **Paul**. En ook **Rein** (†), spelletjesavondenthousiasteling van het eerste uur, die helaas het geluk niet getroffen heeft en niet meer onder ons is.

As most of you know, I also spent half a year abroad during my PhD, more precisely at Durham University in the UK. First of all, special thanks to professor **Ian Baxendale** for hosting me in your lab! It has been a unique experience for me to work with an amazing chemist like yourself, and I have learnt a great deal. Moreover, most colleagues from 'CG053' have become good friends. Thanks guys, for all the dinners, the pub nights, the help in the lab, *etc.* **James**, thanks for being such a nice guy and being my occasional lifting pal, for the Indian curry cooking lessons and for all the talks! As you have already noticed, you are always welcome in Belgium! **Carl**, thanks for all the facts and myths about Malta (you apparently know even more expressions about Malta than Google, and you guaranteed you weren't lying...), for all the help in the lab, for the nice meals and for letting me spend the night in ghetto Gilesgate. **Laurens**, thanks for the occasional talks in Dutch, for the 'formal dinner' and for joining me for clay pigeon shooting! **Marcus**, there were a lot of days where I would have been lost without your scientific advice! Pretty sure you will become a great professor. Back into rowing yet? **Laura**, thanks for all the help with my registration when I arrived, all the country talks (I still remember a lot about Guinee-Bassau for some reason...) and with the legal help regarding the situation with the landlord. **Paolo**, I'm pretty sure no one will ever trump you in learning me to swear in Italian, especially when retrieving NMR data. Thanks for the scientific advice as well! **Te**, thanks for the Chinese noodles and all the hilarious moments!

Also thanks to ginger **Ryan**, riders of **Rohan**, playboy **Alex**, **Russel** Morning Wood and **Edward**.

Wanneer ik terugkwam uit het land van thee (met melk, bweik) en fish & chips, ging ik in Heverlee wonen bij **Tim** de turbokakker & **Jeroen**, de Merchtemboy die wel eens een cursus huishoudkunde kan gebruiken! Eerst en vooral, ik heb me serieus geamuseerd met jullie, ook al ging ik veel crossfitten en vissen. Tim, bedankt voor alle filosofische gesprekken (en het waren er véél), en Jeroen, bedankt voor al de chemische praat en alle drinks. Een doctoraat was wat teveel gevraagd voor jou (BURN!), al zal het aan kennis en *knowhow* zeker niet gelegen hebben!

Mensen die hier ook een plaatsje verdienen zijn de vrienden van het vissen, en dan voornamelijk de harde kern van de **VBK regio Vlaams-Brabant**. Bedankt voor de regioavonden, etentjes, *fish-inns*, schunnige avonden op de Oude Markt,... Ondanks dat het vissen zelf op een laag pitje stond tijdens de eerste twee jaar van mijn doctoraat, bleef ik steeds opnieuw uitkijken naar deze activiteiten. *Partner in crime* **Tom Cochet** verdient toch een extra vermelding. Of het nu gaat over minikarpertjes, monsterkarpers, SKPs, wulpse deernen of de dagelijkse roddels, ik kon steeds bij u terecht voor wat *fish talk* of om wat te zeveren, iets dat de dagen toch altijd wel wat aangenamer maakte. Ondanks je zelfverklaarde titel van “De Tildonkse Leeuw” betrap ik je er toch steeds meer op dat je hummus en guacamole met smaak begint te vreten. De boerenzoon van Bertem *goes vegi*? Pikant detail voor alle lezers is dat Tom van plan is een boek uit te brengen in de nabije toekomst: “*How to become a real man*”, met massa’s handige *tips & tricks*. Ook wederhelft **Steffi Verbeeck**, mijn allerbeste Lync buddy en eten-in-de-zetel vriendin (soms tot ergernis van de Leeuw) heeft hier een plaatsje verdiend. Ik weet alleen niet hoe je dit Lync verlies binnen een kleine maand gaat oplossen? Hopelijk kan je hiervoor ergens terecht...

Also crossfit (a crazy workout regime where bones are broken when you are clumsy...) has been a significant “hobby” during my PhD, in which I have made a lot of good friends. Special thanks to **Redneck Abhi**, **Roid Boy Job**, **Apekop Thomas**, **Chest Pump Robin**, **Enkelmans Pieter**, **Engine Dries**, **Early Bird Brandon**, **Pretty Boy Jorn**, **Boerenbond Kris**, **Eikel Bart**, all the **coaches**, and many, many more...

Op het thuisfront zijn er niet zoveel vriendschappen die door de jaren heen deftig onderhouden zijn, maar één waar dat wel het geval is, is sowieso

diegene met **Ruben** (of Costello, Roebymon, Ginger, De Becker,...). Sinds de dagen dat we samen in een band zaten zijn we goeie maten, en daar heb ik toch wel veel aan. Het feit dat jij ook graag diepe gesprekken voert, ligt hier sowieso aan de basis. En zelfs ook beginnen crossfitten seg, wat een invloed heb ik wel niet op u, hoho! Chapeau dat je al die jaren een goede vriend van mij bent gebleven, merci!

Mijn familie kan hier zeker ook niet ontbreken. Er zijn er zelfs twee waarvan ik overtuigd ben dat ze de wetenschapsvlam reeds vanop zeer jonge leeftijd bij mij hebben aangewakkerd, en de kans lijkt me groot dat ik zonder hen nooit beland was in het wetenschappelijk onderzoek. Enerzijds is dat **papa**, die me kritisch leerde denken over alledaagse zaken, tot ab-so-lu-te ergernis van menig (godsdienst)leerkracht! Ook de grootste passie uit mijn leven, het vissen, vloeit voort uit jou. Hoog tijd dat je wat meer krediet neemt voor dergelijke dingen. Anderzijds is dat **mijn grootvader** (Carlos), die door zijn onuitputbaar enthousiasme zowat alles op een zeer jonge Seger afvuurde: vlaggen, wereldkaarten, (dieren)encyclopedieën,... De lijst is eindeloos en ik was zo leergierig dat ik er soms niet van kon slapen! Daarnaast is er natuurlijk ook nog **mama** voor haar onbegrensd positivisme, haar nogal unieke humor en extreem talent voor verhalen klaar en duidelijk te vertellen. En ook de luidste van heel de familie (of Asse, of het heelal) **Liese & Lore**, die een gedeelde eerste plaats op het wereldkampioenschap schaterlachen behaalden, horen in dit dankwoord meer dan thuis. Jullie geven me tevens psychologisch advies wanneer ik dat wens, maar vooral ook wanneer ik dat niet wens! Haha! Onze band vind ik vrij uniek, en ik hoop dat dat mag duren tot ze ons onder de grond stoppen! De rest van mijn familie zoals mijn grootouders, tantes, nonkels, neven en nichten zijn mensen waarop ik kan terugvallen, waarvoor mijn oprechte dank.

Tot slot wil ik graag mijn vriendin **Maïté** bedanken, die door de meeste lezers van dit dankwoord waarschijnlijk beter gekend is als De Dikke Prot en/of Protmans. Van bijna in het begin van mijn doctoraat tot helemaal op het einde stond je aan mijn zijde, zowel in goede als slechte dagen. Het blijven om kunnen gaan met mijn zwerverslust, vissersdrang en filosofische trekjes verdient sowieso al verschillende trofeeën. Dat er nog vele jaren mogen volgen, gevuld met een grote portie humor en/of samouraisaus. *Aj mou kinjth, ek zien a toch geire, zenne!*

Na 4 jaar zit het er op. Ik kan het zelf amper vatten. Hetgeen men 'doctoreren' noemt, man, wat heeft dat mij veranderd! Ik vind het bijna

schrijnend hoeveel dat heeft bijgedragen aan de persoon die ik vandaag ben. Het doet je echt beseffen dat je eigenlijk niets weet, en dat je je visie constant moet veranderen bij nieuwe wetenschappelijke bevindingen. En dat is bij het gros van de mensen bijna onmogelijk, *tunnel vision* weet je wel... Ik heb de indruk dat veel collega's hun wetenschappelijke, kritische denkwijze van zich kunnen afzetten wanneer ze de deuren van Chem & Tech buiten wandelen op het einde van de dag, maar dat is bij mij precies niet meer mogelijk (sorry, Maïté). Het is tevens niet evident om als wetenschapper het bewijs/je interesse te blijven volgen, niet wetende naar waar het leiden zal. Ik kijk dan ook vaak op naar wetenschappers die, ondanks geld, macht, politiek, reputatie, etc. toch hun pad blijven volgen. *Follow the evidence!* Als wetenschapper zit je namelijk op de eerste rij: je ziet dat algemeen aanvaarde wetenschappelijke bevindingen niet noodzakelijk worden doorgetrokken naar de samenleving, omdat ze niet stroken met de maatschappelijke visie of er gewoon teveel geld mee gemoeid is, ongeacht de bergen bewijs. Het hard optreden tegen drugs (de zogenaamde *war on drugs*) is hier één van de vele voorbeelden hoe we de bal volledig blijven misslaan. In ieder geval, mijn wereldbeeld is door de jaren heen voorgoed veranderd en écht *open minded* proberen zijn is voor mij is een van de mooiste dingen die uit doctoreren voortgevloeid is. In vraag stellen houdt mij scherp, en leidt tot zingeving. *With all my heart, thank you, science...*

Na "10 jaar studeren", zoals sommige personen mijn tijd in het Leuvense wel eens omschrijven, vragen velen zich af of het nu genoeg is geweest. Kort antwoord: neen! Leergierig ben je, en dat blijf je. Voor mij is het dus tijd voor een nieuw avontuur. Ik kijk er alvast naar uit, niet wetende wat komen zal.

En jij, ga jij er nu maar eerst even bij zitten, want ik wil je over chemie vertellen.

Segar, November 2017

"When the idea of a new substance is born, nothing exists but symbols, a collage of odd atoms hooked together with bonds, all scribbled out on a blackboard or a napkin at the dinner table. The structure, of course, and perhaps even some spectral characteristics and physical properties are inescapably pre-ordained. [...] [Other] properties cannot yet be known, for at this stage they do not exist."

Alexander Shulgin, PIHKAL

Table of Contents

Summary	IV
Samenvatting	V
List of abbreviations	VI
Acknowledgements - Dankwoord	X
Table of Contents	XXI
1. General introduction	3
1.1 Flow chemistry	5
1.2.1 General	5
1.2.2 Gas reactions in flow	14
1.2.2.1 General	14
1.2.2.2 Tube-in-Tube reactors	15
1.2 Gas surrogates	17
1.3 Two-chamber reactors	19
1.4 Objectives	22
2. In search of a new CO precursor	27
2.1 Literature and discovery	27
2.2 New CO precursor: applied in palladium-catalyzed carbonylation	32
2.2.1 Flow approach	32
2.2.2 Two-chamber approach	38
2.3 New CO precursor: further considerations and conclusions	43
3. The assembly of pyrazine based oligoamide alpha-helix mimetics	49
3.1 Literature and objectives	49
3.1.1 Protein-Protein Interactions	49
3.1.2 Strategies for protein-protein interaction inhibitor design	51
3.1.3 Rational Design of small molecule PPI inhibitors	52
3.2 Results and discussion	57
3.2.1 Retrosynthesis	57
3.2.2 Synthesis	59

3.2.3 Towards analogues of tRNA synthetase inhibitors	70
3.3 Conclusions and future perspectives	74
4 The use of sulfur dioxide in organic synthesis	77
4.1 Literature and objectives.....	77
4.2 Results and discussion	83
4.3 Preparation of DABSO	87
5 Towards a continuous synthesis of glycerol carbonate using glycerol and dimethyl carbonate	95
5.1 Literature and objectives.....	95
5.2 Results and discussion	97
6. Conclusions & Future Perspectives	107
6.1 General conclusions	107
6.2 Future perspectives	110
7. Experimental	115
7.1 General.....	115
7.2 Chemical safety.....	117
7.3 In search of a new CO precursor	120
7.3.1 Flow approach	120
7.3.2 Two chamber approach.....	123
7.3.3 Economic comparison	133
7.4 The assembly of pyrazine based oligoamide alpha-helix mimetics... 136	
7.5 The use of sulfur dioxide in organic synthesis	177
7.6 Towards a continuous synthesis of glycerol carbonate using dimethyl carbonate	180
Publications, awards and posters	184
Publications.....	184
Awards	184
Posters.....	184
References.....	185

CHAPTER 1

GENERAL INTRODUCTION

1. General introduction

In this thesis, we are particularly interested in performing organic reactions with gases. In an academic lab setting, organic reactions involving gaseous reagents require special precautions. First, a gas is not easily contained and leakages are rather difficult to prevent when using conventional glassware. This implies serious dangers, especially if the gas is highly flammable and/or toxic. Whilst for relatively safe gases such as oxygen, a balloon filled with gas can be used in the reaction setup, this is far from the case with gases such as carbon monoxide, hydrogen fluoride, *etc.* In the latter cases, safety and practical restrictions limit the use of such a setup (Figure 1). Another main limiting factor when using a gas for a chemical transformation is the solubility of the gas in the reaction medium. Since a lot of gases used in synthesis are poorly soluble in solvents (*e.g.* carbon monoxide),¹ high pressures are often required and a rapid decrease in solubility with increasing temperature is observed, according to Henry's law. Working under high pressures, of course, also implies extra safety precautions for the lab chemist. Specialized high-pressure facilities are equipped with leakage and pressure detectors and require specialized training of personnel. The scale of high-pressure reactions is often restricted to mitigate risks, which contributes to a challenging scale-up. Another problem is one of thermodynamics. Gas-liquid reactions require a high interfacial area for an efficient mass transfer rate. Round bottomed flasks do not provide solace here, as the interfacial area decreases rapidly with increasing size of the flask (Figure 2). (Note that when stirring, the vortex increases the interfacial area, which is dependent on the stirring rate.) This is again problematic for a potential scale-up.

All of the represented problems mentioned above (safety, scale-up, mass transfer rate, low solubility, high pressure) keep the academic chemist from performing organic reactions involving gases. There are however several ways to overcome these problems, *e.g.* flow chemistry,² making use of gas surrogates,³⁻⁵ with the possibility of performing the reaction in a two-chamber reactor.⁶⁻⁹

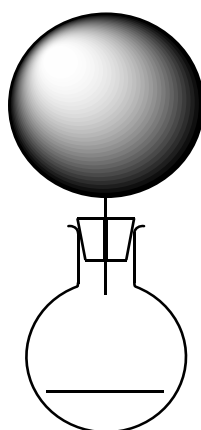
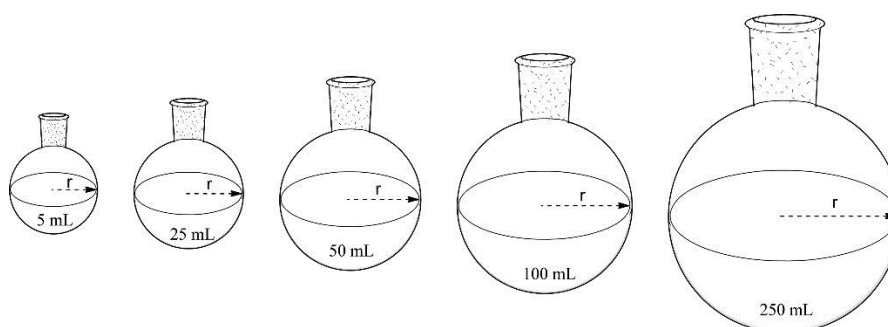


Figure 1: Schematic representation of a balloon setup.



Radius r (m)				
0.014	0.021	0.025	0.033	0.043
Interfacial area a (m^2m^{-3})				
107	71	60	46	35

Figure 2: Interfacial area decrease with increasing flask volume. Reprinted with permission from *Org. Process. Res. Dev.*, **2015**, 327-360. Copyright American Chemical Society.

1.1 Flow chemistry

1.2.1 General

Synthetic organic chemistry research and round bottom flasks go hand in hand. Since the early stages of this field, the basic way in which one conducts a chemical synthesis has remained fairly unchanged for over two centuries.¹⁰ Condensers, measuring cylinders, test tubes and round bottom flasks are still used on a daily basis by the synthetic chemist after being invented almost 200 years ago. The era of batch chemistry is undergoing a drastic change in the last two decades, as several other potent methods are gaining more attention among researchers, such as continuous flow techniques,¹¹ microwave chemistry¹² or ball milling.¹³

When a reaction is performed under batch conditions, reagents are added into a vessel, forming a reaction mixture left to react. Temperature, reaction time, concentration and stoichiometry are typical key parameters. When having a look at the processing steps one has to perform for a single chemical transformation, up to six manipulations can be required (Figure 3). These supplementary manipulations are expensive and labor intensive, and are necessary due to low reactivity, poor selectivity, incomplete conversion and/or formation of side products. This is often attributed due to bad mixing and temperature control combined with highly reactive reagents.¹¹ In addition, the physical dimensions of the devices used drastically limit the scale at which reactions can be carried out. The combination of the mentioned issues make change inevitable, and alternative approaches should be encouraged.

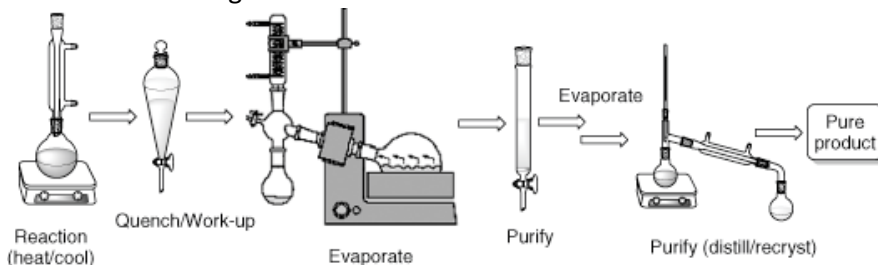


Figure 3: Sequence involving a chemical transformation in batch. Reprinted with permission from Baxendale IR, *J. Chem. Technol. Biotechnol.*, **2013**, 519-552. Copyright Wiley.

Such an alternative approach is flow chemistry. Flow chemistry is in its most basic sense defined as performing a chemical transformation in a continuous manner by pumping the reagents through a tube or pipe. Examples of flow syntheses at industrial scale are known for almost a century.¹⁴ The

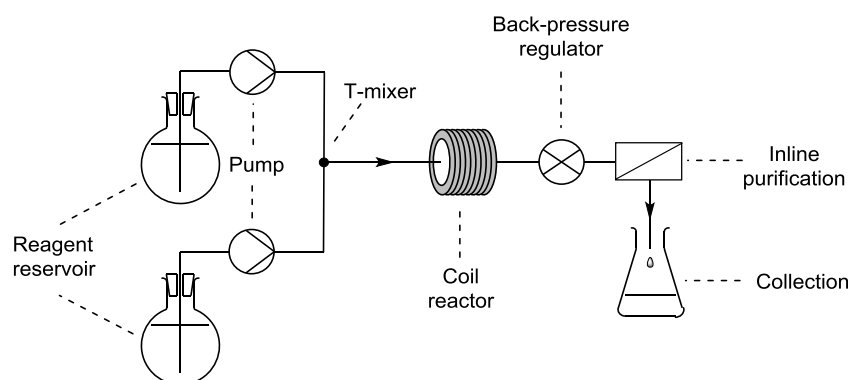
application of flow techniques in an academic research environment is more recent. In the last two decades an increasing interest in flow based synthesis methods is observed, with commercial lab scale flow platforms (*e.g.* Syrris,¹⁵ Chemtrix,¹⁶ VapourTec,¹⁷ Uniqsis,¹⁸ ThalesNano¹⁹ and many more) being considered the main driver of this phenomenon. A distinction is made between modular systems, where the setup is custom built from loose parts, and monolithic systems, where all components are integrated into a single device. In between, one has semi-modular systems, where a device can be edited in various ways by adding/removing functional modules. Due to the versatility of the semi-modular systems (such as the VapourTec R- and E-series), these are becoming more popular, albeit at a higher price than their monolithic counterparts. More recently, researchers at MIT developed a refrigerator-sized flow system with incredible versatility (Figure 4).²⁰ This state-of-the-art flow platform is able to synthesize pharmaceuticals starting from commercially available starting materials, over multiple synthesis steps, performing purification, solvent switches, crystallization and formulation inline. The synthesized pharmaceuticals meet the U.S. Pharmacopeia standards.



Figure 4: (A) Upstream synthesis modules. (B) Downstream purification and formulation modules. (C) Close-up of PFA tube reactor and membrane separation unit. (D) Detailed images of downstream modules. Reprinted with permission from Science, **2016**, 61-67. Copyright AAAS.

A schematic representation of a basic flow setup is depicted in Scheme 1. Reagent reservoirs contain the reagents (and often solvents) that are needed. From here, the use of pumps (from normal HPLC pumps to peristaltic ones) brings the reagent streams together in the T-mixer piece, where mixing occurs. The mixture is pumped through the reactor, where the actual reaction occurs. A plethora of energy input means can be used, going from (extreme) temperature,²¹⁻²² microwave irradiation,²³⁻²⁴ UV and visible light,²⁵⁻²⁷ and sonication.²⁸ Besides a coil reactor, reactor chips (for microflow and lab-on-a-chip applications)²⁹ and packed bed reactors (for heterogeneous

catalysts and scavengers)³⁰⁻³¹ are common alternatives. The *residence* time is defined as reactor volume divided by the total flow rate. Some exceptions to this are for example when using a packed bed reactor (PBR) filled with heterogeneous catalyst. In here, the reactor volume will be overestimated since one needs to subtract the total volume of the catalyst present in the PBR. Residence time is equivalent to reaction time in batch conditions, and can be seen as the time every fraction of reaction mixture spends in the reactor. A back-pressure regulator (BPR) is installed after the reactor, which could serve multiple purposes, such as bringing solvents above their boiling point or pushing multiphasic flows to homogeneity, without significantly increasing the risk of explosions. In a final stage, the reaction mixture can be subjected to some form of inline purification, such as scavenging (trapping side products),³⁰ liquid-liquid extraction,³² catch-and-release,³³ etc. The stream is then collected in a recipient, where quenching or precipitation of the product often already occurs.

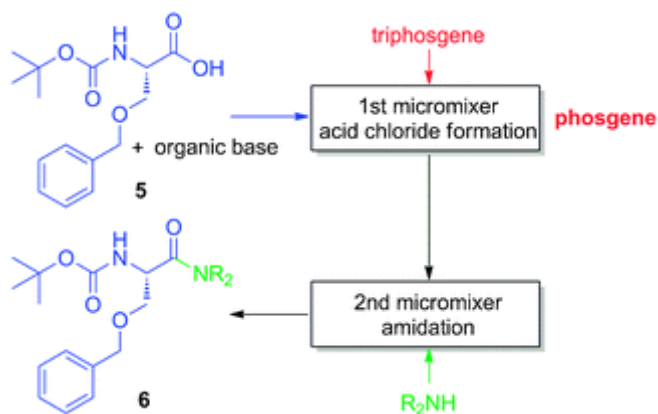


Scheme 1: Schematic flow setup.

Some advantages of continuous flow technology include the following:

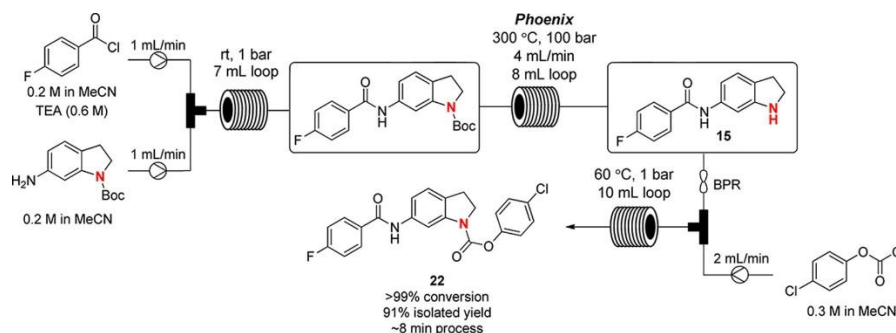
- Scalability:** When compared to batch chemistry, the continuous nature of flow technology in combination with the far superior control of reaction parameters drastically enhances scale up.³⁴ While multiple strategies exist for readily scaling up flow processes, like leaving the setup run for a longer time (*scaling out*), or running the reaction in parallel via multiple setups (*numbering up*),³⁵ the scale up of the reactor itself is more difficult. This requires careful scaling of relevant parameters and additional calculations.

- Safety:** Continuous flow processes are in most cases safer than their batch counterparts. In a synthesis where a toxic/dangerous intermediate is formed, the actual amount of intermediate in a flow setup will be very low, compared to performing this in batch. As a result, the risk is significantly reduced. In analogy, when working under pressure in a flow setup, the risk of an actual explosion is very low. As a result, flow chemistry provides solace to revive the academic use of useful reagents such as diazomethane³⁶ or phosgene³⁷ (Scheme 2).



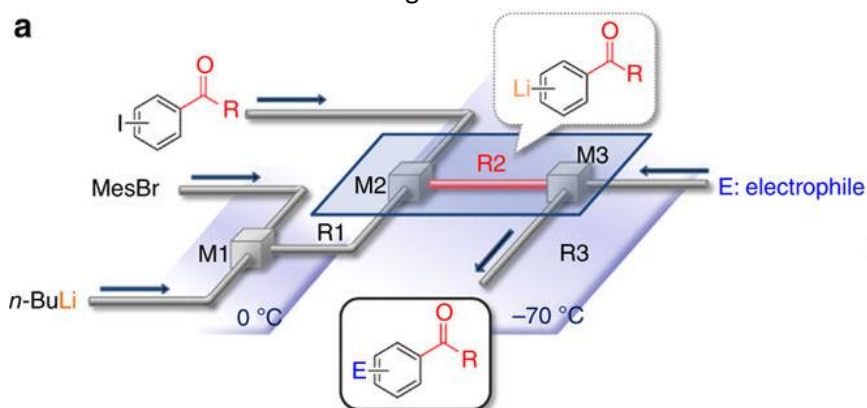
Scheme 2: Continuous flow system of the amidation of N-Boc-Phe using phosgene in situ. Reprinted with permission from Chem. Commun., **2011**, 12661-12663. Copyright Royal Society of Chemistry.

- Extreme conditions:** Flow setups are able to reach temperatures and pressures which are completely impossible to obtain in batch chemistry, in an academic environment.³⁸ Several examples are reported in literature.³⁹⁻⁴⁰ Industry picked up on this, since ThalesNano brought the Phoenix Flow Reactor® on the market, a flow platform for high temperature and pressure reactions (up to 450 °C and 200 bar).⁴¹ An example is depicted in Scheme 3.⁴² The Boc deprotection step occurs at 300 °C and 100 bar, with a residence time of 2 minutes.



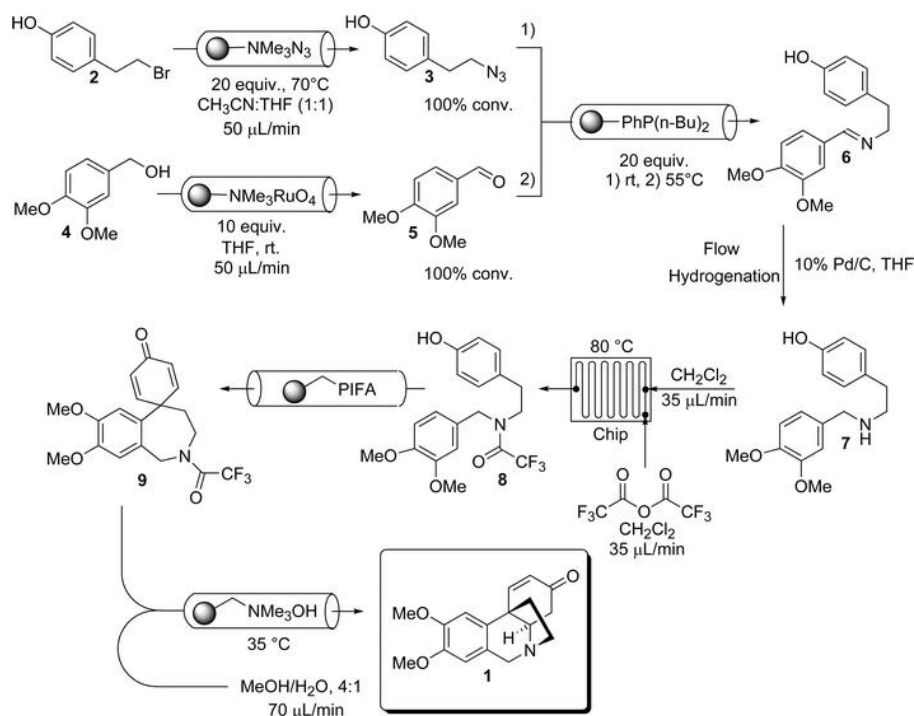
Scheme 3: Flow setup of reference 42. In the second reactor, a high temperature Boc-deprotection takes place. Reprinted with permission from *Organic Letters*, **2016**, 1732-1735. Copyright American Chemical Society.

- Flash chemistry:** In a nutshell, flash chemistry is chemistry performed in flow which simply cannot be done in batch.⁴³ These are usually extremely fast reactions involving very unstable species on time scales less than a second, which are not achievable in batch. An example is a protecting-group-free synthesis, an emerging field in flash chemistry (Scheme 4).⁴⁴ An aryllithium species is formed in reactor R2, which in turn can react with a variety of electrophiles in reactor R3. Since the aryllithium species bears a ketone group, this intermediate is extremely reactive. The researchers found that the residence time of R2 needed to be 0.003 seconds or less, in order to prevent side reactions such as dimerization. As one can imagine, this is of course not possible in batch. Flash chemistry stresses the extreme control of parameters in flow chemistry, which is considered a main advantage.



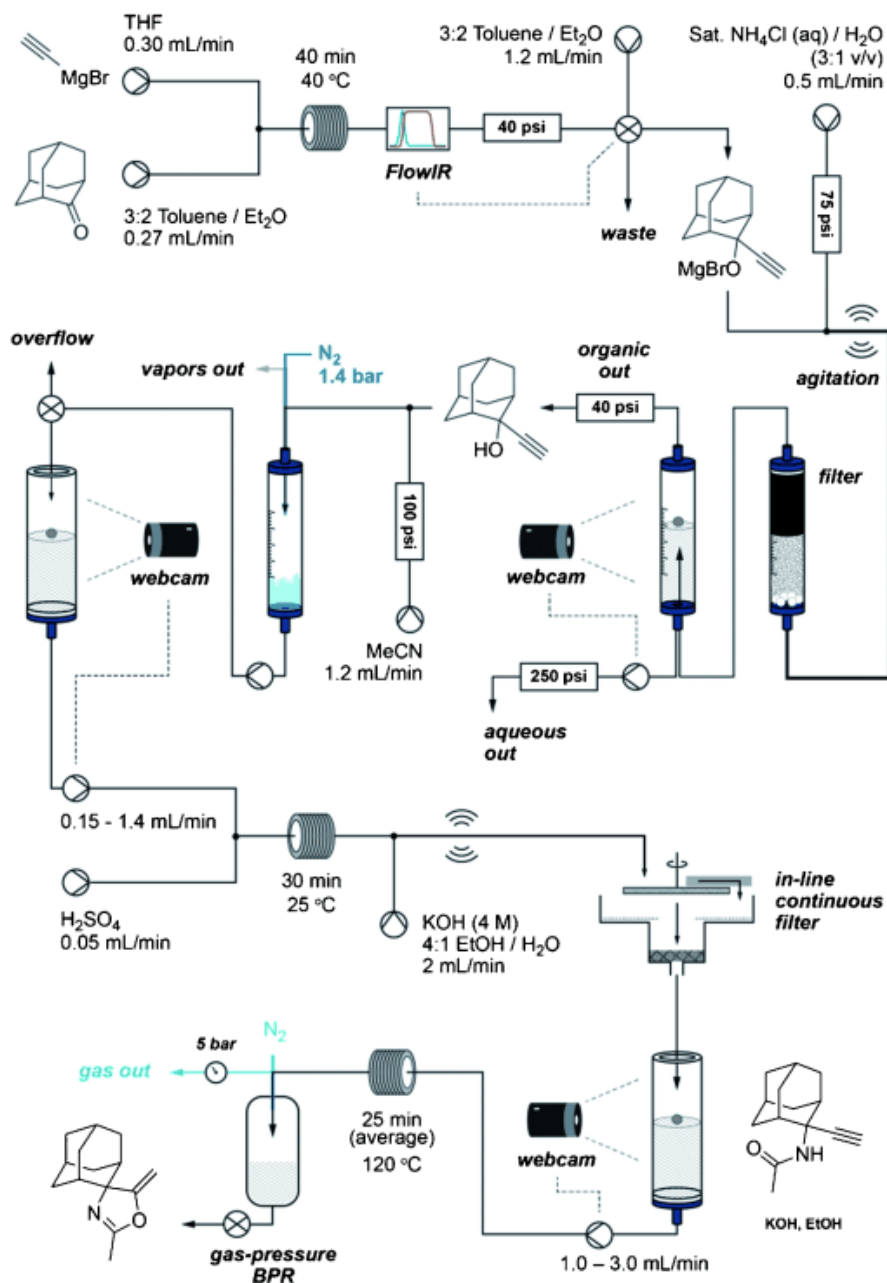
Scheme 4: Flow setup of a flash chemistry example. Reprinted with permission from *Nat. Commun.*, **2011**, 264. Copyright Nature Publishing Group.

- Telescoping:** In modern flow chemistry, telescoping (or cascade or multi-step synthesis) is considered a hot topic, since it demonstrates the versatility and capability of flow chemistry. Telescoping can be used for pharmaceutical²⁰ and natural product synthesis, where it is often combined with several types of inline purification. An example by the Ley group is depicted below (Scheme 5).⁴⁵ In this report, oxomaritidine, an alkaloid natural product, is prepared in a 7 step synthesis linked into one single continuous flow sequence. The researchers started from commercially available building blocks and most of the reagents are polymer supported in packed bed reactors (PBRs), easing purification of the final product. After evaporation, the product was isolated in a purity of >90%. The overall yield of this 7 step synthesis is 40%. The authors were curious what happened to the rest of the starting materials. It was found that the phenolic oxidation gave only a 50% yield. The remaining phenol was unexpectedly scavenged out of solution by the polymer supported base.



Scheme 5: Flow synthesis of (±)-oxomaritidine. Reprinted with permission from Chem. Commun., **2006**, 2566-2568. Copyright Royal Society of Chemistry.

- **Automation:** In recent years, automation is gaining more attention in flow technologies, with software and camera controlled state-of-the-art protocols being reported by well-known academics in the field, such as Steven Ley and Klavs Jensen. A fully automated, self-controlling, telescoped seven-step synthesis is reported by Ingham *et al.* and is partially depicted below (Scheme 6).⁴⁶ This process incorporates Grignard, Ritter and cyclization reactions and extraction, solvent-switching, filtration and quenching are all performed inline. Cameras carefully observed reservoir levels upon which feedback was given to the control system, which monitored all parameters. The control system was designed with algorithms to handle minor deviations from steady state behavior without human interference. In turn, this was remotely monitored by a single researcher on his cell phone. After 7 steps, the product was collected and purified offline, providing an output of 8 mmol per hour.



Scheme 6: The fully telescoped flow process, which was controlled by one system and managed by a single researcher. Reprinted with permission from *Angew. Chem. Int. Ed.*, 2015, 2-18. Copyright Wiley.

As a concluding remark we can definitely state that flow chemistry has earned an important spot in synthetic organic chemistry research, but it has,

of course, drawbacks as well. Very slow reactions for example are usually difficult to perform in flow because they would need an excessive residence time in the reactor. Another key problem is that every time when a new stream is introduced, the mixture gets more and more diluted. However, this problem can be overcome by inline evaporation and inline solvent switching. It is also believed that other non-scientific factors hamper complete adoption of flow techniques: flow platform systems are expensive, and when compared to batch processes, more chemical engineering aspects are involved (flow rate, retention time, *etc.*).

1.2.2 Gas reactions in flow

1.2.2.1 General

As stated earlier, gas-liquid reactions require an efficient mass transfer rate which can be achieved by a high interfacial area.² The latter is usually below $100 \text{ m}^2 \text{ m}^{-3}$ in conventional flasks, and can be up to $18000 \text{ m}^2 \text{ m}^{-3}$ in a microchannel flow reactor.⁴⁷ In general, flow is a better platform for gas reactions, as the higher pressure capability in flow systems enhances dissolution and allows a more controlled gas volume delivery. Under increased pressure all gas can dissolve and a homogeneous gas-liquid reaction takes place. This is often not the case, and the most common biphasic flow regime is known as segmented flow (Figure 5). However, the toroidal currents deliver excellent mixing and enhance mass transfer.⁴⁸

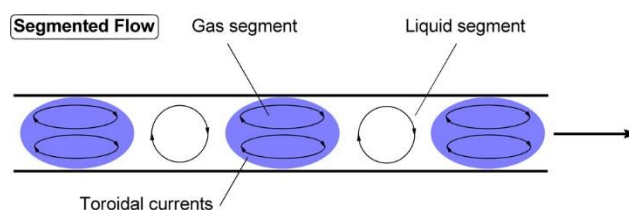


Figure 5: Segmented gas-liquid flow. Reprinted with permission from *Org. Process Res. Dev.*, **2015**, 327-360. Copyright American Chemical Society.

The area of flow-based gas-liquid reactions has become an increasingly popular field. Reports with carbon monoxide, ozone, hydrogen, carbon dioxide, oxygen, ammonia, dimethyl amine, ethylene, diazomethane, *etc.* have been published in the last decade.^{36-37, 49} In this thesis we will make use of gas-liquid reactions in flow, with using carbon monoxide.

1.2.2.2 Tube-in-Tube reactors

Another approach for delivering gas to a reaction makes use of a gas-permeable membrane that serves as a barrier. This is usually called a tube-in-tube reactor and is made up of a Teflon AF-2400 membrane, which has high permeability for gases but not liquids. This was reported by the group of Steven Ley.⁴⁹⁻⁵⁰ VapourTec® picked up on this and now sells tube-in-tube reactors for their E- and R-series.⁵¹ A tube-in-tube design is depicted in Figure 6.

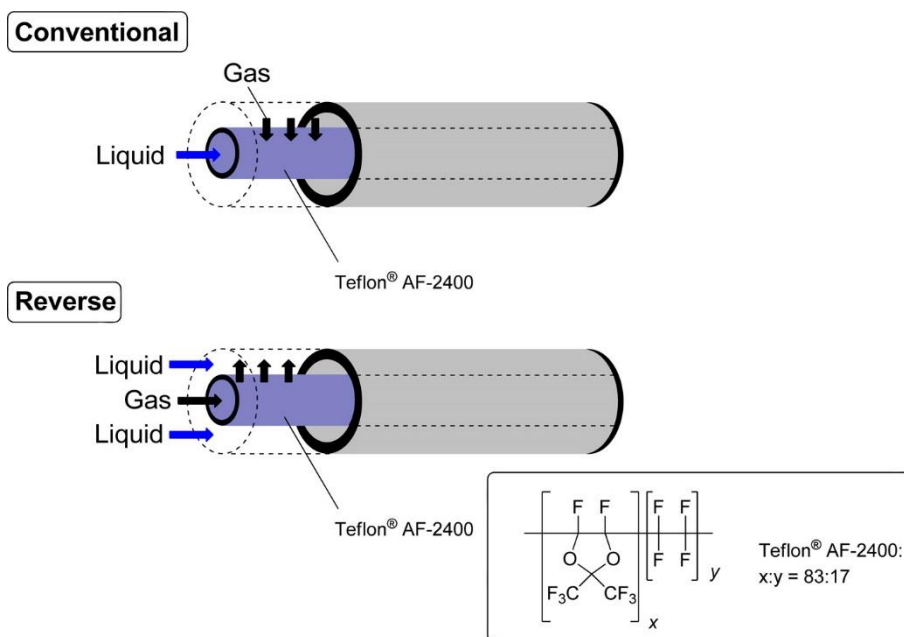
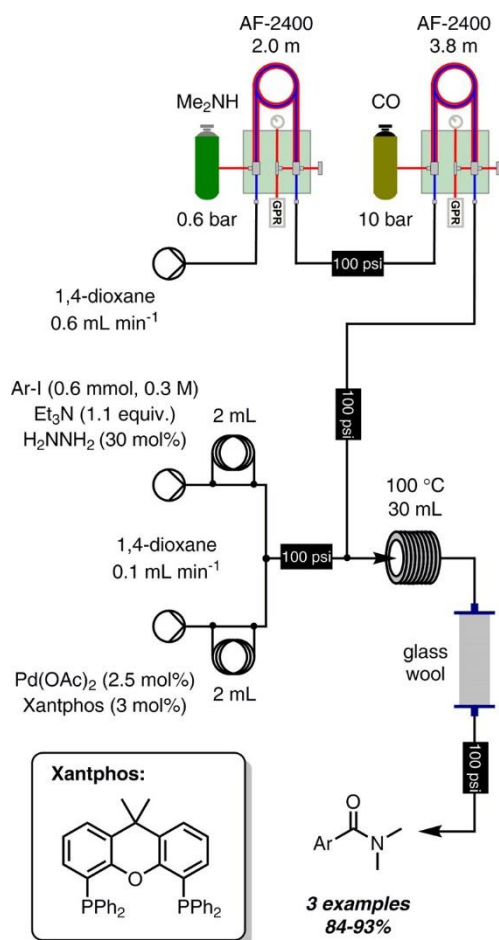


Figure 6: Conventional vs. reverse tube-in-tube design. Reprinted with permission from *Org. Process Res. Dev.*, **2015**, 327-360. Copyright American Chemical Society.

A novel example is depicted in Scheme 7, again reported by the Ley group.⁵² Herein, the authors made use of two tube-in-tube reactors to enrich a stream of dioxane with carbon monoxide and dimethyl amine for a palladium-catalyzed aminocarbonylation. A BPR before and after the second tube-in-tube reactor was necessary to keep the carbon monoxide in solution, hereby avoiding segmented flow. Various aryl iodides were transformed into their respective *N,N*-dimethylamides, which were isolated in high yields. The authors obtained better results when using hydrazine to efficiently reduce Pd^{II} species to Pd^0 .



Scheme 7: Aminocarbonylation of aryl iodides using two different gases. Reprinted with permission from *Eur. J. Org. Chem.*, **2014**, 6418-6430. Copyright Wiley.

1.2 Gas surrogates

As demonstrated earlier, working with gases in synthetic organic chemistry can be quite problematic, at least on lab scale. While researchers continue to report on low-pressure transformations,⁵³ other potential problems of certain gases such as toxicity, smell, flammability and storage of the gas are not fully addressed by means of working at lower pressure. A controlled generation and consumption of a gas in a closed setup overcomes these issues greatly. It is here that gas surrogates (also called gas precursors) can provide solace and these gas-releasing moieties have become popular when working at lab scale. In the case of very toxic gases, such as carbon monoxide (CO), sulfur dioxide (SO₂), hydrogen cyanide (HCN) and fluorine (F₂), the storage of pressured vessels on its own already brings serious safety risks and is often not very suited for an academic lab setting (extra costs, specialized fume hoods, requirement of trained personnel, *etc.*). Examples of gas surrogates include DABSO for sulfur dioxide⁵⁴, SelectFluor for fluorine⁵⁵⁻⁵⁶ (SelectFluor is not a precursor of the actual gas, but it is an electrophilic F-source, and is therefore a substitute of using fluorine gas) and potassium hexacyanoferrate, a non-toxic precursor for hydrogen cyanide,⁵⁷ to name a few (Figure 7).

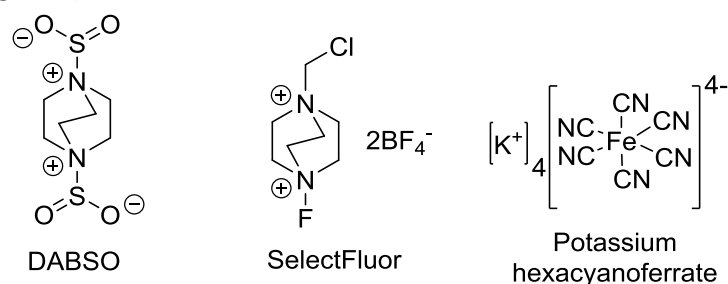


Figure 7: DABSO, a gas surrogate for SO₂, SelectFluor, a gas surrogate for F₂ (i.e. electrophilic fluorine source) and potassium hexacyanoferrate as a gas surrogate for HCN.

The search of gas surrogates is the most extensively studied for carbon monoxide.³ This is of course due to the notorious toxicity of carbon monoxide, in combination with being odorless and colorless, making it completely undetectable by human senses. It is therefore that this gas is considered extremely dangerous and is also called ‘the silent killer’. Examples of CO surrogates include metal carbonyl complexes,⁵⁸ formamides,⁵⁹ *N*-formyl saccharin,⁶⁰⁻⁶¹ aryl formates,⁶²⁻⁶³ aldehydes,⁶⁴⁻⁶⁵ chloroform⁶⁶ and formic acid.⁶⁷⁻⁶⁸ These precursors are usually used in palladium-catalyzed carbonylation, reported by Heck and coworkers in the seventies (Figure 8).⁶⁹

This chemistry gives rise to numerous carboxylic acid derivatives such as amides and esters. Other examples include carbonylative Suzuki,⁷⁰ carbonylative Sonogashira,⁷¹ etc. Some of these reported CO surrogates are very toxic themselves, expensive and/or generate byproducts. These byproducts can be unreactive spectator compounds, therefore complicating work-up and purification, or participate in the reaction. In both cases the application window of these substances is narrowed (due to functional group tolerance). These problems are all arising when using these CO precursors *in situ*. There is however the possibility of generating the gas *ex situ*, overcoming the aforementioned issues. This is possible via tube-in-tube reactors in continuous flow,⁷² as stated above, or by the use of two-chamber reactors when working under batch conditions (see below).

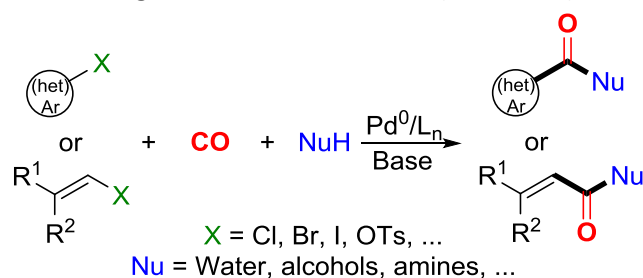


Figure 8: Palladium-catalyzed carbonylation.

1.3 Two-chamber reactors

Some examples of DIY reactors where two reaction tubes are connected with each other are reported in literature,^{66,73-75} often specifically designed for the migration of a moiety (often a gas) from one chamber to the other. In 2010, Troels Skrydstrup and coworkers from Aarhus University in Denmark revolutionized this field. They initiated a research program in palladium-catalyzed carbonylation⁹ and were also hesitant of using pressured carbon monoxide vessels and gas filled balloons. The development of COware, a patented two-chamber system,⁸ for the *ex situ* generation of CO was a consequence of this, overcoming numerous safety issues (Figure 9).

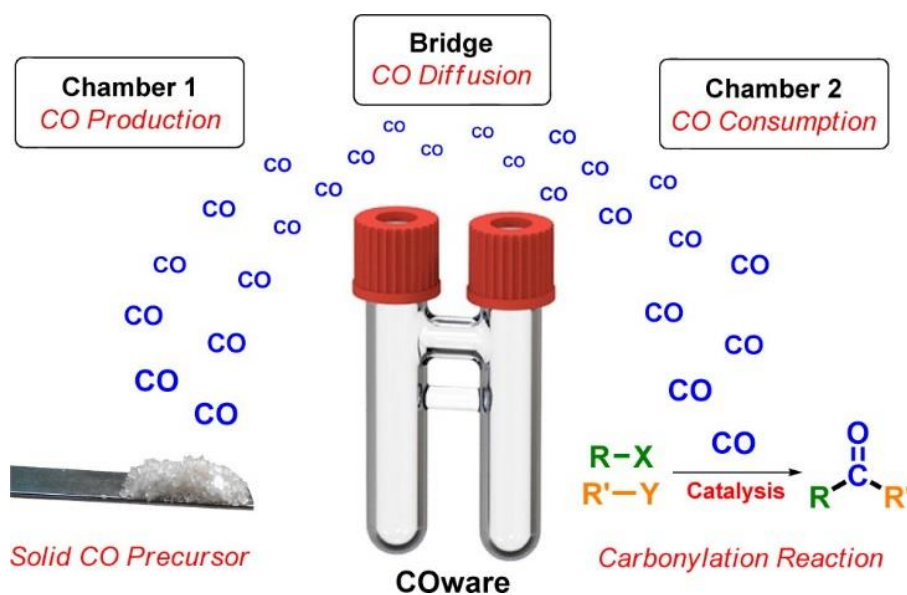
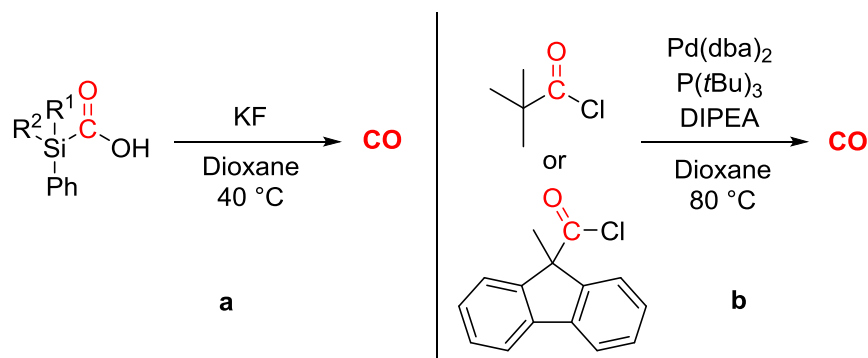


Figure 9: COware, the patented two-chamber system of the Skrydstrup group. CO production from a solid precursor in the left chamber, which migrates through the bridge to undergo a CO consuming reaction in the right chamber. Reprinted with permission from Acc. Chem. Res., 2016, 594-605. Copyright American Chemical Society.

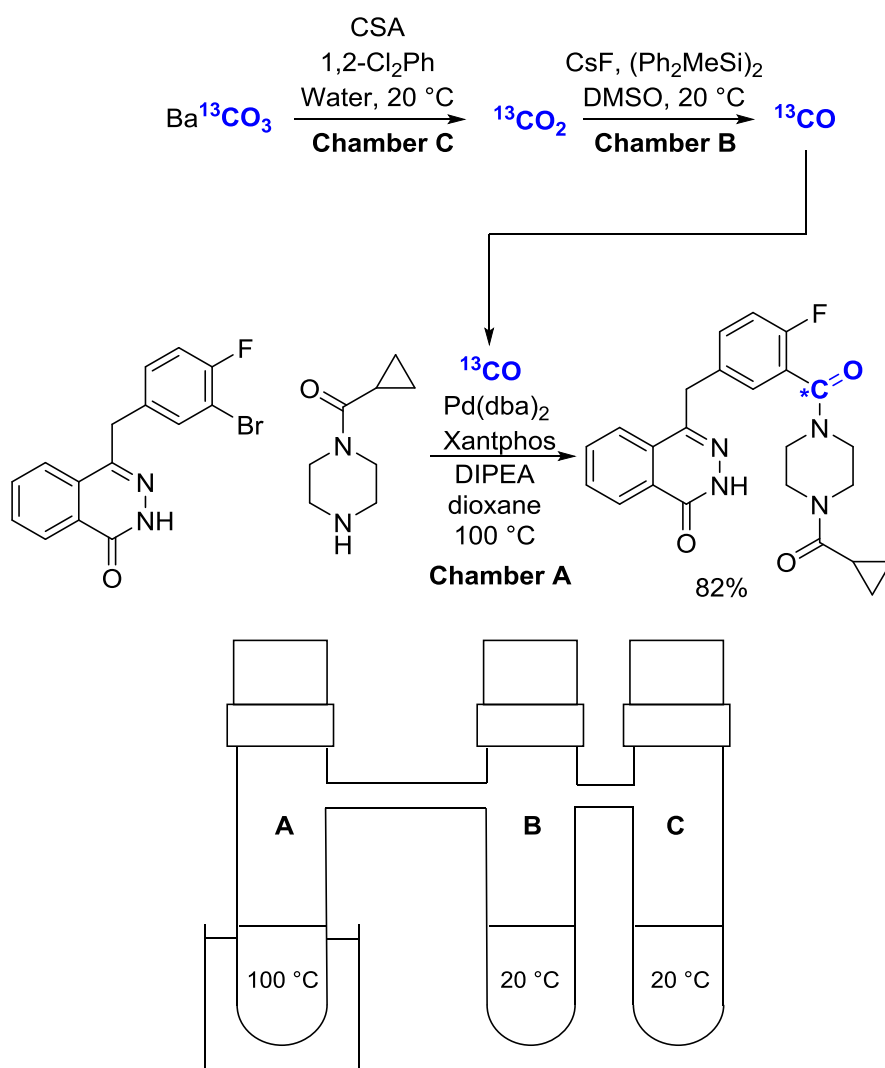
The group simultaneously reported solid CO surrogates, such as silacarboxylic acids⁶ and bulky acyl chlorides.⁷ Their use is depicted in Scheme 8. In the case of silacarboxylic acids, CO is released under the influence of potassium fluoride at 40 °C. On the other hand, bulky acyl chlorides generate CO under palladium catalysis. The bulkiness of both the ligand and the acyl chloride promotes reductive elimination of the palladium complex, by decarbonylation and β -hydride elimination.⁷ With both types of CO surrogates, a COware two-chamber setup was used. The generated near-

stoichiometric carbon monoxide was consumed in the other chamber by means of palladium-catalyzed carbonylation.



Scheme 8: CO precursors reported by the Skrydstrup group. (a) Silicarboxylic acids. (b) Bulky acyl chlorides.

Skrydstrup and coworkers later reported the use of a three chamber reactor (Scheme 9).⁷⁶ In chamber C, carbon-13 enriched barium carbonate was decomposed by acid, releasing $^{13}\text{CO}_2$. This carbon dioxide was subsequently captured in chamber B by a disilane in the presence of cesium fluoride. Carbon-13 enriched CO was thereby generated, which was then consumed in chamber A in a palladium-catalyzed carbonylation. This novel report demonstrates the capability of multi-chamber reactors for the migration of multiple gases at the same time, with the possibility to synthesize ^{13}C -labeled pharmaceuticals directly from commercially available carbon-13 enriched barium carbonate.

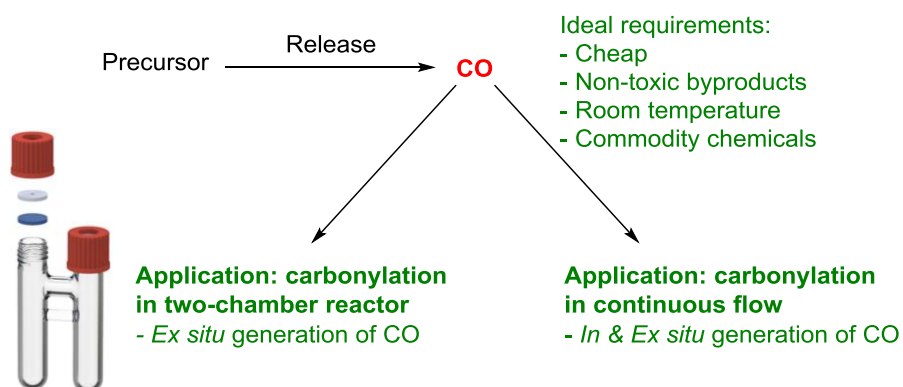


Scheme 9: Application of a three-chamber reactor. CO_2 is generated in chamber C and subsequently consumed in chamber B. Hereby, CO is generated and is consumed in an aminocarbonylation in chamber A.

1.4 Objectives

In what preceded, we have seen that the enhancement of working with (dangerous) gases in an academic setting is a widely studied topic. Gas surrogates often provide solace, and techniques such as two-chamber technology or continuous flow processes are convenient tools for the application of these surrogates. It is our intention to contribute to this field, making organic reactions involving gases more approachable for the academic chemist by developing novel and safe ways for their utilization.

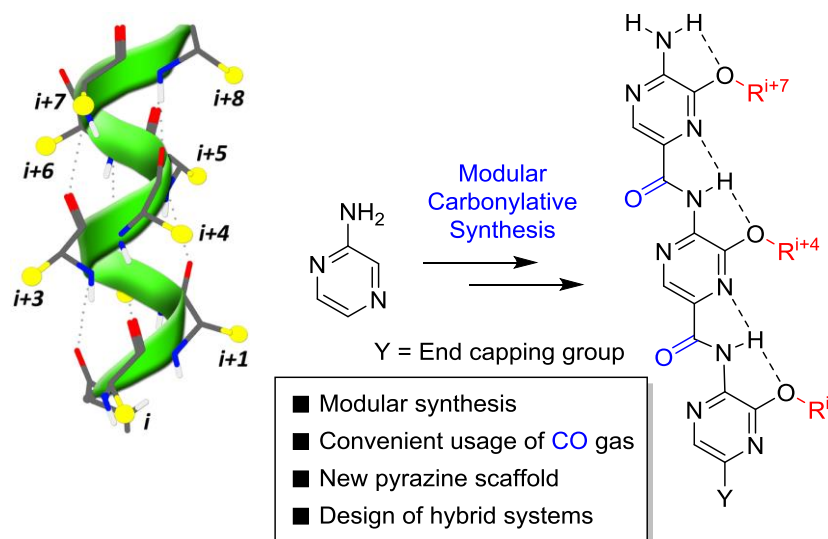
Chapter 2 will focus on the discovery of a new carbon monoxide precursor. Currently, numerous CO precursors have been reported as a substitute for carbon monoxide on a laboratory scale. However, most of these CO surrogates are very toxic themselves, need elevated temperatures to release CO, are expensive and/or are specialty chemicals requiring multiple synthesis steps before use. It is our goal to contribute to this field by developing another CO precursor which preferably is cheaper, more efficient, safer and convenient in use. In addition, the CO precursor will be applied for palladium-catalyzed carbonylation, which will be optimized. Some syntheses of medicinally relevant compounds will be added as well as isotopic ^{13}C -labelling. Both two-chamber reactors and continuous flow will be used as tools for this precursor (Scheme 10).



Scheme 10: Strategy for the design of a new carbon monoxide precursor.

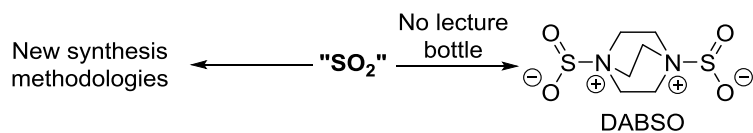
Chapter 3 will cover the synthesis of unreported pyrazine based oligoamide α -helix peptidomimetics. The bridging amide linkers will be synthesized via palladium-catalyzed carbonylation, using the developed technology of

chapter 2. This will serve as an alternative strategy for the assembly of monomers, where usually amide coupling reagents are used. The use of catalytic carbonylation chemistry as a coupling method is advantageous since (1) no stoichiometric amounts of coupling reagents are used, (2) it offers a broad functional group tolerance and (3) it is able to handle substrates which are very low in nucleophilicity, such as aminopyrazines.⁷⁷ Moreover, this methodology should allow the synthesis of hybrid systems (Scheme 11).



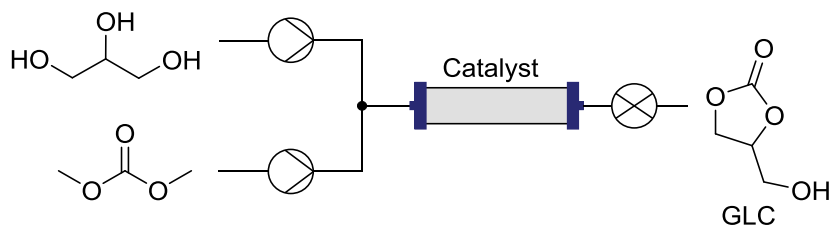
Scheme 11: Strategy for the design of pyrazine based oligoamide α -helix peptidomimetics.

In **chapter 4**, the switch was made to sulfur dioxide gas, which is in many aspects similar to carbon monoxide (interesting synthetic properties but very toxic). Sulfur dioxide is a ubiquitous commodity chemical which has several chemical applications in industrial processes, but is not researched thoroughly in academia. However, considering the importance of functional groups such as sulfones and sulfonamides in agrochemicals, pharmaceuticals and materials, there is a high interest in new and enhanced synthesis methods. It is here that we aim to contribute to new technologies using sulfur dioxide as a reactant for the synthesis of SO_2 -containing functional groups. Moreover, an attempt will be made to enhance the safety aspects of the synthesis of popular SO_2 surrogates, such as DABSO. Key in this approach is the aim to step away from sulfur dioxide pressurized gas vessels, which imply serious safety concerns (Scheme 12).



Scheme 12: Objectives for working with sulfur dioxide.

Finally, in **chapter 5** we will aim to develop a continuous flow process starting from glycerol to synthesize glycerol carbonate (GLC) and/or glycidol in a scalable, green manner. It will be attempted to optimize a protocol which has industrial applicability. Therefore, dimethyl carbonate (DMC), due to its considered greenness, was the phosgene surrogate of choice and glycerol the other reagent, due to being an industrial waste product in biodiesel synthesis. In this way, DMC can be seen as a substitute for carbon monoxide (CO use is discussed in **chapter 2 & chapter 3**). Different catalysts will be screened, keeping in mind that industry prefers easy to separate, cheap and non-toxic ones. Both reported catalysts as new catalysts will be tested (Scheme 13).



Scheme 13: Development of a continuous flow protocol for the synthesis of glycerol carbonate (GLC).

CHAPTER 2

IN SEARCH OF A NEW CO PRECURSOR

2. In search of a new CO precursor

2.1 Literature and discovery

As already stated in **chapter 1.2**, the search for and application of new gas surrogates is well documented for the case of synthetically useful carbon monoxide (CO), due to it being odorless, colorless, extremely toxic and flammable.³ Globally, carbon monoxide might be responsible for more than half of lethal poisonings.⁷⁸ In mammals, it binds to hemoglobin, thereby inhibiting oxygen transfer *in vivo*. The binding affinity of carbon monoxide for hemoglobin is about 200 times stronger than that of oxygen.⁷⁹ The lack of oxygen transfer quickly results in permanent damage or even death. Symptoms of carbon monoxide exposure can be found in Table 1. The main natural sources of CO are volcanoes, fires and photochemical reactions in the troposphere.⁸⁰

Table 1: Symptoms of carbon monoxide exposure. Readopted from reference 78.

Concentration (ppm)	Symptoms
35	Headache and dizziness within 6 to 8 hours of constant exposure
100	Slight headache in 2 to 3 hours
200	Slight headache within 2 to 3 hours, loss of judgement
400	Frontal headache within 1 to 2 hours
800	Dizziness, nausea and convulsions within 45 minutes. Insensible within 2 hours
1600	Headache, tachycardia, dizziness and nausea within 20 minutes, death in less than 2 hours
3200	Headache, dizziness and nausea in 5 to 10 minutes, death in less than 30 minutes
6400	Headache and dizziness in 1 to 2 minutes. Death within 20 minutes
12800	Death within 3 minutes

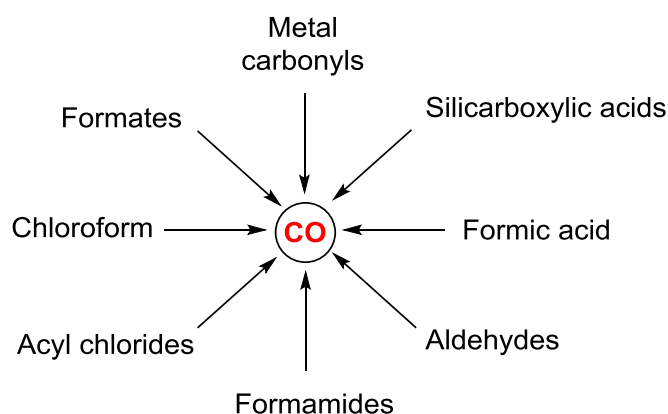
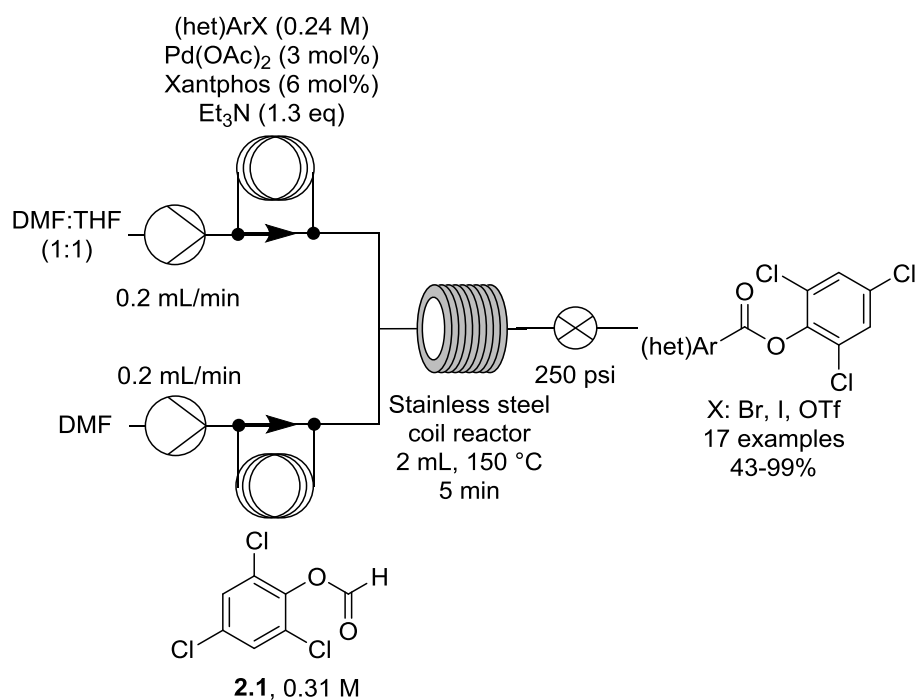


Figure 10: Examples of reported CO surrogates.

Currently, numerous CO precursors have been reported as a substitute for carbon monoxide on a laboratory scale (Figure 10). However, most of these CO surrogates are very toxic themselves, need elevated temperatures to release CO, are expensive and/or are specialty chemicals requiring multiple synthesis steps before use.

It is our goal to contribute to this field by developing a CO precursor which is cheaper, more efficient, safer and convenient in use. In addition, the CO precursor will be applied to palladium-catalyzed carbonylation, which will be optimized. Some syntheses of medically relevant compounds will be added as well as isotopic ^{13}C -labelling.

Earlier work in our group demonstrated the use of 2,4,6-trichlorophenyl formate (**2.1**) as a useful CO surrogate in flow (Scheme 14).⁸¹ The byproduct of the CO generation, 2,4,6-trichlorophenolate, acted as nucleophile in the carbonylation, forming an active ester in the process. If one wants to avoid this, an *ex situ* CO generation would provide solace (two-chamber reactor or tube-in-tube flow reactor). Later experiments however showed that 2,4,6-trichlorophenyl formate is not fully stable in solution since CO formation (bubbles) was sometimes observed when preparing stock solutions in DMF, making it unpredictable to handle. Also the trichlorophenol released during the reaction is a potentially harmful byproduct.



Scheme 14: Flow setup of earlier work from our group with 2,4,6-trichlorophenyl formate as CO precursor.

While 2,4,6-trichlorophenyl formate (**2.1**) was used previously as CO precursor both by others and ourselves, the fact that it was not stable in solution was not ideal. Indeed, it is important to strike a balance: a gas surrogate should be intrinsically stable and only decompose in a predictable manner under well-defined conditions. Hence, at this point, it was our intention to look for alternatives. Several potential CO surrogates were hypothesized where formic acid was equipped with a leaving group (Figure 11). For **2.2**, a standard formylation protocol should be suited to synthesize the respective compound, while for **2.3** and **2.4** it was hypothesized that these could be synthesized from cheap and readily available tosyl chloride or cyanuric chloride, respectively, and formic acid under basic conditions. Pentafluorophenyl formate (**2.2**) was synthesized and isolated, but unfortunately, as could be expected fully degraded in a couple of days. Moreover, pentafluorophenol is fairly expensive and toxic, making it not ideal as a CO precursor building block. A mixture of cyanuric chloride and formic acid in the presence of base did not result in **2.3**, no conversion was observed. A final idea was attempted with the synthesis of a mixed anhydride type system **2.4** (Scheme 15). Equimolar amounts of formic acid and tosyl

chloride were dissolved in THF. After this, 2 eq of triethylamine were added, and instant vigorous bubble formation was observed and confirmed to be CO gas by the alarm of the carbon monoxide detector. It was hypothesized that formic acid reacts with tosyl chloride once it is deprotonated, thereby forming a highly unstable intermediate (**2.4**), which upon deprotonation immediately leads to carbon monoxide formation since sulfonates are excellent leaving groups. Note that the generated byproducts are fairly innocent organic salts (ammonium chlorides and sulfonates), in contrast with other CO precursors generating toxic byproducts.

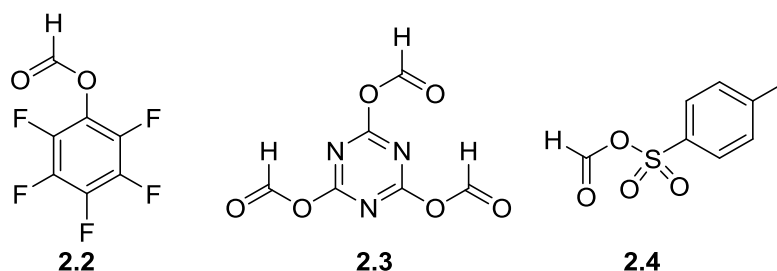
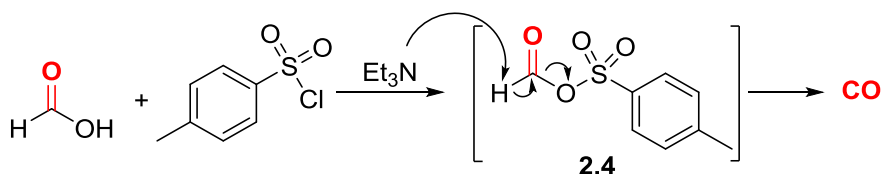


Figure 11: Potential new CO precursors.



Scheme 15: Discovery of a new CO precursor

Being interested in the versatility of this reaction, as well as the solubility of the side products (an important factor for flow experiments), other reagents and solvents were tested. These revealed that this unreported CO precursor system is quite versatile: the sulfonyl chloride, the base and the solvent could all be varied, still resulting in CO liberation (Table 2). As it appears, decomposition occurs at 0 °C, room temperature and 60 °C. With these results in hand, palladium-catalyzed carbonylation was chosen as test case for this CO precursor system.

Table 2: Variation of parameters of new CO surrogate system. Equimolar amounts of sulfonyl chloride and formic acid were dissolved in the solvents and subsequently 2 equivalents of base were added.

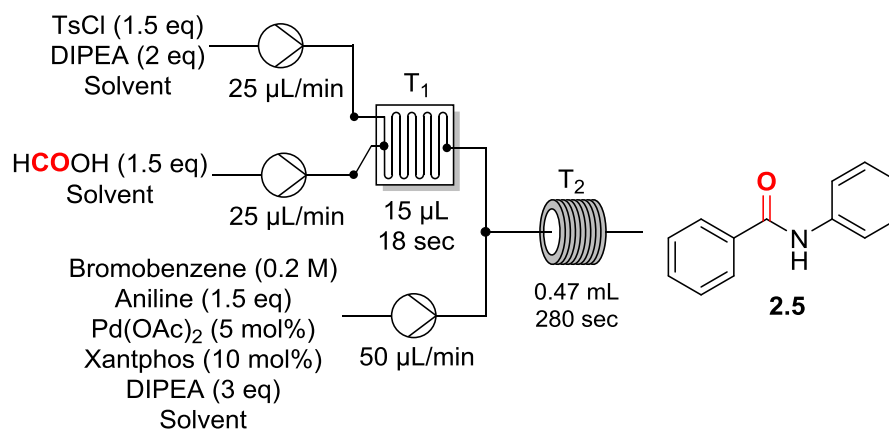
Entry	Sulfonyl chloride	Base	Solvent	CO?
a	TsCl	Et ₃ N	THF	Yes
b	TsCl	Et ₃ N	DMF	Yes
c	TsCl	DIPEA	Dioxane	Yes
d	TsCl	DIPEA	ACN	Yes
e	TsCl	DIPEA	Toluene	Yes
f	TsCl	DIPEA	THF	Yes
g	TsCl	Et ₃ N	Toluene	Yes
h	MsCl	Et ₃ N	Toluene	Yes
i	MsCl	Et ₃ N	THF	Yes
j	MsCl	Et ₃ N	DMF	Yes
k	MsCl	Et ₃ N	Dioxane	Yes
l	NsCl	Et ₃ N	THF	Yes

2.2 New CO precursor: applied in palladium-catalyzed carbonylation

2.2.1 Flow approach

The first approach to apply our CO precursor system was in a continuous flow setup. In theory, one has the choice to generate CO *in situ* via traditional flow reactors, or *ex situ*, via a tube-in-tube flow reactor. Both approaches will be explored. The combination of tosyl chloride as sulfonyl source and DIPEA as base delivered the most soluble organic salts. Therefore, these were the reagents of choice for following flow experiments.

The *in situ* approach was first explored. The setup is depicted in Scheme 16. A solution of tosyl chloride and DIPEA was mixed with a formic acid solution in a glass microchip. This reagent stream was subsequently mixed with the catalytic system and substrated in a PTFE coil reactor. Note that no back pressure regulator was used. The reaction temperatures and solvents were varied, and the results are summarized in Table 3.



Scheme 16: Flow setup of *in situ* CO generation and subsequent carbonylation.

Table 3: Results of in situ CO generation and subsequent carbonylation (Scheme 16). Variation of reaction temperatures and used solvents.

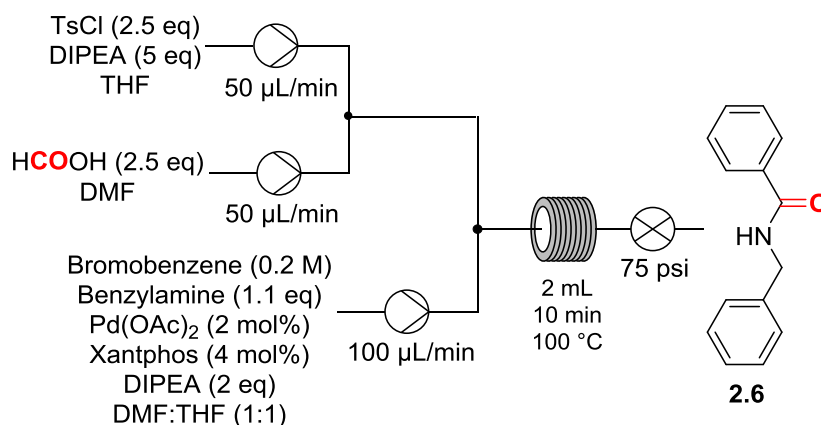
Run	Solvent	T ₁ (°C)	T ₂ (°C)	GC Yield ^a
a	DMF	60	80	0%
b	DMF	60	100	0%
c	DMF	60	120	3%
d	DMF	60	150	14%
e	Toluene	60	120	0%
f	Toluene	60	150	1%
g	Toluene	100	150	2%
h	THF	60	120	3%
i	THF	60	150	5%
j	THF	100	150	10%

^a Based on GC-MS without internal standard.

While the temperature of the glass reactor chip was assumed to be not important, a temperature of 60 °C was anyway applied in the initial experiments. First, DMF was used as solvent and no product formation was observed at 80 and 100 °C (run **a** & **b**). We did however observe bubble formation in the glass microreactor, indicating carbon monoxide release. Further raising the temperature of the coil reactor to 120 and 150 °C (run **c** & **d**) resulted in a GC yield of 3% and 14%, respectively. One could argue that at temperatures of 150 °C, DMF itself might contribute to CO formation. This should however not be the case, according to literature.³ Toluene was the solvent of use in following experiments (runs **e-g**). As it appeared, only very low amounts of product **2.5** were formed in toluene. THF as solvent gave better results (runs **h-j**). Unexpectedly, a better result was obtained when increasing the temperature of the glass reactor chip. However, no exclusion of experimental variation is possible. Moreover, in all runs, segmented flow was observed (gassing out of carbon monoxide).

Keeping in mind that only 1.5 equivalents of CO are used, it was hypothesized that segmented flow was not in our favor. Therefore, a new flow setup was

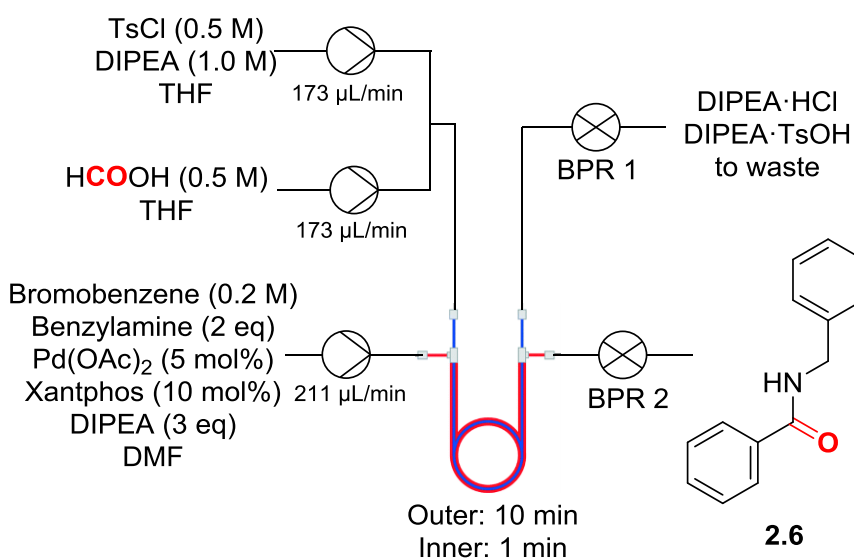
used, depicted in Scheme 17. The nucleophile was changed from aniline to benzylamine, since aniline is a poor nucleophile and therefore not ideal for use in a model system. The number of equivalents of CO was raised to 2.5, the residence time was raised to 10 min and a back-pressure regulator at 75 psi was used in order to avoid segmented flow. Unfortunately, the BPR got clogged, most probably due to precipitation of organic salts (DIPEA·HCl and DIPEA·TsOH).



Scheme 17: Edited flow setup for *in situ* CO generation and subsequent carbonylation.

At this stage, it was decided to stop pursuing the *in situ* CO generation flow setup and to switch to an *ex situ* CO generation, using a tube-in-tube flow setup. As described in **chapter 1.2.2**, this device contains a membrane which separates an outer and inner reactor. This membrane is only permeable to gases such as CO. The results are summarized in Table 4.

Table 4: Ex situ CO generation using a tube-in-tube reactor.



Run	Temperature	BPR 1	BPR 2	GC yield
a	100 °C	40 psi	N/A	20%
b	140 °C	40 psi	N/A	30%
c^a	rt	100 psi	75 psi	0%
d^a	60 °C	100 psi	75 psi	0%
e^a	100 °C	100 psi	75 psi	0%
f	100 °C	40 psi	N/A	40%

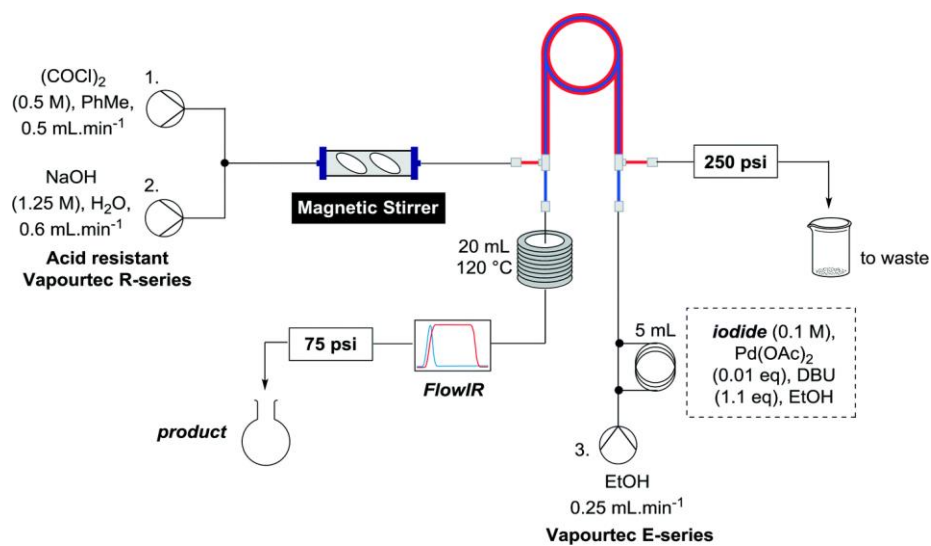
^a THF:DMF (1:1) used instead of DMF in the outer tube.

Initial results appeared promising (run **a** & **b**) when 20% and 30% GC yield were obtained at 100 and 140 °C, respectively. However, a clear segmented flow was observed, again due to outgassing of carbon monoxide. Again it was hypothesized that this was the main problem of these fairly low conversions. Furthermore, the reported GC yield was the average of obtained results (GC sample taken from collection flask. Over time, conversion varied when sampling every 5 minutes, ranging randomly from 15% to 70% (*ergo* not taking a sample from the total collection volume but directly filling a GC vial from the outlet). This indicated that no steady state was obtained. Based on a report by Ley and coworkers,⁵² the BPR of the inner reactor was raised to

100 psi and a BPR in the outer reactor was added that was set to 75 psi. Moreover, the solvent of the outer reactor was changed from DMF to THF:DMF (1:1). This resulted in a homogenous flow, in line with the Ley publication. However, to our surprise, 3 runs (**c-e**) did not result in any product. Run **f** was then performed as a repetition of run **a**, where again segmented flow was observed, but still a GC yield of 40% was obtained. The difference in GC yield with run **a** is fairly big (20%). It should be noted that again shifting results were obtained from GC samples from collecting a sample every 5 minutes. Therefore, it was assumed that no steady state was reached.

In retrospect, it was realized that the gassing out we observed might have been due to raising the temperature above the used solvent its boiling point when no BPR was used.

In early 2016 a report from Ley and coworkers was published, where oxalyl chloride, another known CO precursor,⁸² generated carbon monoxide which diffused through the membrane of a tube-in-tube reactor (Scheme 18).⁷² Via this setup, which applied significant longer residence times than our experiments (80 minutes vs. 10 minutes), 3 vinyl iodides and 7 (hetero)aryl iodides underwent alkoxycarbonylation. Although we believe our described approach could be further optimized, the combination of this report and the interest in a two-chamber approach (see **chapter 2.2.2**), our flow approach route was abandoned. In retrospect, 1,4-dioxane might have been a better solvent choice, since numerous reports use it for palladium-catalyzed carbonylation in flow.^{52, 72, 83} Another remark is that aryl iodides might be easier model systems, since they undergo palladium-catalyzed reactions more readily than aryl bromides. A final suggestion is raising the residence time, maybe by adding a coil reactor after the tube-in-tube reactor and, of course, preventing segmented flow.



Scheme 18: Alkoxy carbonylation of vinyl and aryl iodides via a tube-in-tube reactor setup.
 Reprinted with permission from *React. Chem. Eng.*, **2016**, 280-287. Copyright Royal Society of Chemistry.

2.2.2 Two-chamber approach

This section is based on:

C. Veryser, S. Van Mileghem, B. Egle, P. Gilles and W.M. De Borggraeve, Low-cost instant CO generation at room temperature using formic acid, mesyl chloride and triethylamine, *React. Chem. Eng.*, **2016**, 142-146.⁸⁴ *The author came up with applying the CO precursor in a two-chamber setup, performed the initial experiments and contributed to further follow-up of the experiments and write-up of the paper.*

A lecture of professor Troels Skrydstrup at the Belgian Organic Synthesis Symposium 2014 described the use of two-chamber reactors as tools for *ex situ* carbon monoxide generation.⁶⁻⁸ It is here that the idea was sparked to instead of using a flow concept for our newly discovered CO precursor system, a two-chamber approach would be a more convenient way to demonstrate its utility in palladium-catalyzed carbonylation. As described in **chapter 1.3**, a two-chamber reactor consists of two chambers connected via a bridge (Figure 12). Usually, in one chamber, a gas is generated which diffuses to the other chamber, where it is consumed. As already stated, this *ex situ* approach was chosen over an *in situ* approach since sulfonyl chlorides are not compatible with a vast amount of nucleophiles, *e.g.* amines when one wants to perform an aminocarbonylation. Therefore, a two-chamber setup was chosen.

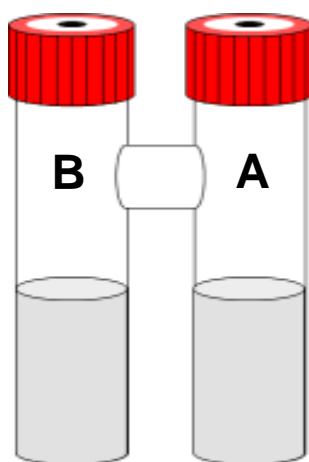
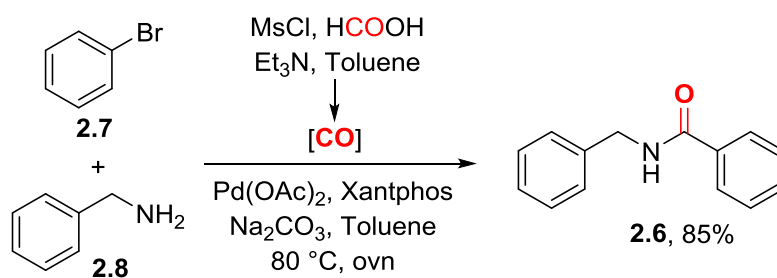


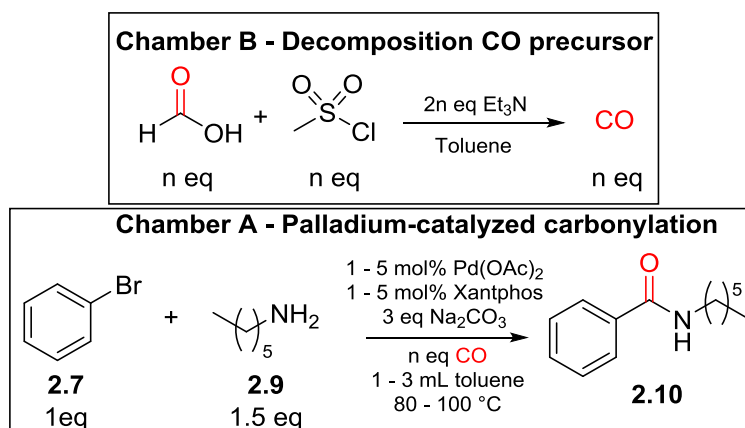
Figure 12: Patented two-chamber reactor design.

In a first two-chamber experiment, a palladium-catalyzed carbonylation was carried out in chamber A, using bromobenzene (**2.7**, limiting reagent) and benzylamine (**2.8**) as aryl halide and nucleophile, respectively (Scheme 19). In chamber B, 1.5 equivalents of both formic acid and mesyl chloride were dissolved in toluene and 3 equivalents of triethylamine were added. Mesyl chloride was indeed our sulfonyl chloride of choice, mainly due to its low cost (cheaper than other sulfonyl chlorides), its physical properties (liquid at room temperature) and due to atom economy (better than other sulfonyl chlorides). Under the assumption that the conversion in the CO generating reaction is complete, 1.5 equivalents of carbon monoxide are generated. The two-chamber reactor was immersed in an oil bath at 80 °C and left stirring overnight. After purification, the product (**2.6**) was isolated in 85% yield. When repeating the same reaction with a CO balloon instead of the precursor, a significantly lower yield was obtained (71%). This clearly indicated that this was a nice start, needing only near-stoichiometric amounts of carbon monoxide in the process. ¹³C-NMR analysis confirmed that mesyl chloride and formic acid do not react without adding base. When adding base however, both mesyl chloride and formic acid peaks disappeared. A new peak emerged, which was confirmed to be from the mesylate anion, confirming our proposed mechanism in **chapter 2.1**. From this results, we chose bromobenzene (**2.7**) and *n*-hexylamine (**2.9**) as substrates for optimization. The results are summarized in Table 5. In entry a, using 3 equivalents of CO at 80 °C, the product (**2.10**) was obtained in 80% yield. Increasing the temperature to 100 °C already resulted in a nearly quantitative isolated yield (96%). Further lowering the number of equivalents of carbon monoxide (entries **c-d**) did not result in a significant difference in yield, compared to using 1.3 equivalents, which is near-stoichiometric and further avoids pressure build up. Delighted with these results, further parameters were tested. In entry **e**, the amount of palladium catalyst was lowered to 1 mol%, again giving no significant difference in isolated yield. In a final attempt (entry **f**), the reaction time was reduced to two hours. Once again, a nearly quantitative yield was obtained.



Scheme 19: First two-chamber reactor attempt.

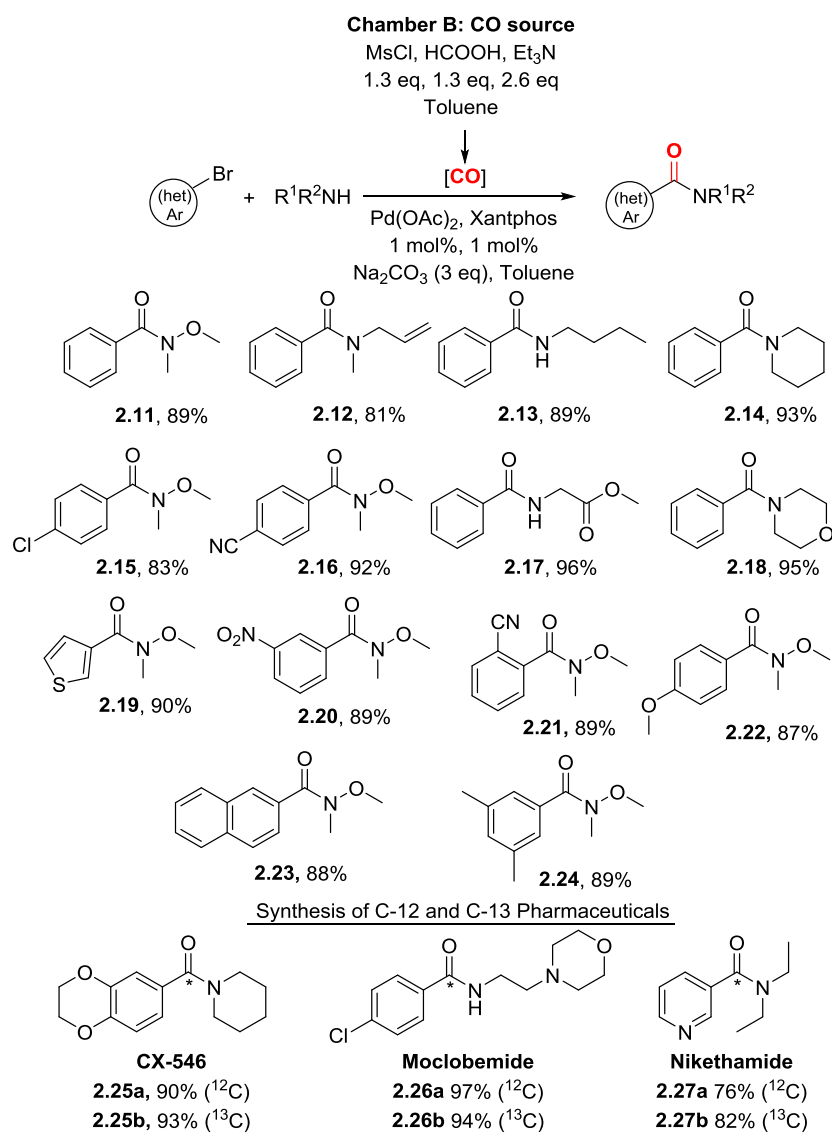
Table 5: Optimization studies of two-chamber carbonylation protocol.



Entry	T (°C)	t (h)	mol% Pd/Xantphos	Eq CO	Yield
a	80	Ovn	5/5	3	80
b	100	Ovn	5/5	3	96
c	100	Ovn	5/5	2	95
d	100	Ovn	5/5	1.3	93
e	100	Ovn	1/1	1.3	94
f	100	2	1/1	1.3	95

With the optimized conditions at hand, it was time to further explore the scope of this protocol. As shown in Scheme 20, different benzamides and Weinreb amides (**2.11-2.27**) were synthesized in mostly good to excellent yields. Heterocycles such as pyridine (**2.27**) and thiophene (**2.19**) were

tolerated, as well as functional groups such as nitrile (**2.16** & **2.21**), chlorine (**2.15** & **2.26**), nitro (**2.20**), methoxy (**2.22**) and allyl (**2.12**). In a final stage three pharmaceuticals were synthesized: CX-546 (**2.25**),⁸⁵ Moclobemide (**2.26**)⁸⁶ and Nikethamide (**2.27**).⁸⁷ There was made use of both formic acid and the commercially available carbon-13 enriched formic acid. The isotopic labelling of pharmaceuticals is useful for *in vivo* studies. CX-546 and Moclobemide were synthesized in excellent yields, and Nikethamide, being a little bit more challenging due to the pyridine ring, was synthesized in a good yield. The yields when using ¹³C-CO were in the same range, successfully obtaining these labelled pharmaceuticals.




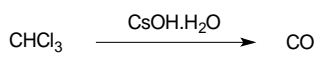
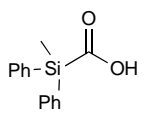
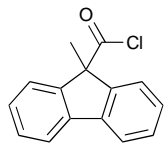
Scheme 20: Scope of palladium-catalyzed carbonylation using two-chamber setup with CO precursor.

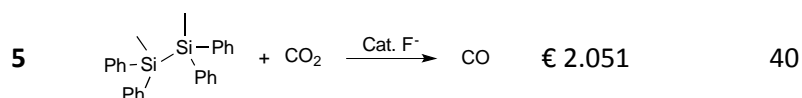
2.3 New CO precursor: further considerations and conclusions

As stated above, this newly developed CO precursor system is convenient in use as mesyl chloride, formic acid and triethylamine are cheap commodity chemicals available in almost every organic synthesis lab. Furthermore, the decomposition occurs at room temperature, while most precursors need higher temperatures for CO liberation.^{7, 59, 66} In addition, some precursors require several synthesis steps and/or the use of a transition metal, a heterogeneous base or other expensive reagents.^{6-7, 76}

A small economical comparison was made between our reported CO precursor and a small selection of examples from literature (*Note: these prices are from December 2015, and may have changed since*). The data is summarized in Table 6. Our system is 30 to >150 times more cost efficient than the other reported precursors. Details of these calculations can be found below. We only evaluated the cost of the starting materials, no costs of solvent, work-up, carbon dioxide, heating, water use, purification, working hours *etc.* were taken into account. This overestimates the relative price of our precursor, since no work-up or purification is needed. With this in mind, it costs € 0.051 to generate 1 mmol of CO, which is even less than the cost of 1 mL of anhydrous DCM (€ 0.08)! Our developed CO precursor is, to the best of our knowledge, one of the cheapest precursors known in literature.

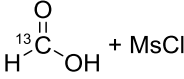
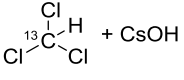
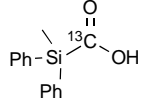
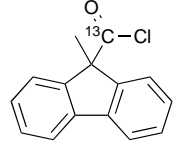
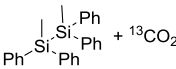
Table 6: Price comparison of recently published CO generating systems. ^a Price per mmol CO. Detailed information can be found in the tables below.

Method	CO generating system	Price ^a	Relative price
1		€ 0.051	1
2		€ 2.294	45
3		€ 1.506	30
4		€ 8.479	166



Another interesting economical aspect is the price comparison of commercially available ^{13}C precursors. Since ^{13}C -formic acid is commercially available, our reported procedure also provides an obvious source of ^{13}CO . Remark that this enriched precursor is at least 9 times less expensive per mmol ^{13}CO than any other reported commercial ^{13}CO precursor (Table 7). Again, complete conversion to CO was assumed. As it appears, our system belongs to one of the most cost efficient ^{13}C -carbonylation methods. Note that these price calculations are only indicative, as they will change over time. However the price difference is significant (≥ 9 factors). Also, the prices of other reagents are not incorporated, as they are significantly less expensive than ^{13}C -labelled reagents. The ^{13}CO precursors from methods 3 and 5 are not commercially available. These methods use $^{13}\text{CO}_2$ gas as their ^{13}CO precursor. This is cheaper than H^{13}COOH , but implies working with gas vessels and requires synthesis steps to obtain the actual ^{13}CO precursor. Indeed, the whole idea behind the CO precursors/two chamber concept is to step away from pressurized gas vessels on a laboratory scale. Therefore, the Skrydstrup group employed a three chamber reactor, where they generate $^{13}\text{CO}_2$ from $\text{Ba}^{13}\text{CO}_3$ (a solid), which is subsequently reacted to ^{13}CO .⁷⁶ Therefore, the price of $\text{Ba}^{13}\text{CO}_3$ is added in Table 7.

Table 7: Price comparison for the generation of 1 mmol of carbon-13 CO.

Method (see above)	CO generating system	Commercial price per gram	Commercial price per mmol ¹³ CO	Relative price
1	 + MsCl	€ 307	€ 14	1
2	 + CsOH	€ 1056	€ 126	9
3		-	-	-
4		€ 653	€ 158	11
5	 + ¹³ CO ₂	-	-	-
3 & 5	¹³ CO ₂	€ 186 per liter = € 151 per gram	€ 7	0.5
-	Ba ¹³ CO ₃	€ 1647	€ 329	23

In conclusion, we have developed an economical and convenient CO precursor. Via a simple two-chamber setup it is possible to use carbon monoxide in a safe and convenient way on a laboratory scale for organic reactions. This precursor is, to the best of our knowledge, one of the cheapest CO precursors known in literature. ¹³C-labelling is easily possible due to the relatively cheap and commercially available carbon-13 enriched formic acid.

CHAPTER 3

THE ASSEMBLY OF PYRAZINE BASED OLIGOAMIDE ALPHA- HELIX MIMETICS

3. The assembly of pyrazine based oligoamide alpha-helix mimetics

This section is based on:

S. Van Mileghem, B. Egle, P. Gilles, C. Veryser, L. Van Meervelt, W. M. De Borggraeve, Carbonylation as a novel method for the assembly of pyrazine based oligoamide alpha-helix mimetics, *Org. Biomol. Chem.*, **2017**, 373-378.⁸⁸
The author contributed to most of the synthetic work, collected all data and wrote the paper.

3.1 Literature and objectives

3.1.1 Protein-Protein Interactions

In a protein-protein interaction (PPI), two or more proteins interact (reversibly or irreversibly) with each other. These interactions can be homomeric (same protein) or heteromeric (different proteins). PPIs are vital biological processes, ranging from cellular communication to programmed cell death.⁸⁹ Therefore, when perturbations emerge in PPIs, diseases and afflictions begin to arise.⁹⁰ This makes PPIs highly attractive drug targets. With over 650 000 interactions, PPIs are a great opportunity for the discovery of new therapeutics.⁹¹ Up to a decade ago, drug development mainly targeted proteins which were considered druggable (*ie.* the possibility of modulating a target with a small molecule). Classic examples include G-protein, proteases and kinases.⁹² PPIs on the other hand were once considered undruggable, which was mainly due to their large (1500-3000 Å²), flat, shallow and dynamic surfaces.⁹³

The question that arises is the following: how can a small molecule (<500 Da) possibly disrupt an interaction between proteins that is significantly bigger than the molecule itself? At first sight it appears that a small molecule inhibitor has to dwell in the outstretched interaction surface for shelter. However, by combining crystallography with site directed mutagenesis (alanine screening), researchers have shown how PPIs function.⁹⁴ It appeared that in most cases, the interaction is highly dependent on just a small number of key amino acid residues. These are located at the interaction surface, forming a so called hot spot.⁹⁵ These hot spots are enriched in arginine, tryptophan and tyrosine.⁹⁴ On top of that, another interesting experiment revealed that protein PPI surfaces are in fast dynamic movement, with pockets opening and closing, all in the order of nanoseconds.⁹⁶ This reveals

that the interaction surface is in fact shifting and moving and cavities could be formed, in where a small molecule can gain access to locations fully enclaved between two proteins. These findings are good news for the potential of small molecule protein-protein interaction inhibitors (SMPPPIs), as binding to a hot spot should be sufficient to disrupt the entire complex. Currently, the number of SMPPPIs is increasing.⁹⁷⁻⁹⁸ Figure 13 depicts the classification of PPIs by whether one side of the interface consists of a primary (linear) protein sequence (a fairly short peptide), a single region of a secondary structure (such as an α -helix) or multiple sequences requiring tertiary structures.⁹⁸ At one extreme, the PPI spans 1-4 amino acids. There are currently 4 examples of small molecule mimetics of this type of PPI in clinical trials.⁹⁸ Also PPIs containing a single secondary structure have been proven to be able to be inhibited by small molecules. Globular interfaces requiring tertiary structures on both sides of a PPI have fewer success, as the PPI consists of a much higher complexity.

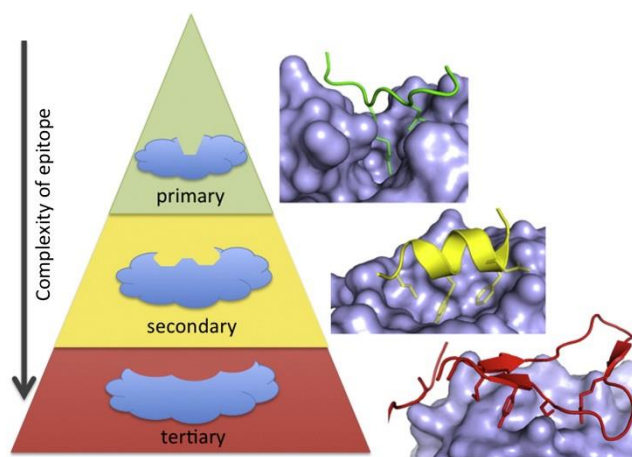


Figure 13: Classification of PPIs. The complexity of the PPI raises from primary to secondary to tertiary structures. Reprinted with permission from *Chemistry & Biology*, **2014**, 1102-1114. Copyright Cell Press.

3.1.2 Strategies for protein-protein interaction inhibitor design

Several strategies have been developed to help develop this challenging field.⁹⁹

Fragment screening and optimization has become a standard part of the medicinal chemists' arsenal for more than a decade.¹⁰⁰ The concept of this approach is conceptually simple: this technique uses fragments which are molecules with a molecular weight of 200 Da or less for screening. These fragments are screened for weak binding with a protein. After this, proper optimization of each unique interaction in the binding site and subsequent linking of these fragments into a single molecular entity should, ideally, yield a compound with a binding affinity that is the sum of the individual interactions. However, using this technique to tackle PPIs is not straight forward, since a low-affinity small fragment hit is not able to disrupt a PPI. To tackle this issue, biophysical analysis techniques such as thermal shift,¹⁰¹ surface plasmon resonance,¹⁰² SAR by NMR¹⁰³ and X-ray crystallography¹⁰⁴ are typically used in this approach. Once a hit is identified, protein NMR is often used to determine whether the fragment binds at the PPI interface. In the last decade, 14 highly potent inhibitors ($IC_{50} < 100$ nM) were developed by fragment based screening, indicating the technique's potential.⁹⁸

Biological screening searches for macromolecular entities (> 5000 Da) from Nature, usually in the form of (complexed) proteins or antibodies.¹⁰⁵ These usually have advantages such as excellent selectivity and a long half-life. However, it is not possible to orally administer these types of drugs, intravenously or subcutaneously administration is necessary. Moreover, membrane permeability is very low, making this approach unsuitable for intracellular targets.

Virtual screening (or computational screening): given the structure of a PPI, it is possible to use computational tools to find potential small molecule binding pockets and assess drugability.⁹⁹ Generated hits can then be tested in a bioassay for binding activity. It speaks for itself that this method is relatively cheap. However, this technique requires a high understanding of structural elements of a specific PPI, as well as molecular dynamics calculations, due to PPIs their dynamics (no static moieties).¹⁰⁶

High throughput screening (HTS) is a method where a library of compounds is screened.¹⁰⁷ Subsequent medicinal chemistry optimization of hits takes place. When performing HTS to alter a PPI, a number of challenges must be

taken into account: low hit rates, weak hits and difficulties in removing false positives.⁹⁹ Nevertheless, success with HTS has been achieved. An example is the successful screen against human papillomavirus E2-E1.¹⁰⁸

Rational design (peptidomimetics) is the design of (PPI) inhibitors that mimic peptides and will be discussed below.

3.1.3 Rational Design of small molecule PPI inhibitors

This approach designs inhibitors that mimic peptides. Usually these inhibitors do not follow Lipinski's rule of five.¹⁰⁹ Their odd druglikeness presents very different challenges and strategies compared to conventional drug design.¹¹⁰⁻¹¹¹ When the target to be mimicked is a protein secondary structure, the inhibitors are termed *peptidomimetics*.¹¹² This field is subdivided based on the mimicked secondary structural element: α -helices, β -sheets and reverse turns.

For PPIs, α -helix mimetics are more intensively studied than other peptidomimetics. This is mainly due to the fact that 60% of all known PPIs utilize an α -helix on the interaction surface, and 60% of these bind a single face of the helix.¹¹³ A protein α -helix adopts a right-hand coiled structure which is stabilized by intramolecular hydrogen bonds between the amides on the backbone (Figure 14). Hence, compounds which mimic one face of an α -helix (usually the i , $i+3/4$ & $i+7$ amino acid residues) can, theoretically, already cover a large part of PPIs.

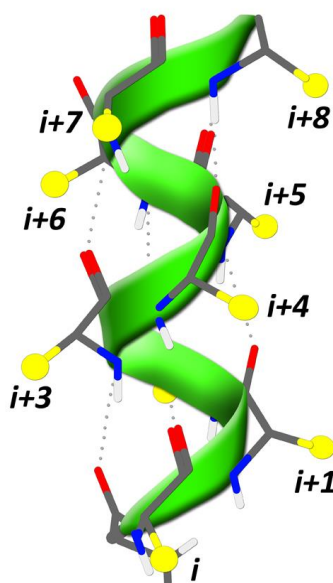


Figure 14: A protein α -helix. Dashed lines represent stabilizing intramolecular hydrogen bonds.

Several approaches exist for the design of α -helix mimetics, as depicted in Figure 15. Mimicry of this three hot-spot residues of an α -helix can be achieved with a linear oligomer with repeating units (**Aa**), a linear molecule assembled from different monomers (**Ab**), a constrained peptide (**Ac**) or an attachment of residues on a central scaffold (**Ad**). Examples are the terphenyl scaffold¹¹⁴ (**Aa** type) or benzodiazepine mimetics¹¹⁵ (**Ad** type) (Figure 16). Both mimic one face of an α -helix.

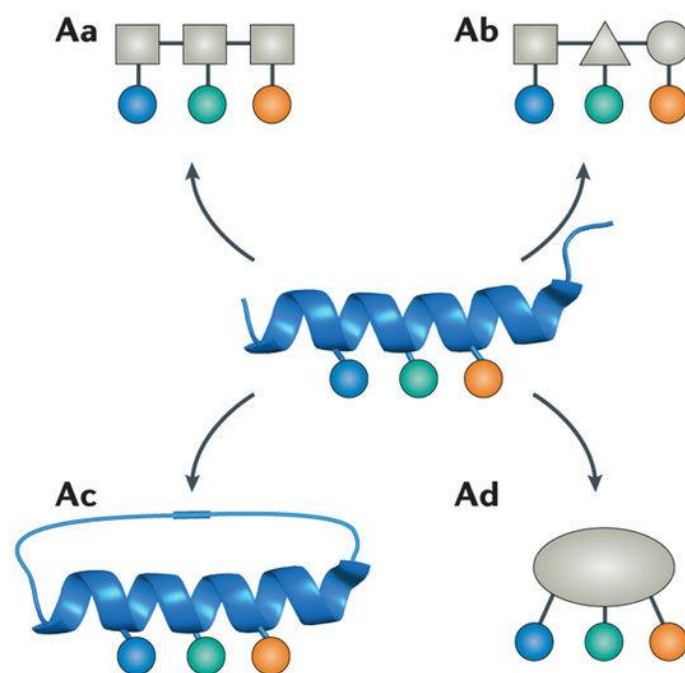


Figure 15: Strategies for the design of α -helix peptidomimetics. Reprinted with permission from *Nature Reviews: Drug Discovery*, **2016**, 533-550. Copyright Nature Publishing Group.

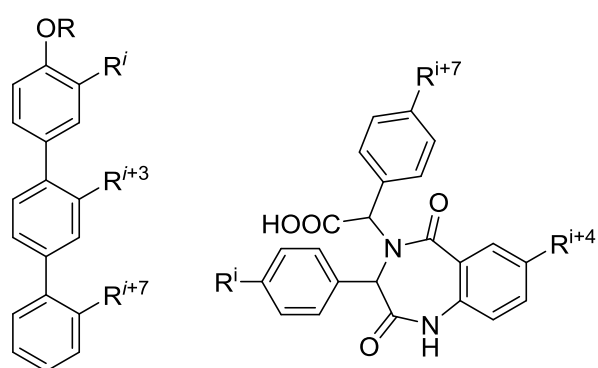


Figure 16: Literature examples of same face α -helix mimetics. Terphenyl scaffold (left) and benzodiazepine scaffold (right).

A remarkable class of molecules which have shown potential in the modulation of protein-protein interactions are the oligoamide systems.¹¹⁶ Central in the design of these oligoamide systems is the modularity in synthesis. This elegant concept provides an unambiguous strategy for the assembly of monomeric units to multimers. Among the oligoamide type systems described in the literature (some examples in Figure 17),¹¹⁷⁻¹¹⁸ amide

bond formation is not always straightforward.¹¹⁹ The amide synthesis is typically performed via acyl chlorides or via the corresponding carboxylic acid with specialty coupling reagents (e.g. Ph_3PCl_2 ,¹²⁰ Ghosez's reagent¹²¹ and Mukaiyama reagent¹²²) since the amine coupling partners are not always nucleophilic. Due to the elaborate synthetic work, significant efforts have been made towards solid phase synthesis and recently, late stage introduction of the amino acid side chains.^{121, 123}

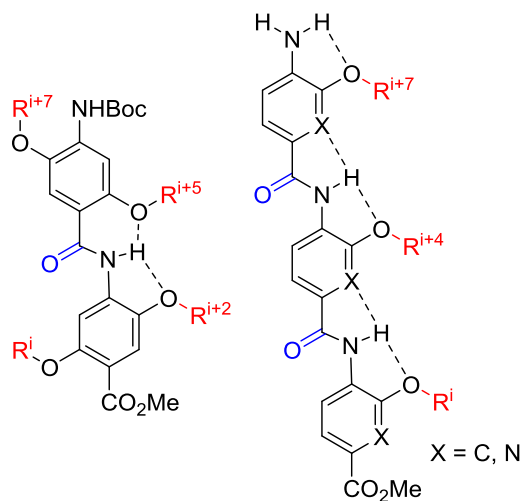


Figure 17: Oligoamide α -helix peptidomimetics.

Here, we report on palladium-catalyzed carbonylation as an alternative strategy for the assembly of monomers (Figure 18). The use of catalytic carbonylation chemistry as a coupling method is advantageous since (1) no stoichiometric amounts of coupling reagents are used, (2) it offers a broad functional group tolerance and (3) it is able to handle substrates which are very low in nucleophilicity.⁷⁷ Previous experience with peptidomimetics¹²⁴ in our group motivated us to pursue the synthesis of unreported pyrazine based oligoamide α -helix peptidomimetics via palladium-catalyzed carbonylation. This scaffold has the interesting feature of increasing hydrophilicity and solubility by adding hydrogen bond acceptors that can contribute to a so called wet edge.¹²⁵⁻¹²⁶ The modularity in design by using carbonylation chemistry enabled us to synthesize both pyrazine based multimers as well as a couple of hybrid dimers.

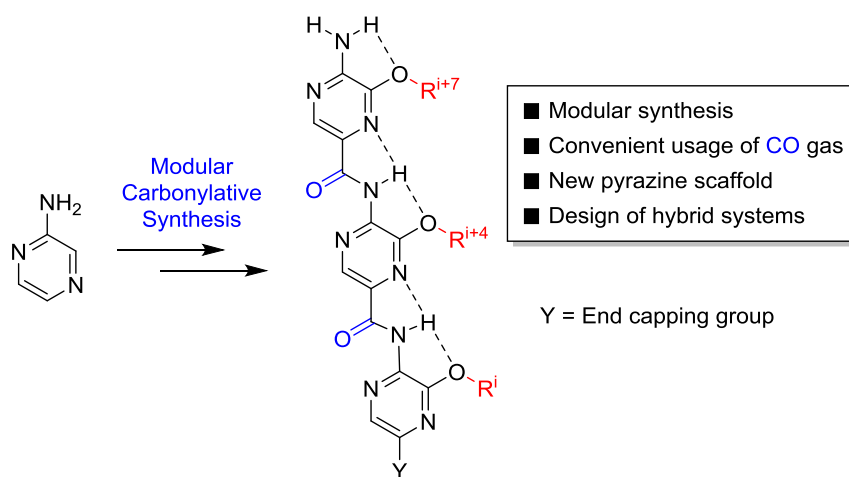
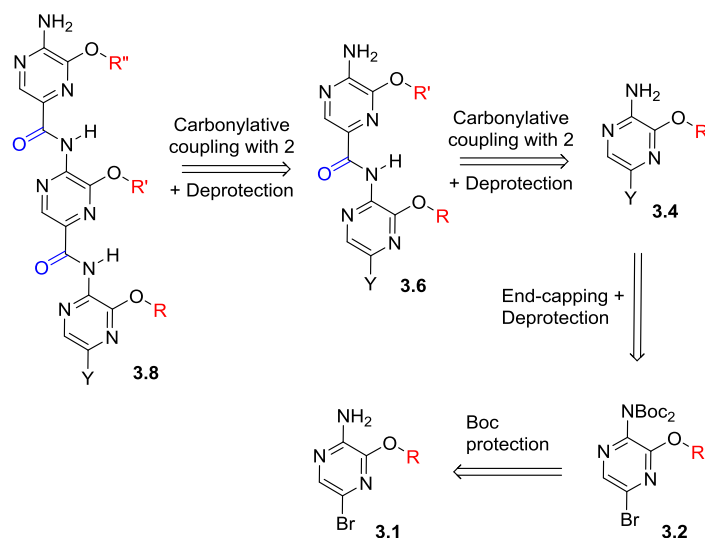


Figure 18: Our proposed pyrazine based oligoamide α -helix mimetics.

3.2 Results and discussion

3.2.1 Retrosynthesis

It was proposed that the pyrazine based multimeric structure (Figure 18) mimics the amino acid residues at the same face of the helix as its phenyl and pyridine counterparts,¹²⁷ namely at the i , $i + 4$ and $i + 7$ positions. Building block **3.1** (or its protected version **3.2**) consists of a pyrazine core which enabled the development of a modular route (Scheme 21). The idea is inspired by peptide synthesis where a sequence of activation, coupling and deprotection is repeated a number of times to synthesize (oligo)peptides. Similarly, in our strategy, building blocks **3.2** serve as a substrate for the growing oligoamide multimers via a palladium-catalyzed carbonylation with CO gas,¹²⁸ which are then deprotected to prepare them for the next coupling. The main reason for using aminocarbonylation as the coupling methodology is due to its ability to couple substrates which are low in nucleophilicity, such as aminopyrazine derivatives.¹²⁹ Moreover, the reaction conditions of carbonylation chemistry are mild and therefore more compatible with sensitive amino acid side chains present on the peptidomimetics.¹²⁸ In order to avoid the use of a CO lecture bottle and CO filled balloons, our developed two-chamber set-up (see **chapter 2.2**) was in a later stage successfully implemented for the sake of safety.



Scheme 21: Retrosynthetic approach to pyrazine based oligoamide α -helix mimetics.

In order to avoid homocoupling and polymerization, the first building block needs to have its halide group replaced with a moiety that cannot interfere in the following palladium-catalyzed coupling. This is a so called end-capping group, which in the peptide synthesis analogy corresponds to blocking the C-terminal amino acid by formation of *e.g.* an ester or attachment to a solid support. The end-capping can be done via carbonylation chemistry or other cross-coupling chemistry, such as Suzuki coupling¹³⁰ forming biaryl type compounds ($Y = Ar$). Deprotection of an end-capped scaffold yields **3.4** that is ready to be coupled with another Boc-protected building block (**3.2**) via carbonylation. Finally, another iteration of the deprotection/coupling followed by a final deprotection yields the pyrazine based α -helix peptidomimetic trimer (**3.8**). To demonstrate this proof of principle, a range of monomeric building blocks was synthesized which were assembled into a set of multimers.

The Boc-protected aminopyrazines (**3.2**, Scheme 21) should allow easy preparation of mixed multimers, containing both pyrazine and other types of monomers (*e.g.* phenyl or pyridine scaffolds). This not only increases the potential structural diversity but also allows tuning the conformational rigidity of the multimers, which has been demonstrated to be advantageous for some PPI targets.¹³¹

3.2.2 Synthesis

In a first stage the synthesis of pyrazine building blocks is performed. Aminopyrazine (**3.9**) is dibrominated using NBS in DMSO.¹³² Following bromination, the desired amino acid mimicking side chain¹³³ was attached using a fully regioselective S_NAr in THF.^{132, 134} Table 8 summarizes the scope of the synthesized pyrazine building blocks. Monomers **3.1a-c** and **3.1h** were prepared in excellent yields. Compound **3.1d** mimics a tyrosine residue¹³³ and is synthesized in a yield of 64%. **3.1e-g** are trityl-protected monomers which are obtained in low to moderate yields. When incorporating trityl protected monomers in a multimer, a non-acidic deprotection protocol is required to remove the Boc groups, *e.g.* by refluxing these compounds in water.¹³⁵ It should be noted that for the synthesis of monomers with an aliphatic amino acid residue (**3.1a**, **3.1b** and **3.1h**), purification is troublesome (similar R_f values for 3,5-dibromoaminopyrazine (**3.10**) and product). In these cases, a larger excess of both base and nucleophile is required if conversion is not complete. Indeed, double S_NAr was not observed in any case so a larger excess was not a problem.

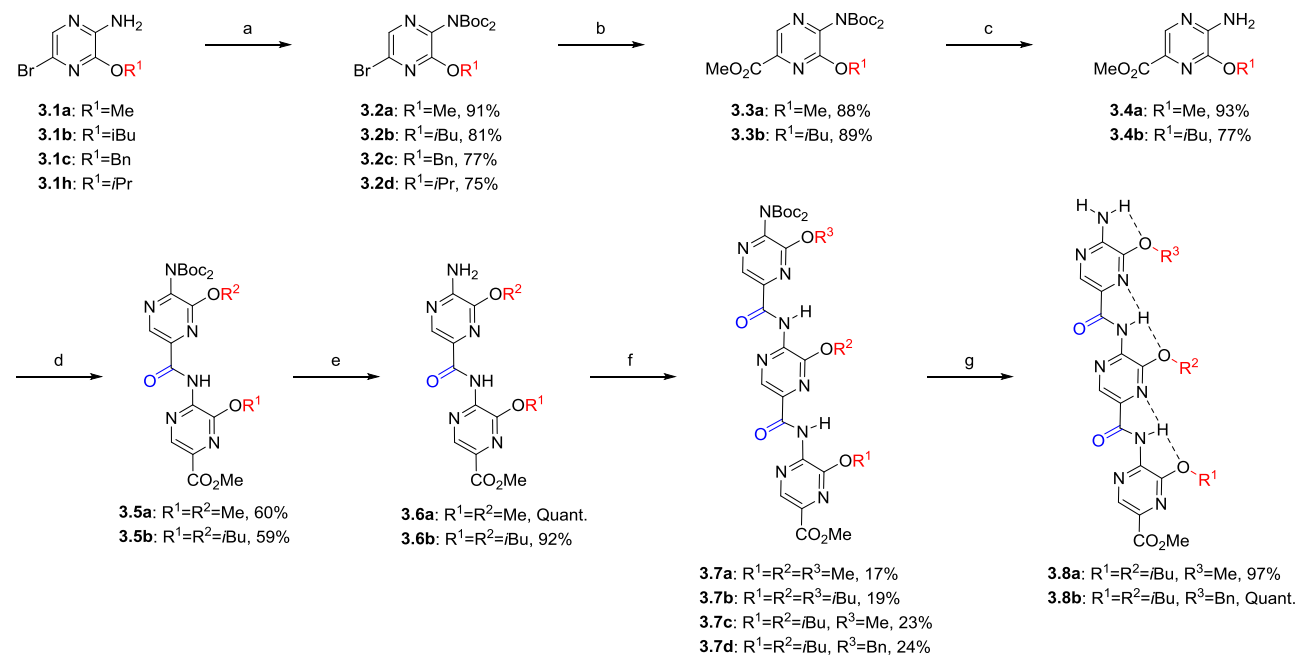
Table 8: Synthesis of the pyrazine building blocks.^a

Entry	Base	Product	Yield (%)	AA Residue
3.1a^b	NaH		83	Ala
3.1b	NaHMDS		88	Leu
3.1c	NaH		81	Phe
3.1d	NaHMDS		64	Tyr
3.1e	NaH		35	His
3.1f	NaHMDS		10	Lys
3.1g	NaHMDS		54	Glu
3.1h^c	NaH		91	Val

^a Conditions: 0.2 M pyrazine in THF, 1.5 eq alcohol, 1.5 eq base, 50 °C, overnight. ^b 1.1 eq NaOMe in MeOH. ^c 10 eq *i*PrOH and 3 eq NaH.

Following the synthesis of the monomers, we embarked upon the assembly of multimers. Some examples are depicted in Scheme 22. Multiple monomers were double Boc-protected in good to excellent yields. After this, an alkoxycarbonylation was performed to synthesize methyl ester end-capped building blocks **3.3a** and **3.3b** in good yields. Subsequently, the Boc groups were removed under acidic conditions. In a following step monomers **3.4a** and **3.4b** were coupled with Boc-protected monomers, again *via* carbonylation. Two protected dimers were synthesized in fairly good yields. Again, acidic deprotection yielded dimers **3.6a** and **3.6b**. In a final sequence, these dimers were carbonylatively coupled with monomers **3.7a-d**, to yield 4 protected trimers in poor yields. TFA deprotection once again resulted in trimers **3.8a** and **3.8b**. While we have nicely proven our synthesis route was effective, the yields of the carbonylative trimerisation are a real bottleneck.

Other solvents commonly used in carbonylation such as 1,4-dioxane or DMF did not result in a higher yield. These unprotected dimers are highly rigid and planar molecules, making intermolecular stacking a readily event. **3.6a** and **3.6b** were highly insoluble in both organic solvents and water, even at elevated temperatures. Since in the carbonylative trimerisation, large amounts of dimer were recovered, it was hypothesized that these low obtained yields are due to a very poor solubility of the dimer starting material.



Scheme 22: Synthesis of pyrazine based methyl ester end-capped α -helix peptidomimetics. Reagents and conditions: (a) Boc₂O, DMAP, DCM, reflux. (b) MeOH, Pd(OAc)₂, Xantphos, CO, Et₃N, 80 °C. (c) TFA, DCM. (d) **3.1a** or **3.1b**, Pd(OAc)₂, Xantphos, CO, Na₂CO₃, toluene, 100 °C. (e) TFA, DCM. (f) **3.1a**, **3.1b** or **3.1c**, Pd(OAc)₂, Xantphos, CO, Na₂CO₃, toluene, 100 °C. (g) TFA, DCM.

X-ray analysis of **3.6b** confirms the presence of intramolecular hydrogen bonds, in analogy to the oligoamide pyridine counterparts.¹³⁶ This type of hydrogen bonding introduces stronger curvature in the molecule's backbone compared to the benzamide systems, which can be beneficial as protein α -helices also have the tendency to curve.¹³⁷ An overlay image of our dimer **3.6b** with a benzamide¹³⁸ and pyridinyl analog¹³⁹ is shown in Figure 19. It was observed that the distance between the O-alkylated sidechains is slightly smaller than is observed for the benzamide system. This is a result of an additional hydrogen bond between the amide proton and pyrazine nitrogen, as was also the case for the pyridine dimer.¹³⁹ The presence of this hydrogen bond is also responsible for the stronger downfield shift of the amide proton in comparison with the one in our hybrid systems (10.09 ppm for **3.6b** vs 8.45 ppm for **3.16**) and the benzamide and pyridinyl amide systems described in literature.^{136, 139} Furthermore, a smaller angle of inclination is observed (155.9° versus 159.6° for our pyrazine system and the reported benzamide system, respectively). This clearly shows the structural resemblance between our and known systems. However, a more exact evaluation of which residues in a helix can be mimicked by these scaffolds would require a more detailed analysis (EKOS).¹⁴⁰

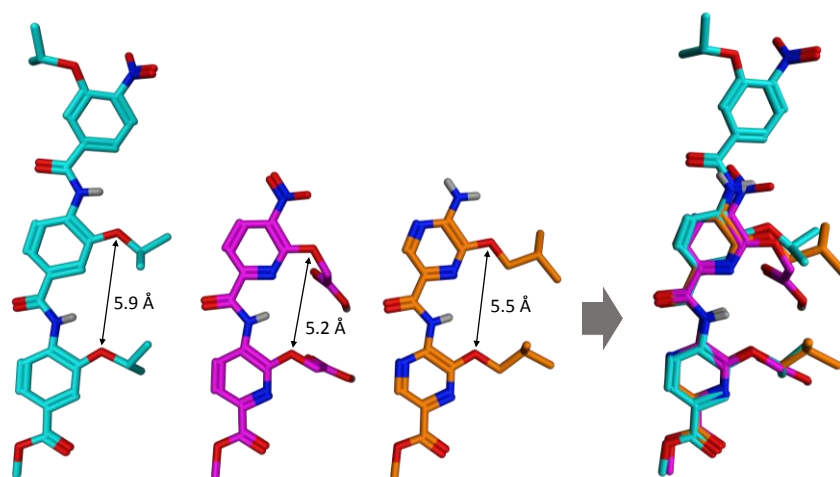
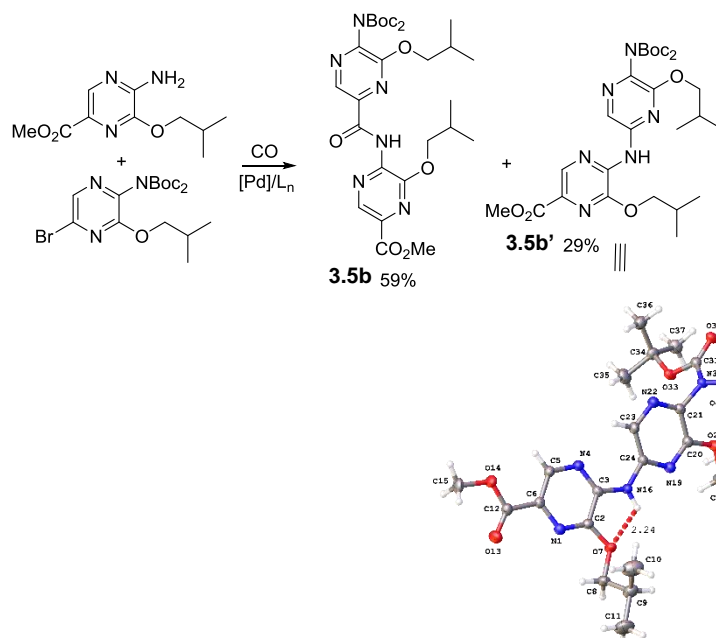


Figure 19: Overlay analysis of (from left to right) Wilson's benzamide crystal (CCDC 870274), Hamilton's pyridine crystal (CCDC 697087) and our pyrazine crystal (CCDC 1512413).

In the case of carbonylative dimer formation, an amount up to 30% of Buchwald–Hartwig amination¹⁴¹ side product was observed, which was confirmed by X-ray crystallography. For the synthesis of **3.5b** the amination product (**3.5b'**) was isolated in 29% yield (Scheme 23). These findings

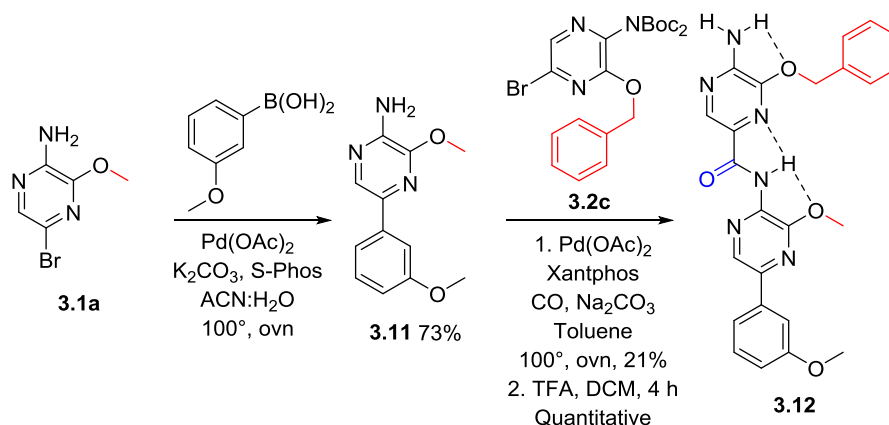
correlate with a report of Buchwald *et al.*,¹⁴² describing that in a palladium/Xantphos system the preferred Buchwald-Hartwig amination reaction conditions are electron deficient aryl halides combined with electron deficient nucleophiles, which is both the case for our pyrazine substrates.



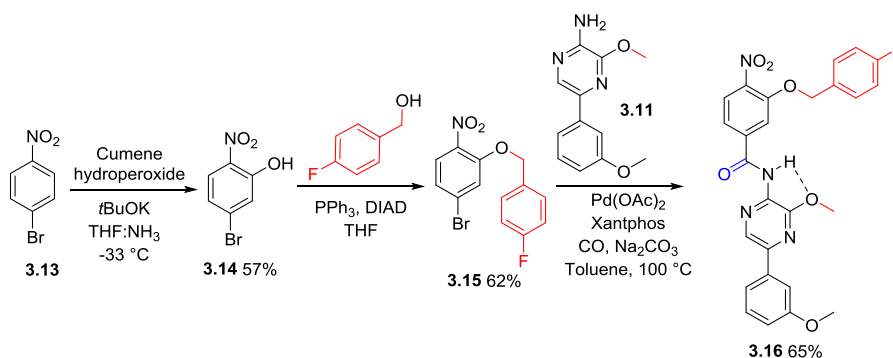
Scheme 23: Buchwald-Hartwig amination as a side reaction in carbonylative dimerisation.

In a next example, Suzuki cross-coupling was used as end-capping strategy. This is demonstrated in Scheme 24. Building block **3.1a** was end-capped to obtain compound **3.11**. Boc-protected building block **3.1c** was attached via carbonylation, which after deprotection led to dimer **3.12**. The yield of this carbonylative dimerization (21%) is lower than other dimerizations. We were not able to explain this significant yield difference. Alternatively, other aryl building blocks can also be introduced as the second monomeric unit via this modular synthesis. This is demonstrated in Scheme 25. Phenyl monomer **3.15** was synthesized starting from p-nitrobromobenzene (**3.13**) via a vicarious nucleophilic substitution which was carried out in a mixture of THF and liquid ammonia.¹⁴³ The resulting phenol **3.14** was treated with p-fluorobenzyl alcohol in a Mitsunobu reaction to yield **3.15**.¹⁴⁴ Finally, this monomer was carbonylatively coupled with **3.11**, which gave rise to hybrid dimer **3.16**, which mimics an alanine and tyrosine residue of an α -helix on

the *i* and *i*+4 position. Note that this carbonylative dimerization yield is again in the usual obtained range (65%).

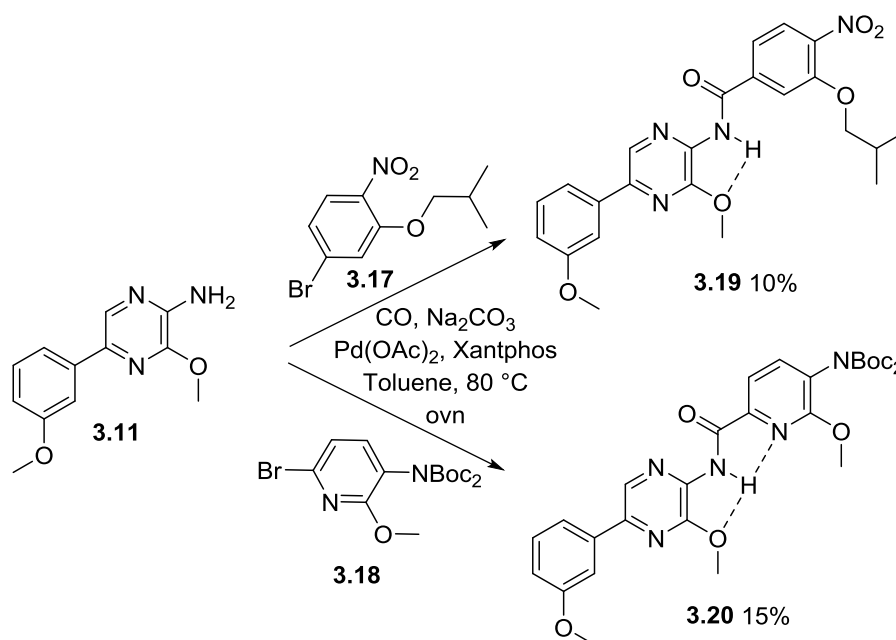


Scheme 24: Alternative end-capping: Suzuki biaryl monomer subsequently transformed into dimer **3.12**.



Scheme 25: Proof of principle for the synthesis of a hybrid dimer, containing both a pyrazine and phenyl monomer.

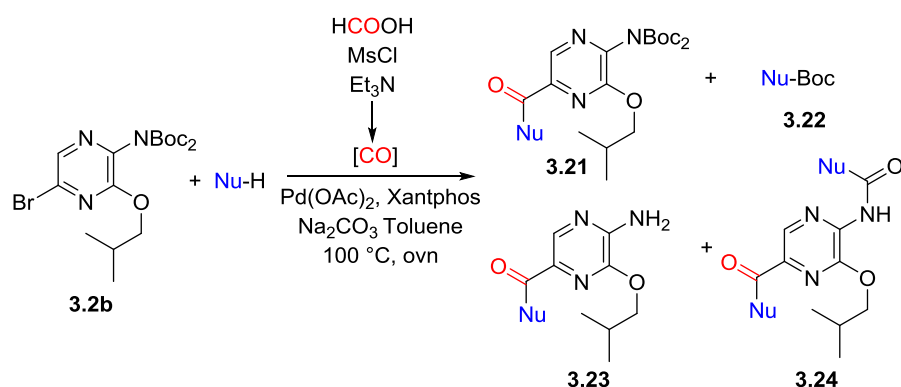
The synthesis of a few others hybrid dimers was attempted. Starting from the Suzuki end-capped pyrazine monomer **3.11**, both a phenyl (**3.17**) and pyridine monomer (**3.18**) were carbonylatively coupled (Scheme 26). The purification was however troublesome. Normal phase MPLC did not result in pure products. Reverse HPLC did purify these mixtures, but the obtained yields were low. Moreover, in both cases, significant amounts of Buchwald-Hartwig amination product were collected as well.

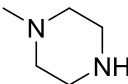
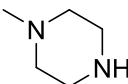
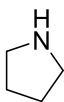
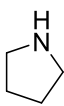
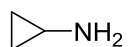


Scheme 26: Further attempts of synthesizing hybrid dimers.

Another extension of our end-capping chemistry is the aminocarbonylation of the pyrazine substrates. However, these reactions were not as straightforward as expected. Using protected monomer **3.2b** as substrate did not result in expected aminocarbonylated product **3.21** (Table 9). After further analysis of the reaction mixture with GC-MS and NMR, 3 unexpected products had formed: Boc-protected *N*-methylpiperazine (**3.22**), deprotected aminocarbonylated product (**3.23**) and a pyrazine urea derivative (**3.24**). When using more equivalents of nucleophile, the ratio of side products changed drastically. Initially it was hypothesized that having synthesized a basic compound, column chromatography was not able to purify them. Therefore, the nucleophile was switched to pyrrolidine. Similar results and trends were observed (entry 3-4). In entry 5, the primary amine cyclopropylamine reacted smoothly to the expected product, without the formation of the formerly obtained side products.

Table 9: Aminocarbonylation as end-capping strategy. Initial investigation.

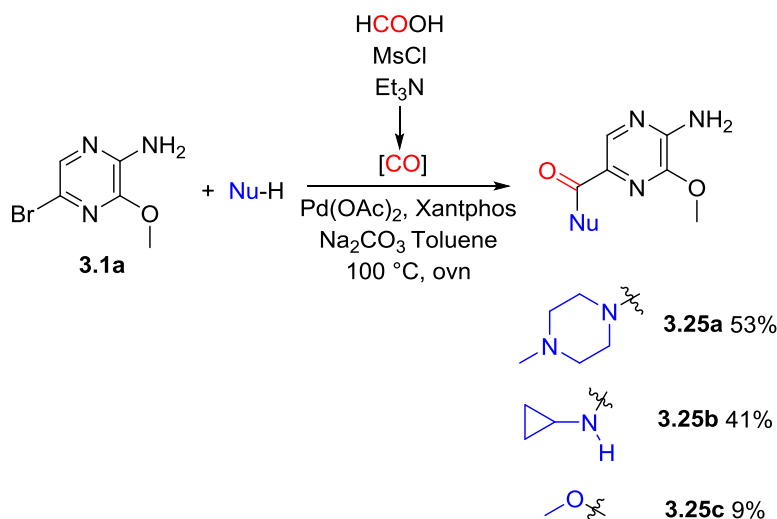


Entry	Nucleophile	Equivalents	Ratio side products ^a	Yield 3.21
1		1.5	1.9	-
2		4	0.2	-
3		1.5	1.8	-
4		4	0.3	-
5		4	-	75%

^a Ratio **3.23**/**3.24**, determined by GC-MS.

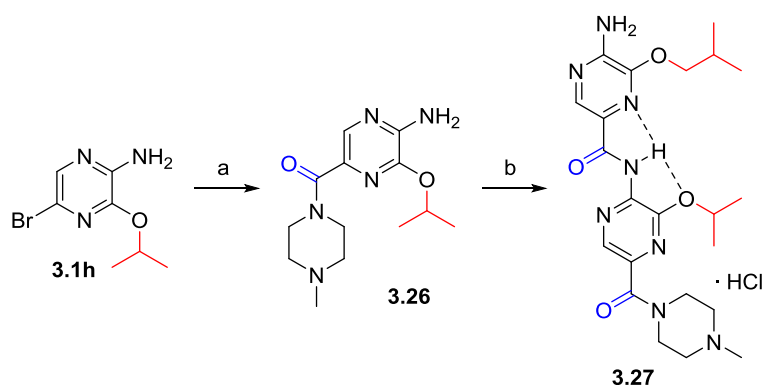
To our surprise, secondary amines react with anilinic carbamate groups, forming unsymmetrical ureas at elevated temperatures and deprotecting the pyrazine, as reported in literature.¹⁴⁵ Hence, these Boc-groups were not stable under these conditions when using secondary amines. They were however completely stable when primary amines were used. This raised the question if it really was necessary to protect the pyrazine monomers with Boc groups. Therefore, we attempted some carbonylations with unprotected pyrazine monomers (Scheme 27). Fortunately, when performing this

carbonylation with unprotected monomer **3.1a**, the piperazine end-capped product **3.25a** was obtained. When using cyclopropylamine as nucleophile, the yield is significantly lower than when using the Boc-protected monomer (41% vs 75%). An attempt with methanol resulted in a poor yield, compared with its protected counterpart (9% vs 88%). Also, after reaction a insoluble solid was retrieved, which was believed to be polymerized pyrazine moieties (speculation based on NMR).



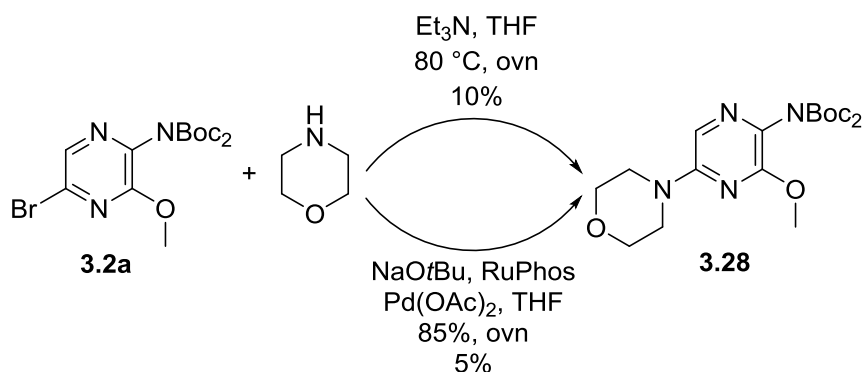
Scheme 27: Carbonylation end-cap with unprotected monomer.

Similar to the reported oligoamide systems, the water solubility of our multimers remains problematic. However, the introduction of a water solubilizing end-capping group is possible via the aminocarbonylation strategy and could solve this problem. When performing this carbonylation with unprotected monomer **3.1h**, the end-capped product **3.26** was obtained (Scheme 28). This was then coupled with **3.2b**. After deprotection this gave **3.27**, which mimics an α -helix with valine and leucine residues. The water solubility problem was however not solved by introducing the piperazine salt.



Scheme 28: Synthesis of dimer HCl salt by piperazine end-cap. Reagents and conditions: (a) *N*-methylpiperazine, Pd(OAc)₂, Xantphos, CO, Na₂CO₃, toluene, 100 °C, 62%. (b) 1. **3.2b**, Pd(OAc)₂, Xantphos, CO, Na₂CO₃, toluene, 100 °C, 17% (43% with recovery of **3.2b**). 2. TFA, DCM, 97%. 3. HCl, dioxane, Quant.

Other possibilities for end-capping were attempted. The introduction of morpholine as end-cap seemed interesting, as it increases the polarity of the molecule and is less planar. Both S_NAr and Buchwald-Hartwig amination were attempted, but the yields were very low (Scheme 29). In both cases, deprotected side products were obtained, hampering purification. This indicated again that these Boc groups were not stable in combination with secondary amines at elevated temperatures. In summary, these transformations would probably work better when working with unprotected monomer (see above).



Scheme 29: Morpholine as end-cap. Performed via S_NAr and Buchwald-Hartwig amination.

3.2.3 Towards analogues of tRNA synthetase inhibitors

After our carbonylation strategy for pyrazine based oligoamide α -helix mimetics was published, we were looking for other applications where amino acid mimics could prove useful. A report by Finn and coworkers described the first example of threonine tRNA synthetase inhibitors with the actual nucleoside scaffold being replaced by a heterocycle. Some of their compounds showed excellent bacterial over human selectivity providing a potential tool in the development of novel antibiotics (Figure 20a). The compounds were developed using structure-based drug design.¹⁴⁶ A crucial part of these threonyl-tRNA synthetase (ThrRS) inhibitors is threonine, which is attached via an *N*-aminoacyl sulfonamide (Figure 20b). This functional group is reported as a non-hydrolysable bioisoster of a phosphate in aminoacyl adenylates.¹⁴⁷ The idea was to develop methodology to modify tRNA synthetase inhibitors with pyrazine analogues of the amino acids.

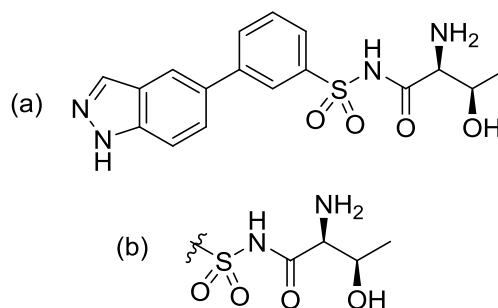


Figure 20: (a) Reported compound with excellent selectivity (bacterial to human). (b) Crucial interaction part of threonine tRNA synthetase inhibitors.

Since colleagues at KU Leuven had a stable isoleucine tRNA synthetase (IleRS) crystal, a proposal was made to develop a methodology for the synthesis of pyrazine **3.29** (Figure 21). This compound bears an isoleucine analogue, is end-capped with an *N*-acylsulfonamide and could be tested as a substructure of an isoleucine tRNA synthetase (IleRS) inhibitor. Other groups also make use of *N*-acylsulfonamides as linker moiety in IleRS inhibitors.¹⁴⁸ In a later stage, the ethyl group could be replaced with heterocycles described the report by Finn and coworkers (Figure 20a).¹⁴⁶ In this preliminary work we wanted to explore methodology to generate the modified amino acid based *N*-acylsulfonamide structure.

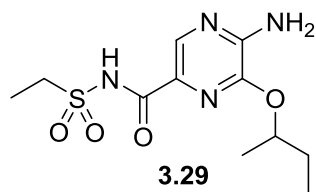
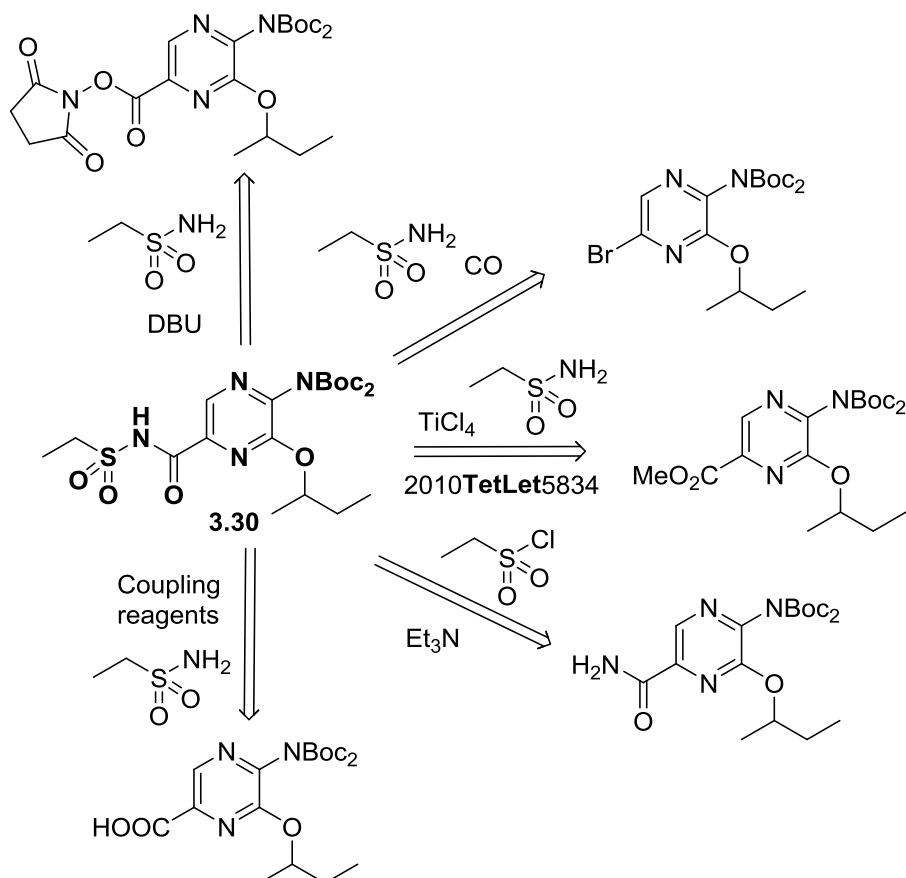


Figure 21: Proposed pyrazine as potential IleRS inhibitor.

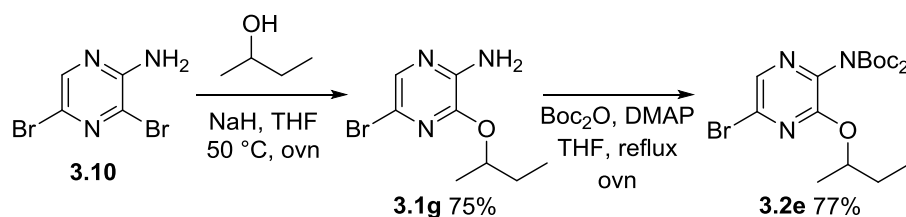
A retrosynthetic analysis of the acylsulfonamide was performed and is depicted in Scheme 30. Several methods should be suitable to synthesize **3.30**, ranging from carbonylation to coupling reagent chemistry, *etc.*



Scheme 30: Retrosynthetic analysis of the crucial step: the acylsulfonamide synthesis.

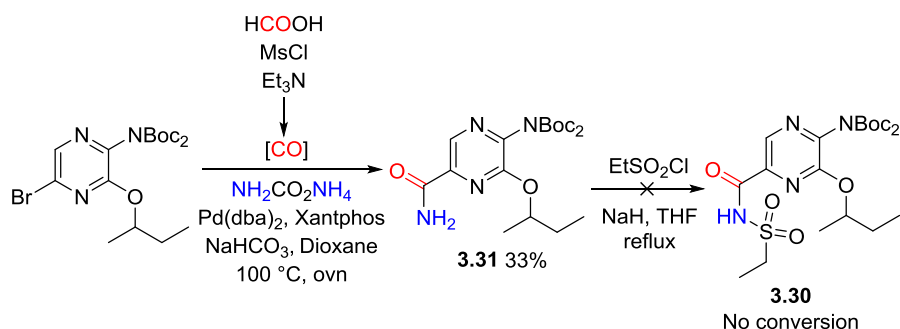
The synthesis commenced from 3,5-dibromoaminopyrazine (**3.10**), by again starting with the fully regioselective nucleophilic aromatic substitution, using

sec-butanol as nucleophile, isolating the product in a 75% yield (Scheme 31). Monomer **3.1g** was subsequently Boc-protected (77%).



Scheme 31: Regioselective S_NAr followed by Boc-protection.

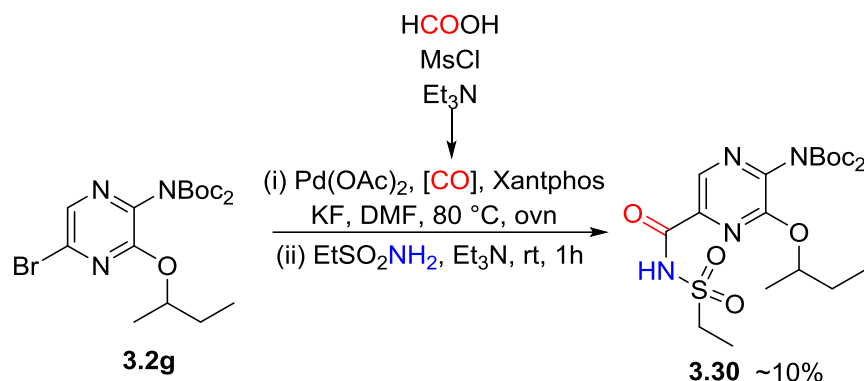
With the protected monomer (**3.2e**) in hand, it was decided to first attempt to synthesize the primary amide by carbonylation and subsequent sulfonylation to yield **3.30**. Nongaseous precursors for both carbon monoxide and ammonia were used similar to a procedure reported by the Skrydstrup group, however our own CO precursor was used (Scheme 32).¹⁴⁹ The product was isolated in moderate yield. After this, the sulfonylation of the primary amide was attempted. Even at reflux conditions, no conversion was observed.



Scheme 32: Synthesis of primary amide via carbonylation and subsequent sulfonylation.

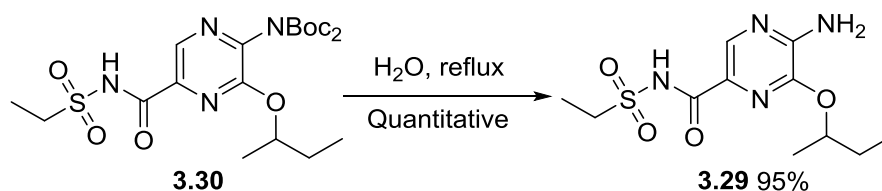
At this point, another route was chosen. A report from the Manabe group used potassium fluoride to carbonylatively generate acyl fluorides from aryl bromides, with subsequent amidation by means of adding an amine.⁶¹ This procedure provided us with **3.30**, albeit in very low yield (about 10%, Scheme 33). In a later stage it was realized that the low yield might have been due to purification: (i) no starting material was retrieved after column chromatography, (ii) the product had an extremely low UV response and (iii) the product smeared out on the column. The combination of almost no UV response and the smearing made us hypothesize that the product did not

dissolve well in the eluent used (Heptanes:Ethyl acetate). In summary, this purification would probably work better in other eluent systems.



Scheme 33: Aminocarbonylation route.

In a final step, the Boc groups were cleaved off by refluxing in water¹³⁵ (Scheme 34). This attempt delivered the product in an excellent yield.



Scheme 34: Neutral Boc deprotection as a final step.

Pyrazine **3.29** was tested for antibacterial activity on 6 different pathogens (see Experimental Section). Unfortunately, it proved to be inactive up to 100 μM . It was hypothesized that once the nucleoside part of the inhibitor is attached, we have a higher chance of finding a hit. Development of such 'complete' scaffolds will be pursued in further research.

3.3 Conclusions and future perspectives

In conclusion, a modular synthesis protocol has been developed towards previously unreported oligoamide pyrazine based α -helix peptidomimetics. A coupling-deprotection sequence was used, utilizing a palladium-catalyzed aminocarbonylation to form the amide bonds between poorly nucleophilic aminopyrazine type building blocks. This methodology enables the flexible synthesis of a diverse set of (hetero)aryl oligoamide α -helix peptidomimetics. The synthesis also features the introduction of various end-capping strategies *via* (carbonylative) cross-coupling reactions. Furthermore, a pyrazine monomer with an isoleucine residue was end-capped with an *N*-acylsulfonamide moiety as new methodology towards non-nucleoside tRNA synthetase inhibitors for the development of new antibiotics.

CHAPTER 4

THE USE OF SULFUR DIOXIDE IN ORGANIC SYNTHESIS

4 The use of sulfur dioxide in organic synthesis

4.1 Literature and objectives

Sulfur dioxide is a ubiquitous commodity chemical which has several chemical applications in industrial processes. Until recently, it was not often used in an academic lab setting.¹⁵⁰ This can partly be ascribed to the gaseous state of sulfur dioxide, as well as its notorious toxicity and smell. It should of course be noted that the foul smell is one of the reasons why sulfur dioxide is less dangerous than carbon monoxide (**chapter 2 & chapter 3**). Sulfur dioxide is easily detected by the nose, while carbon monoxide is odorless. Considering the importance of functional groups such as sulfones and sulfonamides in agrochemicals, pharmaceuticals and materials (Figure 22),⁴ there is a high interest in new and enhanced synthesis methods.¹⁵¹

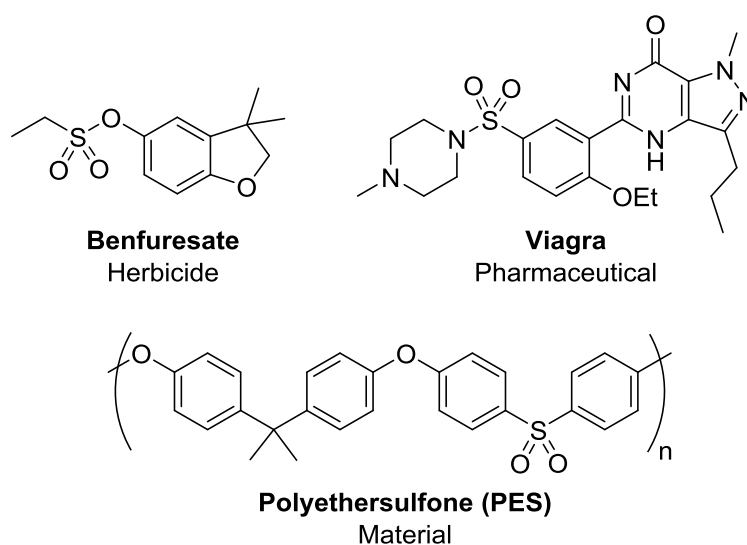


Figure 22: Important industrial compounds containing an SO₂ group.

The reactivity of SO₂ in synthetic organic chemistry is diverse. This is a result of the unique structure of SO₂ (Figure 23).¹⁵² The sulfur atom has amphoteric properties: a lone pair in a high-lying HOMO (black) resulting in nucleophilicity (σ-donor) and a low-lying LUMO (white & grey) with the largest orbital coefficient on the sulfur atom, implying electrophilic properties. Moreover, SO₂ can possess a relatively stable SOMO, which allows it to participate in radical reactions.

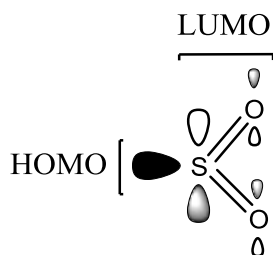


Figure 23: Frontier orbitals of SO_2 . HOMO in black and LUMO in white and grey.

The use of sulfur dioxide in synthetic organic chemistry is reviving. It is believed that the advancement of convenient and stable SO_2 surrogates is an important driver in the rejuvenation of organic synthesis research involving SO_2 .¹⁵³ The Willis group was the first to demonstrate the utility of $\text{DABCO} \cdot (\text{SO}_2)_2$ (abbreviated as DABSO, Figure 24), a bench-stable solid reagent, as a sulfur dioxide equivalent with more than 50 w% SO_2 and an excellent vacuum stability. DABSO is used in the synthesis of *N*-aminosulfonamides, sulfonamides, sulfones and sulfamides.^{54, 154} Since then, numerous synthetic studies using DABSO as SO_2 equivalent have been published.¹⁵⁵⁻¹⁶⁰ Moreover, in some cases the use of DABSO was more successful than using SO_2 gas, presumably due to catalyst poisoning by the excess sulfur dioxide when gas is used.¹⁵⁵

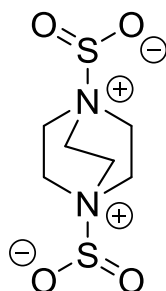
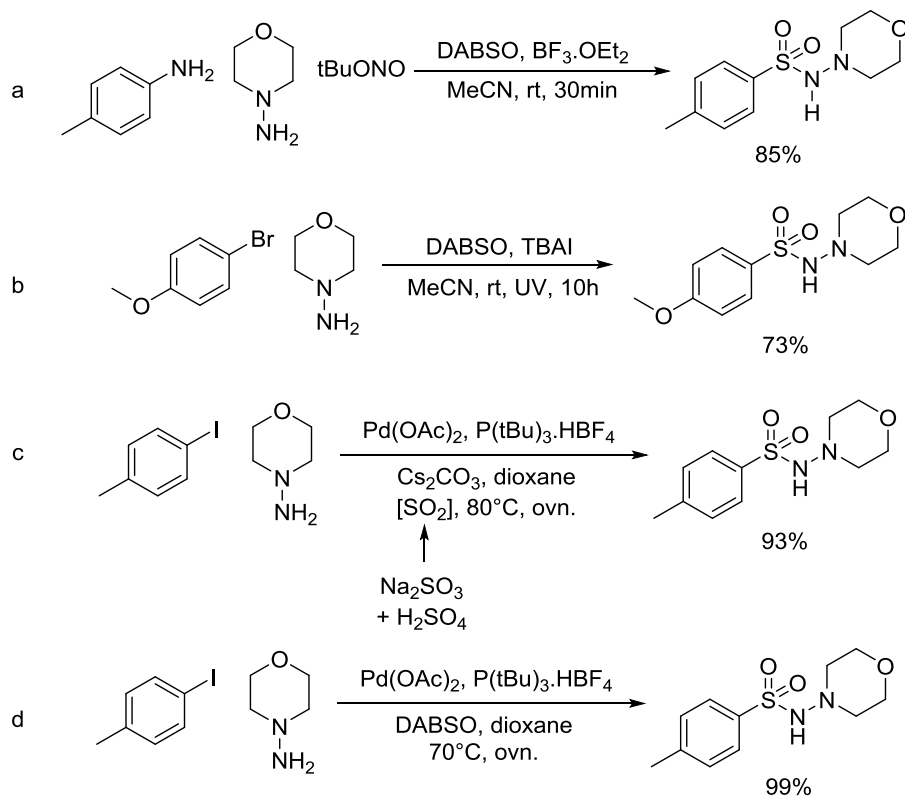


Figure 24: DABSO, a bench-stable SO_2 gas surrogate.

Most reactions involving SO_2 insertion are performed with hydrazines as nucleophiles.^{54, 154-156, 159} Both transition-metal catalyzed and radical SO_2 insertions did not yield product when using amines. This is mostly ascribed due to increased nucleophilicity of hydrazines. Some literature examples are depicted in Scheme 35.^{73, 155, 161-162} Most reports also include one or two simple amines in the scope which show no reactivity. Also, to the best of our knowledge, no mention is made of hydroxylamines as nucleophiles. This is

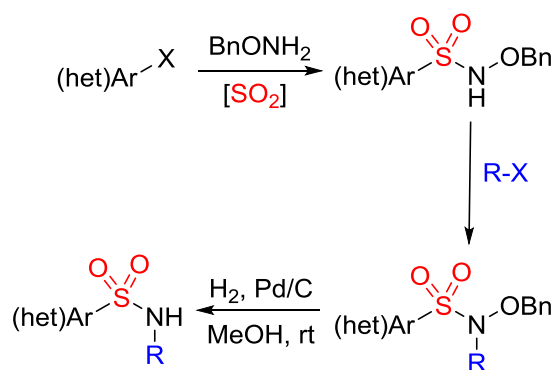
surprising, since their nucleophilicity is higher than that of amines (though lower than that of hydrazines). Moreover, nucleophilicity is probably not the only factor, since a report determined that methylamine is more nucleophilic than hydrazine.¹⁶³ Moreover, the hydrazine scope is not very elaborate. It was noticed that in all cases no hydrazines with a hydrogen on both nitrogens were used, which surprised us as well.



Scheme 35: Examples from literature of both radical and transition-metal catalyzed SO_2 insertion for the synthesis of N-aminosulfonamides.

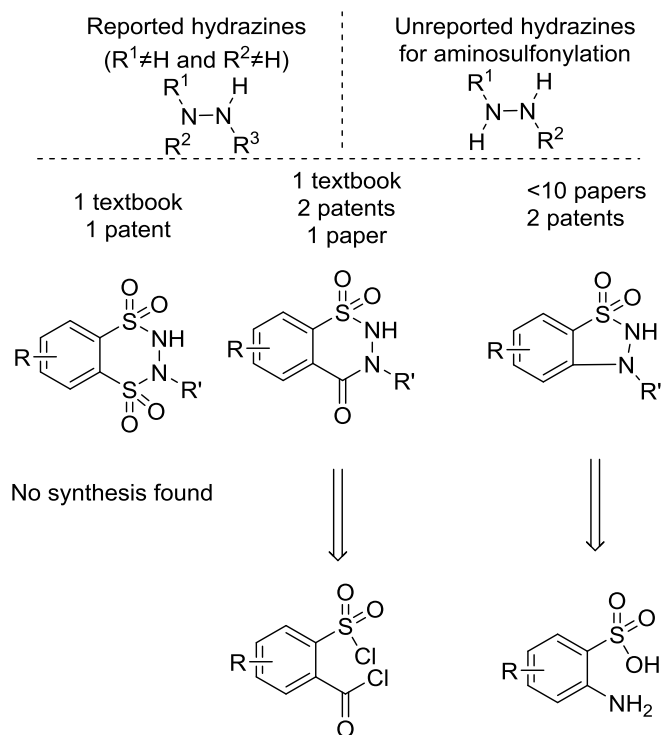
As mentioned above, hydroxylamines were never reported as nucleophiles in SO_2 insertion chemistry. However, a report by King and coworkers showed that N-sulfonylhydroxylamines are easily N-alkylated.¹⁶⁴ This is in contrast with alkylation/arylation of sulfonamides which requires transition metals (e.g. Chan-Lam coupling)¹⁶⁵ and/or elevated temperatures.¹⁶⁶⁻¹⁶⁷ We hypothesized that when combining this with an earlier report from our group to selectively cleave a hydroxylamine,¹⁶⁸ this could lead to a three step

synthesis to highly functionalized sulfonamides (Scheme 36) starting from aryl halides.

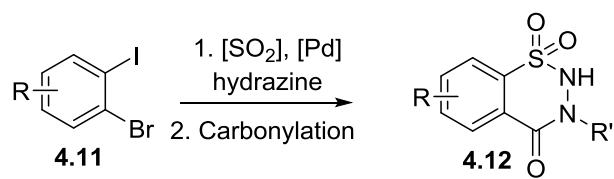
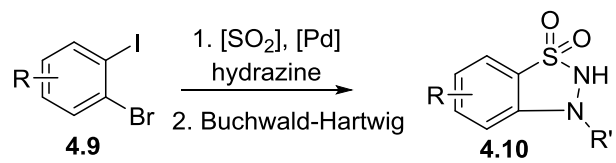
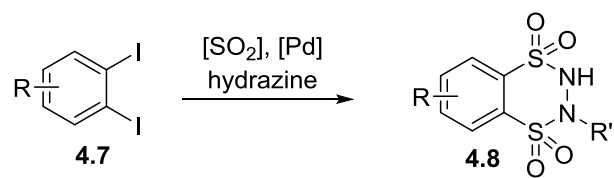


Scheme 36: Proposal for the synthesis of functionalized sulfonamides.

Another objective of this chapter is the following. As already stated, no hydrazine with at least one hydrogen on each nitrogen is reported in SO₂ insertion literature (Scheme 37). This could however be interesting for cyclizations for the synthesis of sulfonyl containing heterocycles (Scheme 37). As it appears, these heterocycles are rare in literature. It could be of interest to synthesize these scaffolds using SO₂ insertion chemistry (Scheme 38). Indeed, these reports¹⁵⁴⁻¹⁵⁵ included examples of functional groups in the ortho position and a complete selectivity of aryl iodides over aryl bromides.



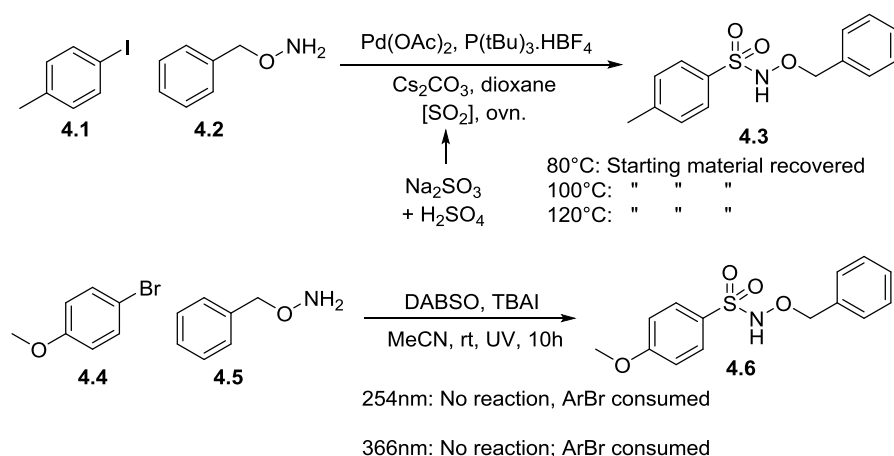
Scheme 37: Upper: Unreported hydrazines for these chemistries. Below: Selected sulfonyl containing heterocycles and their synthesis.



Scheme 38: Synthesis proposals for the selected sulfonyl containing heterocycles with unreported hydrazines.

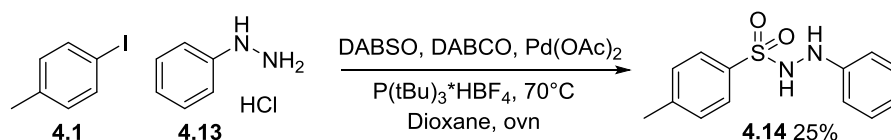
4.2 Results and discussion

Two literature procedures for aminosulfonylation were adapted, changing the nucleophile to *O*-benzylhydroxylamine (**4.2**, Scheme 39). First, a two-chamber procedure was attempted by generating sulfur dioxide from sodium sulfite and sulfuric acid,⁷³ but did not lead to product formation, even at higher temperatures than reported. Also the reported UV reaction¹⁶² did not yield any product. After column chromatography, a complex mixture was obtained without recovering the starting material. As it appears, hydroxylamines do not undergo these type of SO₂ insertions, which makes them similar in reactivity to amines in this respect.



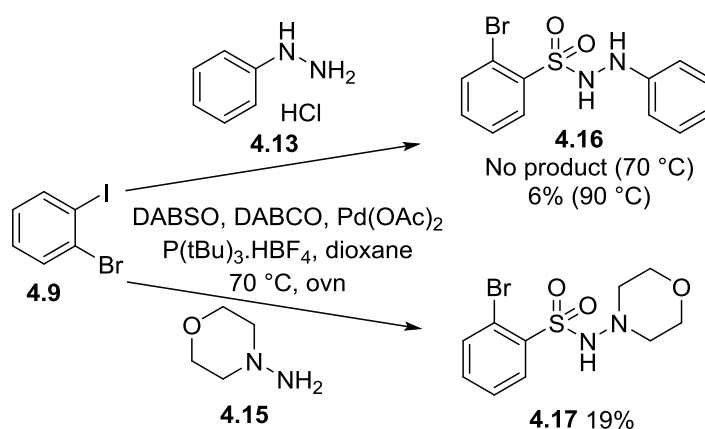
Scheme 39: SO₂ insertions with a hydroxylamine as nucleophile.

Since 1,1-diphenylhydrazine and 1,1-methylphenylhydrazine are used as nucleophiles in multiple transition metal catalyzed SO₂ insertion reports, it was decided to try using phenylhydrazine (**4.13**) as test case (Scheme 40). The reaction between *p*-tolyl iodide (**4.1**) and phenyl hydrazine (**4.13**) was tried in the presence of DABSO in order to produce compound **4.14**. Note that an HCl-salt was used, therefore one extra equivalent of DABCO was added. In a first attempt white crystals were formed upon evaporation of the eluent from chromatographic purification. However, when breaking the vacuum, the crystals turned purple. NMR analysis indicated that the product degraded. Intrigued by this result, it was decided to break the vacuum in the rotavapor using a nitrogen atmosphere, keeping the crystals in a protective environment. The purple color was not intense, and NMR indicated the product had formed and was isolated in 25% yield.



Scheme 40: Palladium-catalyzed SO_2 insertion with a hydrogen on both nitrogens.

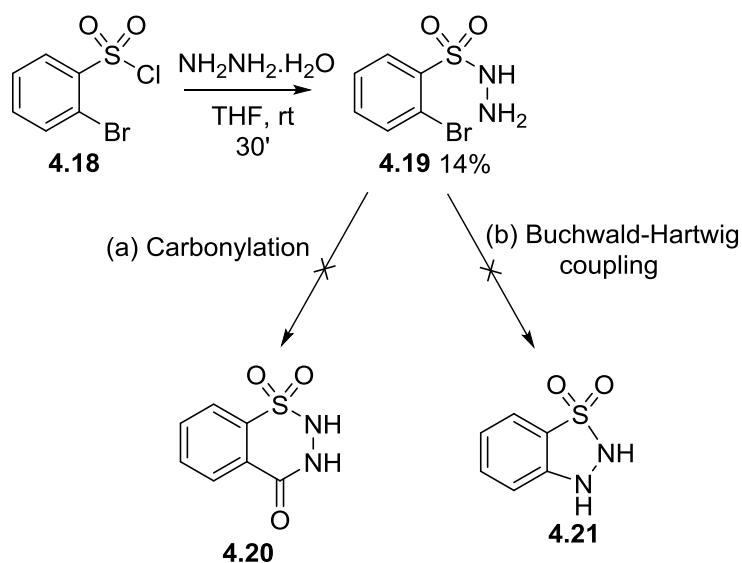
Keeping this sensitivity in mind, in a similar fashion, we attempted to synthesize *o*-bromo derivative **4.16** (Scheme 41). To our delight the product was isolated when applying higher temperatures, albeit in a very low yield. However, significant amounts of starting material were recovered. When *N*-aminomorpholine (**4.15**) was used as nucleophile, **4.17** was isolated in 19% yield. The low yield is surprising since *N*-aminomorpholine is the standard nucleophile in literature reports, and examples with *ortho* substituents are known.¹⁵⁵



Scheme 41: Synthesis of *ortho*-bromo derivatives.

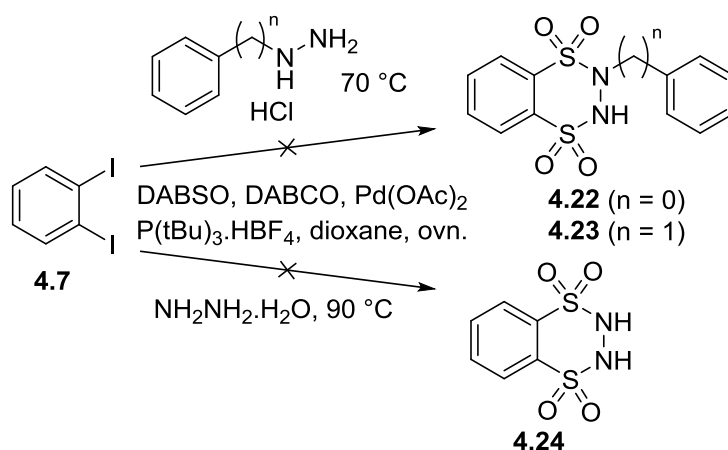
Due to these disappointing yields, another substrate (**4.18**) was used for generating the precursors for cyclization (Scheme 42). The low yield (14%) of the substitution is surprising since we did not obtain dimer product and the starting material appeared to be consumed. It was hypothesized that a lot of product was lost during extraction workup. Indeed, in the water layer both product and dimer product were found. This is due to increased acidity of the NH, resulting in significant product loss during work-up. In a next step, with the little amount of product obtained, ring closures via carbonylation and Buchwald-Hartwig amination were attempted. Both carbonylation and Buchwald-Hartwig amination were palladium-catalyzed and carried out at

100 °C in toluene. In neither case however, conversion was observed and starting materials were recovered.



*Scheme 42: Cyclizations attempts via carbonylation (a) and Buchwald-Hartwig coupling (b).
 (a): two chamber reaction, HCOOH , MsCl , Et_3N , $\text{Pd}(\text{OAc})_2$, Xantphos, Na_2CO_3 , toluene, 100 °C.
 (b) NaOtBu , K_2CO_3 , $\text{Pd}(\text{PPh}_3)_4$, toluene, 100 °C.*

The double SO_2 insertion of *o*-diiodobenzene (**4.7**) was also attempted (Scheme 43). Both benzyl hydrazine and phenylhydrazine appeared to be ineffective, as significant amounts of *o*-diiodobenzene were retrieved after reaction. A higher temperature in combination with hydrazine had the same outcome: no conversion.



Scheme 43: Double SO₂ insertion attempt on ortho-diiodobenzene.

At this point, it was decided to abandon the SO₂ insertion chemistry, mainly due to the disappointing yields. In our hands, when exactly repeating literature procedures, much lower yields were obtained, implying the sensitivity of this chemistry.

4.3 Preparation of DABSO

This section is based on:

S. Van Mileghem and W. M. De Borggraeve, A convenient multigram synthesis of DABSO using sodium sulfite as SO₂ source, *Org. Process Res. Dev.*, **2017**, 785-787.¹⁶⁹

In **chapter 4.2**, DABSO was used as a SO₂ gas surrogate. Since DABSO is a relatively expensive chemical, some research groups synthesize it on site.^{154, 170-171} We also had the intention to synthesize it ourselves. However, the reported procedures include the use of sulfur dioxide gas, implying safety considerations regarding the handling and storage of sulfur dioxide pressurized vessels and using a large excess of the gas. Usually DABSO precipitates out of solution when formed. The Bischoff group circumvented the use of SO₂ vessels by synthesizing DABSO with the commercially available Karl-Fischer reagent.¹⁷²⁻¹⁷³ However, since this reagent is a solution of a base (usually pyridine) and an alcohol (usually methanol) containing 15-20% of SO₂, this protocol leads to more complex mixtures and a low atom economy. Moreover, DABSO is soluble in methanol, resulting in a less efficient precipitation. To the best of our knowledge, no protocol for the synthesis of DABSO is reported where SO₂ is generated in a controlled fashion and consumed in a closed system, omitting multiple safety issues of working with this toxic gas.

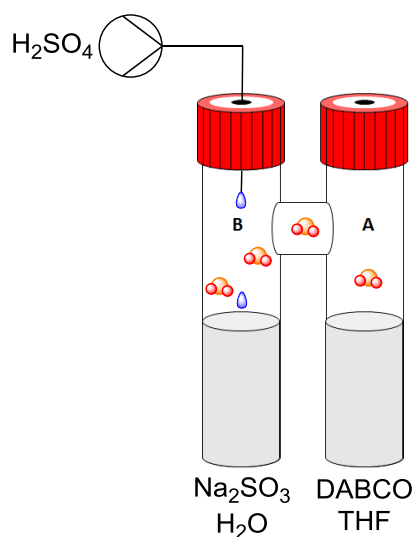
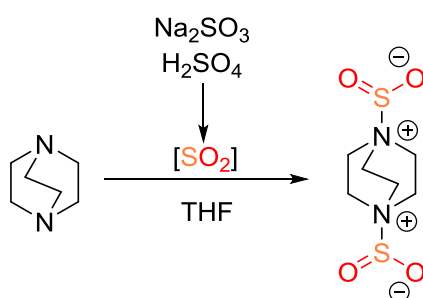


Figure 25: Reaction set-up. SO_2 is gradually generated in chamber B and is consumed in chamber A to form DABSO.

By making use of the elegant two-chamber system (COware) reported by Skrydstrup *et al.*⁶⁻⁷ it is possible to generate sulfur dioxide *ex situ*. The reaction set-up is depicted in Figure 25 and the results are summarized in Table 10. Metal sulfite salts are known to release SO_2 when reacting them with strong acids.⁴ Moreover, the use of sodium sulfite as an SO_2 surrogate has been applied in palladium-catalyzed aminosulfonylation.⁷³ Due to its simplicity and cheap nature, this was our SO_2 surrogate of choice. Since the release of SO_2 from sodium sulfite and strong acid is fast,⁴ a gradual release is needed to avoid generating too high pressure in the reactor. Furthermore, sulfur dioxide is far more soluble in water and organic solvents than other gases used in synthesis (*e.g.* CO and H_2).¹⁷⁴⁻¹⁷⁶ Therefore, sodium sulfite is solubilized in water, and sulfuric acid is slowly added by means of a syringe pump, resulting in a gradual release of SO_2 .

Table 10: Results of two-chamber synthesis of DABSO.



Entry	mmol DABCO	V _{THF} (mL)	V _{Water} (mL)	V _{Sulfuric acid} (μL/min)	V _{Sulfuric acid} (μL)	eq Na ₂ SO ₃	t (h)	Yield (%)
a^a	6	8	8	100	960	2.5	2	94
b^a	6	8	8	100	960	0	2	0
c^a	6	8	8	100	800	2.2	2	92
d^b	45	30	25	50	6000	2.2	ovn	63
e^b	45	60	40	50	6000	2.2	ovn	99
f^b	45	60	40	50	6000	2.2	3	53

ovn = overnight, V = volume, v = syringe flow rate. ^a 20 mL inner volume two-chamber reactor. ^b 400 mL inner volume two-chamber reactor

In a first trial, DABCO (673 mg, 6 mmol) was added in THF (8 mL) in chamber A while 2.5 equivalents (1.89 g) of sodium sulfite were added in water in chamber B (entry **a**). Next, sulfuric acid (960 μL, 3 equivalents) was added dropwise over 10 minutes to chamber B. After 15 minutes, a white precipitate was observed, indicating DABSO formation. After 2 hours of stirring at room temperature, filtration and overnight drying, DABSO was obtained in a yield of 94%. (It should be noted that the overnight drying was performed either on a Schlenk line or in a dessicator. When drying under high vacuum (lyophilizer), a lot of product was lost!) To make sure no other impurities were precipitating in chamber A, a blank reaction was performed without the use of sodium sulfite (entry **b**). No precipitate was formed in chamber A. Using a lower excess of both sodium sulfite and sulfuric resulted in a nearly identical yield (entry **c**). At this stage, it was desirable to perform this reaction at a larger scale. Therefore, the flow rate of sulfuric acid was lowered to 50 μL min⁻¹ to avoid pressure build-up and the reaction was

stirred overnight. A first scale-up resulted in a disappointing yield of 63% (entry **d**). It was hypothesized that this result could be attributed to increasing the molarity of DABCO in THF. After stirring overnight, DABSO was precipitated and barely any THF was visible. This could have led to a physical barrier (DABSO matrix) between the remaining DABCO and SO₂. To our delight, when more THF was used, this issue was resolved and a quantitative yield was obtained (entry **e**). Since first signs of precipitation of DABSO are apparent after about 2 hours of reaction, an attempt to decrease the reaction time was tested (entry **f**). A disappointing yield of 53 % was obtained and hence more time is needed to bring the reaction to completion.

A price comparison between the two protocols can be found in Table 11. Comparison was done on a 45 mmol scale reaction. Reagents of the Bischoff protocol are carefully adopted.¹⁷³ Note that these price calculations are only indicative, as they will change over time. Commercial prices are based on the online catalogues of Sigma-Aldrich (*date of consultation: 24th January 2017*). Remark that costs of glassware, desiccators and working hours are not implemented. Since the difference in yield is very small, this is neglected in the calculation. As it appears, our protocol is about two and a half times less expensive. Furthermore, commercially available DABSO is about 27 times more expensive. Results are summarized in the table below. The most significant price difference is the use of anhydrous solvents: other reports stress the use of anhydrous solvents. In our hands however, no difference was found between anhydrous and wet solvents towards DABSO purity (determined by CHN-analysis).

Table 11: Price comparison between reported DABSO syntheses.

Our protocol			Bischoff protocol		
Reagent	Quantity	Cost	Reagent	Quantity	Cost
DABCO	5.05 g	€ 1.21	DABCO	5.05 g	€ 1.21
THF	60 mL	€ 1.88	THF (anhydrous)	60 mL	€ 7.79
Na ₂ SO ₃	12.48 g	€ 1.47	Karl-Fisher reagent	40 mL	€ 5.40
H ₂ SO ₄	6 mL	€ 0.28	Et ₂ O (anhydrous)	200 mL	€ 15.88
Et ₂ O	200 mL	€ 6.70			
		€ 11.54			€ 30.28
	Relative cost:	1			2.62
	Cost per gram DABSO	€ 1.07 / g			€ 2.81 / g

Cost per gram DABSO from Sigma Aldrich: € 28.9 / g. Relative cost: 27

As an example the theoretical maximum generated pressure will be calculated. Therefore, it was assumed that N₂ and SO₂ behave as ideal gases, and that no gas is soluble in our solvents of choice (which is not the case for SO₂, which dissolves very well in water). In entry e, (see Table 10), the total solvent volume is 100 mL (60 mL THF, 40 mL H₂O). At this point, since the inner volume of our two-chamber reactor is 400 mL, the remaining volume is 300 mL. Therefore, according to the ideal gas law:

$$n = \frac{pV}{RT} = \frac{1 \text{ atm} \times 0.300 \text{ L}}{0.082 \frac{\text{L} \times \text{atm}}{\text{K} \times \text{mol}} \times 298 \text{ K}} = 12.28 \text{ mmol nitrogen}$$

Thus, 12.28 mmol N₂ is present before adding sulfuric acid. When all sulfuric acid is added (neglecting the pressure generated by 6 mL extra liquid) and assuming that the conversion of H₂SO₄ and Na₂SO₃ is 100%, we generate 99 mmol of SO₂ (2.2 equivalents of 45 mmol DABCO). When assuming that no DABSO is formed, 113 mmol of gas is present (14 mmol N₂ + 99 mmol SO₂). Hence the pressure is,

$$p = \frac{nRT}{V} = \frac{0.113 \text{ mol} \times 0.082 \frac{\text{L} \times \text{atm}}{\text{K} \times \text{mol}} \times 298 \text{ K}}{0.300 \text{ L}} = 9.2 \text{ atm}$$

Thus, the theoretical maximum generated pressure in the two-chamber set-up is 9.2 atm. However, the two-chamber reactors septa can resist up to 5 bar, and no pressure release was observed when reactions were carried out at this scale. This is, of course, a consequence of a combination of factors such as gradual SO₂ release, high solubility of SO₂ in water and immediate SO₂ capture by DABCO.

In conclusion, we have developed a convenient multigram synthesis of DABSO. Sulfur dioxide is generated and consumed in a closed two chamber system, hereby avoiding a lot of safety issues of working with the toxic gas. The danger of pressure build-up is avoided by gradually releasing SO₂. No heating or cooling is required, nor is working with anhydrous solvents. High to quantitative yields are obtained. This protocol is suited for synthesizing DABSO on a 10 gram scale.

CHAPTER 5

TOWARDS A CONTINUOUS SYNTHESIS OF GLYCEROL CARBONATE USING GLYCEROL AND DIMETHYL CARBONATE

5 Towards a continuous synthesis of glycerol carbonate using glycerol and dimethyl carbonate

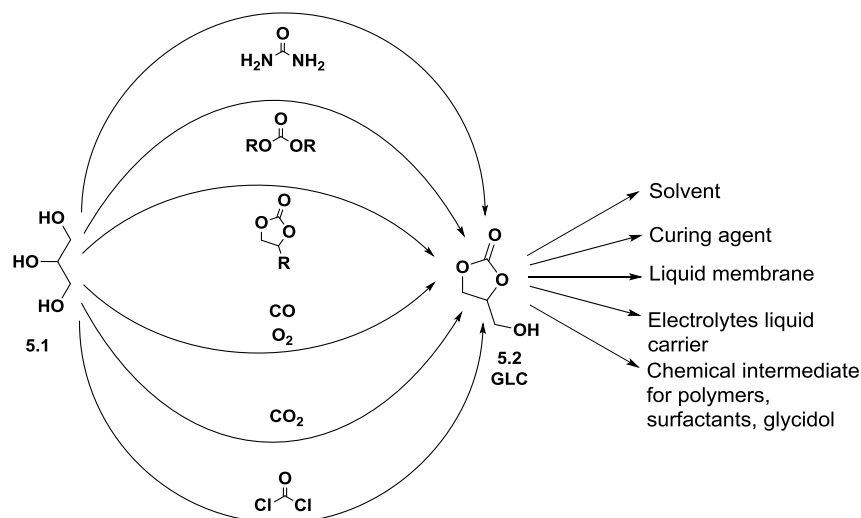
This research was performed during a 6 month internship at Durham University under the supervision of Prof. Ian R. Baxendale.

5.1 Literature and objectives

There is a lot of industrial interest in the valorisation of glycerol in recent years, mainly due to glycerol (**5.1**) being a waste product from biodiesel production. The growth of this industry accounted for 2247 kilotons of glycerol in 2013 and the global glycerol market is expected to reach \$2.52 billion by 2020.¹⁷⁷ The conversion of glycerol to value-added products has therefore received considerable attention. Some examples are hydrogenolysis to 1,2-propanediol,¹⁷⁸ dehydration to allyl alcohol¹⁷⁹ and gasification to syngas.¹⁸⁰ Glycerol carbonate (**5.2**, abbreviated as GLC) is another interesting product derived from glycerol, and is considered a renewable building block due to its versatility.¹⁸¹ Applications of GLC include its use as curing agent,¹⁸² surfactant,¹⁸³ chemical intermediate for polymer production¹⁸⁴ and electrolyte liquid carrier.¹⁸⁵ GLC is also becoming increasingly popular as a safe bio-based alternative to organic solvents, due to a high boiling point (115 °C at 0.1 mbar) and low volatility (vapour pressure of 8 mbar at 177 °C).¹⁸⁶ Moreover, GLC is water-soluble, non-toxic, readily biodegradable and non-flammable.

The conversion of glycerol to GLC has been extensively studied (Scheme 44).¹⁸¹ Examples of its synthesis include the use of phosgene, carbon monoxide and carbon dioxide.¹⁸¹ Other reagents such as organic carbonates and urea have also been used. The direct use of carbon dioxide is desirable, but known processes for direct GLC synthesis from CO₂ often include the use of toxic tin reagents and glycerol conversions are low (up to 30%). These processes are therefore not feasible for application on an industrial scale.¹⁸⁷ Dimethyl carbonate (DMC) is widely studied as a carbonyl source to synthesise GLC since it is considered an environmentally benign chemical. It is also used in industry to synthesise GLC.^{188,189-192} A lot of catalysts are known for this transformation, *e.g.* inorganic bases,¹⁹³⁻¹⁹⁶ tertiary amines,¹⁹⁷⁻¹⁹⁹ lipases,²⁰⁰⁻²⁰² and *N*-heterocyclic carbenes.²⁰³ However, to our surprise only a few continuous processes are known for this transformation.²⁰⁴⁻²⁰⁵ In general, continuous processes more often meet the basic criteria for potential industrial feasibility and scale up. To the best of our knowledge, inorganic

bases are the catalysts of choice for industrial preparation of GLC from glycerol and DMC.¹⁸⁹⁻¹⁹²



Scheme 44: Main routes for the synthesis of glycerol carbonate from glycerol.

The objective of this project was the development of a continuous flow process starting from glycerol to synthesize either glycerol carbonate or glycidol in a scalable, green manner. The goal was to optimize a protocol which has industrial applicability. Therefore, dimethyl carbonate, due to its considered greenness, was the phosgene surrogate of choice to be combined with glycerol an industrial waste product from biodiesel synthesis. Different catalysts had to be screened, keeping in mind that industry prefers easy to separate, cheap and non-toxic ones. Both reported catalysts and new catalysts had to be tested.

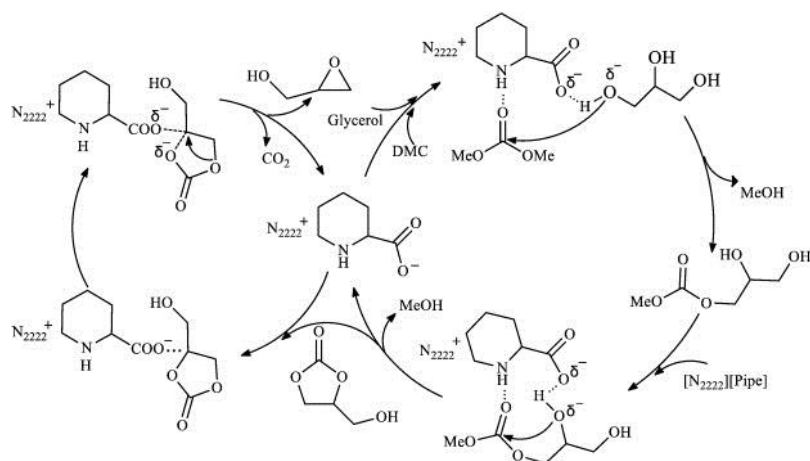
5.2 Results and discussion

Our applied strategy existed of first repeating reported batch procedures, and second, translating them to an optimized flow process. As a starting point of our investigation, reported neat batch experiments with homogeneous catalysts were performed, in order to get a better understanding of this transformation and testing if this chemistry was reproducible (Table 12). It quickly became clear that basicity of the catalyst is an important parameter: the stronger the base, the higher the observed GC yield, which is in accordance with the literature findings (entries 1-4).¹⁸¹ Increasing the temperature also yields better results (entries 4-5). In previous work performed on the attempted synthesis of glycidol, an experiment of Tao and coworkers was repeated:²⁰⁶ tetraethyl ammonium amino acid ionic liquids were reported as efficacious catalysts for the one-pot neat synthesis of glycidol, starting from glycerol and dimethyl carbonate under reflux conditions. However, when we repeated their experiments, we were not able to get selectivity towards glycidol. Instead, a high selectivity towards GLC was obtained (entries 6-7). Intrigued by the results of this type of catalyst, some alternatives were used for this transformation (entries 8-10). The low yields could suggest that both an NH-moiety and carboxylate are required for efficient catalysis, which is in line with the mechanism proposed for the formation of the GLC intermediate in the paper by Zhou *et al* (Scheme 45).²⁰⁶

Table 12: Initial batch investigation.^a

Entry	Catalyst	Temp	Duration	GC Yield (%)
1	KOH	rt	ovn	79
2	nBuLi	rt	ovn	93
3	NEt ₄ I	rt	ovn	20
4	tBuOK	rt	ovn	66
5	tBuOK	60	ovn	95
6		reflux	2h	92
7		reflux	2h	91
8	NBu ₄ OAc	reflux	2h	5
9		reflux	2h	Trace
10		reflux	2h	5

^a rt = room temperature, ovn = overnight. Conditions: 5 mmol scale, 3.5 equivalents DMC, 5 mol% catalyst



Scheme 45: Proposed mechanism from reference 206. As stated, the catalytic cycle ended with GLC formation (only traces of glycidol were observed). Reprinted with permission from *Cat. Commun.*, **2015**, 25-29. Copyright Elsevier.

With these preliminary results at hand, it was desirable to translate these experiments to a continuous flow process. Compound **5.3** (Table 12, entry 6)

was chosen as the catalyst of choice for homogeneous catalysis flow experiments since it is a cheap and mild catalyst. A Vapourtec® R-series system which was equipped with a PTFE coil reactor was used as flow platform. Since DMC and glycerol are immiscible at room temperature, a two stream setup was used as depicted in Table 13. The relative flow rate was adjusted in such a way to obtain 3.5 equivalents of DMC. Initially we adopted the protocol from the de Souza group,²⁰⁴ using neat glycerol with catalyst, preheated at 70°C (entry 1). It was immediately observed that pumping this viscous mixture was not possible. A solvent which is able to dissolve both glycerol and DMC was desired, *e.g.* aliphatic alcohols. Therefore glycerol and **5.3** were dissolved in ethanol for further experiments. It quickly became clear that GLC formation increased with temperature. Applying a temperature of 140 °C yielded a 90% conversion and 85% selectivity (entry 4). When repeating these conditions in absence of catalyst **5.3**, almost no GLC formation was observed (entry 5). Variation of residence time resulted in small differences in conversion, while a slight decrease in selectivity was seen when increasing residence time (entries 6-7). It is worth noting that small amounts of diethyl carbonate were formed in experiments involving ethanol as evidenced by ¹H NMR. In a final experiment, water instead of ethanol was used as solvent and a low conversion was obtained (entry 8). This might be due to a biphasic segmented flow, while a homogeneous flow was observed when ethanol was used as solvent. Another reason is that under these conditions water could have hydrolyzed GLC. The synthesis of GLC using catalyst **5.3** gave some nice results in flow. A key aspect of industrial applicability however is ease of purification of the product. In this case, the catalyst removal was not very straightforward. However, this catalyst would be easily removed from the reaction mixture if it were heterogeneous.

Table 13: Homogeneous catalysis flow experiments.^a

Entry	Catalyst	Temp (°C)	t _R (min)	V _R (mL)	C (%)	S (%)
1 ^b		100	30	10	/	/
2		100	30	10	15	71
3		120	30	10	53	84
4		140	30	10	90	85
5	None	140	30	10	<5	/
6		140	40	20	85	83
7		140	15	10	82	92
8 ^c		140	30	10	10	75

^a t_R = residence time, V_R = reactor volume, C = conversion, S = selectivity. Conditions: 3.5 equivalents of DMC. BPR = 100 psi. ^b Neat glycerol + catalyst preheated at 70 °C used. ^c Water (1M) used instead of ethanol.

As stated above, the ease of separation of catalyst after reaction is one of the key requirements for industrial applicability and we therefore wanted to see if good results would be obtained as well when making use of a heterogeneous catalyst, similar to **5.3**. Therefore, additional batch experiments were carried out, this time using polymer supported catalysts (Table 14). Pipecolic acid was loaded on to a solid support via a simple neutralisation reaction of Ambersep® 900 Hydroxide (**5.5**) to generate catalyst **5.4** (Table 14). When testing this catalyst in a batch reaction under neat reflux conditions, a nearly quantitative conversion towards GLC was obtained (entry 1). To rule out the catalytic effect was due to residual hydroxide present in the catalyst starting material, a blank experiment was performed using Ambersep® 900 Hydroxide as catalyst (**5.5**, entry 2). Low conversion was obtained, attributing the catalytic effect to the pipecolic acid. Note that this result differs greatly from potassium hydroxide as catalyst, where a good conversion was obtained (Table 12, entry 1). This could be

explained due to mass transport limitations. Only a slight increase in yield was observed when methanol was used as cosolvent (entry 3) or when the reaction was carried out at 120 °C in a microwave reactor (entry 4). These results strongly suggest that a different mechanism takes place when using weakly basic catalysts of type **5.4** than strongly basic catalysts, as proposed by the report of Tao and coworkers.²⁰⁶

Table 14: Heterogeneous catalysis experiments in batch.^a

Reaction scheme: Glycerol (HO-CH₂-CH(OH)-CH₂-OH) + Dimethyl carbonate (CH₃O-CO-OCH₃) $\xrightarrow{\text{Cat.}}$ 2-(hydroxymethyl)-1,3-dioxolane-4-one

Entry	Catalyst	GC Yield (%)
1	 5.4	95
2	 5.5	10
3^b	 5.5	27
4^c	 5.5	40

^a Conditions: reflux (2h), 20 mmol scale, 3.5 equivalents DMC, 1 g polymer (about 1 mol%). ^b Methanol used as cosolvent. ^c Microwave, 1 hour, 120 °C.

As **5.4** was deemed a suitable catalyst for this transformation, it was again attempted to translate this to a continuous flow process. A column reactor was filled with catalyst and heated to the appropriate temperature while the reagents are being pumped through. The results are summarised in Table 15. *[It should be noted that mentioned residence times might be slightly underestimated since the polymer beads have the tendency to contract when being heated!]* Methanol was the solvent of choice for dissolving glycerol, since it is more easily removed than ethanol and results in less complex mixtures as methanol is generated as by-product in the reaction as well. Moreover, this time a more concentrated solution than in Table 13 was used, since minimisation of solvent volume is also desired in industrial applications. Also, reaction of methanol and GLC yields the starting materials instead of side products. In a first trial, the reaction was run with a residence time of 15 minutes at 100 °C and resulted in 85% conversion with a 89% selectivity for

GLC (entry 1). Since we were interested if the observed tendencies in batch would be equal in flow, these conditions were repeated with the strongly basic catalyst **5.5**. A 73% conversion and 93% selectivity were obtained (entry 2), which is in stark contrast to the results in batch (Table 14, entries 1-2), where the difference in efficacy between both catalysts was far more pronounced. Moreover, in the continuous flow setup, the differences in the results are relatively small. Also, polymer supported basic catalysts have been used before for the neat batch synthesis of GLC, without much success.¹⁹⁶ It should be noted that there is of course a significant difference in the reported batch processes and our flow experiments since no methanol is used in the batch experiments. Moreover, **5.5** is a cheap and commercially available catalyst. It was therefore decided to further optimise this process with catalyst **5.5** instead of with catalyst **5.4**. High conversion and selectivity were obtained when raising the reactor temperature to 120 °C (entry 3). To our delight, when further increasing the temperature to 140 °C, the residence time could be lowered to 3 minutes without significant differences in GLC formation (entry 4). It was observed that a higher excess of DMC resulted in higher glycerol conversion, but decreased the selectivity due to formation of diglycerol tricarboxylate, in accordance with the literature (entry 5).²⁰⁷ Using neat glycerol was attempted by making use of peristaltic pumps (VapourTec E-series system) and following the the protocol of de Souza *et al.*,²⁰⁴ *i.e.* preheating glycerol to 70°C (entry 6). Only 30% conversion was obtained. Methanol seems to be a required cosolvent enhancing the homogeneity of the liquid phase and therefore, allowing better mixing and short residence times in combination with high conversion and selectivity. This is in this case not possible when using neat glycerol. Ochoa-Gómez *et al.* hypothesized that formation of GLC only occurs if the glyceroxide anion is formed.¹⁹⁶ Therefore, close contact between the catalytic sites and glycerol is required, which is of course enhanced by homogeneity of the liquid phase. According to the Ochoa-Gómez group, mass transport limitations also explain why their results are poor when using heterogeneous strongly basic ion exchange resins Amberlyst A260H and Amberjet 4400 OH in batch.¹⁹⁶ Also in our hands only low conversion in batch under reflux conditions was obtained with our heterogeneous, strongly basic catalyst, Ambersep 900 Hydroxide (**5.5**, entry 2). The success of the flow methodology is hypothesized to be a combined effect of (a) using higher temperatures, (b) inducing a homogeneous liquid phase by adding methanol and (c) performing the reaction in a continuous column reactor, thus inducing more turbulence

than conventional batch stirring. Motivated by these findings, it was decided to keep using methanol as cosolvent.

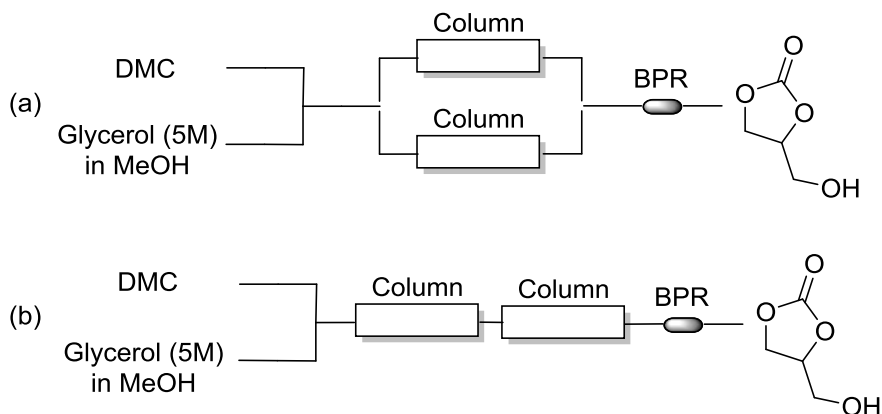
Table 15: Heterogeneous catalysis flow experiments.^a

Entry	Catalyst	Temp (°C)	t _R (min)	C (%)	S (%)
1		100	15	85	89
2		100	15	73	93
3		120	15	90	94
4		140	3	90	83
5 ^b		120	5	100	67
6 ^c		120	5	30	90

^a 3.5 equivalents DMC. t_R = residence time, BPR = back pressure regulator (250 psi used at 140 °C, otherwise 100 psi), C = conversion, S = selectivity. ^b 10 equivalents DMC used. ^c Neat glycerol preheated at 70 °C used.

Since conversion and selectivity were quite similar in both homogeneous and heterogeneous flow catalysis, but residence time was longer for the former, attempts to demonstrate the scalability of the heterogeneous flow setup were performed. As depicted in Scheme 46a, the use of parallel columns was tested. As it appears, no significant differences in GLC formation were obtained, both at 120 and 140 °C and using 3.5 equivalents of DMC, in comparison with single column usage. Distribution of the flow stream to two parallel reactors with theoretically same residence times often gives different results in our experience. In a first scale up experiment a total flow rate of 2 mL min⁻¹ was used at 140 °C and using 4 equivalents of DMC, resulting in a residence time of 4 minutes (Scheme 46b). A conversion of 95% and selectivity of 80% were obtained and maintained for 4 hours without losing efficiency, consuming 82 grams of glycerol. GLC was isolated in a 75% yield and this resulted in a space-time yield of 2.50 kg GLC per L reactor per hour. When repeating this experiment but lowering the residence time to 2 minutes, 62% isolated yield of GLC was obtained, resulting in a space-time yield of 3.38 kg GLC per L reactor per hour. A useful further extension involved the reusability of the catalyst (see **chapter 7** Experimental Section).

The catalyst was used 4 times at 120 °C for about 60 minutes per run without losing efficiency. In between runs, the catalyst beads were rinsed with methanol and dried overnight. At 140 °C a 10% decrease in conversion was observed at fourth usage. It appears that the catalyst is robust and air-stable after use.



Scheme 46: (a) The use of parallel columns. (b) Set up for scale up experiments.

While these results are not bad, further investigation is needed because of issues with reproducibility of the results. In a number of runs, for unclear reasons, we observed a significantly lower conversion when repeating certain conditions. This is of course problematic for both publication and industrial application. Indeed, reproducibility is considered one of the biggest issues in organic chemistry literature.²⁰⁸ In the meantime, follow up research in the Baxendale group showed that even better results were obtained with other heterogeneous catalysts such as polymer supported tetraalkyl ammonium derivatives with anions such as fluorides, malononitriles and triflated amines.²⁰⁹

CHAPTER 6

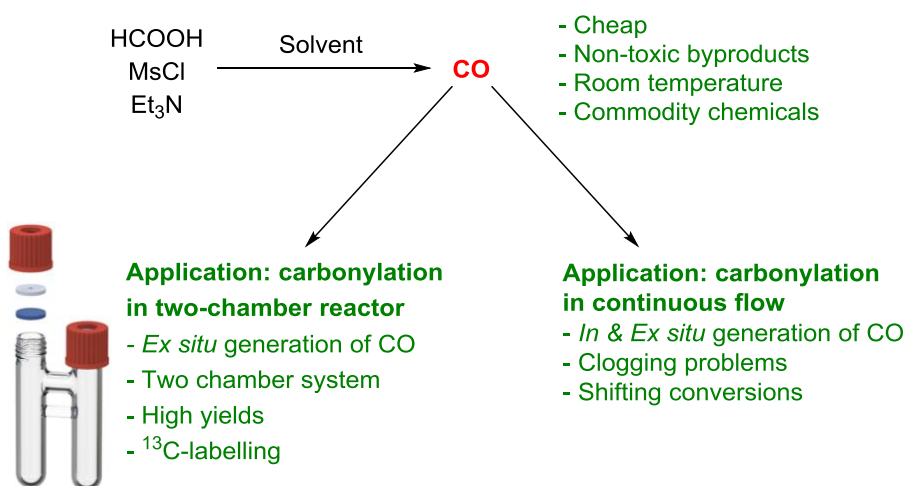
CONCLUSIONS AND FUTURE PERSPECTIVES

6. Conclusions & Future Perspectives

6.1 General conclusions

In general, contributions were made to make working with very dangerous gases in an academic lab environment more accessible. These developed procedures exceed reported ones in cost and safety.

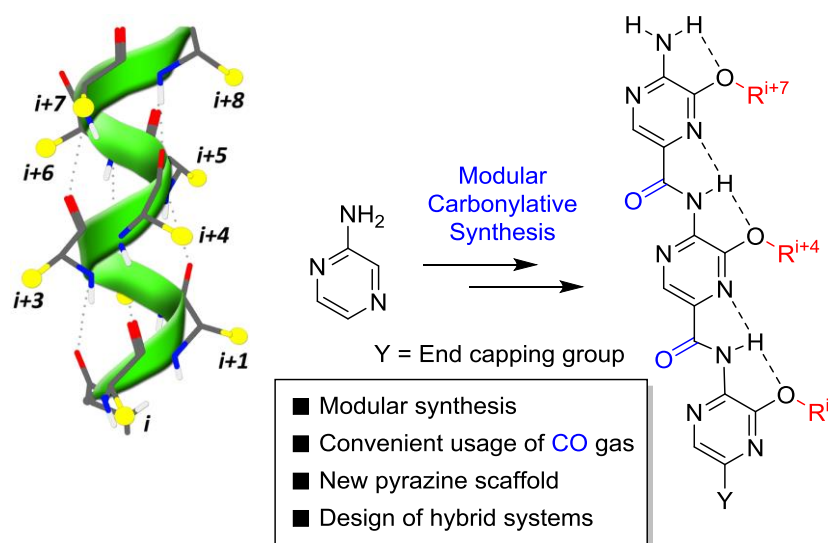
First, a convenient and safe method was developed to generate carbon monoxide. This new method uses formic acid, mesyl chloride and triethylamine to generate carbon monoxide, 3 commodity chemicals available in every organic synthesis lab and is one of the cheapest ways known to generate carbon monoxide on laboratory scale (**chapter 2.1**). This methodology was applied by means of a two-chamber reactor where in the other chamber the carbon monoxide was consumed *via* a palladium-catalyzed carbonylation (**chapter 2.2**). High yields were achieved and some biologically active compounds were synthesized via this method, with the existing possibility of labelling carbon monoxide with commercially available ^{13}C -enriched formic acid. Moreover, attempts were undertaken to use this CO precursor in continuous flow, however without much success. This is summarized in Scheme 47.⁸⁴



Scheme 47: CO generation and applications.

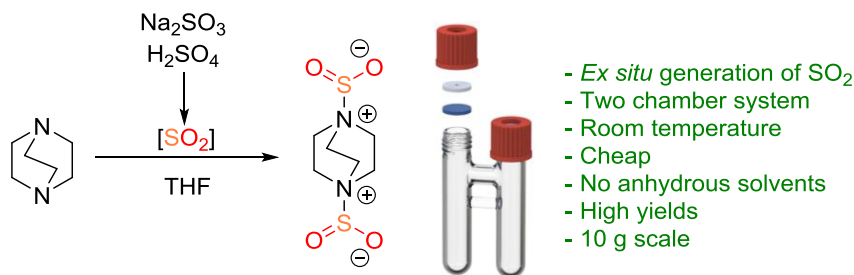
Second, the developed methodology in **chapter 2** was applied to the synthesis of minimalist α -helix peptidomimetics, scaffolds that can display amino acid side chains in a geometrically similar way as a protein α -helix

(**chapter 3**). Palladium-catalyzed aminocarbonylation reactions were used to assemble the helix mimetics. Previously unreported pyrazine based oligoamide α -helix mimetics were generated in this fashion, as well as hybrid type multimers (Scheme 48).⁸⁸



Scheme 48: A protein α -helix (left) and our developed modular synthesis of the mimetics (right).

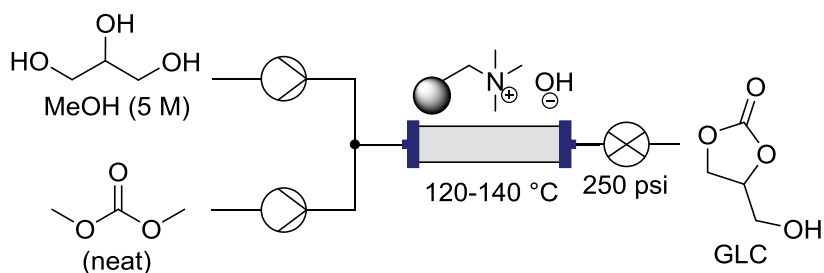
Next, the use of sulfur dioxide as reactant in organic synthesis was examined (**chapter 4.2**). Facing similar dangers as working with carbon monoxide, we developed a method for the large scale laboratory synthesis of DABSO, a common gas surrogate for sulfur dioxide, again making use of two-chamber reactors (**chapter 4.3** and Scheme 49).¹⁶⁹



Scheme 49: Two-chamber protocol of the DABSO synthesis using sodium sulfite as SO_2 source.

Finally, flow chemistry was used to expand classic batch synthetic tools. The application of flow chemistry for the synthesis of glycerol carbonate from

glycerol. Glycerol is an industrial waste product of the production of biodiesel while glycerol carbonate is considered a green chemical. In literature however, a lot of batch processes are known for this transformation while almost no flow protocols were reported. This led to the development of a flow protocol where high conversion and selectivity were achieved by making use of a heterogeneous basic catalyst in a packed bed column reactor (**chapter 5**). The residence could be lowered to 3-5 minutes, leading to high space-time yields. Reuse of catalyst (up to 4 times) was possible with only slight decrease in conversion (from 90% to 80%).



Scheme 50: Continuous flow protocol for the synthesis of glycerol carbonate (GLC) from glycerol and dimethyl carbonate (DMC) using a solid supported catalyst in a packed bed reactor.

6.2 Future perspectives

Our group aims to continue to contribute to the enhancement of safe ways of working with (dangerous) gases for the organic synthesis researcher. Recently, a safe protocol of working with sulfuryl fluoride (SO_2F_2) was published, again making use of a two-chamber reactor setup.²¹⁰ Other ideas with gases are emerging as we speak and this topic will undoubtedly continue to prove its utility in our research group during future work. Figure 26 summarizes the ideal requirements for new two-chamber ideas.

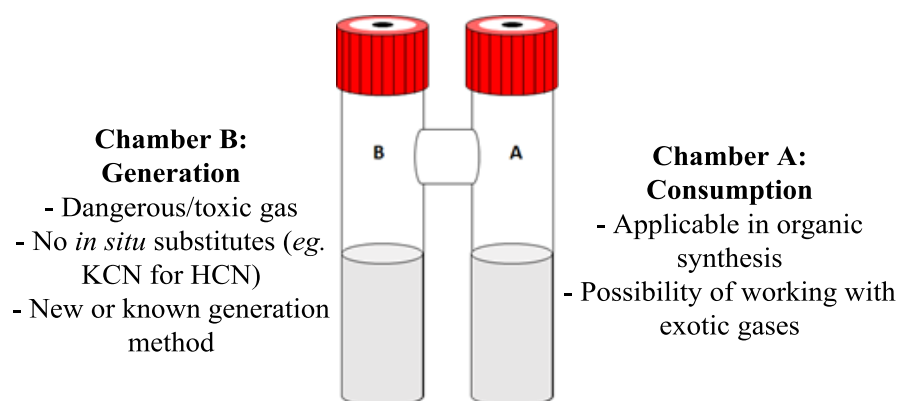
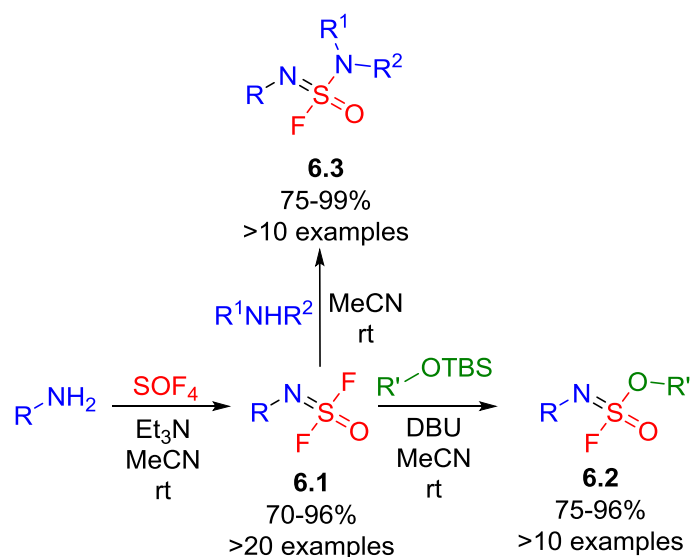


Figure 26: Ideal requirements for new two-chamber projects.

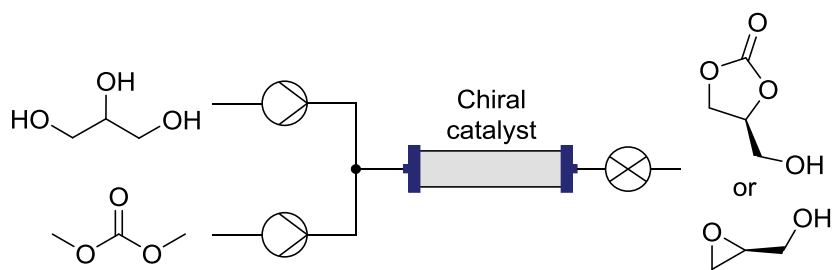
One specific idea is the generation of SOF_4 , a rather exotic but highly useful gas. Indeed, the Sharpless group developed click chemistry using this gas, and is phrased SuFEx: sulfur (VI) fluoride exchange.²¹¹ A demonstration of this highly selective chemistry is depicted in Scheme 51. First, SOF_4 reacts with primary amines/anilines under basic conditions to form iminosulfur oxydifluorides **6.1**. Next, one can couple silyl ethers in the presence of DBU with **6.1**, resulting in sulfurofluoridoimides **6.2**, substituting one fluorine in the process. Another possibility is reacting **6.1** with secondary amines. This yields in **6.3** type compounds. These steps (amination or phenolation) can be repeated on the remaining fluorine of **6.3** (not shown). All these steps are very selective, occur at room temperature and often require no column chromatography with mostly excellent yields. In our opinion, the main disadvantage is the storage and handling of a pressurized gas vessel containing SOF_4 . As stated before, this implies a lot of safety considerations. Therefore, it would be highly interesting to develop a method to make this recent chemistry more accessible in academic laboratories by means of

generating and consuming SOF_4 in a closed system, thereby avoiding the use of a lecture gas bottle.



Scheme 51: SuFEx click chemistry using SOF_4 .

In agreement with the general consensus of continuous flow chemistry as a novel emerging field for organic synthesis, our group will continue to contribute to research with this tool as well. In the case of the continuous flow synthesis of glycerol carbonate (GLC), further investigation is required. Currently, other catalysts are being screened and additional experiments are being carried out. In addition to the project discussed in **chapter 5**, the development of chiral catalysts for the asymmetric synthesis of GLC or glycidol would be highly interesting, since these are relevant chiral industrial building blocks (Scheme 52). A couple *N*-heterocyclic carbenes (NHCs) are known for the synthesis of (racemic) GLC from glycerol and DMC.^{203, 212} Interestingly, chiral NHCs are popular catalysts in asymmetric synthesis,²¹³⁻²¹⁴ and could, in our opinion, be a good starting point for further investigation. Moreover, NHCs could be easily immobilized on a polymer support, such as hyperbranched polymers, a topic which our group is also investigating.



Scheme 52: Flow process proposal for the synthesis of chiral GLC or glycidol.

CHAPTER 7

EXPERIMENTAL

7. Experimental

7.1 General

All reagents and solvents were purchased from commercial sources (Sigma-Aldrich, Acros, FluoroChem, TCI, Strem, Fluka, AK Scientific, Manchester Organics) and used without further purification. All anhydrous solvents were purchased from commercial sources with the exception of diethyl ether, toluene and THF, which were dried in large quantities using an Mbraun SPS 800 drying setup.

^1H NMR, ^{13}C NMR and 2D measurements were recorded on a Bruker Avance 300 MHz (operating at 75 MHz for ^{13}C measurements) and a Bruker Avance 400 MHz spectrometer (operating at 100 MHz for ^{13}C measurements). Chemical shifts are reported in parts per million (ppm) and are referenced to the internal standard tetramethylsilane (TMS) in CDCl_3 and DMSO. Alternatively, the deuterated solvent was used as internal standard. s = singlet, d = doublet, t = triplet, q = quartet, bs = broad singlet.

IR spectra were recorded using a Bruker Alpha-P coupled to OPUS software.

GC-MS measurements were performed with a ThermoFinnigan Trace GC Gas Chromatographer with non-automated PTV injector, temperature program from 40 to 300 °C (rate: 20 °C/min, hold 5 min), coupled to a ThermoScientific ITQ900 full scan EI mass spectrometry detector.

Melting points were obtained using a Mettler Toledo DSC1 system. Alternatively, a Reichert-Jung Thermovar electrochemical 9200 instrument was used. The measurements are not corrected.

High-resolution mass spectra (HRMS) were measured with a Waters Synapt G2 HDMS quadrupole orthogonal acceleration time-of-flight mass spectrometer. Samples were infused at 3 $\mu\text{L}/\text{min}$ and spectra were obtained in positive ionization mode with a resolution of 15000 (FWHM) using leucine enkephalin as lock mass. Alternatively, a Kratos MS50TC machine was used with an ionization energy of 70 eV at 150-250 °C (as required), coupled to a MASSPEC II data acquiring system. The high resolution mass spectra were recorded with a resolution of 10000.

Column chromatography was carried out using self-packed flash columns containing flash silica (Davisil® Chromatography Silica, Medium Type LC 60A, 40-63 micron) on a Büchi Sepacore™ flash apparatus, consisting of a C-660

Büchi fraction collector, C-615 pump manager, C-635 UV-photometer, two C-605 pump modules and a Linseis D120S plotter. Thin layer chromatography (TLC) was carried out on pre-coated plates SIL G-25 (Machery-Nagel) with UV₂₅₄ fluorescence indicator.

Reverse phase HPLC was performed on a Waters Delta 600 analytical/preparative system equipped with Waters 996 Photo Diode Array Detector. Preparative column size: Alltech C18 Prevail 5 μ m, 150x22 mm, and Phenomenex Luna C18, 5 μ m, 150x22 mm

Crystal structures were determined on a Agilent SuperNova diffractometer (single source at offset, Eos detector). Using Olex2, the structure was solved with the ShelXS structure solution program using Direct Methods and refined with the ShelXL refinement package using least-squares minimization.

For flow experiments a VapourTec R2+R4 unit, a VapourTec E-series unit with peristaltic pumps or DIY reactors with PTFE tubing were used. Omnifit glass columns (10 mm i.d. x 100 mm length) were used as reactors for heterogeneous catalysis experiments.

7.2 Chemical safety

All experimental work in this thesis was carried out in accordance with the Code of Practice for Safety in the Lab,²¹⁵ and the Departmental Safety Brochure.²¹⁶ Special care and attention are needed when manipulating toxic substances, laboratory glassware and explosive substances. Further information can be found on the web page of The Department of Chemistry, and of the HSE department (Health, Safety & Environment). Additional information and existing risk analyses can be found on a user-contributed sharepoint.²¹⁷

In this thesis, a significant contribution was made towards lab safety by making it less dangerous to work with toxic gases. Therefore, two gases will be briefly discussed in this section of which we have made frequent use, but are highly dangerous.

Carbon monoxide

The incorporation of carbon monoxide as a carbonyl moiety in organic molecules is the main reason why this gas is so synthetically useful, especially from an atom efficiency point of view. However, CO gas is also known as ‘the silent killer’, attributing to numerous deaths each year. Carbon monoxide is highly flammable, odorless and colorless. Upon exposure, CO binds to hemoglobin, the enzyme responsible for oxygen transport throughout a living organism. It binds 200 times stronger than oxygen and is called carboxyhemoglobin (COHb). On top, COHb binds oxygen more strongly than hemoglobin itself (4 binding places in total), leading to an even more pronounced reduced release of oxygen delivery. This quickly leads to oxygen deprivation, and as a consequence, death. Table 16 gives an overview of the signs and symptoms when one is exposed to carbon monoxide.

In the early days of this research in our group, reactions where toxic gases such as carbon monoxide were used needed to be performed in the so-called ‘cyanide room’ with special fumehoods and multiple alarms and detectors, using a balloon setup. This required a special safety training and physical presence of a trained supervisor. Ever since the development of our new CO precursor two-chamber system, it is strongly encouraged to apply this in our lab when carbon monoxide is needed. As stated, this protocol is significantly safer, as the carbon monoxide is produced and consumed, using only near-stoichiometric amounts. Therefore, this two-chamber protocol is not required to be carried out in the ‘cyanide room’.

Table 16: Overview of symptoms related to carbon monoxide exposure.

Concentration (ppm)	Symptoms
35	Headache and dizziness within 6 to 8 hours of constant exposure
100	Slight headache in 2 to 3 hours
200	Slight headache within 2 to 3 hours, loss of judgement
400	Frontal headache within 1 to 2 hours
800	Dizziness, nausea and convulsions within 45 minutes. Insensible within 2 hours
1600	Headache, tachycardia, dizziness and nausea within 20 minutes, death in less than 2 hours
3200	Headache, dizziness and nausea in 5 to 10 minutes, death in less than 30 minutes
6400	Headache and dizziness in 1 to 2 minutes. Death within 20 minutes
12800	Death within 3 minutes

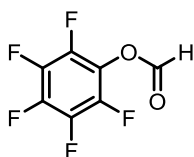
Sulfur dioxide

Sulfur dioxide is a ubiquitous commodity chemical which has several chemical applications in industrial processes. Until recently, it was not often used in an academic lab setting.¹⁵⁰ This can partly be ascribed to the gaseous state of sulfur dioxide, as well as its notorious toxicity and smell. Inhaling sulfur dioxide is associated with increased respiratory symptoms and disease, difficulty in breathing, and death.²¹⁸ In 2010, the EPA revised the primary SO₂ standards by establishing a new one-hour standard at a level of 75 parts per billion (ppb).

However, the use of sulfur dioxide in synthetic organic chemistry is reviving. It is believed that the advancement of convenient and stable SO₂ surrogates (such as DABSO) is an important driver in the rejuvenation of organic synthesis research involving SO₂. In this sense, our developed protocol helped contribute to safer usage of sulfur dioxide in organic chemistry. A safe alternative to synthesize DABSO on site, which is relatively expensive, is described. Key in this protocol is of course the removal of a pressurized SO₂ gas vessel, which implies serious safety concerns. The SO₂ source was in this case the innocent salt sodium sulfite. In analogy with our two-chamber protocol of using carbon monoxide, sulfur dioxide is generated and consumed in a closed two-chamber setup. The generation occurs quite slow, leading to a gradual release of the gas, and thereby avoiding pressure buildup.

7.3 In search of a new CO precursor

Pentafluorophenyl formate (4.14)

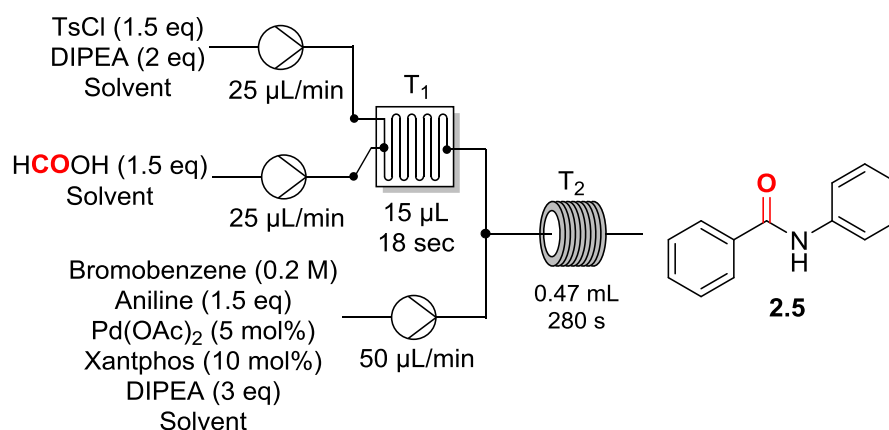


Pentafluorophenol (1 g, 5.43 mmol) was dissolved in 6 mL of dry chloroform. The solution was cooled to 0 °C, DCC (1.35 g, 6.52 mmol) and formic acid (0.25 mL, 6.52 mmol) was added slowly while keeping the temperature at 0 °C. Afterwards the reaction was stirred for an additional 90 minutes at 0 °C. The suspension was then filtered and the filtrate was evaporated *in vacuo*. The residue was redissolved in Et₂O and the organic phase was washed with 5% aq. NaHCO₃, water and brine. It was then dried over MgSO₄, filtered and the filtrate was evaporated *in vacuo* to give the product as a colorless oil (1 g, 87% yield). The product is not stable and decomposes on standing, even at -20 °C.

7.3.1 Flow approach

Procedure for aminocarbonylation in flow using a Teflon coil reactor

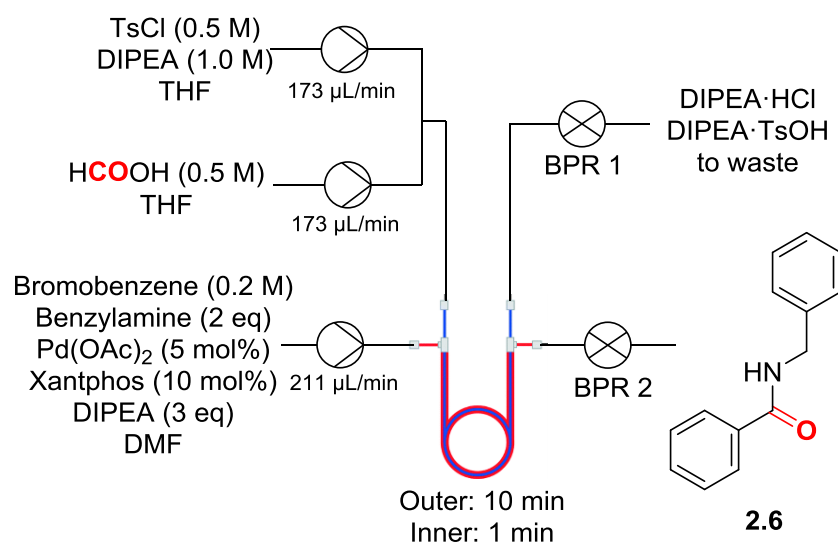
Three solutions were prepared: A) Tosyl Chloride (0.3 M) and DIPEA (0.4 M), B) Formic acid (0.3 M) and C) PhBr (0.2 M), aniline (0.3 M), Pd(OAc)₂ (0.01 M), Xantphos (0.02 M) in the solvent of choice. Solutions A and B were loaded in separate syringes and pumped, using a Chemyx Fusion 200 syringe pump. The solutions were mixed in an PTFE T-tube fitting and passed through a Chemtrix glass reactor chip (residence time 18 s), heated using the Chemtrix Start Unit, with temperature control provided by a Laird Technologies MTTC1410 unit. Next, the reagent stream was mixed with solution C (pumped via a separate syringe pump) in another T-tube fitting before being passed through a Teflon coil reactor (residence time 280 s). The product was then collected at the outlet and subjected to GC-MS analysis to determine conversion.



Scheme 53: In situ CO precursor flow protocol.

Procedure for aminocarbonylation using a Tube-in-Tube reactor

Tosyl Chloride (0.5 M) and DIPEA (1.0 M), B) Formic acid (0.5 M) and C) Bromobenzene (0.2 M), benzylamine (0.4 M), Pd(OAc)₂ (0.01 M), Xantphos (0.02 M) and DIPEA (0.6 M) were dissolved in the solvent of choice. Solutions A and B were loaded in separate syringes and pumped, using a Chemyx Fusion 200 syringe pump. The solutions were mixed in an PTFE T-tube fitting (Dolomite²¹⁹ part r. 3000397) and passed through the inner tube of the Tube-in-Tube reactor (residence time 1 min). Simultaneously, solution C was passed through the outer tube of the Tube-in-Tube reactor (residence time 10 min). The outlet stream of the inner tube was disposed as waste, the outlet stream of the outer tube was collected and subjected to GC-MS analysis to determine conversion.

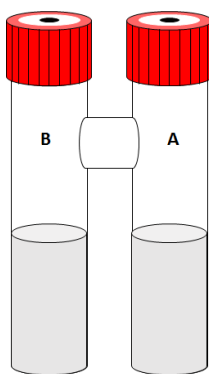


Scheme 54: Ex situ CO precursor flow protocol: making use of a tube-in-tube reactor.

7.3.2 Two chamber approach

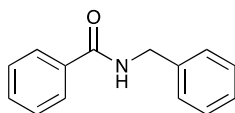
General procedure

Chamber A of a flame-dried two-chamber reactor was filled with 1 mg Palladium(II) acetate (5 μ mol, 1 mol%), 3 mg Xantphos (5 μ mol, 1 mol %) and 159 mg sodium carbonate (1.5 mmol, 3 eq). The reactor was brought under argon atmosphere by two consecutive vacuum-argon cycles. Next, chamber B was filled with 2 mL dried degassed toluene, 51 μ L mesyl chloride (0.65 mmol, 1.3 eq) and 25 μ L formic acid (0.65 mmol, 1.3 eq). In chamber A, 1 mL dried degassed toluene was added, followed by 0.5 mmol aryl bromide (1 eq) and 0.75 mmol amine (1.5 eq). Then the reactor was placed in an oil-bath at 100 °C. Finally, 181 μ L triethylamine (1.3 mmol, 2.6 eq) was added by injection through the septum in chamber B and instant gas formation was observed. After this, the reactor was brought to room temperature and the generated pressure was released by removing one of the caps. As carbon monoxide is a highly toxic gas, the reaction was stirred at room temperature for 15 minutes to ensure that all carbon monoxide gas was extracted out of the fume hood. Next, the content of chamber A was transferred to a 100 mL round bottomed flask. This chamber was washed 5 times with 2 mL of EtOAc, these fractions were added to the same flask. After the addition of 1 gram Celite® 535, the solvent was removed under reduced pressure. The crude product was purified by solid-phase flash column chromatography on silica gel.



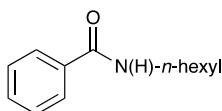
Representation of the two-chamber reactor. Inner volume = 20 mL.

***N*-benzylbenzamide (2.6)**



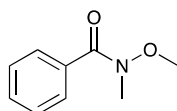
The general procedure was followed using 53 μ L bromobenzene (0.5 mmol, 1 eq) and 82 μ L phenylmethanamine (0.75 mmol, 1.5 eq). The crude mixture was purified by solid-phase flash column chromatography on silica gel (85:15 heptanes/ethyl acetate). The title compound was obtained as a white solid (96 mg, 91%). ^1H NMR (400 MHz, DMSO) 9.04 (bs, 1H), 7.95 – 7.86 (m, 2H), 7.58 – 7.43 (m, 3H), 7.33 (d, J = 4.3 Hz, 4H), 7.24 (dd, J = 8.6 & 4.4 Hz, 1H), 4.49 (d, J = 6.0 Hz, 2H). ^{13}C NMR (101 MHz, DMSO) 166.2, 139.7, 134.3, 131.2, 128.3, 128.2, 127.2, 127.2, 126.7, 42.6, 39.5. Melting point: 105-107 $^{\circ}\text{C}$.

***N*-hexylbenzamide (2.10)**



The general procedure was followed using 53 μ L bromobenzene (0.5 mmol, 1 eq) and 99 μ L *n*-hexylamine (0.75 mmol, 1.5 eq). The crude mixture was purified by solid-phase flash column chromatography on silica gel (85:15 heptanes/ethyl acetate). The title compound was obtained as a waxy solid (101 mg, 98%). ^1H NMR (300 MHz, CDCl_3) 7.85 – 7.30 (m, 5H), 6.65 (m, 1H), 3.39 (m, 2H), 1.65 – 1.50 (m, 2H), 1.42 – 1.16 (m, 6H), 0.86 (t, J = 6.7 Hz, 3H). ^{13}C NMR (75 MHz, CDCl_3) 167.7, 134.9, 131.2, 128.5, 127.0, 40.2, 31.6, 29.6, 26.7, 22.6, 14.1. Melting point: 42-44 $^{\circ}\text{C}$.

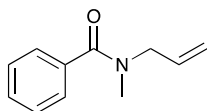
***N*-methoxy-*N*-methylbenzamide (2.11)**



The general procedure was followed using 53 μ L bromobenzene (0.5 mmol, 1 eq) and 73 mg *N,O*-dimethylhydroxylamine hydrochloride (0.75 mmol, 1.5 eq). The crude mixture was purified by solid-phase flash column chromatography on silica gel (80:20 heptanes/ethyl acetate). The title compound was obtained as a colorless oil (73 mg, 89%). ^1H NMR (300 MHz,

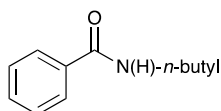
CDCl₃) 7.69 – 7.34 (m, 5H), 3.54 (s, 3H), 3.35 (s, 3H). ¹³C NMR (75 MHz, CDCl₃) 170.1, 134.2, 130.7, 128.2, 128.1, 61.1, 33.9.

***N*-allyl-*N*-methylbenzamide (2.12)**



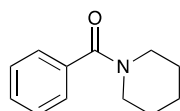
The general procedure was followed using 53 μ L bromobenzene (0.5 mmol, 1 eq) and 71 μ L *N*-methylprop-2-en-1-amine (0.75 mmol, 1.5 eq). The crude mixture was purified by solid-phase flash column chromatography on silica gel (80:20 heptanes/ethyl acetate). The title compound was obtained as a colorless oil (71 mg, 81%). ¹H NMR (600 MHz, DMSO) 7.47 – 7.35 (m, 5H), 5.89 – 5.75 (m, 1H), 5.24 – 5.15 (m, 2H), 3.94 (s, 2H), 2.90 (s, 3H). ¹³C NMR (151 MHz, DMSO) 170.0, 136.3, 133.1, 128.8, 127.8, 126.1, 116.5, 50.8, 34.0.

***N*-butylbenzamide (2.13)**



The general procedure was followed using 53 μ L bromobenzene (0.5 mmol, 1 eq) and 74 μ L *N*-butylamine (0.75 mmol, 1.5 eq). The crude mixture was purified by solid-phase flash column chromatography on silica gel (85:15 heptanes/ethyl acetate). The title compound was obtained as a colorless oil (79 mg, 89%). ¹H NMR (400 MHz, DMSO) 8.42 (bs, 1H), 7.48 (m, 5H), 3.26 (dd, *J* = 12.8 & 6.9 Hz, 2H), 1.57 – 1.45 (m, 2H), 1.39 – 1.27 (m, 2H), 0.90 (t, *J* = 7.3 Hz, 3H). ¹³C NMR (101 MHz, DMSO) 166.1, 134.7, 130.9, 128.2, 127.1, 38.8, 31.2, 19.6, 13.7. Melting point: 41-42 °C.

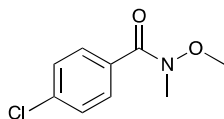
Phenyl(piperidin-1-yl)methanone (2.14)



The general procedure was followed using 53 μ L bromobenzene (0.5 mmol, 1 eq) and 74 μ L piperidine (0.75 mmol, 1.5 eq). The crude mixture was purified by solid-phase flash column chromatography on silica gel (80:20 heptanes/ethyl acetate). The title compound was obtained as a colorless oil

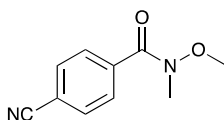
(88 mg, 93%). ^1H NMR (300 MHz, CDCl_3) 7.36 (m, 5H), 3.68 (m, 2H), 3.31 (m, 2H), 1.64 (m, 4H), 1.49 (m, 2H). ^{13}C NMR (75 MHz, CDCl_3) 170.3, 136.5, 129.3, 128.4, 126.8, 48.7, 43.1, 26.5, 25.7, 24.6. Melting point: 47-48 °C.

4-chloro-*N*-methoxy-*N*-methylbenzamide (2.15)



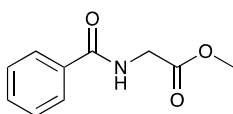
The general procedure was followed using 144 mg 1-bromo-4-chlorobenzene (0.75 mmol, 1.5 eq) and 49 mg *N,O*-dimethylhydroxylamine hydrochloride (0.50 mmol, 1.0 eq). The crude mixture was purified by solid-phase flash column chromatography on silica gel (80:20 heptanes/ethyl acetate). The title compound was obtained as a colorless oil (83 mg, 83%). ^1H NMR (300 MHz, CDCl_3) 7.64 (d, J = 8.7 Hz, 2H), 7.36 (d, J = 8.7 Hz, 2H), 3.52 (s, 3H), 3.34 (s, 3H). ^{13}C NMR (75 MHz, CDCl_3) 168.7, 136.8, 132.3, 129.9, 128.4, 77.2, 61.2, 33.6.

4-cyano-*N*-methoxy-*N*-methylbenzamide (2.16)



The general procedure was followed using 91 mg 4-bromobenzonitrile (0.5 mmol, 1 eq) and 73 mg *N,O*-dimethylhydroxylamine hydrochloride (0.75 mmol, 1.5 eq). The crude mixture was purified by solid-phase flash column chromatography on silica gel (60:40 heptanes/ethyl acetate). The title compound was obtained as a light yellow oil (87 mg, 92%). ^1H NMR (300 MHz, CDCl_3) 7.72 (dd, J = 20.6 & 8.5 Hz, 4H), 3.50 (s, 3H), 3.35 (s, 3H). ^{13}C NMR (75 MHz, CDCl_3) 168.0, 138.3, 131.9, 128.9, 118.2, 114.2, 61.4, 33.3.

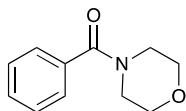
Methyl 2-benzamidoacetate (2.17)



The general procedure was followed using 53 μL bromobenzene (0.5 mmol, 1 eq) and 94 mg methyl glycinate hydrochloride (0.75 mmol, 1.5 eq). The crude mixture was purified by solid-phase flash column chromatography on

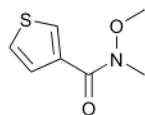
silica gel (80:20 heptanes/ethyl acetate). The title compound was obtained as a white solid (93 mg, 96%). ^1H NMR (300 MHz, CDCl_3) 7.82 – 7.75 (m, 2H), 7.52 – 7.34 (m, 3H), 7.06 (bs, 1H), 4.18 (d, J = 5.3 Hz, 2H), 3.73 (s, 3H). ^{13}C NMR (75 MHz, CDCl_3) 170.2, 167.3, 133.2, 131.4, 128.2, 126.7, 52.0, 41.3. Melting point: 82-83 °C.

Morpholino(phenyl)methanone (2.18)



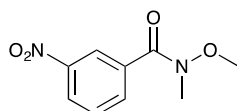
The general procedure was followed using 53 μL bromobenzene (0.5 mmol, 1 eq) and 66 μL morpholine (0.75 mmol, 1.5 eq). The crude mixture was purified by solid-phase flash column chromatography on silica gel (50:50 heptanes/ethyl acetate). The title compound was obtained as a colorless oil (91 mg, 95%). ^1H NMR (400 MHz, CDCl_3) 7.38 (m, 5H), 3.63 (m, 8H). ^{13}C NMR (101 MHz, CDCl_3) 170.5, 135.7, 129.9, 128.6, 127.2, 67.0, 46.9. Melting point: 73-74 °C.

***N*-methoxy-*N*-methylthiophene-3-carboxamide (2.19)**



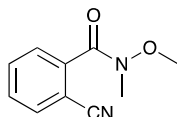
The general procedure was followed using 47 μL 3-bromothiophene (0.5 mmol, 1 eq) and 73 mg *N,O*-dimethylhydroxylamine hydrochloride (0.75 mmol, 1.5 eq). The crude mixture was purified by solid-phase flash column chromatography on silica gel (80:20 heptanes/ethyl acetate). The title compound was obtained as a light yellow oil (77 mg, 90%). ^1H NMR (300 MHz, CDCl_3) 8.06 (dd, J = 3.0 & 1.2 Hz, 1H), 7.56 (dd, J = 5.1 & 1.2 Hz, 1H), 7.27 (dd, J = 5.1 & 3.0 Hz, 1H), 3.64 (s, 3H), 3.35 (s, 3H). ^{13}C NMR (75 MHz, CDCl_3) 163.4, 134.1, 130.5, 128.7, 124.5, 60.9, 32.9.

***N*-methoxy-*N*-methyl-3-nitrobenzamide (2.20)**



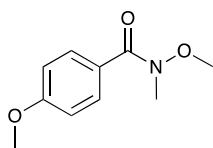
The general procedure was followed using 101 mg 1-bromo-3-nitrobenzene (0.5 mmol, 1 eq) and 73 mg *N,O*-dimethylhydroxylamine hydrochloride (0.75 mmol, 1.5 eq). The crude mixture was purified by solid-phase flash column chromatography on silica gel (75:25 heptanes/ethyl acetate). The title compound was obtained as a light yellow oil (90 mg, 86%). ¹H NMR (300 MHz, CDCl₃) 8.57 – 8.53 (m, 1H), 8.34 – 8.27 (m, 1H), 8.05 – 7.99 (m, 1H), 7.60 (t, *J* = 8.0 Hz, 1H), 3.54 (s, 3H), 3.38 (s, 3H). ¹³C NMR (75 MHz, CDCl₃) 167.3, 147.9, 135.6, 134.4, 129.3, 125.4, 123.6, 61.5, 33.3. Melting point: 41-43 °C.

2-cyano-*N*-methoxy-*N*-methylbenzamide (2.21)

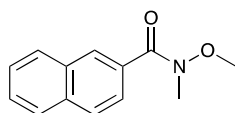


The general procedure was followed using 92 mg 2-bromobenzonitrile (0.5 mmol, 1 eq) and 73 mg *N,O*-dimethylhydroxylamine hydrochloride (0.75 mmol, 1.5 eq). The crude mixture was purified by solid-phase flash column chromatography on silica gel (70:30 heptanes/ethyl acetate). The title compound was obtained as a colorless oil (85 mg, 89%). ¹H NMR (400 MHz, CDCl₃) 7.74 – 7.45 (m, 4H), 3.52 (s, 3H), 3.36 (s, 3H). ¹³C NMR (101 MHz, CDCl₃) 166.9, 139.1, 132.9, 132.5, 129.9, 128.0, 116.9, 110.9, 61.5, 33.4.

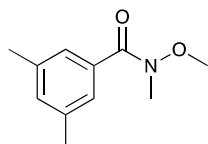
N-4-dimethoxy-*N*-methylbenzamide (2.22)



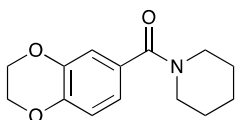
The general procedure was followed using 63 μL 1-bromo-4-methoxybenzene (0.5 mmol, 1 eq) and 73 mg *N,O*-dimethylhydroxylamine hydrochloride (0.75 mmol, 1.5 eq). The crude mixture was purified by solid-phase flash column chromatography on silica gel (80:20 heptanes/ethyl acetate). The title compound was obtained as a colorless oil (85 mg, 87%). ¹H NMR (300 MHz, CDCl₃) 7.70 (d, *J* = 8.9 Hz, 2H), 6.87 (d, *J* = 8.9 Hz, 2H), 3.81 (s, 3H), 3.53 (s, 3H), 3.32 (s, 3H). ¹³C NMR (75 MHz, CDCl₃) 169.0, 161.1, 130.1, 125.6, 112.8, 60.5, 54.9, 33.5.

***N*-methoxy-*N*-methyl-2-naphthamide (2.23)**

The general procedure was followed using 104 mg 2-bromonaphthalene (0.5 mmol, 1 eq) and 73 mg *N,O*-dimethylhydroxylamine hydrochloride (0.75 mmol, 1.5 eq). The crude mixture was purified by solid-phase flash column chromatography on silica gel (85:15 heptanes/ethyl acetate). The title compound was obtained as a colorless oil (94 mg, 88%). ¹H NMR (300 MHz, CDCl₃) 8.22 (s, 1H), 7.92 – 7.73 (m, 4H), 7.58 – 7.47 (m, 2H), 3.55 (s, 3H), 3.40 (s, 3H). ¹³C NMR (75 MHz, CDCl₃) 169.9, 134.2, 132.5, 131.4, 128.9, 128.7, 127.7, 127.6, 127.4, 126.5, 125.1, 61.2, 33.9.

***N*-methoxy-*N*,3,5-trimethylbenzamide (2.24)**

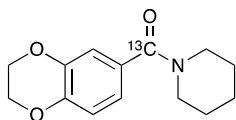
The general procedure was followed using 68 μL 1-bromo-3,5-dimethylbenzene (0.5 mmol, 1 eq) and 73 mg *N,O*-dimethylhydroxylamine hydrochloride (0.75 mmol, 1.5 eq). The crude mixture was purified by solid-phase flash column chromatography on silica gel (70:30 heptanes/ethyl acetate). The title compound was obtained as a colorless oil (86 mg, 89%). ¹H NMR (300 MHz, CDCl₃) 7.22 (s, 2H), 7.06 (s, 1H), 3.56 (s, 3H), 3.31 (s, 3H), 2.32 (s, 6H). ¹³C NMR (75 MHz, CDCl₃) 170.5, 137.7, 134.2, 132.2, 125.6, 77.2, 61.0, 34.1, 21.3.

(2,3-dihydrobenzo[*b*][1,4]dioxin-6-yl)(piperidin-1-yl)methanone or CX-546 (2.25a)

The general procedure was followed using 67 μL 6-bromo-2,3-dihydrobenzo[*b*][1,4]dioxine (0.5 mmol, 1 eq) and 74 μL piperidine (0.75 mmol, 1.5 eq). The crude mixture was purified by solid-phase flash column chromatography on silica gel (80:20 heptanes/ethyl acetate). Compound

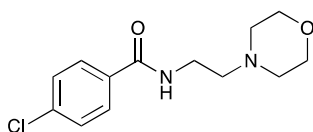
2.25a was obtained as a white solid (111 mg, 90%). ^1H NMR (600 MHz, CDCl_3) 6.95 – 6.82 (m, 3H), 4.25 (m, 4H), 3.52 (m, 4H), 1.68 – 1.64 (m, 2H), 1.57 (m, 4H). ^{13}C NMR (151 MHz, CDCl_3) 170.0, 144.9, 143.6, 130.0, 120.6, 117.3, 116.7, 64.6, 64.5, 46.0, 26.3, 24.8.

Carbon-13 labelled (2,3-dihydrobenzo[*b*][1,4]dioxin-6-yl)(piperidin-1-yl)methanone or CX-546 (2.25b)



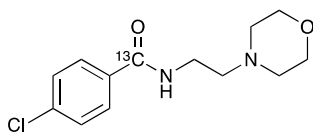
The general procedure was followed using 67 μL 6-bromo-2,3-dihydrobenzo[*b*][1,4]dioxine (0.5 mmol, 1 eq) and 74 μL piperidine (0.75 mmol, 1.5 eq). The crude mixture was purified by solid-phase flash column chromatography on silica gel (80:20 heptanes/ethyl acetate). Compound **2.25b** was obtained as a white solid (124 mg, 94%). **Remark:** for the C-13 labelled CX-546, 25 μL of ^{13}C -HCOOH (95 wt. % in H_2O) was used. ^1H NMR (600 MHz, CDCl_3) 6.94 – 6.81 (m, 3H), 4.26 – 4.20 (m, 4H), 3.66 – 3.38 (m, 4H), 1.68 – 1.62 (m, 2H), 1.61 – 1.52 (m, 4H). ^{13}C NMR (151 MHz, CDCl_3) 169.9 (s), 144.9 (s), 143.5 (s), 129.9 (d, $J = 67.7$ Hz), 120.6 (s), 117.20 (d, $J = 4.9$ Hz), 116.6 (d, $J = 2.3$ Hz), 64.6 (s), 64.5 (s), 46.2 (bs), 26.2 (s), 24.8 (s).

4-chloro-*N*-(2-morpholinoethyl)benzamide or Moclobemide (2.26a)



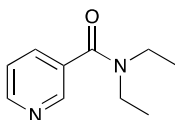
The general procedure was followed using 98 mg 1-bromo-4-chlorobenzene (0.5 mmol, 1 eq) and 99 μL 2-morpholinoethan-1-amine (0.75 mmol, 1.5 eq). The crude mixture was purified by solid-phase flash column chromatography on silica gel (96:4 dichloromethane/methanol). Compound **2.26a** was obtained as a white solid (130 mg, 97%). ^1H NMR (300 MHz, CDCl_3) 7.75 – 7.68 (m, 2H), 7.45 – 7.37 (m, 2H), 6.76 (bs, 1H), 3.77 – 3.68 (m, 4H), 3.57 – 3.48 (m, 2H), 2.63 – 2.56 (m, 2H), 2.54 – 2.43 (m, 4H). ^{13}C NMR (75 MHz, CDCl_3) 166.4, 137.8, 133.1, 129.0, 128.5, 67.1, 56.9, 53.4, 36.2. Melting point: 137 °C.

Carbon-13 labelled 4-chloro-*N*-(2-morpholinoethyl)benzamide or Moclobemide (2.26b)



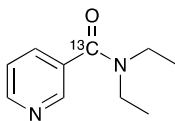
The general procedure was followed using 98 mg 1-bromo-4-chlorobenzene (0.5 mmol, 1 eq) and 99 μ L 2-morpholinoethan-1-amine (0.75 mmol, 1.5 eq). The crude mixture was purified by solid-phase flash column chromatography on silica gel (96:4 dichloromethane/methanol). Compound **2.26b** was obtained as a white solid (126 mg, 94%). **Remark:** for the C-13 labelled Moclobemide, 25 μ L of ^{13}C -HCOOH (95 wt. % in H_2O) was used. ^1H NMR (300 MHz, CDCl_3) 7.70 (m, 2H), 7.39 (m, 2H), 6.80 (bs, 1H), 3.78 – 3.64 (m, 4H), 3.59 – 3.48 (m, 2H), 2.58 (m, 2H), 2.54 – 2.41 (m, 4H). ^{13}C NMR (75 MHz, CDCl_3) 166.4 (s), 137.7 (s), 133.0 (d, J = 65.2 Hz), 128.9 (d, J = 4.4 Hz), 128.5 (d, J = 2.5 Hz), 67.1 (s), 56.9 (s), 53.4 (s), 36.2 (s).

***N,N*-diethylnicotinamide or Nikethamide (2.27a)**



The general procedure was followed using 49 μ L 3-bromopyridine (0.5 mmol, 1 eq) and 78 μ L diethylamine (0.75 mmol, 1.5 eq). The crude mixture was purified by solid-phase flash column chromatography on silica gel (97:3 dichloromethane/methanol). Compound **2.27a** was obtained as a yellow oil (68 mg, 76%). ^1H NMR (300 MHz, CDCl_3) 8.58 (m, 2H), 7.71 – 7.62 (m, 1H), 7.34 – 7.26 (m, 1H), 3.36 (m, 4H), 1.14 (m, 6H). ^{13}C NMR (75 MHz, CDCl_3) 168.6, 150.3, 147.2, 134.3, 133.0, 123.4, 43.4, 39.6, 14.3, 12.9.

Carbon-13 labelled *N,N*-diethylnicotinamide or Nikethamide (2.27b)



The general procedure was followed using 49 μ L 3-bromopyridine (0.5 mmol, 1 eq) and 78 μ L diethylamine (0.75 mmol, 1.5 eq). The crude mixture was purified by solid-phase flash column chromatography on silica gel (97:3

dichloromethane/methanol). Compound **2.27b** was obtained as a yellow oil (73 mg, 82%). **Remark:** for the C-13 labelled Nikethamide, 25 μ L of ^{13}C -HCOOH (95 wt. % in H_2O) was used. ^1H NMR (300 MHz, CDCl_3) 8.60 (m, 2H), 7.78 – 7.57 (m, 1H), 7.38 – 7.26 (m, 1H), 3.37 (m, 4H), 1.15 (m, 6H). ^{13}C NMR (75 MHz, CDCl_3) 168.6 (s), 150.3 (s), 147.2 (d, $J = 3.0$ Hz), 134.3 (d, $J = 1.6$ Hz), 133.0 (d, $J = 66.7$ Hz), 123.5 (s), 43.5 (s), 39.6 (s), 14.3 (s), 12.9 (s).

7.3.3 Economic comparison

Note that these prices are calculated for the generation of 1 mmol of CO (implying a 100 % conversion)

1- Low-Cost Instant CO Generation at Room Temperature from Formic Acid, Mesityl Chloride and Triethylamine⁸⁴

Chemicals	mmol	Commercial price	Commercial price per mmol	Price
Formic acid	1	€ 43.50 per 1 L	€ 0.002	€ 0.002
Mesityl chloride	1	€ 24.10 per 100 mL	€ 0.019	€ 0.019
Triethylamine	2	€ 107.00 per 1 L	€ 0.015	€ 0.03
Total price per mmol CO: € 0.051				

2- Chloroform as a Carbon Monoxide Precursor: In or Ex Situ Generation.⁶⁶

Chemicals	mmol	Commercial price	Commercial price per mmol	Price
Chloroform	1	€ 72.20 per 1 L	€ 0.003	€ 0.003
CsOH·H₂O	3.33	€ 40.9 per 10 grams	€ 0.688	€ 2.291
Total price per mmol CO: € 2.294				

*3- Silacarboxylic Acids as Efficient Carbon Monoxide Releasing Molecules: Synthesis and Application in Palladium-Catalyzed Carbonylation Reactions.*⁶

The yield of 77% for the first synthesis step (CO₂ + Lithium + chlorodiphenyl (methyl)silane) was taken into account.

Chemicals	mmol	Commercial price	Commercial price per mmol	Price
Lithium	5.844	€ 82.9 per 25 grams	€ 0.023	€ 0.134
Chlorodiphenyl (methyl)silane	1.299	€ 91.50 per 25 grams	€ 0.855	€ 1.111
Potassium Fluoride	1.06	€ 734.00 per 100 grams	€ 0.246	€ 0.261
Total price per mmol CO: € 1.506				

*4- Ex Situ Generation of Stoichiometric and Substoichiometric ¹²CO and ¹³CO and Its Efficient Incorporation in Palladium Catalyzed Aminocarbonylations.*⁷

The CO generating system in this article consists of 1 eq of 9-methyl-9H-fluorene-9-carbonyl chloride, 5 mol% Pd(dba)₂, 5 mol% P(tBu)₃ and 1.5 eq of DIPEA.

Chemicals	mmol	Commercial price	Commercial price per mmol	Price
9-methyl-9H-fluorene-9-carbonyl chloride	1	€ 128.50 per 5 grams	€ 6.24	€ 6.24
Pd(dba)₂	0.05	€ 93.00 per 2 grams	€ 26.72	€ 1.336
P(tBu)₃	0.05	€ 79.50 per 1 gram	€ 16.09	€ 0.805
DIPEA	1.5	€ 371 per 1 L	€ 0.065	€ 0.098
Total price per mmol CO: € 8.479				

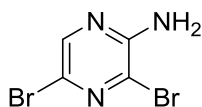
5- Efficient Fluoride-Catalyzed Conversion of CO₂ to CO at Room Temperature.⁷⁶

The CO generating system in this article consists of 1.5 eq of tetraphenyldimethyldisilane, 2 eq of carbon dioxide and 0.1 eq of cesium fluoride. However the tetraphenyldimethyldisilane additive is not commercially available, but can be prepared via one extra synthesis step (lithium + chlorodiphenyl (methyl)silane). The yield of 60% of this synthesis step was taken into account.

Chemicals	mmol	Commercial price	Commercial price per mmol	Price
Lithium	1.67	€ 83.90 per 25 grams	€ 0.023	€ 0.038
Chlorodiphenyl (methyl)silane	2.31	€ 91.50 per 25 grams	€ 0.855	€ 1.975
Cesium Fluoride	0.1	€ 63.00 per 25 grams	€ 0.38	€ 0.038
Total price per mmol CO: € 2.051				

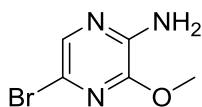
7.4 The assembly of pyrazine based oligoamide alpha-helix mimetics

3,5-Dibromo-2-aminopyrazine (3.10)



Pyrazin-2-amine (5 g, 52.6 mmol) was dissolved in a mixture of DMSO (100 mL) and water (2.5 mL). The solution was subsequently cooled to <15 °C. NBS (20 g, 112 mmol) was added slowly over a period of approximately 50 min. Afterwards the reaction was stirred at RT for 6 hours. The reaction mixture was then poured into 300 mL of ice water. The aqueous phase was extracted with EtOAc. The organic fraction was washed with sat. NaHCO₃ solution, water and afterwards dried over MgSO₄. The solvent was evaporated *in vacuo* to obtain a brown colored solid. The crude product was purified by column chromatography (60:40 heptanes/EtOAc) to give 3,5-dibromopyrazin-2-amine (11.5 g, 72%) as white-yellow crystals. Melting point: 86-88 °C. ¹H NMR (300 MHz, CDCl₃, ppm): δ 8.04 (s, 1H), 5.06 (bs, 2H). ¹³C NMR (75 MHz, CDCl₃, ppm): δ 151.9, 143.1, 123.9, 123.6. FT-IR (cm⁻¹): 3338, 2953. HR-MS: Calculated mass: 251.8768 Mass found: 251.8779.

5-Bromo-3-methoxypyrazin-2-amine (3.1a)



A solution of 3,5-dibromopyrazin-2-amine (1 g, 3.95 mmol) in 3 mL of dry methanol was prepared and cooled to 0 °C. NaOMe (1 mL of a 25% solution in MeOH) was then added dropwise while vigorous stirring the mixture. After addition, the reaction mixture was set to reflux for 16 hours. Afterwards the solution was allowed to cool to RT and left standing overnight. The resulting precipitate was filtered, washed with ice-cold methanol and air-dried to give 5-bromo-3-methoxypyrazin-2-amine **3.1a** (670 mg, 83%) as a white solid. All analytical data were found to be in accordance with the literature.²²⁰ Melting point: 137-139 °C. ¹H NMR (300 MHz, CDCl₃, ppm): δ 7.64 (s, 1H), 4.78 (s, 2H), 4.01 (s, 3H). ¹³C NMR (75 MHz, CDCl₃, ppm): δ 147.7, 144.2, 134.4, 121.0,

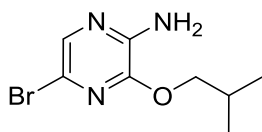
54.4. FT-IR (cm⁻¹): 3484 (s, -NH₂). HR-MS: Calculated mass: 202.9694 Mass found: 202.9703.

General Procedures for S_NAr with alcohols on 3,5-dibromo-2-aminopyrazine

Procedure A: *with NaH*: The alcohol (1.5 eq) was dissolved in dry THF (0.25 M) under an argon atmosphere. This solution was then cooled to 0 °C and NaH (1.5 eq) was slowly added (**Caution: evolution of hydrogen gas!**), keeping the temperature at 0 °C. The suspension was then allowed to stir at 0 °C for 30 min. 3,5-dibromo-2-aminopyrazine (**3.10**, 1 eq), dissolved in dry THF (0.4 M), was then slowly added while keeping the temperature at 0 °C. After addition, the reaction mixture is allowed to heat to RT and then heated at 50 °C for 18 hours. The reaction mixture was subsequently cooled to RT and diluted with EtOAc. The organic phase was then washed with water and brine before being dried over MgSO₄ and evaporated *in vacuo*. The crude product was then purified using MPLC.

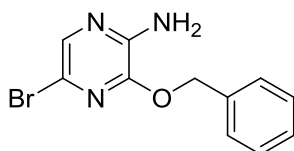
Procedure B: *with NaHMDS*: The alcohol (1.5 eq) was dissolved in dry THF (0.15 M) under an argon atmosphere. This solution was then cooled to 0 °C and NaHMDS (1.5 eq, 1 M solution in THF) was slowly added, keeping the temperature at 0 °C. The suspension was then allowed to stir at RT for 30 min. 3,5-dibromo-2-aminopyrazine (**3.10**, 1 eq), dissolved in dry THF (0.4 M), was then slowly added while keeping the temperature at 0 °C. After addition, the reaction mixture is allowed to heat to RT and then heated at 50 °C for 18 hours. The reaction mixture was subsequently cooled to RT and diluted with EtOAc. The organic phase was then washed with water and brine before being dried over MgSO₄ and evaporated *in vacuo*. The crude product was then purified using MPLC.

5-Bromo-3-isobutoxypyrazin-2-amine (3.1b)



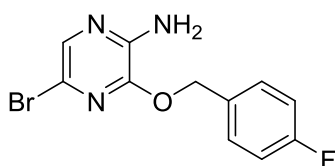
Using **procedure B**, purified by reverse phase HPLC in ACN/water (from 0% to 80% ACN in 30 minutes), **3.1b** was obtained as a red oil (88%). ¹H NMR (300 MHz, CDCl₃, ppm): δ 7.62 (s, 1H), 4.77 (bs, 2H), 4.13 (d, J = 6.7 Hz, 2H), 2.12 (m, 1H), 1.02 (d, J = 6.7 Hz, 6H). ¹³C NMR (150MHz, CDCl₃, ppm): δ 147.5, 144.2, 134.1, 121.1, 73.4, 27.8, 19.2. HR-MS: Calculated mass: 246.0237. Mass found: 246.0254.

3-(Benzyloxy)-5-bromopyrazin-2-amine (3.1c)



Using general **procedure A**, purified using MPLC (7/3 heptanes/EtOAc), **3.1c** was obtained as yellow crystals (81%). All analytical data were found to be in accordance with the literature.²²¹

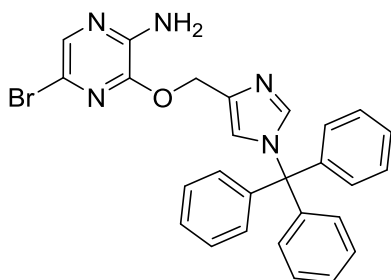
5-Bromo-3-[(4-fluorobenzyl)oxy]pyrazin-2-amine (3.1d)



Using **procedure B**, purified using MPLC (7/3 heptanes/EtOAc), **3.1d** obtained as a yellow solid (64%). Melting point: 102-104 °C. ¹H NMR (300 MHz, CDCl₃, ppm): δ 7.69 (s, 1H), 7.45 (dd, J = 8.8 Hz, 11 Hz, 2H), 7.10 (t, J = 8.8 Hz, 2H), 5.37 (s, 2H), 4.79 (bs, 2H). ¹³C NMR (75 MHz, CDCl₃, ppm): δ 147.7 (d, J =

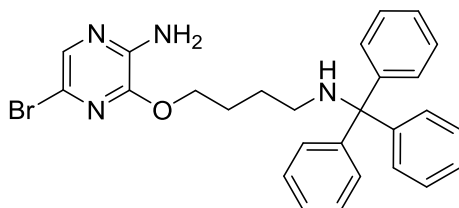
148.5Hz), 146.9, 144.1, 134.7, 130.7 (d, J = 7 Hz), 127.8, 120.8, 115.6 (d, J = 21.4 Hz), 68.3. HR-MS: Calculated mass: 296.9913 Mass found: 296.9918.

5-Bromo-3-[(1-trityl-1H-imidazol-4-yl)methoxy]pyrazin-2-amine (3.1e)



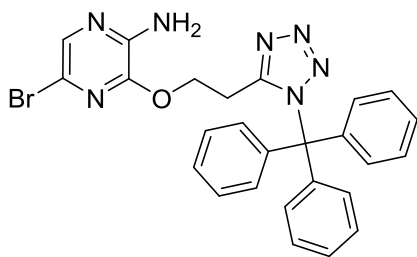
Using **procedure A**, purified using MPLC (40:60 heptanes/EtOAc), **3.1e** was obtained as a white solid (35%). Melting point: 213-215 °C. ¹H NMR (300 MHz, CDCl₃, ppm): δ 7.61 (s, 1H), 7.48 (s, 1H), 7.32-7.36 (bm, 9H), 7.10-7.14 (bm, 6H), 7.00 (s, 1H), 5.32 (s, 2H), 4.88 (bs, 2H). ¹³C NMR (75 MHz, CDCl₃, ppm): δ 146.9, 144.4, 143.5, 142.2, 139.2, 135.4, 134.3, 129.7, 128.2, 128.1, 122.5, 75.6, 62.8. HR-MS: Calculated mass: 165.0651 Mass found: 165.0646 (M – C₂₁H₁₅Br).

5-bromo-3-[4-(tritylamino)butoxy]pyrazin-2-amine (3.1f)



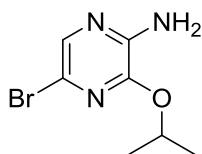
Using **procedure B**, purified using MPLC (90:10 heptanes/EtOAc), **3.1f** was obtained as a light yellow solid (10%). Melting point: 148-150 °C. ¹H NMR (300 MHz, CDCl₃, ppm): δ 7.61 (s, 1H), 7.47 (m, 6H), 7.27 (m, 6H), 7.18 (m, 3H), 4.73 (bs, 2H), 4.33 (t, J = 6.80 Hz, 2H), 2.20 (t, J = 7.4 Hz, 2H), 1.84 (m, 2H), 1.62 (m, 2H). ¹³C NMR (75 MHz, CDCl₃, ppm): δ 147.3, 146.2, 144.1, 134.2, 128.6, 127.8, 126.3, 121.1, 70.9, 67.4, 43.3, 27.4, 26.6. HR-MS: Calculated mass: 260.1201 Mass found: 260.1222.

5-Bromo-3-[2-(1-trityl-1H-tetrazol-5-yl)ethoxy]pyrazin-2-amine (3.1g)



Using **procedure B**, purified using MPLC (50:50 heptanes/EtOAc), **3.1g** was obtained as a yellow solid (54%). Melting point: 153-156 °C. ¹H NMR (300 MHz, CDCl₃, ppm): δ 7.62 (s, 1H), 7.28-7.36 (bm, 9H), 7.06-7.09 (bm, 6H), 4.72 (t, J = 6.19 Hz, 2H), 4.56 (bs, 2H), 3.43 (t, J = 6.19 Hz, 2H). ¹³C NMR (75 MHz, CDCl₃, ppm): δ 162.0, 146.6, 144.2, 141.2, 134.8, 130.2, 128.6, 128.4, 128.0, 127.8, 120.7, 83.0, 64.6, 25.7. HR-MS: [M-Trt] Calculated mass: 286.1416 Mass found: 286.1442.

5-Bromo-3-isopropoxy pyrazin-2-amine (3.1h)



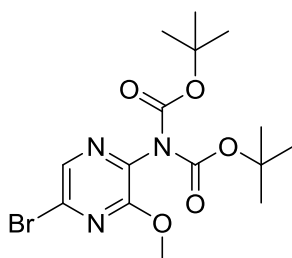
Using general **procedure A** (but 10 eq IPA and 3 eq NaH), **3.1h** was obtained as a yellow solid (91%) and was used after extraction (EtOAc/H₂O) without further purification. Melting point: 105-106 °C. ¹H NMR (300 MHz, CDCl₃, ppm): δ 7.60 (s, 1H), 5.32 (m, J = 6 Hz, 1H), 4.77 (bs, 2H), 1.37 (s, 6H). ¹³C NMR (75 MHz, CDCl₃, ppm): δ 146.9, 144.3, 133.3, 121.0, 70.5, 21.8.

Procedure C: For diBoc protection of pyrazine building blocks:

The amine (1 eq) and DMAP (0.1 eq) were dissolved in dry DCM (0.2 M) under an argon atmosphere. Boc₂O (2.5 eq) was then slowly added at RT, while stirring vigorously. Afterwards the reaction was heated to reflux for 16 hours. The mixture was then cooled to RT and the solvent was evaporated *in vacuo*.

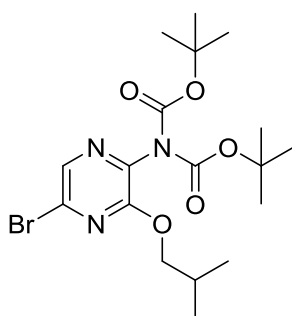
The residue was suspended in EtOAc and washed with water and brine. The organic phase was then dried over MgSO₄, filtered and evaporated *in vacuo*.

di-tert-Butyl (5-bromo-3-methoxypyrazin-2-yl)imidodicarbonate (3.2a)



5-Bromo-3-methoxypyrazin-2-amine (**3.1a**) (1 g, 4.90 mmol) was dissolved in THF (Volume: 20 mL) and cooled to <5 °C in an ice bath. Boc₂O (2.84 mL, 12.25 mmol) was slowly added and the mixture was stirred for 1 hour in the ice bath. Afterwards the solution was allowed to warm to RT and left stirring overnight. Water was added (20 mL) and the aqueous phase was extracted with EtOAc. The combined EtOAc fractions were washed with sat. NaHCO₃, water and subsequently dried over MgSO₄. The solvent was evaporated *in vacuo* to give the crude product. Purification was carried out by MPLC (9/1 heptanes/EtOAc) to give **3.2a** as white crystals (1.8 g, 91%). Melting point: 74-76 °C. ¹H NMR (300 MHz, CDCl₃, ppm): δ 8.12 (s, 1H), 4.02 (s, 3H), 1.42 (s, 18H). ¹³C NMR (75 MHz, CDCl₃, ppm): δ 155.2, 149.9, 136.9, 136.3, 134.9, 83.6, 54.9, 27.8. FT-IR (cm⁻¹): 1797 (s, carbamate). HR-MS: Calculated mass: 403.0768 Mass found: 403.0743.

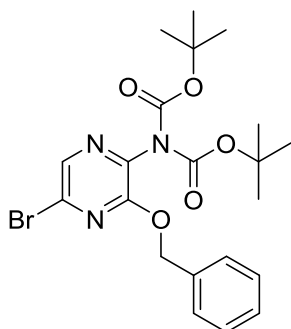
di-tert-Butyl (5-bromo-3-isobutoxypyrazin-2-yl)imidodicarbonate (3.2b)



Prepared using **procedure C**, purified using MPLC (8/2 heptanes/EtOAc), **3.2b** was obtained as an off-white solid (81%). Melting point 73-76 °C. ¹H NMR

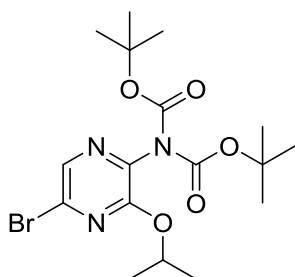
(300 MHz, CDCl₃, ppm): δ 8.09 (s, 1H), 2.08 (m, 1H), 4.16 (d, J = 6.5 Hz, 2H), 1.41 (s, 18H), 1.00 (d, J = 6.5 Hz, 6H). ¹³C NMR (75 MHz, CDCl₃, ppm): δ 155.4, 149.9, 136.8, 136.0, 135.1, 83.6, 74.0, 27.9, 27.4, 19.1. HR-MS: Calculated mass: 445.1212 Mass found: 445.1246.

di-tert-Butyl [3-(benzyloxy)-5-bromopyrazin-2-yl]imidodicarbonate (3.2c)



Prepared using **procedure C**, purified using MPLC (8/2 heptanes/EtOAc), **3.2c** was obtained as orange crystals (77%). Melting point: 69-72 °C. ¹H NMR (300 MHz, CDCl₃, ppm): δ 8.13 (1H), 7.36 (5H), 5.45 (2H), 1.35 (18H). ¹³C NMR (75 MHz, CDCl₃, ppm): δ 154.7, 149.9, 136.9, 136.5, 135.3, 134.8, 128.4, 128.3, 83.7, 69.3, 27.8. HR-MS: Calculated mass: 502.0949 Mass found: 502.0949.

di-tert-Butyl (5-bromo-3-ispropoxy-pyrazin-2-yl)imidodicarbonate (3.2d)



Prepared using **procedure C** (but 4 eq of Boc₂O), purified using MPLC (8/2 heptanes/EtOAc), **3.2d** was obtained as yellow crystals (79%). Melting point: 81-83 °C. ¹H NMR (300 MHz, CDCl₃, ppm): δ 8.07 (s, 1H), 5.46-5.28 (m, 1H), 1.41 (s, 18H), 1.35 (d, J = 6 Hz, 6H). ¹³C NMR (75 MHz, CDCl₃, ppm): δ 154.7, 149.8, 137.0, 135.7, 134.9, 83.4, 71.3, 27.9, 21.7. HR-MS: Calculated mass: 454.0949 Mass found: 454.0939 [M+Na].

General procedures for carbonylative coupling

Procedure D: *Alkoxy carbonylation of monomers with CO balloon.*

All solid reagents ($\text{Pd}(\text{OAc})_2$ (5 mol%), the pyrazine monomer (1 eq) and Xantphos (10 mol%) were brought into an oven-dried 2-necked flask with a septum, under an atmosphere of argon. The flask was evacuated and backfilled with argon, this was repeated 2 times. Methanol (10 eq) and triethylamine (0.2 M) were added with a syringe via the septum. The resulting mixture was purged with carbon monoxide for 2 minutes (**Caution!** *Carbon monoxide is a highly toxic and flammable gas*). The reaction was then placed under a carbon monoxide atmosphere by means of a balloon and heated to 80 °C in an oil bath for 24 hours. After this time, the mixture was cooled, diluted with EtOAc and filtered over Celite®. The resulting filtrate was evaporated *in vacuo* to obtain the crude product. Purification was carried out by MPLC.

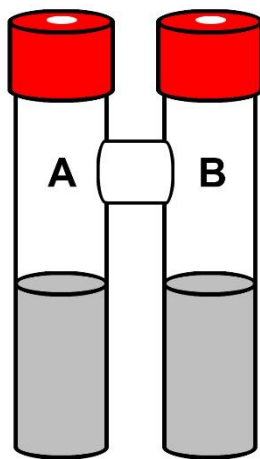
Procedure E: General procedure for CO precursor two-chamber system

Chamber A of a flame-dried two-chamber reactor was filled with 1 mg palladium(II) acetate (0.005 mmol, 1 mol%), 3 mg Xantphos (0.005 mmol, 1 mol%) and 159 mg sodium carbonate (1.50 mmol, 3 eq). The reactor was brought under argon atmosphere by two consecutive vacuum-argon cycles. Next, chamber B was filled with 2 mL dry degassed toluene, 51 μL mesyl chloride (0.65 mmol, 1.3 eq) and 25 μL formic acid (0.65 mmol, 1.3 eq). In chamber A, 1 mL dry degassed toluene was added, followed by 0.50 mmol aryl bromide (1 eq) and 0.75 mmol amine/alcohol (1.1 eq). Then the reactor was placed in an oil-bath at 100 °C. Finally, 181 μL triethylamine (1.30 mmol, 2.6 eq) was added by injection through the septum in chamber B and instant gas formation was observed.

[Remark: when the aryl bromide and/or amine are solids at room temperature, they were added to Chamber A after the addition of palladium(II) acetate and Xantphos.]

After 2 to 24 hours, the reactor was brought to room temperature and the residual pressure was released carefully by removing one of the caps. As carbon monoxide is a highly toxic gas, the reaction was stirred at room temperature for 15 minutes to ensure that all carbon monoxide gas was extracted out of the fume hood. Next, the content of chamber A was transferred to a 100 mL round bottomed flask. Chamber A was rinsed five

times with 2 mL of EtOAc and these fractions were added to the same flask. After the addition of 1 g Celite®, the solvent was removed under reduced pressure. For purification, the crude product was dry-loaded onto the MPLC system.

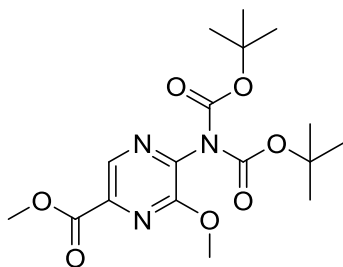


Representation of the two-chamber reactor. Inner volume = 20 mL.

Procedure F: Aminocarbonylative coupling of monomers with CO balloon

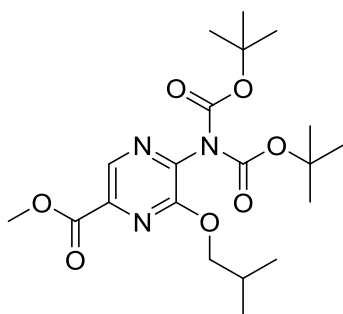
All solid reagents: monomer A (1 eq), monomer B (1 eq), Pd(OAc)₂ (5 mol%), Na₂CO₃ (3 eq) and Xantphos (5 mol%) were brought in a dry two-necked flask with a cooler and a septum, under an atmosphere of argon. The flask was evacuated and subsequently purged with argon. This was repeated 2 times. Dry degassed toluene (0.2 M) was added via a syringe. The mixture was purged with carbon monoxide for 2 minutes via a needle through the septum. (**Caution!** Carbon monoxide is a highly toxic and flammable gas). Then a carbon monoxide atmosphere was created by means of a balloon. The mixture was stirred at 80 °C, for 24 hours. Afterwards, the reaction was cooled to room temperature, diluted with EtOAc and filtered over a plug of Celite®. The filtrate was evaporated to afford the crude product which was purified by MPLC.

Methyl 5-[bis(*tert*-butoxycarbonyl)amino]-6-methoxypyrazine-2-carboxylate (3.3a)



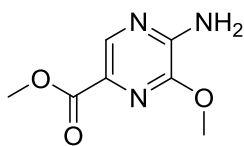
Using **Procedure D**, after purification by MPLC (8/2 heptanes/EtOAc), **3.3a** was obtained as white crystals (88%). Melting point: 99-102 °C. ¹H NMR (300 MHz, CDCl₃, ppm): δ 8.55 (s, 1H), 4.10 (s, 3H), 4.05 (s, 3H), 1.40 (s, 18H). ¹³C NMR (75 MHz, CDCl₃, ppm): δ 164.2, 155.4, 149.6, 141.4, 139.0, 136.6, 83.7, 75.5, 54.5, 52.9. FT-IR (cm⁻¹): 1742, 1705 (carbamate). HR-MS: Calculated mass: 283.1180 Mass found: 283.1182 [M – Boc].

Methyl 5-[bis(*tert*-butoxycarbonyl)amino]-6-isobutoxypyrazine-2-carboxylate (3.3b)



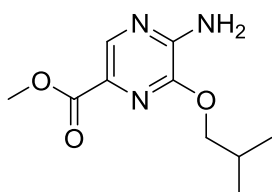
Using **Procedure D**, after purification by MPLC (8/2 heptanes/EtOAc), **3.3b** was obtained as a white solid (89%). Melting point 59-62 °C. ¹H NMR (300 MHz, CDCl₃, ppm): δ 8.71 (s, 1H), 4.26 (d, J = 6 Hz, 2H), 4.00 (s, 3H), 2.10 (m, 1H), 1.39 (s, 18H), 1.01 (d, J = 6.8 Hz, 6H). ¹³C NMR (75 MHz, CDCl₃, ppm): δ 164.2, 155.6, 149.6, 141.3, 139.1, 136.3, 83.7, 73.5, 52.9, 27.9, 27.8, 19.1. HR-MS: Calculated mass: 425.2162 Mass found: 425.2125.

Methyl 5-amino-6-methoxypyrazine-2-carboxylate (**3.4a**)



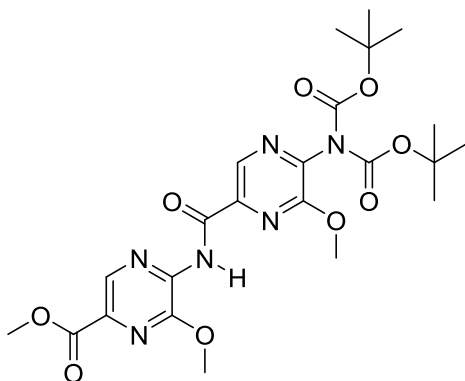
Methyl 5-[bis(tert-butoxycarbonyl)amino]-6-methoxypyrazine-2-carboxylate (**3.3a**) (800 mg, 2.1 mmol) was dissolved in 10 mL of dry DCM and the solution was cooled in an ice bath. To this TFA (3.2 mL, 41.7 mmol) was added dropwise while stirring. After the addition of TFA, the reaction was stirred at RT for 6 hours. Afterwards, the solvent was evaporated *in vacuo*. The residue was purified using MPLC (7/3 EtOAc/heptanes) to obtain the pure product **3.3b** as off-white crystals (350 mg, 92%). Melting point: 87-88 °C. ¹H NMR (300 MHz, CDCl₃, ppm): δ 8.35 (s, 1H), 5.81 (bs, 2H), 4.11 (s, 3H), 3.93 (s, 3H). ¹³C NMR (75 MHz, CDCl₃, ppm): δ 165.3, 147.8, 147.3, 138.1, 128.6, 54.0, 52.2. FT-IR (cm⁻¹): 3338, 3111, 2953, 2876, 1715, 1551, 1447. HR-MS: Calculated mass: 183.0644 Mass found: 183.0650.

Methyl 5-amino-6-isobutoxypyrazine-2-carboxylate (**3.4b**)



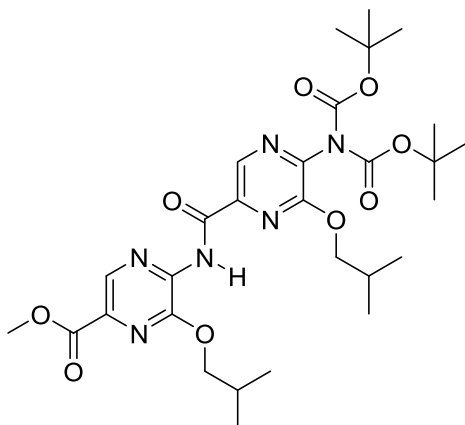
In a sealed vessel under an argon atmosphere, methyl 5-[bis(tert-butoxycarbonyl)amino]-6-isobutoxypyrazine-2-carboxylate (**3.3b**) (220 mg, 0.517 mmol) was suspended in 15 mL of water. The mixture was stirred vigorously while heating to 100 °C for 24 hours. The suspension was then allowed to cool to RT and extracted three times with EtOAc. The combined organic phases were washed with water, brine and dried over MgSO₄. After filtration, the filtrate was evaporated *in vacuo* to give the pure product (**3.4b**) as white crystals (90 mg, 77%). Melting point: 115-117 °C. ¹H NMR (300 MHz, CDCl₃, ppm): δ 8.37 (s, 1H), 5.33 (bs, 2H), 4.25 (d, J = 6.6 Hz, 2H), 3.92 (s, 3H), 2.13 (m, 1H), 1.04 (d, J = 6.6 Hz, 6H). ¹³C NMR (75 MHz, CDCl₃, ppm): δ 165.3, 147.8, 147.2, 137.9, 128.6, 72.9, 52.2, 29.7, 27.9, 19.3. HR-MS: Calculated mass: 226.11860 Mass found: 226.1201.

Methyl 5-[(5-[bis(*tert*-butoxycarbonyl)amino]-6-methoxypyrazin-2-yl)11-carbonyl)amino]-6-methoxypyrazine-2-carboxylate (3.5a)



Using **procedure F**, after purification using MPLC (9/1 heptanes/EtOAc), **3.5a** was obtained as white crystals (60%). Melting point: 242 °C (decomposition). ^1H NMR (300 MHz, CDCl_3 , ppm): δ 10.53 (s, 1H), 8.98 (s, 1H), 8.81 (s, 1H), 4.21 (s, 3H), 4.17 (s, 3H), 3.99 (s, 3H), 2.17 (s, 18H). ^{13}C NMR (75 MHz, CDCl_3 , ppm): δ 164.3, 159.7, 154.2, 149.7, 149.1, 142.1, 140.3, 139.1, 137.6, 135.4, 134.0, 84.0, 55.0, 54.2, 52.7, 27.8. HR-MS: Calculated mass: 534.2074 Mass found: 534.2103.

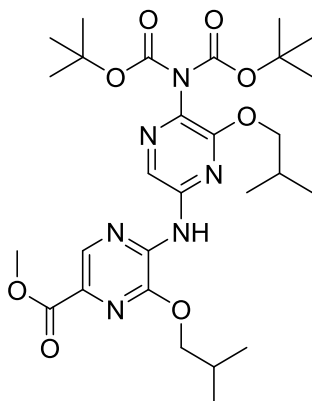
Methyl 5-[(5-[bis(*tert*-butoxycarbonyl)amino]-6-isobutoxypyrazin-2-yl)carbonyl)amino]-6-isobutoxypyrazine-2-carboxylate (3.5b)



Using **procedure F**, after purification using MPLC (1/1 heptanes/EtOAc), **3.5b** was obtained as a yellow oil (59%). ^1H NMR (300 MHz, CDCl_3 , ppm): δ 10.39

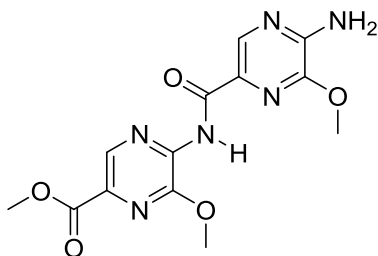
(s, 1H), 8.98 (s, 1H), 8.80 (s, 1H), 4.37 (d, $J = 6.4$ Hz, 2H), 4.25 (d, $J = 6.4$ Hz, 2H), 3.99 (s, 3H), 2.18 (bm, 2H), 1.43 (s, 18H), 1.10 (d, $J = 7$ Hz, 6H), 1.07 (d, $J = 7$ Hz, 6H). ^{13}C NMR (75 MHz, CDCl_3 , ppm): δ 164.4, 159.9, 154.5, 149.8, 148.9, 142.2, 140.3, 139.4, 137.3, 135.4, 134.0, 83.9, 73.9, 73.5, 52.7, 28.1, 21.1, 19.4, 19.2. HR-MS: Calculated mass: 618.3013, Mass found: 618.3000.

Methyl-[(5-(bis[(tert-butoxy)carbonyl]amino) -6-(2-methylpropoxy)pyrazin-2-yl)amino]-6-(2-methylpropoxy)pyrazine-2-carboxylate (3.5b')



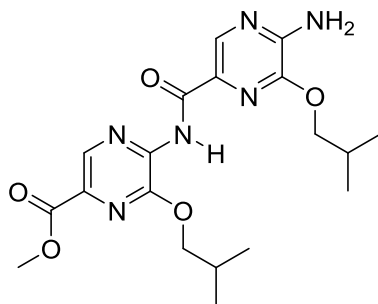
Using **procedure F**, after purification using MPLC (1/1 heptanes/EtOAc), **3.5b'** was obtained as off-white crystals (59%). Melting point: 130-133 °C. ^1H NMR (300 MHz, CDCl_3 , ppm): δ 9.28 (s, 1H), 8.60 (s, 1H), 7.82 (s, 1H), 4.36 (d, $J = 6.7$ Hz, 2H), 4.12 (d, $J = 6.5$ Hz, 2H), 3.95 (s, 3H), 2.32 – 2.16 (m, 1H), 2.15 – 2.00 (m, $J = 13.3, 6.7$ Hz, 1H), 1.40 (s, 18H), 1.09 (d, $J = 6.7$ Hz, 6H), 1.01 (d, $J = 6.7$ Hz, 6H). ^{13}C NMR (101 MHz, CDCl_3 , ppm): δ 165.1, 154.3, 150.6, 147.5, 145.1, 142.3, 137.1, 132.6, 130.6, 123.8, 83.0, 73.7, 73.1, 52.5, 28.1, 28.0, 19.4, 19.3. HR-MS: Calculated mass: 591.3137 Mass found: 591.3120 $[\text{M}+\text{H}]$

Methyl 5-[[[(5-amino-6-methoxypyrazin-2-yl)carbonyl]amino]-6-methoxypyrazine-2-carboxylate (3.6a)



Methyl-5-[[[(5-[bis(*tert*-butoxycarbonyl)amino]-6-isobutoxypyrazin-2-yl)carbonyl) amino]-6-isobutoxypyrazine-2-carboxylate (**3.5a**) (200 mg, 0.374 mmol) was dissolved in 20 mL of DCM under an atmosphere of argon. The solution was cooled to 0 °C in an ice bath and TFA (0.577 mL, 7.48 mmol) was slowly added while stirring. The reaction mixture was then stirred at RT for 4 hours. Afterwards, the solvent was evaporated *in vacuo* to give a white-yellow powder, which was washed with water, MeOH, heptanes, EtOAc and DCM to afford **3.6a** as an off-white powder (125 mg, quant.). Melting point: 290 °C (decomposition). Due to the poor solubility of this product in all solvents tried, analytical data are not available.

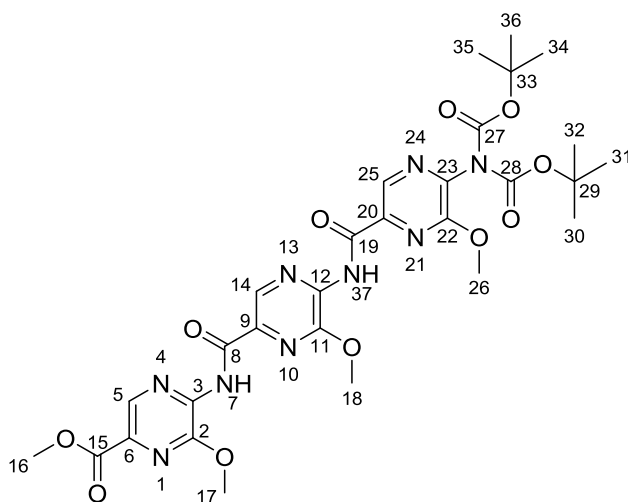
Methyl 5-[5-amino-6-(2-methylpropoxy)pyrazine-2-amido]-6-(2-methylpropoxy) pyrazine-2-carboxylate (3.6b)



In a sealed vessel under an argon atmosphere, methyl 5-[[[(5-[bis(*tert*-butoxycarbonyl)amino]-6-isobutoxypyrazin-2-yl)carbonyl) amino]-6-isobutoxypyrazine-2-carboxylate (**3.5b**) (115 mg, 0.186 mmol) was suspended in 7 mL of water. The mixture was stirred vigorously while heating to 100 °C for 72 hours. The suspension was then allowed to cool to RT and

extracted three times with EtOAc. The combined organic phases were washed with water, brine and dried over MgSO₄. After filtration, the filtrate was evaporated *in vacuo* to give the pure product (**3.6b**) as white crystals (72 mg, 92%). Melting point: 196-198 °C. ¹H NMR (300 MHz, CDCl₃, ppm): δ 8.77 (s, 1H), 8.59 (s, 1H), 5.60 (bs, 2H), 4.23 (d, J = 6 Hz, 2H), 3.97 (s, 3H), 2.19 (m, 2H), 1.10 (d, J = 6.8 Hz, 6H), 1.09 (d, J = 6.8 Hz, 6H). ¹³C NMR (75 MHz, CDCl₃, ppm): δ 164.9, 161.3, 148.8, 148.4, 146.0, 141.0, 137.4, 136.8, 133.0, 129.5, 73.7, 72.9, 52.6, 28.1, 28.0, 19.5, 19.3. HR-MS: Calculated mass: 418.1965. Mass found: 418.1971.

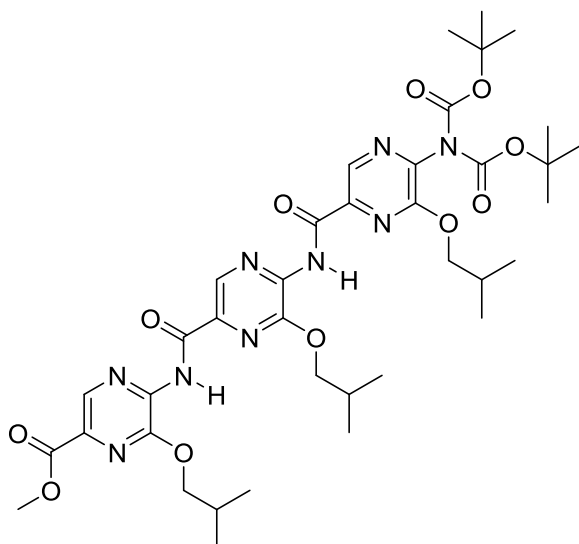
Methyl 5-[[[(5-[[[bis(*tert*-butoxycarbonyl)amino]-6-methoxypyrazin-2-yl)carbonyl)amino]-6-methoxypyrazin-2-yl)carbonyl)amino]-6-methoxypyrazine-2-carboxylate (3.7a**)**



Using **procedure F**, after purification using MPLC (9/1 EtOAc/heptanes), **3.7a** was obtained as a white solid (17%). Peak assignments of the ¹³C and ¹H NMR spectra were confirmed using 2D NMR experiments. ¹H NMR (300 MHz, CDCl₃, ppm): δ 10.50 (s, 1H, H³⁷), 10.40 (s, 1H, H⁷), 9.04 (s, 1H, H⁵), 9.00 (s, 1H, H²⁵), 8.81 (s, 1H, H¹⁴), 4.27 (s, 3H, H¹⁷), 4.21 (s, 3H, H¹⁸), 4.18 (s, 3H, H²⁶), 3.99 (s, 3H, H¹⁶), 1.44 (s, 18H, H^{30-32, 34-37}). ¹³C NMR (75 MHz, CDCl₃, ppm): δ 164.3 (C¹⁵), 159.8 (C¹⁹), 159.5 (C⁸), 154.2 (C²²), 149.7 (C^{27,28}), 149.0 (C¹¹), 148.0 (C²), 142.2 (C²³), 140.9 (C³), 140.5 (C¹²), 139.0 (C²⁰), 137.6 (C¹⁴), 136.3 (C²⁵), 135.5 (C⁵), 134.5 (C⁶), 133.8 (C⁹), 84.1 (C^{29,33}), 55.0 (C²⁶), 54.7 (C¹⁷), 54.2 (C¹⁸),

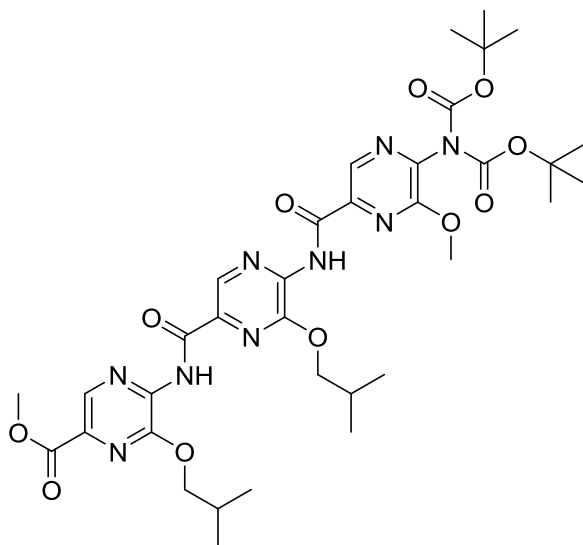
52.7 (C¹⁵), 27.9 (C^{30-32, 34-36}). HR-MS: Calculated mass: 483.1266 Mass found: 483.1278 [M-2Boc].

Methyl 5-[[[(5-[[[5-bis(*tert*-butoxycarbonyl)amino]-6-isobutoxypyrazin-2-yl)carbonyl)amino]-6-isobutoxypyrazin-2-yl)carbonyl)amino]-6-isobutoxypyrazine-2-carboxylate (3.7b)



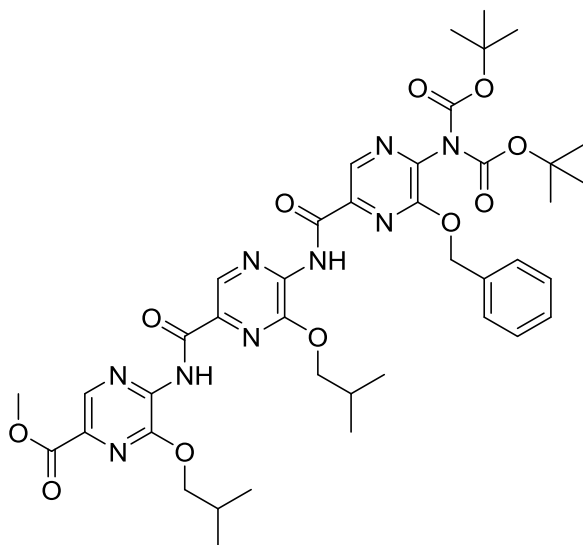
Using **procedure F**, after purification using MPLC (8/2 EtOAc/heptanes), **3.7b** was obtained as an off-white wax (19%). ¹H NMR (300 MHz, CDCl₃, ppm): δ 1.08 (d, J = 6.8 Hz, 6H), 1.11 (d, J = 6.8 Hz, 6H), 1.16 (d, J = 6.8 Hz, 6H), 1.44 (s, 18H), 2.19 (m, 1H), 3.99 (m, 2H), 4.26 (d, J = 6.8 Hz, 2H), 4.35 (d, J = 6.8 Hz, 2H), 4.37 (d, J = 6.8 Hz, 2H), 8.79 (s, 1H), 9.00 (s, 1H), 9.06 (s, 1H), 10.26 (s, 1H), 10.37 (s, 1H). ¹³C NMR (75 MHz, CDCl₃, ppm): δ 164.4, 160.0, 159.8, 154.5, 149.8, 148.9, 147.9, 142.3, 141.0, 140.5, 139.3, 137.4, 136.3, 135.5, 134.6, 133.8, 84.0, 73.8, 73.5, 52.7, 28.2, 28.1, 28.0, 27.9, 19.5, 19.4, 19.2.

Methyl-[5-(5-(bis[(tert-butoxy)carbonyl]amino)12-6-methoxypyrazine-2-amido)-6-(2-methylpropoxy)pyrazine-2-amido]-6-(2-methylpropoxy)pyrazine-2-carboxylate (3.7c)



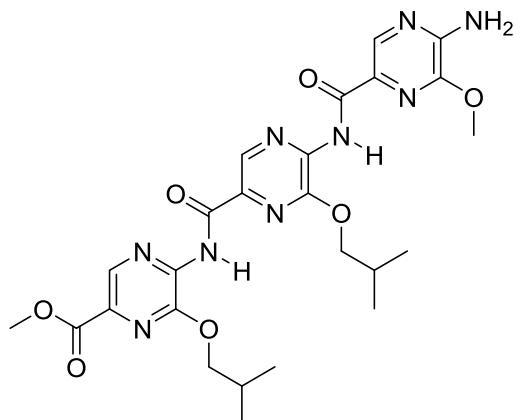
Using **procedure F**, after purification using MPLC (95/5 DCM/MeOH), **3.7c** was obtained as a yellow solid (23%). Melting point: 215-219 °C. ^1H NMR (400 MHz, CDCl_3) δ 10.43 (s, 1H), 10.25 (s, 1H), 9.05 (s, 1H), 9.01 (s, 1H), 8.78 (s, 1H), 4.40 – 4.32 (m, 4H), 4.14 (s, 3H), 3.98 (s, 3H), 1.44 (s, 18H), 1.15 (d, J = 6.6 Hz, 6H), 1.10 (d, J = 6.6 Hz, 6H). ^{13}C NMR (101 MHz, CDCl_3) δ 164.4, 160.0, 159.6, 154.3, 149.8, 148.9, 147.9, 142.3, 141.0, 140.5, 139.1, 137.4, 136.4, 135.8, 134.7, 133.8, 84.1, 73.8, 73.7, 54.2, 52.7, 28.2, 28.1, 27.9, 19.5, 19.4. HR-MS: Calculated mass: 770.3468 Mass found: 770.3480 $[\text{M}+\text{H}]$.

Methyl-(5-[6-(benzyloxy)-5-(bis[(tert-butoxy)carbonyl]amino)pyrazine-2-amido]-6-(2-methylpropoxy)pyrazine-2-amido)-6-(2-methylpropoxy)pyrazine-2-carboxylate (3.7d)



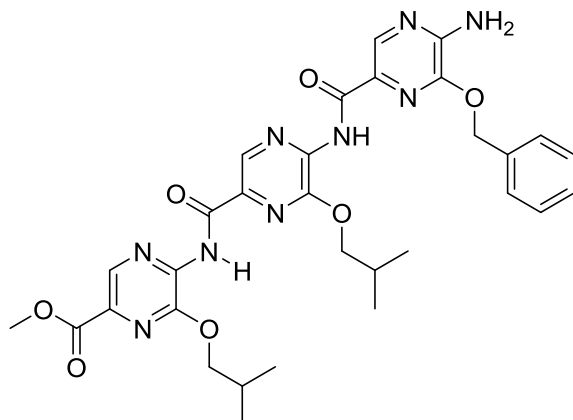
Using **procedure F**, after purification using MPLC (95/5 DCM/MeOH), **3.7d** was obtained as a yellow solid (24%). ^1H NMR (400 MHz, CDCl_3) δ 10.45 – 10.41 (m, 1H), 10.25 (s, 1H), 9.07 (s, 1H), 9.04 (s, 1H), 8.79 (s, 1H), 7.45 – 7.38 (m, J = 5.2, 3.6 Hz, 5H), 5.54 (s, 2H), 4.40 – 4.28 (m, J = 10.5, 6.6 Hz, 4H), 3.98 (s, 3H), 2.25 – 2.11 (m, J = 13.3, 6.6 Hz, 2H), 1.38 (s, 18H), 1.11 – 1.06 (m, J = 6.7, 2.4 Hz, 12H). ^{13}C NMR (101 MHz, CDCl_3) δ 164.4, 160.0, 159.6, 153.9, 149.8, 148.9, 147.9, 142.3, 141.0, 140.5, 139.1, 137.4, 136.4, 135.9, 134.7, 133.8, 128.9, 128.8, 128.1, 84.1, 73.8, 73.8, 69.1, 52.7, 28.2, 28.1, 27.8, 19.5. HR-MS: Calculated mass: 846.3781 Mass Found: 846.3801 $[\text{M}+\text{H}]$.

Methyl-5-[5-(5-amino-6-methoxypyrazine-2-amido)-6-(2-methylpropoxy)pyrazine-2-amido]-6-(2-methylpropoxy)pyrazine-2-carboxylate (3.8a**)**



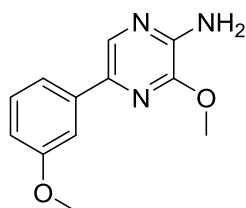
3.7c was dissolved in dry DCM (0.2 M) and the solution was cooled in an ice bath. Subsequently, TFA (20 eq) was added dropwise while stirring. After the addition of TFA, the reaction was stirred at RT for 6 hours. Afterwards, the solvent was evaporated *in vacuo* to obtain the pure product (**3.8a**) as a yellow solid (98%). Due to the poor solubility of this product in all solvents tried, NMR data are not available. FT-IR (cm⁻¹): 3499 (-NH₂), 3338, 2919, 1719. HR-MS: Calculated mass: 570.2419 Mass found: 570.2416 [M+H].

Methyl-5-(5-[5-amino-6-(benzyloxy)pyrazine-2-amido]-6-(2-methylpropoxy)pyrazine-2-amido)-6-(2-methylpropoxy)pyrazine-2-carboxylate (3.8b)



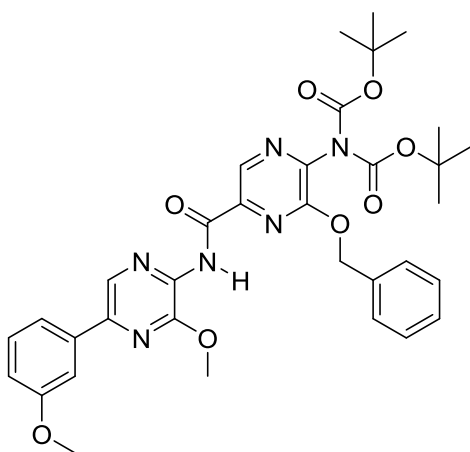
3.7d was dissolved in dry DCM (0.2 M) and the solution was cooled in an ice bath. Subsequently, TFA (20 eq) was added dropwise while stirring. After the addition of TFA, the reaction was stirred at RT for 6 hours. Afterwards, the solvent was evaporated *in vacuo* to obtain the pure product (**3.8b**) as a yellow solid (quant.). Melting point: 244-246 °C. ^1H NMR (400 MHz, CDCl_3) δ 10.34 (s, 1H) 10.26 (s, 1H), 9.03 (s, 1H), 8.78 (s, 1H), 8.65 (s, 1H), 7.51 – 7.43 (m, 5H), 5.48 (s, 4H), 4.39 – 4.28 (m, 4H), 3.97 (d, J = 2.3 Hz, 3H), 2.27 – 2.09 (m, 2H), 1.13 – 1.04 (m, J = 6.7, 1.9 Hz, 12H). ^{13}C NMR (101 MHz, CDCl_3) δ 164.6, 161.0, 160.4, 149.0, 148.5, 147.8, 145.7, 141.8, 140.8, 137.6, 137.6, 137.5, 136.6, 135.2, 133.9, 133.8, 129.2, 129.1, 128.7, 73.9, 73.8, 69.0, 52.8, 28.3, 28.2, 19.6, 19.5. HR-MS: Calculated mass: 846.3781 Mass found: 846.3801 $[\text{M}+\text{H}]$.

3-methoxy-5-(3-methoxyphenyl)pyrazin-2-amine (3.11)



5-bromo-3-methoxypyrazin-2-amine (**3.1a**) (246 mg, 1.21 mmol), (2-methoxyphenyl)boronic acid, (220 mg, 1.45 mmol), S-Phos (4 mol%), Pd(OAc)₂ (2 mol%) and K₂CO₃ (500 mg, 3.62 mmol) were brought in a dry two-necked flask with a cooler and a septum, under an atmosphere of argon. The flask was evacuated and subsequently purged with argon. This was repeated two times. A degassed mixture of ACN/water (3/2, 6.5 mL, 0.2 M) was added via a syringe. The mixture was stirred at 100 °C, for 24 hours. Afterwards, the reaction was cooled to RT, diluted with EtOAc and filtered over a plug of Celite®. The filtrate was dried over MgSO₄, filtered and evaporated *in vacuo*. The reaction mixture was purified using MPLC (75/25 heptanes/EtOAc) to give 3-methoxy-5-(3-methoxyphenyl)pyrazin-2-amine (**3.11**) as a white solid (203 mg, 73%). Melting point: 92-94 °C. ¹H NMR (300 MHz, CDCl₃, ppm): δ 8.03 (s, 1H), 7.48 (m, 2H), 7.33 (m, 1H), 6.87 (m, 1H), 4.95 (s, 2H), 4.08 (s, 3H), 3.87 (s, 3H). ¹³C NMR (75 MHz, CDCl₃, ppm): δ 156.0, 147.7, 144.4, 138.7, 138.0, 130.0, 129.7, 117.8, 112.9, 111.3, 55.3, 53.4. HR-MS: Calculated mass: 231.1008 Mass found: 231.1007.

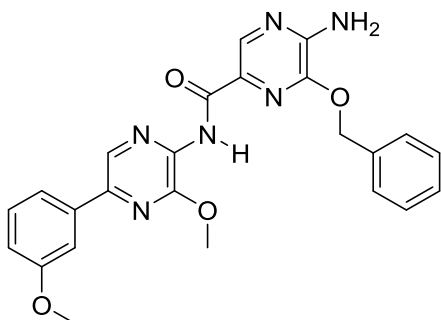
di-tert-butyl [3-(benzyloxy)-5-([(3-methoxy-5-(3-methoxyphenyl)pyrazin-2-yl]amino)carbonyl)pyrazin-2-yl]imidodicarbonate



Using **procedure F**, after purification using MPLC (9/1 heptanes/EtOAc), the product was obtained as white crystals (21%). Melting point: 101-103 °C. ¹H NMR (300 MHz, CDCl₃, ppm): δ 10.19 (s, 1H), 8.98 (s, 1H), 8.54 (s, 1H), 7.58 - 7.37 (m, 9H), 5.62 (s, 2H), 4.20 (s, 3H), 3.90 (s, 3H), 1.37 (s, 18H). ¹³C NMR (75 MHz, CDCl₃, ppm): δ 160.1, 153.6, 149.7, 149.4, 144.1, 141.7, 139.6, 137.4, 136.0, 135.4, 135.3, 131.2, 130.0, 128.7, 128.6, 127.9, 118.8, 114.4, 112.4,

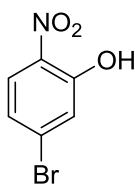
83.9, 68.9, 55.4, 54.2, 27.8. HR-MS: Calculated mass: 659.2824 Mass found: 659.2829.

Methyl 5-([5-amino-6-(benzyloxy)pyrazin-2-yl]carbonyl)amino)-6-methoxypyrazine-2-carboxylate (3.12)

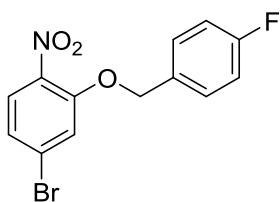


di-*tert*-butyl [3-(benzyloxy)-5-([3-methoxy-5-(3-methoxyphenyl)pyrazine-2-yl]amino) carbonyl]pyrazin-2-yl]imidodicarbonate (65 mg, 0.01 mmol) was dissolved in 8 mL of DCM under an atmosphere of argon. The solution was cooled to 0 °C in an ice bath and TFA (0.15 mL, 1.97 mmol) was slowly added while stirring. The reaction mixture was then stirred at RT for 4 hours. Afterwards, the solvent was evaporated to give a white-yellow powder, which was dissolved in EtOAc and extracted with NaHCO₃. The organic phase was evaporated *in vacuo* to give **3.12** as a yellow powder (45 mg, quant.). Melting point: 240-243 °C. ¹H NMR (300 MHz, CDCl₃, ppm): δ 10.0 (s, 1H), 8.60 (s, 1H), 8.51 (s, 1H), 7.59 - 7.37 (m, 5H), 6.98 - 6.94 (m, 4H), 5.55 (bs, 2H), 5.40 (s, 2H), 4.17 (s, 3H), 3.89 (s, 3H). ¹³C NMR (75 MHz, CDCl₃, ppm): δ 161.0, 160.1, 149.2, 148.0, 145.3, 143.1, 137.7, 136.8, 136.5, 135.6, 131.1, 129.9, 129.8, 128.8, 128.7, 128.5, 118.7, 114.1, 112.2, 68.6, 55.4, 54.1. HR-MS: Calculated mass: 459.1775 Mass found: 459.1772.

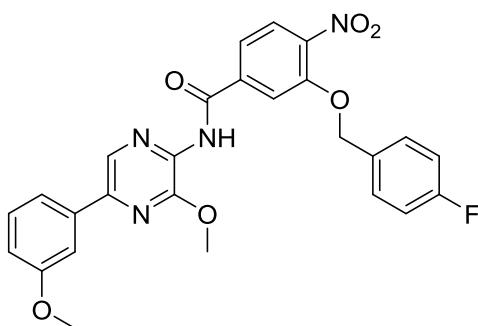
5-bromo-2-nitrophenol (**3.14**)



KOtBu (5.54 g, 49.40 mmol) was added to 20 mL of $\text{NH}_{3(l)}$ under an argon atmosphere while stirring. A solution of cumene hydroperoxide (1.56 mL, 10.86 mmol) and 1-bromo-4-nitrobenzene (2 g, 9.90 mmol) in 7 mL of dry THF was then added dropwise. The reaction mixture was refluxed at $-33\text{ }^{\circ}\text{C}$ for 30 minutes, after which the reaction was quenched by first slowly adding solid NH_4Cl , followed by sat. aqueous NH_4Cl . Aqueous HCl (1 M) was then added until an acidic pH was observed on a pH indicator strip. The mixture was subsequently extracted with EtOAc (3x50 mL), dried and evaporated *in vacuo*. Purification was performed using MPLC (9/1 heptanes/EtOAc) to give **3.14** as bright yellow crystals (1.23 g, 57%). Melting point: $28\text{--}29\text{ }^{\circ}\text{C}$. ^1H NMR (300 MHz, CDCl_3 , ppm): δ 7.14 (dd, $J = 2.9\text{ Hz}$, 1H), 7.38 (d, $J = 2\text{ Hz}$, 1H), 7.98 (d, $J = 9\text{ Hz}$, 1H), 10.63 (s, 1H). ^{13}C NMR (75 MHz, CDCl_3 , ppm): δ 155.3, 132.7, 132.3, 126.1, 123.9, 123.0. FT-IR (cm^{-1}): 1521, 1310 (s, $-\text{NO}_2$). HR-MS: Calculated mass: 215.9302 Mass found: 215.9294.

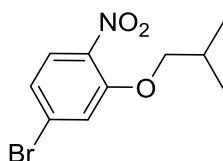
4-bromo-2-[(4-fluorobenzyl)oxy]-1-nitrobenzene (3.15)

5-Bromo-2-nitrophenol (**3.14**) (500 mg, 2.29 mmol), *p*-fluorobenzylalcohol (318 mg, 2.52 mmol) and PPh₃ (902 mg, 3.44 mmol) were dissolved in 4 mL of dry THF under an argon atmosphere. The solution was then cooled to 0 °C and DIAD (696 mg, 3.44 mmol) was slowly added while keeping the temperature at 0 °C. Afterwards the reaction mixture was allowed to warm to RT and stirred for an additional 18 hours. Then the solvent was evaporated and the residue was redissolved in EtOAc and filtered over silica gel. The filtrate was once again evaporated *in vacuo* to deliver the crude product. Purification was performed using MPLC (9/1 heptanes/EtOAc) to give product **3.15** as a yellow solid (462 mg, 62%). Melting point: 80-82 °C. ¹H NMR (300 MHz, CDCl₃, ppm): δ 7.78 (d, *J* = 8.6 Hz, 1H), 7.44 (dd, *J* = 8.8, 5.3 Hz, 2H), 7.29 (d, *J* = 1.9 Hz, 1H), 7.21 (dd, *J* = 8.6, 1.9 Hz, 1H), 7.10 (t, *J* = 8.7 Hz, 2H), 5.18 (s, 2H). ¹³C NMR (75 MHz, CDCl₃, ppm): 162.8 (d, *J* = 247.2 Hz), 152.4 (s), 139.0 (s), 130.6 (d, *J* = 3.2 Hz), 129.0 (d, *J* = 8.3 Hz), 128.4 (s), 127.0 (s), 124.1 (s), 118.5 (s), 115.8 (d, *J* = 21.7 Hz), 71.0 (s). HR-MS: Several ionization methods tried. Suspicion that compound is not ionisable.

3-[(4-fluorobenzyl)oxy]-*N*-(3-methoxy-5-morpholin-4-yl)pyrazin-2-yl)-4-nitrobenzamide (3.16)

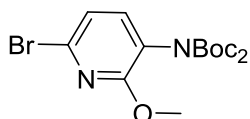
Using **procedure F**, after purification using reverse phase HPLC in ACN/water (from 0% to 80% ACN in 30 minutes), **3.16** was obtained as yellow crystals (65%). Melting point: 83-85 °C. ^1H NMR (300 MHz, CDCl_3 , ppm): δ 8.50 (s, 1H), 8.45 (s, 1H), 7.94 (d, J = 9Hz, 1H), 7.79 (s, 1H), 7.60-7.54 (m, 2H), 7.51-7.37 (m, 3H), 7.09 (t, J = 9Hz, 2H), 6.99 (d, J = 9Hz, 1H), 5.30 (s, 2H), 4.18 (s, 3H), 3.90 (s, 3H). ^{13}C NMR (75 MHz, CDCl_3 , ppm): δ 162.7 (d, J = 123.7 Hz), 162.6 (s), 160.1 (s), 151.9 (s), 149.6 (s), 144.9 (s), 142.3 (s), 139.2 (s), 137.2 (s), 135.8 (s), 131.0 (s), 130.7 (d, J = 3.3 Hz), 13.0 (s), 129.2 (d, J = 8.3 Hz), 125.9 (s), 118.8 (s), 118.4 (s), 115.8 (d, J = 21.7 Hz), 115.3 (s), 114.6 (s), 112.4 (s), 70.9 (s), 55.4 (s), 54.2 (s). HR-MS: Calculated mass: 505.1518 Mass found: 505.1520.

4-bromo-2-isobutoxy-1-nitrobenzene (**3.17**)



5-Bromo-2-nitrophenol (**3.14**) (500 mg, 2.29 mmol), isobutyl alcohol (318 mg, 2.52 mmol) and PPh_3 (902 mg, 3.44 mmol) were dissolved in 4 mL of dry THF under an argon atmosphere. The solution was then cooled to 0 °C and DIAD (696 mg, 3.44 mmol) was slowly added while keeping the temperature at 0 °C. Afterwards the reaction mixture was allowed to warm to RT and stirred for an additional 18 hours. Then the solvent was evaporated and the residue was redissolved in EtOAc and filtered over silica gel. The filtrate was once again evaporated *in vacuo* to deliver the crude product. Purification was performed using MPLC (9/1 heptanes/EtOAc) to give product **3.17** as a yellow solid (60%). Melting point: 80-82 °C. ^1H NMR (300 MHz, CDCl_3) δ 7.74 (d, J = 8.6 Hz, 1H), 7.24 – 7.06 (m, 2H), 3.85 (d, J = 6.4 Hz, 2H), 2.16 (m, 1H), 1.06 (d, J = 6.7 Hz, 6H).

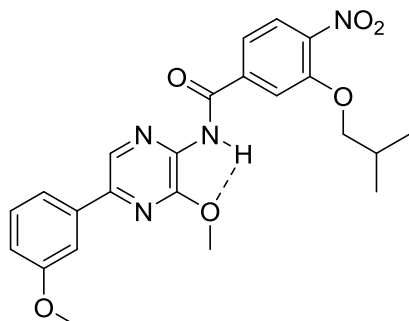
ditert-butyl (6-bromo-2-methoxypyridin-3-yl)carbamate (**3.18**)



Prepared from 6-bromo-2-methoxypyridin-3-amine using **procedure C**, purified using MPLC (8/2 heptanes/EtOAc), **3.18** was obtained as a yellow oil

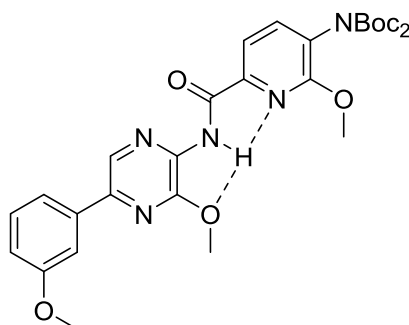
(67%). ^1H NMR (300 MHz, CDCl_3 , ppm): δ 7.38 (d, J = 7.8 Hz, 1H), 7.24 (d, J = 7.8 Hz, 2H), 3.94 (s, 3H), 1.41 (s, 18H).

3-[isobutoxy]-*N*-(3-methoxy-5-morpholin-4-ylpyrazin-2-yl)-4-nitrobenzamide (3.19)



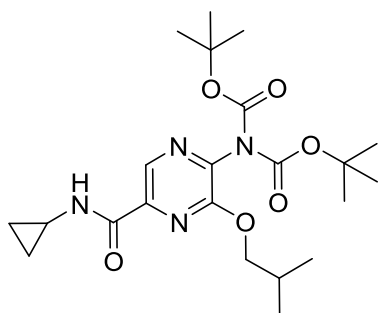
Using **procedure E**, after purification using reverse phase HPLC (100% H_2O \rightarrow 100% MeCN in 20 minutes), **3.19** was obtained as yellow crystals (10%). ^1H NMR (300 MHz, CDCl_3 , ppm): δ 8.50 (s, 2H), 7.91 (d, J = 8.3 Hz, 1H), 7.69 (s, 1H), 7.58 (d, J = 7.2 Hz, 2H), 7.42 (d, J = 8.2 Hz, 1H), 6.99 (d, J = 8.6 Hz, 1H), 4.18 (s, 2H), 3.97 (d, J = 6.4 Hz, 1H), 3.90 (s, 2H), 2.27 – 2.07 (m, 1H), 1.07 (d, J = 6.7 Hz, 4H).

3.20



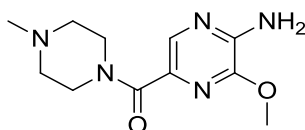
Using **procedure E**, after purification using reverse phase HPLC (100% H_2O \rightarrow 100% MeCN in 20 minutes), **3.20** was obtained as a white solid (15%). ^1H NMR (300 MHz, CDCl_3 , ppm): δ 10.66 (s, 1H), 8.51 (s, 1H), 8.07 – 7.88 (m, 2H), 7.69 – 7.28 (m, 4H), 4.19 (s, 3H), 4.13 (s, 3H), 3.90 (s, 3H), 1.42 (s, 18H). ^{13}C NMR (75 MHz, CDCl_3) δ 160.6, 160.1, 157.8, 150.5, 149.4, 145.3, 143.5, 138.5, 137.66, 136.6, 131.1, 129.9, 127.2, 118.7, 116.6, 114.2, 112.3, 83.4, 55.4, 54.1, 53.7, 27.9.

tert-Butyl *N*-[(tert-butoxy)carbonyl]-*N*-[5-(cyclopropylcarbamoyl)-3-(2-methylpropoxy)pyrazin-2-yl]carbamate (3.21)



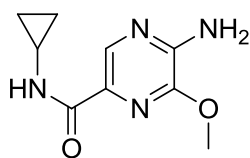
General **procedure E** was followed using **3.2a** (75 mg, 0.168 mmol). As cyclopropylamine is a liquid, it was injected after addition of dry degassed toluene to chamber A. The crude product was purified using MPLC (8/2 heptanes/EtOAc) to obtain the title compound (**3.21**) as a yellow solid (79%). ¹H NMR (400 MHz, CDCl₃) δ 8.78 (s, 1H), 7.47 (bs, 1H), 4.12 (d, J = 6.4 Hz, 2H), 2.94 – 2.79 (m, J = 7.0, 3.3 Hz, 1H), 2.21 – 1.95 (m, 1H), 1.36 (s, 18H), 1.00 (d, J = 6.7 Hz, 6H), 0.94 – 0.83 (m, J = 6.9 Hz, 2H), 0.73 – 0.59 (m, 2H). ¹³C NMR (101 MHz, CDCl₃) δ 164.1, 154.3, 149.8, 141.0, 140.2, 134.0, 83.6, 73.3, 27.9, 27.8, 22.6, 19.2, 6.8.

3-methoxy-5-(4-methylpiperazine-1-carbonyl)pyrazin-2-amine (3.25a)



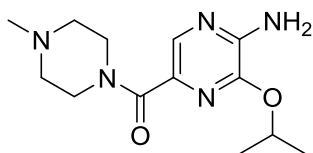
General **procedure E** was followed using **3.1a** (75 mg, 0.368 mmol). As *N*-methylpiperazine is a liquid, it was injected after addition of dry degassed toluene to chamber A. The crude product was purified using MPLC (95/5 dichloromethane/methanol) to obtain the title compound (**3.25a**) as a yellow solid (53%). ¹H NMR (400 MHz, CDCl₃) δ 8.01 (s, 1H), 5.32 (bs, 2H), 3.94 (s, 3H), 3.76 (bs, 4H), 2.46 (bs, 4H), 2.30 (s, 3H). ¹³C NMR (101 MHz, CDCl₃) δ 166.1, 146.2, 145.8, 136.2, 133.3, 55.0, 54.6, 53.7, 47.2, 46.0, 42.6. FTIR (cm⁻¹): 3394 (-NH₂), 2996, 2805, 1611. Melting Point: 167-170 °C. HRMS: Calculated mass: 252.1455 Found mass: 252.1453 (M+H)

5-amino-*N*-cyclopropyl-6-methoxypyrazine-2-carboxamide (3.25b)



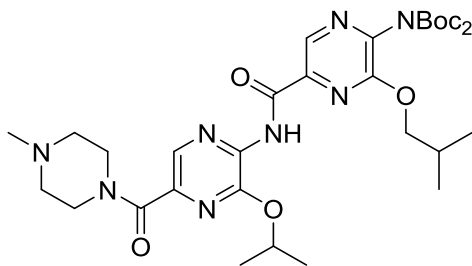
General procedure E was followed using **3.1a** (50 mg, 0.245 mmol). As cyclopropylamine is a liquid, it was injected after addition of dry degassed toluene to chamber A. The crude product was purified using MPLC (99/1 ethyl acetate/triethylamine) to obtain the title compound (**3.25b**) as a yellow solid (41%). ¹H NMR (400 MHz, CDCl₃) δ 8.41 (s, 1H), 7.30 (bs, 1H), 5.35 (bs, 2H), 4.00 (s, 3H), 2.92 – 2.82 (m, *J* = 10.5, 3.5 Hz, 1H), 0.92 – 0.79 (m, 2H), 0.69 – 0.56 (m, 2H). ¹³C NMR (101 MHz, CDCl₃) δ 165.7, 147.8, 146.3, 134.9, 130.4, 53.8, 22.5, 6.8. Melting Point: 175-177 °C. HRMS: Calculated mass: 209.1033 Found mass: 209.1031 (M+H)

(5-amino-6-isopropoxy-pyrazin-2-yl)(4-methylpiperazin-1-yl)methanone (3.26)



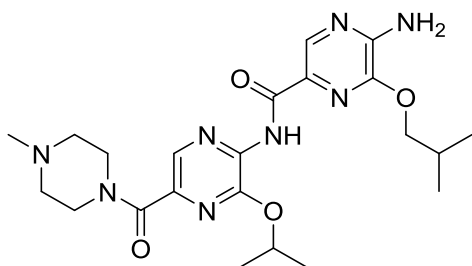
Using **procedure E**, after purification using MPLC (95/5 DCM/MeOH), **3.26** was obtained as yellow crystals (62%). ¹H NMR (300 MHz, CDCl₃, ppm): δ 8.02 (s, 1H) 5.30 – 5.21 (m, 1H), 5.04 (s, 2H), 3.76 (s, 3H), 2.46 (s, 4H), 2.32 (s, 4H), 1.38 (d, *J* = 6.2 Hz, 6H). ¹³C NMR (75 MHz, CDCl₃, ppm): δ 166.2, 146.2, 145.0, 135.7, 133.6, 77.2, 77.0, 69.6, 46.1, 22.0.

***tert*-butyl *N*-[(*tert*-butoxy)carbonyl]-*N*-(5-([5-(4-methylpiperazine-1-carbonyl)-3-(propan-2-yloxy)pyrazin-2-yl]carbamoyl)-3-(2-methylpropoxy)pyrazin-2-yl)carbamate**



Using **procedure E** and **3.2b** as aryl bromide, after purification using MPLC (95/5 DCM/MeOH), the product was obtained as yellow crystals (16% (43% with recovery of starting material)). ¹H NMR (400 MHz, CDCl₃, ppm): δ 10.33 (s, 1H), 8.95 (s, 1H), 8.36 (s, 1H), 5.46 – 5.35 (m, 1H), 4.26 (d, *J* = 6.5 Hz, 2H), 3.81 (s, 2H), 3.61 (s, 2H), 2.52 (s, 2H), 2.41 (s, 2H), 2.33 (s, 4H), 2.23 – 2.10 (m, 1H), 1.79 (s, 2H), 1.45 (d, *J* = 6.2 Hz, 6H), 1.42 (s, 18H), 1.07 (d, *J* = 6.7 Hz, 6H). ¹³C NMR (101 MHz, CDCl₃) 165.2, 159.7, 154.4, 149.8, 147.3, 141.9, 139.5, 138.3, 135.2, 134.7, 83.9, 73.5, 70.9, 46.1, 28.1, 27.9, 22.1, 19.3. HR-MS: Calculated mass: 673.3668 Mass found: 673.3690 [M+H].

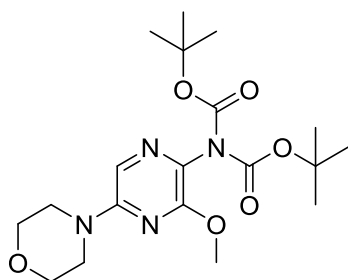
5-amino-6-isobutoxy-*N*-(3-isopropoxy-5-(4-methylpiperazine-1-carbonyl)pyrazin-2-yl)pyrazine-2-carboxamide (3.26)



tert-butyl *N*-[(*tert*-butoxy)carbonyl]-*N*-(5-([5-(4-methylpiperazine-1-carbonyl)-3-(propan-2-yloxy)pyrazin-2-yl]carbamoyl)-3-(2-methylpropoxy)pyrazin-2-yl)carbamate (20 mg, 0.030 mmol) was dissolved in 1 mL of DCM under an atmosphere of argon. The solution was cooled to 0 °C in an ice bath and TFA (46 µL, 0.60 mmol) was slowly added while stirring. The reaction mixture was then stirred at RT for 4 hours. After evaporation, the residue was diluted in saturated Na₂CO₃-solution and extracted with DCM. Afterwards, the organic phase was dried and evaporated *in vacuo* to

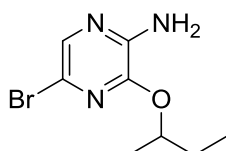
give **3.26** as a yellow solid. ^1H NMR (400 MHz, CDCl_3) δ 10.19 (s, 1H) 8.57 (s, 1H), 8.34 (s, 1H), 5.43 (bs, 2H), 5.42 – 5.31 (m, 1H), 3.82 (s, 2H), 3.64 (s, 2H), 2.52 (s, 2H), 2.42 (s, 1H), 2.34 (s, 3H), 2.26 – 2.16 (m, 1H), 1.45 (d, J = 6.2 Hz, 6H), 1.10 (d, J = 6.7 Hz, 6H). ^{13}C NMR (101 MHz, CDCl_3) δ 19.4, 22.1, 28.0, 29.7, 46.0, 54.7, 55.3, 70.6, 72.9, 129.8, 134.8, 136.4, 138.4, 139.1, 145.9, 147.1, 148.2, 161.1, 165.4. HR-MS: Calculated mass: 473.2619 Mass found: 473.2617 [M+H].

tert-Butyl N-[(tert-butoxy)carbonyl]-5-morpholine-3-(2-methylpropoxy)pyrazin-2-yl]carbamate (3.28)



A solution of **3.2a** (100 mg), morpholine (33 μL , 1.5 eq) and triethylamine (52 μL , 1.5 eq) in 1 mL of dry THF was prepared and was set to reflux for 18 hours. Afterwards the solution was allowed to cool to RT. THF was evaporated and a water/ethyl acetate extraction was performed. After this, the mixture was purified using MPLC (heptanes/EtOAc 7:3) to give **3.28** (30 mg, 10%) as a yellow oil. ^1H NMR (400 MHz, CDCl_3) δ 7.45 (s, 1H), 3.91 (s, 3H), 3.83 (m, 4H), 3.58 – 3.50 (m, 4H), 1.43 (s, 18H).

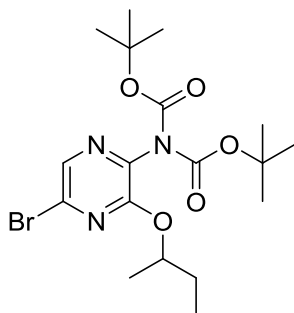
5-bromo-3-(sec-butoxy)pyrazin-2-amine (3.1g)



A flame-dried flask was charged with a stirring bar and NaH (285 mg, 3 eq) was added. The atmosphere was evacuated and back-filled with nitrogen three times. 10 mL *sec*-BuOH was slowly added at 0 °C (**Caution: evolution of hydrogen gas!**). The mixture was stirred for 30 minutes at room temperature. After this, a solution of 1 g 3,5-dibromo-2-aminopyrazine in 10 mL THF:*sec*-BuOH (1:1) was added dropwise at 0 °C. The mixture was then stirred overnight at 50 °C. Evaporation of THF and *sec*-BuOH was followed by an

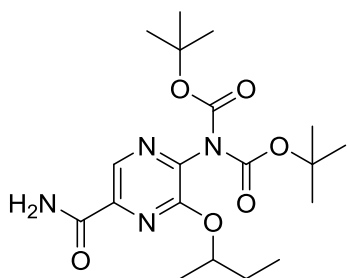
EtOAc/H₂O extraction. The products were purified via MPLC (heptanes/EtOAc 85:15). **3.1g** was obtained as a red oil (735 mg, 76%). ¹H NMR (300 MHz, CDCl₃, ppm): δ 7.59 (s, 1H), 5.15 (m, 1H), 4.82 (bs, 2H), 1.72 (m, 2H), 1.34 (d, J = 6.2 Hz, 3H), 0.96 (t, J = 7.5 Hz, 3H). ¹³C NMR (75 MHz, CDCl₃, ppm): δ 147.0, 144.4, 133.7, 121.0, 77.0, 75.0, 28.8, 19.2, 9.7.

di-tert-Butyl (5-bromo-3-(sec-butoxy)pyrazin-2-yl)imidodicarbonate (3.2e)



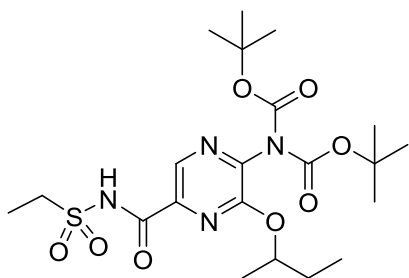
5-bromo-3-(sec-butoxy)pyrazin-2-amine (**3.1g**) (1.39 g) and DMAP (70 mg, 0.1 eq) were dissolved in dry DCM (20 mL, 0.2 M) under an argon atmosphere. A solution of Boc₂O (4.93 g, 4 eq) in 10 mL dry DCM was then slowly added at RT, while stirring vigorously. Afterwards the reaction was refluxed overnight. The mixture was then cooled to RT and the solvent was evaporated *in vacuo*. The residue was suspended in EtOAc and washed with water and brine. The organic phase was then dried over Na₂SO₄, filtered and evaporated *in vacuo*. MPLC (heptanes/EtOAc 85:15) afforded product **3.2e** as a yellow solid (1.95 g, 77%). ¹H NMR (300 MHz, CDCl₃, ppm): δ 8.06 (s, 1H), 5.25 – 5.12 (m, 1H), 1.69 (m, 2H), 1.40 (s, 18H), 1.32 (d, J = 6.2 Hz, 3H), 0.94 (t, J = 7.4 Hz, 3H). ¹³C NMR (75 MHz, CDCl₃, ppm): δ 155.0, 149.8, 136.9, 135.6, 134.9, 83.4, 75.9, 28.8, 27.8, 19.2, 9.6.

di-*tert*-Butyl (5-carboxamide-3-(sec-butoxy)pyrazin-2-yl)imidodicarbonate (3.31)



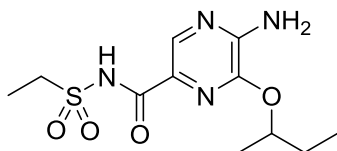
di-*tert*-Butyl (5-bromo-3-(sec-butoxy)pyrazin-2-yl)imidodicarbonate (**3.2e**) (179 mg), Pd(dba)₂ (12 mg, 5 mol%), Xantphos (12 mg, 5 mol%), ammonium carbamate (41 mg, 1.3 eq), sodium bicarbonate (44 mg, 1.3 eq) were added in chamber A of a two-chamber reactor (inner volume = 20 mL). The reactor was brought under a nitrogen atmosphere by two consecutive vacuum-nitrogen cycles. Anhydrous degassed toluene (2 mL), formic acid (20 μ L, 1.3 eq) and mesyl chloride (41 μ L, 1.3 eq) were added to chamber B and anhydrous degassed dioxane (2 mL) to chamber A. At this point, Et₃N (145 μ L, 2.6 eq) was added to chamber B and vigorous gas formation is observed. The reaction was stirred overnight at 100 °C. After this, chamber A was rinsed with EtOAc and evaporated over Celite®. Solid phase MPLC (heptanes/EtOAc 9:1 to 4:6 in 30 minutes) afforded **3.31** as yellow crystals (55 mg, 33%). ¹H NMR (400 MHz, CDCl₃) δ 8.80 (s, 1H), 7.35 (s, 1H), 6.38 (s, 1H), 5.20 (m, 1H), 1.84 – 1.66 (m, 2H), 1.40 (s, 18H), 1.37 (d, *J* = 6.1 Hz, 3H), 0.97 (t, *J* = 7.4 Hz, 3H). ¹³C NMR (101 MHz, CDCl₃) δ 165.4, 154.1, 149.7, 141.4, 139.9, 134.1, 83.6, 75.4, 28.9, 27.8, 19.2, 9.7.

di-*tert*-Butyl (5-*N*-[ethylsulfonyl]carboxamide-3-secbutoxy)pyrazin-2-yl)imidodicarbonate (3.30)



3.2e (268 mg, 0.6 mmol), Pd(OAc)₂ (4 mg, 3 mol%), Xantphos (16 mg, 5 mol%) and potassium fluoride (87 mg, 2.5 eq) were charged in chamber A of a flame-dried two chamber reactor. Air was evacuated three times and back-filled with argon. Degassed anhydrous DMF (3 mL, 0.2 M) was added to chamber A under positive pressure by means of a balloon. Next, formic acid (35 μ L, 1.5 eq), mesyl chloride (70 μ L, 1.5 eq) and degassed anhydrous DMF (2 mL) were added to chamber B. The balloon was removed and thiethylamine (251 μ L, 3 eq) was added to chamber B. The two-chamber reactor was submerged in an oil bath of 80 °C and was left stirring overnight. After this, the mixture was allowed to cool to room temperature and ethylsulfonamide (98 mg, 1.5 eq) and triethylamine (209 μ L, 2.5 eq) dissolved in degassed anhydrous DMF (1 mL) was added dropwise to the reaction mixture in chamber A. This was stirred for 3 hours at room temperature. After this, Celite® was added and DMF was evaporated. MPLC (heptanes/ethyl acetate 70:30 \rightarrow 20:80) was used to give pure **3.30** as a yellow oil (30 mg, 10%). ¹H NMR (300 MHz, CDCl₃) δ 9.32 (s, 1H), 8.81 (s, 1H), 5.20 (m, 1H), 3.63 (d, *J* = 7.4 Hz, 2H), 1.75 (m, 2H), 1.49 (t, *J* = 6.8 Hz, 3H), 1.42 (s, 18H), 1.37 (t, *J* = 6.2 Hz, 3H), 0.98 (t, *J* = 7.4 Hz, 3H).

5-amino-6-(sec-butoxy)-N-(ethylsulfonyl)pyrazine-2-carboxamide (3.29)



3.30 was dissolved in water (0.2 M) and refluxed overnight. After cooling to room temperature, this was extracted three times with ethyl acetate, dried and evaporated. MPLC (DCM \rightarrow 5% MeOH in 30 minutes) was used to give pure product **3.29** as a yellow oil (95%). ¹H NMR (300 MHz, CDCl₃) δ 9.19 (s, 1H), 8.42 (s, 1H), 5.72 (bs, 2H), 5.17 (m, 1H), 3.60 (q, *J* = 7.4 Hz, 2H), 1.86 – 1.69 (m, 3H), 1.45 (t, *J* = 7.4 Hz, 3H), 1.39 (d, *J* = 6.2 Hz, 2H), 1.00 (t, *J* = 7.5 Hz, 3H).

Bacterial tests of compound 3.29

1. Bacterial strains

- *Staphylococcus aureus* ATCC 6538P
- *Staphylococcus epidermidis* RP62A
- *Escherichia coli* NCIB 8743
- *Pseudomonas aeruginosa* PAO1
- *Candida albicans* CO11
- *Sarcina lutea* ATCC9341

2. Stock solutions of products

- 16 mg of compound was dissolved in 1 mL DMSO to afford 52.92 mM solution.
- Further 10 mM solution was prepared in DMSO.
- From this stock solutions, working stock solutions (2 mM, 1 mM and 0.5 mM) were prepared by diluting with water.
- All solutions are stored at -20 °C.

3. Growth of bacteria

- Inoculate 10 µL of glycerol stock ~ 5 ml liquid LB and shake (at 180 rpm) at 37°C for overnight.
- Inoculate 50-100 µl of the overnight-culture in 5 ml liquid LB (1/50-1/100 dilution).
- Grow cultures till OD ~ 0.5 (at 180 rpm and 37 °C) and dilute 1/100 in LB (OD ~ 0.005)

4. Microdilution method (MIC determination in 96-well plate with 100 µl/well)

A) Preliminary test

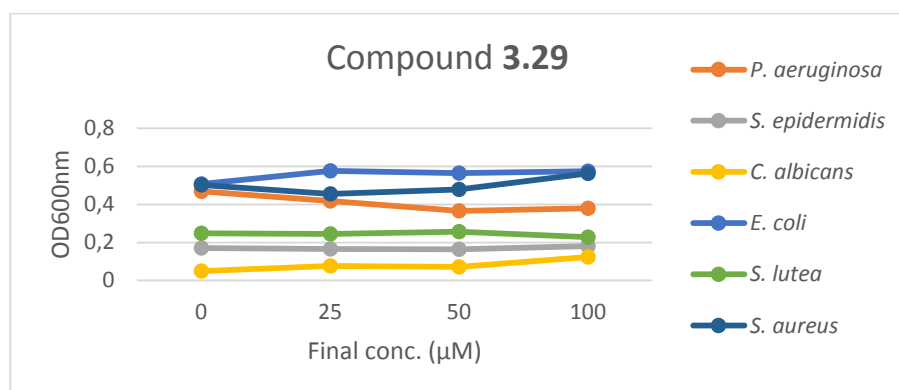
For preliminary testing 2 mM, 1 mM and 0.5 mM working solutions of each compound were chosen to see if the compound possesses antibacterial activity.

- 5 μ L of inhibitor solution was added to 96-well microtitre plate well 1-3 (as shown in plate layout).
- 5 μ L DMSO was used as a control in well 4.
- Further 85 μ L of LB medium was added from row 1 to 4.
- 90 μ L of LB medium was added to well 5.
- 100 μ L of LB was added to well 6 (sterility control).
- 10 μ L of bacterial suspension (OD \sim 0.005) was added to well 1-5.
- The microtitre plate was incubated at 37 $^{\circ}$ C for overnight.
- Next day, OD was measured at 600nm between 20 to 24 h.

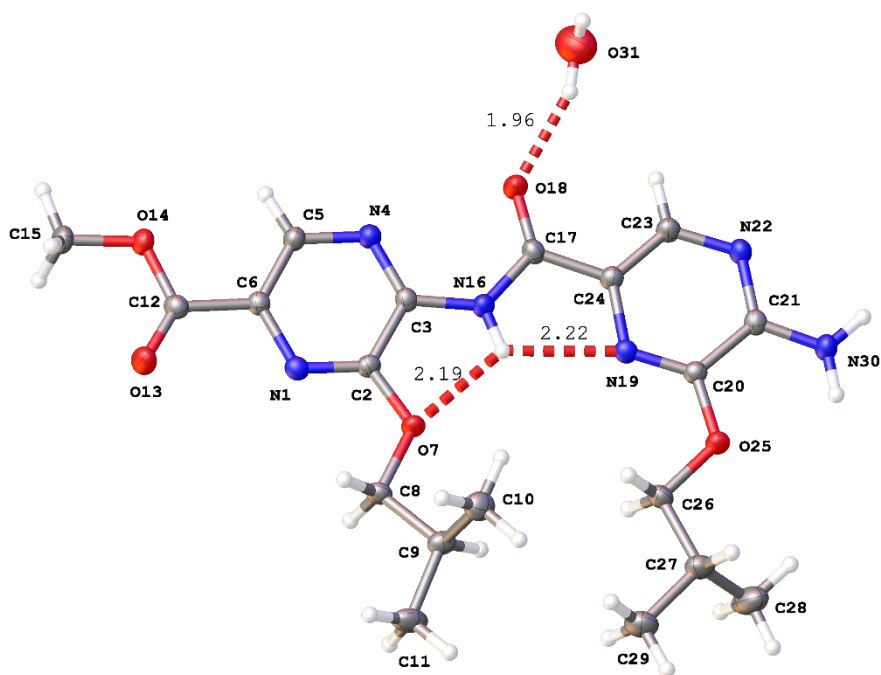
Notes:

1. final dilution will be 20-fold (5 μ L to 100 μ L). Therefore, final concentration in the well will be 100 μ M, 50 μ M and 25 μ M respectively.

2. As **3.29** did not show inhibitory activity up to 100 μ M (final concentration) against tested bacterial strains, detailed MIC determination was abandoned.



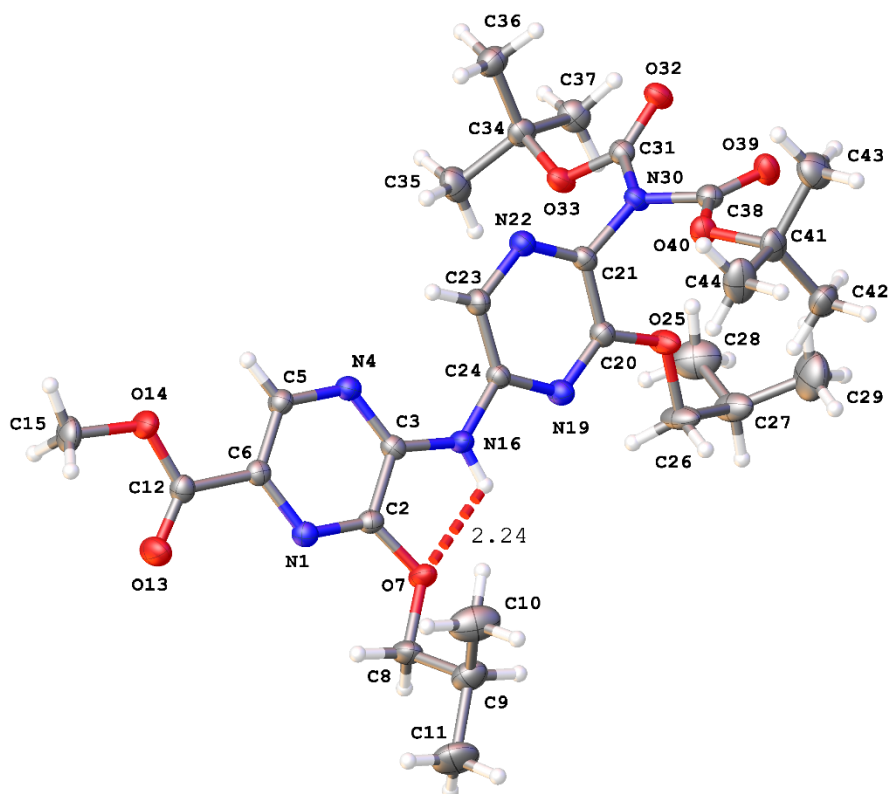
X-ray structures



Molecular structure of **3.6b** (CCDC 1512413) with ellipsoids drawn at the 50% probability level. Dashed lines represent hydrogen bonds.

Empirical formula	C ₁₉ H ₂₈ N ₆ O ₆
Formula weight	436.47
Temperature/K	120.0
Crystal system	orthorhombic
Space group	Pbca
a/Å	17.7469(6)
b/Å	8.5054(3)
c/Å	28.7562(10)
$\alpha/^\circ$	90

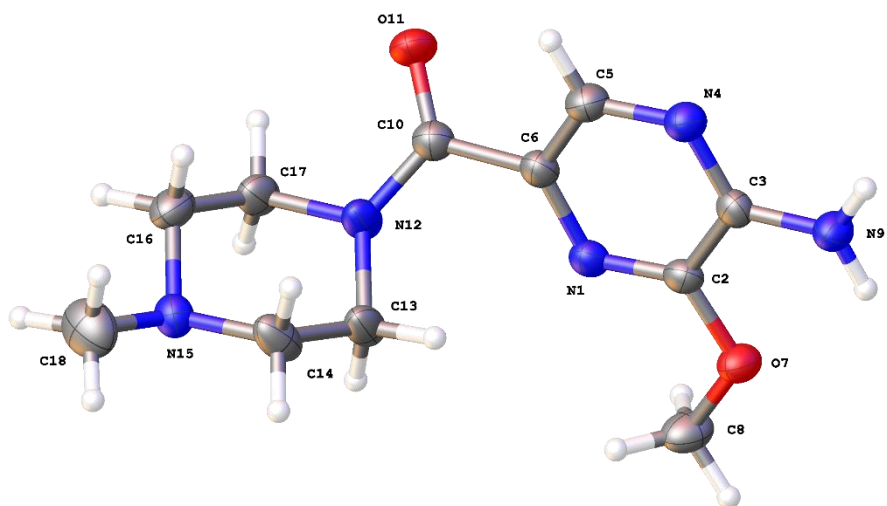
$\beta/^\circ$	90
$\gamma/^\circ$	90
Volume/ \AA^3	4340.6(3)
Z	8
$\rho_{\text{calc}}/\text{cm}^3$	1.336
μ/mm^{-1}	0.101
F(000)	1856.0
Crystal size/ mm^3	$0.5 \times 0.15 \times 0.15$
Radiation	MoK α ($\lambda = 0.71073 \text{ \AA}$)
2 θ range for data collection/ $^\circ$	5.496 to 52.742
Index ranges	$-22 \leq h \leq 22, -9 \leq k \leq 10, -34 \leq l \leq 35$
Reflections collected	28743
Independent reflections	4434 [$R_{\text{int}} = 0.0375, R_{\text{sigma}} = 0.0257$]
Data/restraints/parameters	4434/0/288
Goodness-of-fit on F ²	1.061
Final R indexes [$ I \geq 2\sigma(I)$]	$R_1 = 0.0530, wR_2 = 0.1498$
Final R indexes [all data]	$R_1 = 0.0652, wR_2 = 0.1607$
Largest diff. peak/hole / e \AA^{-3}	0.35/-0.74



Molecular structure of **3.5b'** (CCDC 1512412) with ellipsoids drawn at the 50% probability level. Dashed lines represent hydrogen bonds.

Empirical formula	C ₂₈ H ₄₂ N ₆ O ₈
Formula weight	590.67
Temperature/K	110.02(13)
Crystal system	monoclinic
Space group	P21/c
a/Å	9.6767(4)
b/Å	13.4665(5)
c/Å	25.2462(7)

$\alpha/^\circ$	90
$\beta/^\circ$	100.061(3)
$\gamma/^\circ$	90
Volume/ \AA^3	3239.3(2)
Z	4
$\rho_{\text{calc}}/\text{cm}^3$	1.211
μ/mm^{-1}	0.090
F(000)	1264.0
Crystal size/ mm^3	$0.5 \times 0.3 \times 0.3$
Radiation	MoK α ($\lambda = 0.71073 \text{ \AA}$)
2 θ range for data collection/ $^\circ$	4.912 to 52.744
Index ranges	$-11 \leq h \leq 12$, $-16 \leq k \leq 11$, $-31 \leq l \leq 31$
Reflections collected	17986
Independent reflections	6598 [$R_{\text{int}} = 0.0307$, $R_{\text{sigma}} = 0.0440$]
Data/restraints/parameters	6598/0/390
Goodness-of-fit on F ²	1.095
Final R indexes [$ I \geq 2\sigma(I)$]	$R_1 = 0.0618$, $wR_2 = 0.1284$
Final R indexes [all data]	$R_1 = 0.0904$, $wR_2 = 0.1448$
Largest diff. peak/hole / e \AA^{-3}	0.45/-0.27



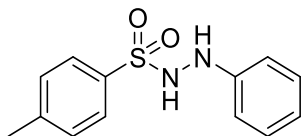
Molecular structure of **3.25a** (CCDC 1512414) with ellipsoids drawn at the 50% probability level.

Empirical formula	C ₁₁ H ₁₇ N ₅ O ₂
Formula weight	251.29
Temperature/K	150
Crystal system	orthorhombic
Space group	P212121
a/Å	12.7749(11)
b/Å	10.4901(10)
c/Å	9.5080(13)
α/°	90
β/°	90
γ/°	90
Volume/Å ³	1274.2(2)
Z	4

$\rho_{\text{calc}}/\text{cm}^3$	1.310
μ/mm^{-1}	0.094
F(000)	536.0
Crystal size/ mm^3	$0.5 \times 0.35 \times 0.25$
Radiation	$\text{MoK}\alpha$ ($\lambda = 0.71073 \text{ \AA}$)
2 θ range for data collection/ $^\circ$	5.024 to 52.734
Index ranges	$-15 \leq h \leq 15$, $-13 \leq k \leq 11$, $-11 \leq l \leq 11$
Reflections collected	7542
Independent reflections	2589 [$R_{\text{int}} = 0.0267$, $R_{\text{sigma}} = 0.0346$]
Data/restraints/parameters	2589/0/165
Goodness-of-fit on F ²	1.064
Final R indexes [$I \geq 2\sigma(I)$]	$R_1 = 0.0393$, $wR_2 = 0.0869$
Final R indexes [all data]	$R_1 = 0.0511$, $wR_2 = 0.0945$
Largest diff. peak/hole / e \AA^{-3}	0.13/-0.18
Flack parameter	0.8(7)

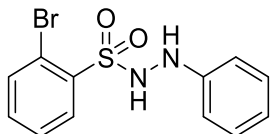
7.5 The use of sulfur dioxide in organic synthesis

4-methyl-*N'*-phenylbenzenesulfonohydrazide (**4.14**)



A glass reaction tube was charged with 4-iodotoluene (**4.1**, 100 mg, 0.46 mmol), phenylhydrazine hydrochloride (**4.13**, 1.5 eq), DABSO (0.6 eq), DABCO (1.5 eq), Pd(OAc)₂ (0.1 eq) and P(*t*Bu)₃.HBF₄ (0.2 eq) and sealed under nitrogen atmosphere. Dioxane (3.2 mL, 0.15 M) was added and the tube was heated to 70 °C by means of an oil bath. The reaction mixture was stirred for 18 hours. After cooling, Celite® was added and the solvent was evaporated. Purification by MPLC (heptanes/ethyl acetate 80:20 → 60:40) afforded the product (**4.14**, 30 mg, 25%). When breaking the vacuum after evaporation, the product is immediately brought under nitrogen atmosphere. ¹H NMR (400 MHz, CDCl₃) δ 7.79 – 7.74 (m, 2H), 7.26 (m, 2H), 7.13 – 7.07 (m, 2H), 6.81 (t, *J* = 7.4 Hz, 1H), 6.74 – 6.70 (m, 2H), 6.24 (bs, 1H), 5.65 (bs, 1H), 2.40 (s, 3H). ¹³C NMR (101 MHz, CDCl₃) δ 146.2, 144.5, 134.9, 129.7, 129.0, 128.3, 121.2, 113.4, 21.6.

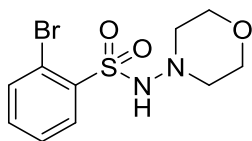
2-bromo-*N'*-phenylbenzenesulfonohydrazide (**4.16**)



A glass reaction tube was charged with 1-bromo-2-iodobenzene (**4.9**, 58 μL, 0.45 mmol), phenylhydrazine hydrochloride (**4.13**, 1.5 eq), DABSO (0.6 eq), DABCO (1.5 eq), Pd(OAc)₂ (0.1 eq) and P(*t*Bu)₃.HBF₄ (0.2 eq) and sealed under nitrogen atmosphere. Dioxane (3.2 mL, 0.15 M) was added and the tube was heated to 90 °C by means of an oil bath. The reaction mixture was stirred for 18 hours. After cooling, Celite® was added and the solvent was evaporated. Purification by MPLC (heptanes/ethyl acetate 80:20 → 60:40) afforded the product (**4.16**, 9 mg, 6%). When breaking the vacuum after evaporation, the product is immediately brought under nitrogen atmosphere. ¹H NMR (400 MHz, CDCl₃) δ 7.91 – 7.87 (m, 2H), 7.47 (dd, *J* = 8.1, 1.8 Hz, 1H), 7.17 (d, *J* =

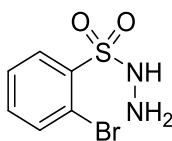
7.9 Hz, 1H), 7.09 (t, $J = 7.9$ Hz, 2H), 6.81 (t, $J = 7.4$ Hz, 1H), 6.71 (d, $J = 7.7$ Hz, 2H), 6.23 (bs, 1H), 5.69 (bs, 1H).

2-bromo-N-morpholinobenzenesulfonamide (**4.17**)



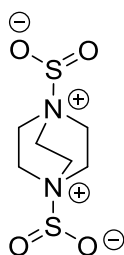
A glass reaction tube was charged with 1-bromo-2-iodobenzene (**4.9**, 64 μ L, 0.5 mmol), DABSO (0.6 eq), DABCO (1.5 eq), Pd(OAc)₂ (0.1 eq) and P(tBu)₃.HBF₄ (0.2 eq) and sealed under nitrogen atmosphere. Dioxane (3.5 mL, 0.15 M) and *N*-aminomorpholine (72 μ L, 1.5 eq) were added and the tube was heated to 70 °C by means of an oil bath. The reaction mixture was stirred for 18 hours. After cooling, Celite® was added and the solvent was evaporated. Purification by MPLC (heptanes/ethyl acetate 80:20 \rightarrow 60:40) afforded the product (**4.17**, 30 mg, 6%). ¹H NMR (400 MHz, CDCl₃) δ 8.25 (dd, $J = 7.7, 1.8$ Hz, 1H), 7.74 (dd, $J = 7.7, 1.2$ Hz, 1H), 7.54 – 7.42 (m, 2H), 6.14 (s, 1H), 3.60 – 3.53 (m, 4H), 2.73 – 2.68 (m, 4H). ¹³C NMR (101 MHz, CDCl₃) δ 137.9, 135.0, 134.2, 133.3, 127.8, 120.0, 66.4, 56.6.

2-bromobenzenesulfonylhydrazide (**4.19**)



A round bottomed flask was charged with *o*-bromobenzenesulfonyl chloride (**4.18**, 1.278 g, 5 mmol) and THF (25 mL). Hydrazine hydrate (486 μ L, 2 eq) was added at 0 °C. The mixture was stirred for 1 hour at room temperature and subsequently THF was evaporated. Water was added to the reaction mixture and this was extracted with DCM three times. Purification by MPLC (heptanes/ethyl acetate 70:30 \rightarrow 50:50) afforded the product (**4.19**) in 14% yield. ¹H NMR (400 MHz, CDCl₃) δ 8.17 (dd, $J = 7.5, 2.1$ Hz, 1H), 7.76 (dd, $J = 7.6, 1.5$ Hz, 1H), 7.54 – 7.44 (m, 2H), 6.66 (bs, 1H), 3.79 (bs, 2H).

DABCO·(SO₂)₂ (abbreviated as DABSO)



A symmetrical two-chamber reactor (inner volume = 400 mL) is charged with a Teflon-coated oval stirring bar in each chamber. 5.050 g of DABCO (45 mmol) is added in chamber A and 12.480 g of Na₂SO₃ (99 mmol, 2.2 eq) is added in chamber B. Two screw caps with septa are fitted on the reactor and air is evacuated and back-filled with nitrogen. This process is repeated three times. THF (60 mL) is added via a syringe in chamber A and similarly water (40 mL) is added in chamber B under a positive pressure by means of a nitrogen balloon. After 10 minutes of stirring at room temperature, the balloon was removed and H₂SO₄ (6 mL) is gradually added *via* a syringe pump (50 μL min⁻¹, added over 2 hours). The mixtures were stirred overnight at room temperature. After this, the solution in chamber B is removed and the suspension in chamber A is transferred to a 100 mL sintered-glass funnel under reduced pressure. The white solid is washed five times with 50 mL diethyl ether. DABSO is known to be hygroscopic and therefore, it is transferred to a flask and dried in a desiccator under vacuum overnight to afford the product as a white powder (10.75 g, 99%). Analytical properties in accordance with the literature.¹⁷³ mp 141-143 °C. ¹H NMR (400 MHz, CD₃OD): δ 3.22 (s). ¹³C NMR (100 MHz, CD₃OD): δ 45.4. CHN-analysis: C 29.99, H 5.03, N 11.66; found C 30.38, H 5.24, N 11.60.

7.6 Towards a continuous synthesis of glycerol carbonate using dimethyl carbonate

Flow equipment

A VapourTec® R2 + R4 unit was used for all flow reactions. An exception to this was when using neat glycerol: a VapourTec E-series system with peristaltic pumps was used. Omnifit® glass columns (10 mm x 100 mm, inner diameter x length) were used as reactors for heterogeneous catalysis experiments.

Large scale flow procedure

Two Omnifit® glass columns (10 mm i.d. x 100 mm) are filled with 4.4 grams of Ambersep® 900 Hydroxide beads each. Both ends of each column were sealed using PTFE plugs and after linking the two columns, MeOH was pumped through at a rate of 1 mL min⁻¹. After 10 minutes, temperature is gradually increased to 140 °C over a 10 minute period. After this, a solution of glycerol (5 M) in MeOH was pumped at 740 µL min⁻¹ and combined via a T-piece with a second stream containing DMC (neat, 4 equivalents) at 1.26 mL min⁻¹. The combined stream was directed into the two linked columns (residence time of approximately 4 minutes) and a backpressure regulator of 17 bar was added in-line. The output was collected for analysis and after evaporation of MeOH and DMC, GLC was purified via either vacuum distillation or column chromatography (DMC:MeOH 95:5).

Analysis

GC-MS experiments were carried out on a Shimadzu QP2010-Ultra. EI is carried at 70eV and the working mass range is 35 – 650 u for all experiments. The samples were prepared by dissolving 10 µL of collection volume in 1 mL of methanol. 0.5 µL of this sample was split injected (25:1) into the Shimadzu QP2010-Ultra equipped with a Rxi-17Sil MS column using helium as carrier gas (0.41 mL min⁻¹). The temperature of the oven was increased from 30 to 300 °C with a 50 °C min⁻¹ rate. Finally, the oven was maintained at 300 °C for 5 min.

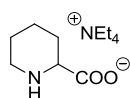
It was found that glycerol and GLC have the same response when plotting peak area in function of concentration (see Supporting Information). Therefore the following terms are defined as follows: conversion as the relative peak area of glycerol with all other peaks, selectivity as the relative

peak area excluding the glycerol signal and GC yield as the relative peak area ratio of GLC with glycerol.

General procedure for the synthesis of homogeneous catalysts

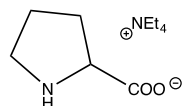
Catalysts are synthesized via simple acid-base neutralization reactions. A slight excess of carboxylic acid was added to a tetraethyl ammonium hydroxide aqueous solution. The mixture was then stirred at room temperature for 2 hours. After evaporation of water at 60 °C under reduced pressure, the residue was washed with ethanol. Ethanol was removed *in vacuo* after filtration and the residue was dried overnight under high vacuum.

Tetraethylammonium piperidine-2-carboxylate (5.3)



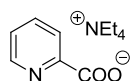
5.3 was prepared using the general procedure and all analytical data were found to be in accordance with the literature.²⁰⁶

Tetraethylammonium prolininate



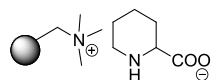
The catalyst was prepared using the general procedure and all analytical data were found to be in accordance with the literature.²⁰⁶

Tetraethylammonium picolinate



The catalyst was prepared using the general procedure and obtained as a yellow solid. ¹H NMR (300MHz, D₂O, ppm): δ 8.55 (d, *J* = 3.5 Hz, 1H), 7.96 (td, *J* = 7.7, 1.6 Hz, 1H), 7.90 (d, *J* = 7.7 Hz, 1H), 7.56 – 7.50 (m, 1H), 3.23 (q, *J* = 7.3 Hz, 7H), 1.28 – 1.19 (m, 11H).

Polymer supported piperidine-2-carboxylate (5.4)



Ambersep® 900 Hydroxide (2 grams) and pipecolic acid (1.3 grams, 1.1 eq) were subsequently added to an RBF containing 20 mL methanol. The flask was then shaken overnight at room temperature (without stirring bar). After this, the polymer beads were filtered, rinsed with methanol and dried overnight to give **5.4**.

Calculation of relative flow rate for heterogeneous continuous column experiments

When using 3.5 equivalents of DMC, the following ratio should be achieved when mixing:

$$\frac{3.5 \text{ mol DMC}}{1 \text{ mol glycerol}} = \frac{315 \text{ g DMC}}{92 \text{ g glycerol}} = \frac{294 \text{ mL DMC}}{73 \text{ mL glycerol}} = 4.03$$

Note that this result is the required volume ratio when using both *neat* DMC and *neat* glycerol. This result changes when a solution of glycerol (5 M) in methanol is used.

Therefore, the volume percent of glycerol is:

$$5 \text{ M} = \frac{5 \text{ mol glycerol}}{L} = \frac{460 \text{ g glycerol}}{1 L} = \frac{365 \text{ mL glycerol}}{1 L} = 0.365$$

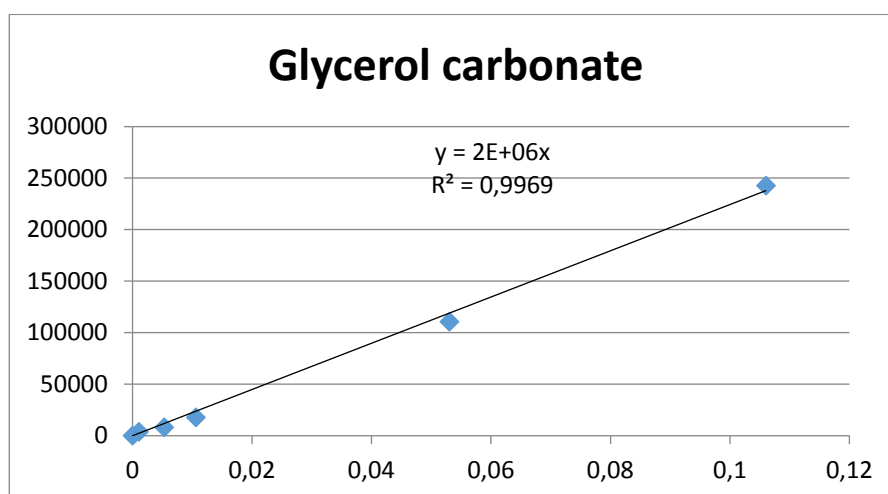
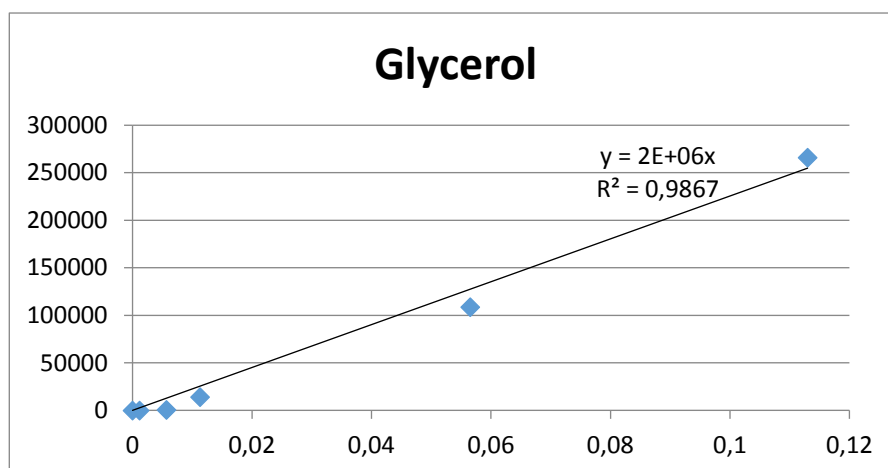
Hence the relative flow rate becomes:

$$4.03 * 0.365 = 1.47$$

The relative flow rate of neat DMC should be about 1.47 times the flow rate of glycerol (5 M) in MeOH when 3.5 equivalents DMC are desired.

Calibration curves for glycerol and glycerol carbonate

Several samples were prepared for following GC-MS experiment. Glycerol was dissolved in MeOH (0.113 M) and serial diluted to have samples in between 0.1 M and 0.001 M, the typical concentration range for prepared GC-MS samples. In the same way glycerol carbonate samples were prepared. The same response curve for peak area in function of concentration was obtained for both glycerol and glycerol carbonate. This was considered sufficient for estimation of GC yield, conversion and selectivity.



Publications, awards and posters

Publications

- C. Veryser, S. Van Mileghem, B. Egle, P. Gilles and W. M. De Borggraeve. Low-cost instant CO generation at room temperature using formic acid, mesyl chloride and triethylamine. *React. Chem. Eng.*, **2016**, 142-146.
- S. Van Mileghem, B. Egle, P. Gilles, C. Veryser, L. Van Meervelt and W. M. De Borggraeve. Carbonylation as a novel method for the assembly of pyrazine based oligoamide alpha-helix mimetics. *Org. Biomol. Chem.*, **2017**, 373-378.
- S. Van Mileghem and W. M. De Borggraeve. A convenient multigram synthesis of DABSO using sodium sulfite as SO₂ source. *Org. Process Res. Dev.*, **2017**, 785-787.

Awards

- SELECTBIO ePosters.net Award Winner for best poster at 'Flow Chemistry Europe 2015' in Berlin, Germany.

Posters

- Flow Chemistry Europe, Berlin, The Use of Carbon Monoxide Precursors under Continuous Flow Conditions, February **2014**.
- Flow Chemistry Europe, Cambridge, Towards A Continuous Synthesis of Glycerol Carbonate Using Dimethyl Carbonate, February **2015**.
- Belgian Organic Synthesis Symposium, Antwerp, Towards A Continuous Synthesis of Glycerol Carbonate Using Dimethyl Carbonate, July **2016**.
- Chemical Research in Flanders Symposium, Blankenberge, Towards A Continuous Synthesis of Glycerol Carbonate Using Dimethyl Carbonate, October **2016**.
- Sigma Aldrich Symposium, Blankenberge, Towards A Continuous Synthesis of Glycerol Carbonate Using Dimethyl Carbonate, December **2016**.

References

1. Colquhoun, H. M.; Thompson, D. J.; Twigg, M. V., Carbonylation: Direct Synthesis of Carbonyl Compounds. *Plenum Press: New York* **1991**.
2. Mallia, C. J.; Baxendale, I. R., The Use of Gases in Flow Synthesis. *Org. Process Res. Dev.* **2016**, *20* (2), 327-360.
3. Morimoto, T.; Kakiuchi, K., Evolution of carbonylation catalysis: No need for carbon monoxide. *Angew. Chem. Int. Ed.* **2004**, *43* (42), 5580-5588.
4. Emmett, E. J.; Willis, M. C., The Development and Application of Sulfur Dioxide Surrogates in Synthetic Organic Chemistry. *Asian J. Org. Chem.* **2015**, *4* (7), 602-611.
5. Gautam, P.; Bhanage, B. M., Recent advances in the transition metal catalyzed carbonylation of alkynes, arenes and aryl halides using CO surrogates. *Catal. Sci. Technol.* **2015**, *5* (10), 4663-4702.
6. Friis, S. D.; Taaning, R. H.; Lindhardt, A. T.; Skrydstrup, T., Silacarboxylic Acids as Efficient Carbon Monoxide Releasing Molecules: Synthesis and Application in Palladium-Catalyzed Carbonylation Reactions. *J. Am. Chem. Soc.* **2011**, *133* (45), 18114-18117.
7. Hermange, P.; Lindhardt, A. T.; Taaning, R. H.; Bjerglund, K.; Lupp, D.; Skrydstrup, T., Ex Situ Generation of Stoichiometric and Substoichiometric (CO)-C-12 and (CO)-C-13 and Its Efficient Incorporation in Palladium Catalyzed Aminocarbonylations. *J. Am. Chem. Soc.* **2011**, *133* (15), 6061-6071.
8. Taaning, R. H.; Hermange, P.; Lindhardt, A. T.; Friis, S. D.; Skrydstrup, T. WO2012079583 A1, 2012.
9. Friis, S. D.; Lindhardt, A. T.; Skrydstrup, T., The Development and Application of Two-Chamber Reactors and Carbon Monoxide Precursors for Safe Carbonylation Reactions. *Acc. Chem. Res.* **2016**, *49* (4), 594-605.
10. Mann, J., Classics in total synthesis: Targets, strategies, methods - Nicolaou, K.C., Sorenson, E.J. *Nature* **1996**, *380* (6572), 308-308.
11. Baxendale, I. R., The integration of flow reactors into synthetic organic chemistry. *J. Chem. Technol. Biotechnol.* **2013**, *88* (4), 519-552.
12. de la Hoz, A.; Diaz-Ortiz, A.; Moreno, A., Microwaves in organic synthesis. Thermal and non-thermal microwave effects. *Chem. Soc. Rev.* **2005**, *34* (2), 164-178.
13. Stolle, A.; Szuppa, T.; Leonhardt, S. E. S.; Ondruschka, B., Ball milling in organic synthesis: solutions and challenges. *Chem. Soc. Rev.* **2011**, *40* (5), 2317-2329.
14. Karnatz, F. A.; Whitmore, F. C., Dehydration of diethylcarbinol. *J. Am. Chem. Soc.* **1932**, *54* (8), 3461.
15. <https://syrris.com/solutions/flow-chemistry/>

16. <http://www.chemtrix.com/>
17. <https://www.vapourtec.com/>
18. <http://www.uniqsis.com/>
19. <http://www.thalesnano.com/>
20. Adamo, A.; Beingessner, R. L.; Behnam, M.; Chen, J.; Jamison, T. F.; Jensen, K. F.; Monbaliu, J. C. M.; Myerson, A. S.; Revalor, E. M.; Snead, D. R.; Stelzer, T.; Weeranoppanant, N.; Wong, S. Y.; Zhang, P., On-demand continuous-flow production of pharmaceuticals in a compact, reconfigurable system. *Science* **2016**, 352 (6281), 61-67.
21. Sauks, J. M.; Mallik, D.; Lawryshyn, Y.; Bender, T.; Organ, M., A Continuous-Flow Microwave Reactor for Conducting High-Temperature and High-Pressure Chemical Reactions. *Org. Process Res. Dev.* **2014**, 18 (11), 1310-1314.
22. Reichart, B.; Tekautz, G.; Kappe, C. O., Continuous Flow Synthesis of n-Alkyl Chlorides in a High-Temperature Microreactor Environment. *Org. Process Res. Dev.* **2013**, 17 (1), 152-157.
23. Morschhauser, R.; Krull, M.; Kayser, C.; Boberski, C.; Bierbaum, R.; Puschner, P. A.; Glasnov, T. N.; Kappe, C. O., Microwave-assisted continuous flow synthesis on industrial scale. *Green Process. Synth.* **2012**, 1 (3), 281-290.
24. Glasnov, T. N.; Kappe, C. O., Microwave-assisted synthesis under continuous-flow conditions. *Macromol. Rapid Commun.* **2007**, 28 (4), 395-410.
25. Hernandez-Perez, A. C.; Caron, A.; Collins, S. K., Photochemical Synthesis of Complex Carbazoles: Evaluation of Electronic Effects in Both UV- and Visible-Light Methods in Continuous Flow. *Chem. Eur. J.* **2015**, 21 (46), 16673-16678.
26. He, Z.; Bae, M.; Wu, J.; Jamison, T. F., Synthesis of Highly Functionalized Polycyclic Quinoxaline Derivatives Using Visible-Light Photoredox Catalysis. *Angew. Chem. Int. Ed.* **2014**, 53 (52), 14451-14455.
27. Yavorsky, A.; Shvydkiv, O.; Hoffmann, N.; Nolan, K.; Oelgemoller, M., Parallel Microflow Photochemistry: Process Optimization, Scale-up, and Library Synthesis. *Org. Lett.* **2012**, 14 (17), 4342-4345.
28. Tu, N. P.; Hochlowski, J. E.; Djuric, S. W., Ultrasound-assisted click chemistry in continuous flow. *Molecular Diversity* **2012**, 16 (1), 53-58.
29. Lin, W. Y.; Wang, Y. J.; Wang, S. T.; Tseng, H. R., Integrated microfluidic reactors. *Nano Today* **2009**, 4 (6), 470-481.
30. Seeberger, P. H., ORGANIC SYNTHESIS Scavengers in full flow. *Nat. Chem.* **2009**, 1 (4), 258-260.
31. Garcia-Verdugo, E.; Luis, S. V., Flow Processes Using Polymer-supported Reagents, Scavengers and Catalysts. In *Chemical Reactions and Processes under Flow Conditions*, Luis, S. V.; Garcia-Verdugo, E., Eds. Royal Soc Chemistry: Cambridge, 2010; pp 44-85.

32. O'Brien, M.; Koos, P.; Browne, D. L.; Ley, S. V., A prototype continuous-flow liquid-liquid extraction system using open-source technology. *Org. Biomol. Chem.* **2012**, *10* (35), 7031-7036.
33. Palmieri, A.; Ley, S. V.; Polyzos, A.; Ladlow, M.; Baxendale, I. R., Continuous flow based catch and release protocol for the synthesis of alpha-ketoesters. *Beilstein Journal of Organic Chemistry* **2009**, *5*, 7.
34. Anderson, N. G., Using Continuous Processes to Increase Production. *Org. Process Res. Dev.* **2012**, *16* (5), 852-869.
35. Su, Y. H.; Kuijpers, K.; Hessel, V.; Noel, T., A convenient numbering-up strategy for the scale-up of gas-liquid photoredox catalysis in flow. *React. Chem. Eng.* **2016**, *1* (1), 73-81.
36. Mastronardi, F.; Gutmann, B.; Kappe, C. O., Continuous Flow Generation and Reactions of Anhydrous Diazomethane Using a Teflon AF-2400 Tube-in-Tube Reactor. *Org. Lett.* **2013**, *15* (21), 5590-5593.
37. Fuse, S.; Tanabe, N.; Takahashi, T., Continuous in situ generation and reaction of phosgene in a microflow system. *Chem. Commun.* **2011**, *47* (47), 12661-12663.
38. Hessel, V.; Kralisch, D.; Kockmann, N.; Noel, T.; Wang, Q., Novel Process Windows for Enabling, Accelerating, and Uplifting Flow Chemistry. *Chemsuschem* **2013**, *6* (5), 746-789.
39. Bogdan, A. R.; Wang, Y., A high-throughput synthesis of 1,2,4-oxadiazole and 1,2,4-triazole libraries in a continuous flow reactor. *Rsc Advances* **2015**, *5* (97), 79264-79269.
40. Razzaq, T.; Glasnov, T. N.; Kappe, C. O., Continuous-Flow Microreactor Chemistry under High-Temperature/Pressure Conditions. *Eur. J. Org. Chem.* **2009**, (9), 1321-1325.
41. <http://thalesnano.com/phoenix-flow-reactor>
42. Bogdan, A. R.; Charaschanya, M.; Dombrowski, A. W.; Wang, Y.; Djuric, S. W., High-Temperature Boc Deprotection in Flow and Its Application in Multistep Reaction Sequences. *Org. Lett.* **2016**, *18* (8), 1732-1735.
43. Yoshida, J.; Takahashi, Y.; Nagaki, A., Flash chemistry: flow chemistry that cannot be done in batch. *Chem. Commun.* **2013**, *49* (85), 9896-9904.
44. Kim, H.; Nagaki, A.; Yoshida, J., A flow-microreactor approach to protecting-group-free synthesis using organolithium compounds. *Nature Communications* **2011**, *2*.
45. Baxendale, I. R.; Deeley, J.; Griffiths-Jones, C. M.; Ley, S. V.; Saaby, S.; Tranmer, G. K., A flow process for the multi-step synthesis of the alkaloid natural product oxomaritidine: a new paradigm for molecular assembly. *Chem. Commun.* **2006**, (24), 2566-2568.
46. Ingham, R. J.; Battilocchio, C.; Fitzpatrick, D. E.; Sliwinski, E.; Hawkins, J. M.; Ley, S. V., A Systems Approach towards an Intelligent and Self-Controlling

- Platform for Integrated Continuous Reaction Sequences. *Angew. Chem. Int. Ed.* **2015**, *54* (1), 144-148.
47. Yue, J.; Chen, G. W.; Yuan, Q.; Luo, L. G.; Gonthier, Y., Hydrodynamics and mass transfer characteristics in gas-liquid flow through a rectangular microchannel. *Chem. Eng. Sci.* **2007**, *62* (7), 2096-2108.
48. Sobieszuk, P.; Aubin, J.; Pohorecki, R., Hydrodynamics and Mass Transfer in Gas-Liquid Flows in Microreactors. *Chemical Engineering & Technology* **2012**, *35* (8), 1346-1358.
49. Brzozowski, M.; O'Brien, M.; Ley, S. V.; Polyzos, A., Flow Chemistry: Intelligent Processing of Gas-Liquid Transformations Using a Tube-in-Tube Reactor. *Acc. Chem. Res.* **2015**, *48* (2), 349-362.
50. O'Brien, M.; Baxendale, I. R.; Ley, S. V., Flow Ozonolysis Using a Semipermeable Teflon AF-2400 Membrane To Effect Gas-Liquid Contact. *Org. Lett.* **2010**, *12* (7), 1596-1598.
51. <https://www.vapourtec.com/products/flow-reactors/gas-addition-features/>
52. Gross, U.; Koos, P.; O'Brien, M.; Polyzos, A.; Ley, S. V., A General Continuous Flow Method for Palladium Catalysed Carbonylation Reactions Using Single and Multiple Tube-in-Tube Gas-Liquid Microreactors. *Eur. J. Org. Chem.* **2014**, (29), 6418-6430.
53. Kollar, L., *Modern Carbonylation methods*. Wiley: 2008.
54. Woolven, H.; Gonzalez-Rodriguez, C.; Marco, I.; Thompson, A. L.; Willis, M. C., DABCO-Bis(sulfur dioxide), DABSO, as a Convenient Source of Sulfur Dioxide for Organic Synthesis: Utility in Sulfonamide and Sulfamide Preparation. *Org. Lett.* **2011**, *13* (18), 4876-4878.
55. Banks, R. E.; Mohialdinkhaffaf, S. N.; Lal, G. S.; Sharif, I.; Syvret, R. G., 1-ALKYL-4-FLUORO-1,4-DIAZONIABICYCLO 2.2.2 OCTANE SALTS - A NOVEL FAMILY OF ELECTROPHILIC FLUORINATING AGENTS. *J. Chem. Soc., Chem. Commun.* **1992**, (8), 595-596.
56. Lal, G. S., SITE-SELECTIVE FLUORINATION OF ORGANIC-COMPOUNDS USING 1-ALKYL-4-FLUORO-1,4-DIAZABICYCLO 2.2.2 OCTANE SALTS (SELECTFLUOR REAGENTS). *J. Org. Chem.* **1993**, *58* (10), 2791-2796.
57. Schareina, T.; Zapf, A.; Beller, M., Potassium hexacyanoferrate(II) - a new cyanating agent for the palladium-catalyzed cyanation of aryl halides. *Chem. Commun.* **2004**, (12), 1388-1389.
58. Kaiser, N. F. K.; Hallberg, A.; Larhed, M., In situ generation of carbon monoxide from solid molybdenum hexacarbonyl. A convenient and fast route to palladium-catalyzed carbonylation reactions. *J. Comb. Chem.* **2002**, *4* (2), 109-111.
59. Gomez-Benitez, V.; Olvera-Mancilla, J.; Hernandez-Ortega, S.; Morales-Morales, D., High yield carbonylation of RuCl₂(PPh₃)₃ using dimethylformamide (DMF) as convenient source of CO. The X-ray crystal

- structure of $\text{RuCl}_2(\text{CO})(\text{DMF})(\text{PPh}_3)_2$. *J. Mol. Struct.* **2004**, 689 (1-2), 137-141.
60. Ueda, T.; Konishi, H.; Manabe, K., Palladium-Catalyzed Reductive Carbonylation of Aryl Halides with N-Formylsaccharin as a CO Source. *Angew. Chem. Int. Ed.* **2013**, 52 (33), 8611-8615.
61. Ueda, T.; Konishi, H.; Manabe, K., Palladium-Catalyzed Fluorocarbonylation Using N-Formylsaccharin as CO Source: General Access to Carboxylic Acid Derivatives. *Org. Lett.* **2013**, 15 (20), 5370-5373.
62. Wang, H. N.; Dong, B.; Wang, Y.; Li, J. F.; Shi, Y. A., A Palladium-Catalyzed Regioselective Hydroesterification of Alkenylphenols to Lactones with Phenyl Formate as CO Source. *Org. Lett.* **2014**, 16 (1), 186-189.
63. Ueda, T.; Konishi, H.; Manabe, K., Trichlorophenyl Formate: Highly Reactive and Easily Accessible Crystalline CO Surrogate for Palladium-Catalyzed Carbonylation of Aryl/Alkenyl Halides and Triflates. *Org. Lett.* **2012**, 14 (20), 5370-5373.
64. Shibata, T.; Toshida, N.; Takagi, K., Catalytic Pauson-Khand-type reaction using aldehydes as a CO source. *Org. Lett.* **2002**, 4 (9), 1619-1621.
65. Shibata, T.; Toshida, N.; Takagi, K., Rhodium complex-catalyzed Pauson-Khand-type reaction with aldehydes as a CO source. *J. Org. Chem.* **2002**, 67 (21), 7446-7450.
66. Gockel, S. N.; Hull, K. L., Chloroform as a Carbon Monoxide Precursor: In or Ex Situ Generation of CO for Pd-Catalyzed Aminocarbonylations. *Org. Lett.* **2015**, 17 (13), 3236-3239.
67. Brancour, C.; Fukuyama, T.; Mukai, Y.; Skrydstrup, T.; Ryu, I., Modernized Low Pressure Carbonylation Methods in Batch and Flow Employing Common Acids as a CO Source. *Org. Lett.* **2013**, 15 (11), 2794-2797.
68. Losch, P.; Felten, A. S.; Pale, P., Easy, Green and Safe Carbonylation Reactions through Zeolite-Catalyzed Carbon Monoxide Production from Formic Acid. *Adv. Synth. Catal.* **2015**, 357 (13), 2931-2938.
69. Schoenberg, A.; Heck, R. F., PALLADIUM-CATALYZED FORMYLATION OF ARYL, HETEROCYCLIC, AND VINYLIC HALIDES. *J. Am. Chem. Soc.* **1974**, 96 (25), 7761-7764.
70. Zhu, Z. L.; Zhang, W. Q.; Gao, Z. W., Suzuki-Miyaura Carbonylative Reaction in the Synthesis of Biaryl Ketones. *Progress in Chemistry* **2016**, 28 (11), 1626-1633.
71. Tambade, P. J.; Patil, Y. P.; Nandurkar, N. S.; Bhanage, B. M., Copper-catalyzed, palladium-free carbonylative Sonogashira coupling reaction of aliphatic and aromatic alkynes with Iodoaryls. *Synlett* **2008**, (6), 886-888.
72. Hansen, S. V. F.; Wilson, Z. E.; Ulven, T.; Ley, S. V., Controlled generation and use of CO in flow. *React. Chem. Eng.* **2016**, 1 (3), 280-287.

73. Li, W. F.; Li, H. Q.; Langer, P.; Beller, M.; Wu, X. F., Palladium-Catalyzed Aminosulfonylation of Aryl Iodides by using Na₂SO₃ as the SO₂ Source. *Eur. J. Org. Chem.* **2014**, 2014 (15), 3101-3103.
74. Nordeman, P.; Odell, L. R.; Larhed, M., Aminocarbonylations Employing Mo(CO)(6) and a Bridged Two-Vial System: Allowing the Use of Nitro Group Substituted Aryl Iodides and Aryl Bromides. *J. Org. Chem.* **2012**, 77 (24), 11393-11398.
75. Christensen, S. H.; Olsen, E. P. K.; Rosenbaum, J.; Madsen, R., Hydroformylation of olefins and reductive carbonylation of aryl halides with syngas formed ex situ from dehydrogenative decarbonylation of hexane-1,6-diol. *Org. Biomol. Chem.* **2015**, 13 (3), 938-945.
76. Lescot, C.; Nielsen, D. U.; Makarov, I. S.; Lindhardt, A. T.; Daasbjerg, K.; Skrydstrup, T., Efficient Fluoride-Catalyzed Conversion of CO₂ to CO at Room Temperature. *J. Am. Chem. Soc.* **2014**, 136 (16), 6142-6147.
77. Martinelli, J. R.; Watson, D. A.; Freckmann, D. M. M.; Barder, T. E.; Buchwald, S. L., Palladium-catalyzed carbonylation reactions of aryl bromides at atmospheric pressure: A general system based on xantphos. *J. Org. Chem.* **2008**, 73 (18), 7102-7107.
78. Raub, J. A.; Mathieu-Nolf, M.; Hampson, N. B.; Thom, S. R., Carbon monoxide poisoning - a public health perspective. *Toxicology* **2000**, 145 (1), 1-14.
79. Goldstein, M., CARBON MONOXIDE POISONING. *J. Emerg. Nurs.* **2008**, 34 (6), 538-542.
80. Weinstock, B.; Niki, H., CARBON-MONOXIDE BALANCE IN NATURE. *Science* **1972**, 176 (4032), 290-+.
81. Alonso, N.; Munoz, J. D.; Egle, B.; Vrijdag, J. L.; De Borggraeve, W. M.; de la Hoz, A.; Diaz-Ortiz, A.; Alcazar, J., First Example of a Continuous-Flow Carbonylation Reaction Using Aryl Formates as CO Precursors. *J. Flow Chem.* **2014**, 4 (3), 105-109.
82. Hansen, S. V. F.; Ulven, T., Oxalyl Chloride as a Practical Carbon Monoxide Source for Carbonylation Reactions. *Org. Lett.* **2015**, 17 (11), 2832-2835.
83. Mallia, C. J.; Walter, G. C.; Baxendale, I. R., Flow carbonylation of sterically hindered ortho-substituted iodoarenes. *Beilstein Journal of Organic Chemistry* **2016**, 12, 1503-1511.
84. Veryser, C.; Van Mileghem, S.; Egle, B.; Gilles, P.; De Borggraeve, W. M., Low-cost instant CO generation at room temperature using formic acid, mesyl chloride and triethylamine. *React. Chem. Eng.* **2016**, 1 (2), 142-146.
85. Lipina, T.; Weiss, K.; Roder, J., The ampakine CX546 restores the prepulse inhibition and latent inhibition deficits in mGluR5-deficient mice. *Neuropsychopharmacology* **2007**, 32 (4), 745-756.
86. Laux, G., MOCLOBEMIDE IN ANTIDEPRESSANT THERAPY - A REVIEW. *Psychiatr. Prax.* **1989**, 16, 37-40.

87. Feinsilver, O., ROLE OF NIKETHAMIDE AS A RESPIRATORY STIMULANT IN MANAGEMENT OF PULMONARY INSUFFICIENCY. *Curr. Ther. Res.-Clin. Exp.* **1962**, 4 (4), 165-&.
88. Van Mileghem, S.; Egle, B.; Gilles, P.; Veryser, C.; Van Meervelt, L.; De Borggraeve, W. M., Carbonylation as a novel method for the assembly of pyrazine based oligoamide alpha-helix mimetics. *Org. Biomol. Chem.* **2017**, 15 (2), 373-378.
89. Arkin, M. R.; Wells, J. A., Small-molecule inhibitors of protein-protein interactions: Progressing towards the dream. *Nat. Rev. Drug Discov.* **2004**, 3 (4), 301-317.
90. Schuster-Bockler, B.; Bateman, A., Protein interactions in human genetic diseases. *Genome Biol.* **2008**, 9 (1), 12.
91. Stumpf, M. P. H.; Thorne, T.; de Silva, E.; Stewart, R.; An, H. J.; Lappe, M.; Wiuf, C., Estimating the size of the human interactome. *Proc. Natl. Acad. Sci. U.S.A.* **2008**, 105 (19), 6959-6964.
92. Wermuth, C. G., *The Practice of Medicinal Chemistry*. Third edition ed.; Elsevier: 2008.
93. Voet, A.; Banwell, E. F.; Sahu, K. K.; Heddle, J. G.; Zhang, K. Y. J., Protein Interface Pharmacophore Mapping Tools for Small Molecule Protein: Protein Interaction Inhibitor Discovery. *Curr. Top. Med. Chem.* **2013**, 13 (9), 989-1001.
94. Bogan, A. A.; Thorn, K. S., Anatomy of hot spots in protein interfaces. *J. Mol. Biol.* **1998**, 280 (1), 1-9.
95. Clackson, T.; Wells, J. A., A HOT-SPOT OF BINDING-ENERGY IN A HORMONE-RECEPTOR INTERFACE. *Science* **1995**, 267 (5196), 383-386.
96. Metz, A.; Pfleger, C.; Kopitz, H.; Pfeiffer-Marek, S.; Baringhaus, K. H.; Gohlke, H., Hot Spots and Transient Pockets: Predicting the Determinants of Small-Molecule Binding to a Protein-Protein Interface. *J. Chem Inf. Model.* **2012**, 52 (1), 120-133.
97. Azzarito, V.; Long, K.; Murphy, N. S.; Wilson, A. J., Inhibition of alpha-helix-mediated protein-protein interactions using designed molecules. *Nat. Chem.* **2013**, 5 (3), 161-173.
98. Arkin, M. R.; Tang, Y. Y.; Wells, J. A., Small-Molecule Inhibitors of Protein-Protein Interactions: Progressing toward the Reality. *Chem. Biol.* **2014**, 21 (9), 1102-1114.
99. Scott, D. E.; Bayly, A. R.; Abell, C.; Skidmore, J., Small molecules, big targets: drug discovery faces the protein-protein interaction challenge. *Nat. Rev. Drug Discov.* **2016**, 15 (8), 533-550.
100. Hajduk, P. J.; Greer, J., A decade of fragment-based drug design: strategic advances and lessons learned. *Nat. Rev. Drug Discov.* **2007**, 6 (3), 211-219.

101. Lo, M. C.; Aulabaugh, A.; Jin, G. X.; Cowling, R.; Bard, J.; Malamas, M.; Ellestad, G., Evaluation of fluorescence-based thermal shift assays for hit identification in drug discovery. *Anal. Biochem.* **2004**, *332* (1), 153-159.
102. Navratilova, I.; Hopkins, A. L., Emerging role of surface plasmon resonance in fragment-based drug discovery. *Future Medicinal Chemistry* **2011**, *3* (14), 1809-1820.
103. Shuker, S. B.; Hajduk, P. J.; Meadows, R. P.; Fesik, S. W., Discovering high-affinity ligands for proteins: SAR by NMR. *Science* **1996**, *274* (5292), 1531-1534.
104. Nienaber, V. L.; Richardson, P. L.; Klighofer, V.; Bouska, J. J.; Giranda, V. L.; Greer, J., Discovering novel ligands for macromolecules using X-ray crystallographic screening. *Nat. Biotechnol.* **2000**, *18* (10), 1105-1108.
105. Rader, R. A., (Re)defining biopharmaceutical. *Nat. Biotechnol.* **2008**, *26* (7), 743-751.
106. Gonzalez-Ruiz, D.; Gohlke, H., Targeting protein-protein interactions with small molecules: Challenges and perspectives for computational binding epitope detection and ligand finding. *Curr. Med. Chem.* **2006**, *13* (22), 2607-2625.
107. Hertzberg, R. P.; Pope, A. J., High-throughput screening: new technology for the 21st century. *Curr. Opin. Chem. Biol.* **2000**, *4* (4), 445-451.
108. White, P. W.; Titolo, S.; Brault, K.; Thauvette, L.; Pelletier, A.; Welchner, E.; Bourgon, L.; Doyon, L.; Ogilvie, W. W.; Yoakim, C.; Cordingley, M. G.; Archambault, J., Inhibition of human papillomavirus DNA replication by small molecule antagonists of the E1-E2 protein interaction. *J. Biol. Chem.* **2003**, *278* (29), 26765-26772.
109. Doak, B. C.; Zheng, J.; Dobritsch, D.; Kihlberg, J., How Beyond Rule of 5 Drugs and Clinical Candidates Bind to Their Targets. *J. Med. Chem.* **2016**, *59* (6), 2312-2327.
110. de Vega, M. J. P.; Martin-Martinez, M.; Gonzalez-Muniz, R., Modulation of protein-protein interactions by stabilizing/mimicking protein secondary structure elements. *Curr. Top. Med. Chem.* **2007**, *7* (1), 33-62.
111. Craik, D. J.; Fairlie, D. P.; Liras, S.; Price, D., The Future of Peptide-based Drugs. *Chem. Biol. Drug Des.* **2013**, *81* (1), 136-147.
112. Ko, E.; Liu, J.; Burgess, K., Minimalist and universal peptidomimetics. *Chem. Soc. Rev.* **2011**, *40* (8), 4411-4421.
113. Raj, M.; Bullock, B. N.; Arora, P. S., Plucking the high hanging fruit: A systematic approach for targeting protein-protein interactions. *Bioorg. Med. Chem.* **2013**, *21* (14), 4051-4057.
114. Orner, B. P.; Ernst, J. T.; Hamilton, A. D., Toward proteomimetics: Terphenyl derivatives as structural and functional mimics of extended regions of an alpha-helix. *J. Am. Chem. Soc.* **2001**, *123* (22), 5382-5383.

115. Cummings, M. D.; Schubert, C.; Parks, D. J.; Calvo, R. R.; LaFrance, L. V.; Lattanze, J.; Milkiewicz, K. L.; Lu, T. B., Substituted 1,4-benzodiazepine-2,5-diones as alpha-helix mimetic antagonists of the HDM2-p53 protein-protein interaction. *Chem. Biol. Drug Des.* **2006**, *67* (3), 201-205.
116. Ravindranathan, P.; Lee, T. K.; Yang, L.; Centenera, M. M.; Butler, L.; Tilley, W. D.; Hsieh, J. T.; Ahn, J. M.; Raj, G. V., Peptidomimetic targeting of critical androgen receptor-coregulator interactions in prostate cancer. *Nature Communications* **2013**, *4*, 11.
117. Kulikov, O. V.; Kumar, S.; Magzoub, M.; Knipe, P. C.; Saraogi, I.; Thompson, S.; Miranker, A. D.; Hamilton, A. D., Amphiphilic oligoamide alpha-helix peptidomimetics inhibit islet amyloid polypeptide aggregation. *Tetrahedron Lett.* **2015**, *56* (23), 3670-3673.
118. Marimnganti, S.; Cheemala, M. N.; Ahn, J. M., Novel Amphiphilic alpha-Helix Mimetics Based on a Bis-benzamide Scaffold. *Org. Lett.* **2009**, *11* (19), 4418-4421.
119. Burslem, G. M.; Wilson, A. J., Synthesis of Oligobenzamide alpha-Helix Mimetics. *Synlett* **2014**, *25* (3), 324-335.
120. Plante, J.; Campbell, F.; Malkova, B.; Kilner, C.; Warriner, S. L.; Wilson, A. J., Synthesis of functionalised aromatic oligamide rods. *Org. Biomol. Chem.* **2008**, *6* (1), 138-146.
121. Campbell, F.; Plante, J. P.; Edwards, T. A.; Warriner, S. L.; Wilson, A. J., N-alkylated oligoamide alpha-helical proteomimetics. *Org. Biomol. Chem.* **2010**, *8* (10), 2344-2351.
122. Kulikov, O. V.; Hamilton, A. D., Synthesis of the novel trimeric benzamides-potential inhibitors of protein-protein interactions. *Rsc Advances* **2012**, *2* (6), 2454-2461.
123. Burslem, G. M.; Kyle, H. F.; Prabhakaran, P.; Breeze, A. L.; Edwards, T. A.; Warriner, S. L.; Nelson, A.; Wilson, A. J., Synthesis of highly functionalized oligobenzamide proteomimetic foldamers by late stage introduction of sensitive groups. *Org. Biomol. Chem.* **2016**, *14* (15), 3782-3786.
124. De Borggraeve, W. M.; Verbist, B. M. P.; Rombouts, F. J. R.; Pawar, V. G.; Smets, W. J.; Kamoune, L.; Alen, J.; Van der Eycken, E. V.; Compennolle, F.; Hoornaert, G. J., Design and synthesis of novel type VI-like beta-turn mimetics. Diversity at the i+1 and the i+2 position. *Tetrahedron* **2004**, *60* (50), 11597-11612.
125. Biros, S. M.; Moisan, L.; Mann, E.; Carella, A.; Zhai, D.; Reed, J. C.; Rebek, J., Heterocyclic alpha-helix mimetics for targeting protein-protein interactions. *Bioorg. Med. Chem. Lett.* **2007**, *17* (16), 4641-4645.
126. Prabhakaran, P.; Barnard, A.; Murphy, N. S.; Kilner, C. A.; Edwards, T. A.; Wilson, A. J., Aromatic Oligoamide Foldamers with a "Wet Edge" as

- Inhibitors of the α -Helix-Mediated p53-hDM2 Protein-Protein Interaction. *Eur. J. Org. Chem.* **2013**, (17), 3504-3512.
127. Ernst, J. T.; Becerril, J.; Park, H. S.; Yin, H.; Hamilton, A. D., Design and application of an α -helix-mimetic scaffold based on an oligoamide-foldamer strategy: Antagonism of the bak BH3/Bcl-xL complex. *Angew. Chem. Int. Ed.* **2003**, 42 (5), 535-+.
128. Brennfuhrer, A.; Neumann, H.; Beller, M., Palladium-Catalyzed Carbonylation Reactions of Aryl Halides and Related Compounds. *Angew. Chem. Int. Ed.* **2009**, 48 (23), 4114-4133.
129. Theodorou, V.; Gogou, M.; Giannoussi, A.; Skobridis, K., Insights into the N,N-diacylation reaction of 2-aminopyrimidines and deactivated anilines: an alternative N-monoacylation reaction. *Arkivoc* **2014**, 11-23.
130. Suzuki, A., Recent advances in the cross-coupling reactions of organoboron derivatives with organic electrophiles, 1995-1998. *J. Organomet. Chem.* **1999**, 576 (1-2), 147-168.
131. Yap, J. L.; Cao, X. B.; Vanommeslaeghe, K.; Jung, K. Y.; Peddaboina, C.; Wilder, P. T.; Nan, A.; MacKerell, A. D.; Smythe, W. R.; Fletcher, S., Relaxation of the rigid backbone of an oligoamide-foldamer-based α -helix mimetic: identification of potent Bcl-x(L) inhibitors. *Org. Biomol. Chem.* **2012**, 10 (15), 2928-2933.
132. Jiang, B.; Yang, C. G.; Xiong, W. N.; Wang, J., Synthesis and cytotoxicity evaluation of novel indolylpyrimidines and indolylpyrazines as potential antitumor agents. *Bioorg. Med. Chem.* **2001**, 9 (5), 1149-1154.
133. Patani, G. A.; LaVoie, E. J., Bioisosterism: A rational approach in drug design. *Chem. Rev.* **1996**, 96 (8), 3147-3176.
134. Scales, S.; Johnson, S.; Hu, Q. Y.; Do, Q. Q.; Richardson, P.; Wang, F.; Braganza, J.; Ren, S. J.; Wan, Y. D.; Zheng, B. J.; Faizi, D.; McAlpine, I., Studies on the Regioselective Nucleophilic Aromatic Substitution (S_NAr) Reaction of 2-Substituted 3,5-Dichloropyrazines. *Org. Lett.* **2013**, 15 (9), 2156-2159.
135. Wang, J.; Liang, Y. L.; Qu, J., Boiling water-catalyzed neutral and selective N-Boc deprotection. *Chem. Commun.* **2009**, (34), 5144-5146.
136. Ernst, J. T.; Becerril, J.; Park, H. S.; Yin, H.; Hamilton, A. D., Design and application of an α -helix-mimetic scaffold based on an oligoamide-foldamer strategy: Antagonism of the bak BH3/Bcl-xL complex. *Angew. Chem. Int. Ed.* **2003**, 42, 535-539.
137. Chothia, C., PRINCIPLES THAT DETERMINE THE STRUCTURE OF PROTEINS. *Annu. Rev. Biochem.* **1984**, 53, 537-572.
138. Azzarito, V.; Prabhakaran, P.; Bartlett, A. I.; Murphy, N. S.; Hardie, M. J.; Kilner, C. A.; Edwards, T. A.; Warriner, S. L.; Wilson, A. J., 2-O-Alkylated para-benzamide α -helix mimetics: the role of scaffold curvature. *Org. Biomol. Chem.* **2012**, 10 (32), 6469-6472.

139. Saraogi, I.; Incarvito, C. D.; Hamilton, A. D., Controlling Curvature in a Family of Oligoamide α -Helix Mimetics. *Angew. Chem. Int. Ed.* **2008**, 47 (50), 9691-9694.
140. Xin, D. Y.; Ko, E.; Perez, L. M.; Ioerger, T. R.; Burgess, K., Evaluating minimalist mimics by exploring key orientations on secondary structures (EKOS). *Org. Biomol. Chem.* **2013**, 11 (44), 7789-7801.
141. Guram, A. S.; Rennels, R. A.; Buchwald, S. L., A SIMPLE CATALYTIC METHOD FOR THE CONVERSION OF ARYL BROMIDES TO ARYLAMINES. *Angew. Chem. Int. Ed.* **1995**, 34 (12), 1348-1350.
142. Harris, M. C.; Geis, O.; Buchwald, S. L., Sequential N-arylation of primary amines as a route to alkyldiarylamines. *J. Org. Chem.* **1999**, 64 (16), 6019-6022.
143. Makosza, M.; Sienkiewicz, K., Hydroxylation of nitroarenes with alkyl hydroperoxide anions via Vicarious Nucleophilic Substitution of hydrogen. *J. Org. Chem.* **1998**, 63 (13), 4199-4208.
144. Lipshutz, B. H.; Chung, D. W.; Rich, B.; Corral, R., Simplification of the Mitsunobu reaction. Di-p-chlorobenzyl azodicarboxylate: A new azodicarboxylate. *Org. Lett.* **2006**, 8 (22), 5069-5072.
145. Lamothe, M.; Perez, M.; ColovrayGotteland, V.; Halazy, S., A simple one-pot preparation of N,N'-unsymmetrical ureas from N-Boc protected primary anilines and amines. *Synlett* **1996**, (6), 507-&.
146. Teng, M.; Hilgers, M. T.; Cunningham, M. L.; Borchardt, A.; Locke, J. B.; Abraham, S.; Haley, G.; Kwan, B. P.; Hall, C.; Hough, G. W.; Shaw, K. J.; Finn, J., Identification of Bacteria-Selective Threonyl-tRNA Synthetase Substrate Inhibitors by Structure-Based Design. *J. Med. Chem.* **2013**, 56 (4), 1748-1760.
147. Gadakh, B.; Smaers, S.; Rozenski, J.; Froeyen, M.; Van Aerschoe, A., 5'-(N-aminoacyl)-sulfonamido-5'-deoxyadenosine: Attempts for a stable alternative for aminoacyl-sulfamoyl adenosines as aaRS inhibitors. *Eur. J. Med. Chem.* **2015**, 93, 227-236.
148. Brown, M. J. B.; Mensah, L. M.; Doyle, M. L.; Broom, N. J. P.; Osbourne, N.; Forrest, A. K.; Richardson, C. M.; O'Hanlon, P. J.; Pope, A. J., Rational design of femtomolar inhibitors of isoleucyl tRNA synthetase from a binding model for pseudomonic acid-A. *Biochemistry* **2000**, 39 (20), 6003-6011.
149. Nielsen, D. U.; Taaning, R. H.; Lindhardt, A. T.; Gogsig, T. M.; Skrydstrup, T., Palladium-Catalyzed Approach to Primary Amides Using Nongaseous Precursors. *Org. Lett.* **2011**, 13 (16), 4454-4457.
150. Müller, H., *Ullmann's Encyclopedia of Industrial Chemistry*. Wiley-VCH: Weinheim, 2000.
151. Liu, G.; Fan, C. B.; Wu, J., Fixation of sulfur dioxide into small molecules. *Org. Biomol. Chem.* **2015**, 13 (6), 1592-1599.

152. Lloyd, D. R.; Roberts, P. J., ASSIGNMENT OF PHOTOELECTRON SPECTRUM OF SULFUR-DIOXIDE. *Mol. Phys.* **1973**, *26* (1), 225-230.
153. Deeming, A. S.; Emmett, E. J.; Richards-Taylor, C. S.; Willis, M. C., Rediscovering the Chemistry of Sulfur Dioxide: New Developments in Synthesis and Catalysis. *Synthesis* **2014**, *46* (20), 2701-2710.
154. Nguyen, B.; Emmett, E. J.; Willis, M. C., Palladium-Catalyzed Aminosulfonylation of Aryl Halides. *J. Am. Chem. Soc.* **2010**, *132* (46), 16372-16373.
155. Emmett, E. J.; Richards-Taylor, C. S.; Nguyen, B.; Garcia-Rubia, A.; Hayter, B. R.; Willis, M. C., Palladium-catalysed aminosulfonylation of aryl-, alkenyl- and heteroaryl halides: scope of the three-component synthesis of N-aminosulfonamides. *Org. Biomol. Chem.* **2012**, *10* (20), 4007-4014.
156. Richards-Taylor, C. S.; Blakemore, D. C.; Willis, M. C., One-pot three-component sulfone synthesis exploiting palladium-catalysed aryl halide aminosulfonylation. *Chem. Sci.* **2014**, *5* (1), 222-228.
157. Tsai, A. S.; Curto, J. M.; Rocke, B. N.; Dechert-Schmitt, A. M. R.; Ingle, G. K.; Mascitti, V., One-Step Synthesis of Sulfonamides from N-Tosylhydrazones. *Org. Lett.* **2016**, *18* (3), 508-511.
158. Zheng, D. Q.; An, Y. Y.; Li, Z. H.; Wu, J., Metal-Free Aminosulfonylation of Aryldiazonium Tetrafluoroborates with DABCO center dot(SO₂)(2) and Hydrazines. *Angew. Chem. Int. Ed.* **2014**, *53* (9), 2451-2454.
159. Deeming, A. S.; Russell, C. J.; Willis, M. C., Palladium(II)-Catalyzed Synthesis of Sulfinates from Boronic Acids and DABSO: A Redox-Neutral, Phosphine-Free Transformation. *Angew. Chem. Int. Ed.* **2016**, *55* (2), 747-750.
160. Rocke, B. N.; Bahnck, K. B.; Herr, M.; Laverne, S.; Mascitti, V.; Perreault, C.; Polivkova, J.; Shavnya, A., Synthesis of Sulfones from Organozinc Reagents, DABSO, and Alkyl Halides. *Org. Lett.* **2014**, *16* (1), 154-157.
161. Zheng, D. Q.; Li, Y.; An, Y. Y.; Wu, J., Aminosulfonylation of aromatic amines, sulfur dioxide and hydrazines. *Chem. Commun.* **2014**, *50* (64), 8886-8888.
162. Li, Y. W.; Zheng, D. Q.; Li, Z. H.; Wu, J., Generation of N-aminosulfonamides via a photo-induced fixation of sulfur dioxide into aryl/alkyl halides. *Organic Chemistry Frontiers* **2016**, *3* (5), 574-578.
163. Nigst, T. A.; Antipova, A.; Mayr, H., Nucleophilic Reactivities of Hydrazines and Amines: The Futile Search for the alpha-Effect in Hydrazine Reactivities. *J. Org. Chem.* **2012**, *77* (18), 8142-8155.
164. Banerjee, R.; King, S. B., Synthesis of Cyclic Hydroxamic Acids through -NOH Insertion of Ketones. *Org. Lett.* **2009**, *11* (20), 4580-4583.

165. Raghuvanshi, D. S.; Gupta, A. K.; Singh, K. N., Nickel-Mediated N-Arylation with Arylboronic Acids: An Avenue to Chan-Lam Coupling. *Org. Lett.* **2012**, *14* (17), 4326-4329.
166. Wallach, D. R.; Chisholm, J. D., Alkylation of Sulfonamides with Trichloroacetimidates under Thermal Conditions. *J. Org. Chem.* **2016**, *81* (17), 8035-8042.
167. Marcotullio, M. C.; Campagna, V.; Sternativo, S.; Costantino, F.; Curini, M., A new, simple synthesis of N-tosyl pyrrolidines and piperidines. *Synthesis* **2006**, (16), 2760-2766.
168. Mai, A. H.; De Borggraeve, W. M., Synthesis of N-Hydroxypyrazin-2(1H)-ones via Selective O-Debenzylation of 1-Benzyloxypyrazin-2(1H)-ones Using Flow Methodology. *J. Flow Chem.* **2015**, *5* (1), 6-10.
169. Van Mileghem, S.; De Borggraeve, W. M., A Convenient Multigram Synthesis of DABSO Using Sodium Sulfite as SO₂ Source. *Org. Process Res. Dev.* **2017**, *21* (5), 785-787.
170. Santos, P. S.; Mello, M. T. S., THE RAMAN-SPECTRA OF SOME MOLECULAR-COMPLEXES OF 1-AZABICYCLO 2.2.2 OCTANE AND 1,4-DIAZABICYCLO 2.2.2 OCTANE. *J. Mol. Struct.* **1988**, *178*, 121-133.
171. Mouselmani, R.; Da Silva, E.; Lemaire, M., Dimethyl sulfite a potential agent for methylation. *Tetrahedron* **2015**, *71* (47), 8905-8910.
172. Martial, L.; Bischoff, L., Stoichiometric Release of SO₂ from Adducts: Application to the Direct Synthesis of Protected Dienes. *Synlett* **2015**, *26* (9), 1225-1229.
173. Martial, L.; Bischoff, L., Preparation of DABSO from Karl-Fischer reagent. *Org. Syn.* **2013**, *90*, 301-305.
174. Li, H.; Jiao, X. L.; Chen, W. R., Solubility of sulphur dioxide in polar organic solvents. *Phys. Chem. Liq.* **2014**, *52* (2), 349-353.
175. vanDam, M. H. H.; Lamine, A. S.; Roizard, D.; Lochon, P.; Roizard, C., Selective sulfur dioxide removal using organic solvents. *Ind. Eng. Chem. Res.* **1997**, *36* (11), 4628-4637.
176. Spedding, D. J.; Brimblecombe, P., SOLUBILITY OF SULFUR-DIOXIDE IN WATER AT LOW CONCENTRATIONS. *Atmos. Environ.* **1974**, *8* (10), 1063-1063.
177. . <http://www.grandviewresearch.com/press-release/global-glycerol-market>.
178. Dasari, M. A.; Kiatsimkul, P. P.; Sutterlin, W. R.; Suppes, G. J., Low-pressure hydrogenolysis of glycerol to propylene glycol. *Appl. Catal. A-Gen.* **2005**, *281* (1-2), 225-231.
179. Konaka, A.; Tago, T.; Yoshikawa, T.; Nakamura, A.; Masuda, T., Conversion of glycerol into allyl alcohol over potassium-supported zirconia-iron oxide catalyst. *Appl. Catal. B-Environ.* **2014**, *146*, 267-273.

180. Yoon, S. J.; Choi, Y. C.; Son, Y. I.; Lee, S. H.; Lee, J. G., Gasification of biodiesel by-product with air or oxygen to make syngas. *Bioresour. Technol.* **2010**, *101* (4), 1227-1232.
181. Sonnati, M. O.; Amigoni, S.; de Givenchy, E. P. T.; Darmanin, T.; Choulet, O.; Guittard, F., Glycerol carbonate as a versatile building block for tomorrow: synthesis, reactivity, properties and applications. *Green Chem.* **2013**, *15* (2), 283-306.
182. Magniont, C.; Escadeillas, G.; Oms-Multon, C.; De Caro, P., The benefits of incorporating glycerol carbonate into an innovative pozzolanic matrix. *Cement and Concrete Research* **2010**, *40* (7), 1072-1080.
183. Ghandi, M.; Mostashari, A.; Karegar, M.; Barzegar, M., Efficient synthesis of alpha-monoglycerides via solventless condensation of fatty acids with glycerol carbonate. *J. Am. Oil Chem. Soc.* **2007**, *84* (7), 681-685.
184. Helou, M.; Carpentier, J. F.; Guillaume, S. M., Poly(carbonate-urethane): an isocyanate-free procedure from alpha,omega-di(cyclic carbonate) telechelic poly(trimethylenecarbonate)s. *Green Chem.* **2011**, *13* (2), 266-271.
185. Abraham, D. US Patent. 117445, 2011.
186. Clements, J. H., Reactive applications of cyclic alkylene carbonates. *Ind. Eng. Chem. Res.* **2003**, *42* (4), 663-674.
187. Ochoa-Gomez, J. R.; Gomez-Jimenez-Aberasturi, O.; Ramirez-Lopez, C.; Belsue, M., A Brief Review on Industrial Alternatives for the Manufacturing of Glycerol Carbonate, a Green Chemical. *Org. Process Res. Dev.* **2012**, *16* (3), 389-399.
188. Wang, H.; Lu, B.; Wang, X. G.; Zhang, J. W.; Cai, Q. H., Highly selective synthesis of dimethyl carbonate from urea and methanol catalyzed by ionic liquids. *Fuel Process. Technol.* **2009**, *90* (10), 1198-1201.
189. Yong Ryu, J. US Patent. US 20090203933 A1, 2009.
190. Hyun Joo, L. B. S., A.; Sang Deuk, L.; Jungho J.; Sik Choi S. US Patent. US 20150239858 A1, 2015.
191. Prochazka, R. W., V. US Patent. US 20110201828 A1, 2011.
192. Mignani, G. L., M.; Da Silva, E.; Dayoub, W.; Raoul, Y. US Patent. US 20130345441 A1, 2013.
193. Li, J. B.; Wang, T., On the deactivation of alkali solid catalysts for the synthesis of glycerol carbonate from glycerol and dimethyl carbonate. *React. Kinet. Mech. Catal.* **2011**, *102* (1), 113-126.
194. Simanjuntak, F. S. H.; Kim, T. K.; Lee, S. D.; Ahn, B. S.; Kim, H. S.; Lee, H., CaO-catalyzed synthesis of glycerol carbonate from glycerol and dimethyl carbonate: Isolation and characterization of an active Ca species. *Appl. Catal. A-Gen.* **2011**, *401* (1-2), 220-225.

195. Rokicki, G.; Rakoczy, P.; Parzuchowski, P.; Sobiecki, M., Hyperbranched aliphatic polyethers obtained from environmentally benign monomer: glycerol carbonate. *Green Chem.* **2005**, *7* (7), 529-539.
196. Ochoa-Gomez, J. R.; Gomez-Jimenez-Aberasturi, O.; Maestro-Madurga, B.; Pesquera-Rodriguez, A.; Ramirez-Lopez, C.; Lorenzo-Ibarreta, L.; Torrecilla-Soria, J.; Villaran-Velasco, M. C., Synthesis of glycerol carbonate from glycerol and dimethyl carbonate by transesterification: Catalyst screening and reaction optimization. *Appl. Catal. A-Gen.* **2009**, *366* (2), 315-324.
197. Munshi, M. K.; Gade, S. M.; Rane, V. H.; Kelkar, A. A., Role of cation-anion cooperation in the selective synthesis of glycidol from glycerol using DABCO-DMC ionic liquid as catalyst. *RSC Adv.* **2014**, *4* (61), 32127-32133.
198. Munshi, M. K.; Gade, S. M.; Mane, M. V.; Mishra, D.; Pal, S.; Vanka, K.; Rane, V. H.; Kelkar, A. A., 1,8-Diazabicyclo 5.4.0 undec-7-ene (DBU): A highly efficient catalyst in glycerol carbonate synthesis. *J. Mol. Catal. A-Chem.* **2014**, *391*, 144-149.
199. Ochoa-Gomez, J. R.; Gomez-Jimenez-Aberasturi, O.; Ramirez-Lopez, C.; Maestro-Madurga, B., Synthesis of glycerol 1,2-carbonate by transesterification of glycerol with dimethyl carbonate using triethylamine as a facile separable homogeneous catalyst. *Green Chem.* **2012**, *14* (12), 3368-3376.
200. Lee, K. H.; Park, C. H.; Lee, E. Y., Biosynthesis of glycerol carbonate from glycerol by lipase in dimethyl carbonate as the solvent. *Bioprocess. Biosyst. Eng.* **2010**, *33* (9), 1059-1065.
201. Kim, S. C.; Kim, Y. H.; Lee, H.; Yoon, D. Y.; Song, B. K., Lipase-catalyzed synthesis of glycerol carbonate from renewable glycerol and dimethyl carbonate through transesterification. *J. Mol. Catal. B-Enzym.* **2007**, *49* (1-4), 75-78.
202. Tudorache, M.; Protesescu, L.; Coman, S.; Parvulescu, V. I., Efficient bio-conversion of glycerol to glycerol carbonate catalyzed by lipase extracted from *Aspergillus niger*. *Green Chem.* **2012**, *14* (2), 478-482.
203. Hervert, B.; McCarthy, P. D.; Palencia, H., Room temperature synthesis of glycerol carbonate catalyzed by N-heterocyclic carbenes. *Tetrahedron Lett.* **2014**, *55* (1), 133-136.
204. Nogueira, D. O.; de Souza, S. P.; Leao, R. A. C.; Miranda, L. S. M.; de Souza, R., Process intensification for tertiary amine catalyzed glycerol carbonate production: translating microwave irradiation to a continuous-flow process. *RSC Adv.* **2015**, *5* (27), 20945-20950.
205. Alvarez, M. G.; Pliskova, M.; Segarra, A. M.; Medina, F.; Figueras, F., Synthesis of glycerol carbonates by transesterification of glycerol in a

- continuous system using supported hydrotalcites as catalysts. *Appl. Catal. B-Environ.* **2012**, *113*, 212-220.
206. Zhou, Y.; Ouyang, F.; Song, Z. B.; Yang, Z.; Tao, D. J., Facile one-pot synthesis of glycidol from glycerol and dimethyl carbonate catalyzed by tetraethylammonium amino acid ionic liquids. *Catalysis Communications* **2015**, *66*, 25-29.
207. Cushing, K. A.; Peretti, S. W., Enzymatic processing of renewable glycerol into value-added glycerol carbonate. *RSC Adv.* **2013**, *3* (40), 18596-18604.
208. Baker, M., Reproducibility: Check your chemistry. *Nature* **2017**, *548* (7668), 485-488.
209. Personal communication
210. Veryser, C.; Demaerel, J.; Bieliunas, V.; Gilles, P.; De Borggraeve, W. M., Ex Situ Generation of Sulfuryl Fluoride for the Synthesis of Aryl Fluorosulfates. *Org. Lett.* **2017**.
211. Li, S. H.; Wu, P.; Moses, J. E.; Sharpless, K. B., Multidimensional SuFEx Click Chemistry: Sequential Sulfur(VI) Fluoride Exchange Connections of Diverse Modules Launched From An SOF₄ Hub. *Angew. Chem. Int. Ed.* **2017**, *56* (11), 2903-2908.
212. Stewart, J. A.; Drexel, R.; Arstad, B.; Reubsaet, E.; Weckhuysen, B. M.; Bruijninx, P. C. A., Homogeneous and heterogenised masked N-heterocyclic carbenes for bio-based cyclic carbonate synthesis. *Green Chem.* **2016**, *18* (6), 1605-1618.
213. Gillingham, D. G.; Hoveyda, A. H., Chiral N-heterocyclic carbenes in natural product synthesis: Application of Ru-catalyzed asymmetric ring-opening/cross-metathesis and Cu-catalyzed allylic alkylation to total synthesis of baconipyrone C. *Angew. Chem. Int. Ed.* **2007**, *46* (21), 3860-3864.
214. Merzouk, M.; Moore, T.; Williams, N. A., Synthesis of chiral iminoalkyl functionalised N-heterocyclic carbenes and their use in asymmetric catalysis. *Tetrahedron Lett.* **2007**, *48* (50), 8914-8917.
215. <https://admin.kuleuven.be/sab/vgm/kuleuven/EN/riskactivities/cs>
216. <http://chem.kuleuven.be>
217. <http://groupware.kuleuven.be/sites/depchemrisico/>
218. <https://www.epa.gov/so2-pollution>
219. Dolomite. <http://www.dolomite-microfluidics.com/> (accessed 12/08/2014).
220. Camerino, B.; Palamidessi, G., Derivati della Pirazina.-Nota 1. Aminopirazine.(Derivatives of Pyrazine-Note 1. Aminopyrazine.). *Gazz. chim. ital* **1960**, *90*, 1807-1814.

221. Caldwell, J. J.; Veillard, N.; Collins, I., Design and synthesis of 2(1H)-pyrazinones as inhibitors of protein kinases. *Tetrahedron* **2012**, 68 (47), 9713-9728.